Pulmonary Vascular Defects in Congenital Diaphragmatic Hernia

The quest for early factors and intervention

Daphne Mous

Pulmonary Vascular Defects in Congenital Diaphragmatic Hernia

The quest for early factors and intervention

Daphne Mous

Printing of this thesis was financially supported by SBOH, employer of GP trainees.

SBOH
voor artsen in opleiding

ISBN: 978-94-6295-783-1

Layout: Paul Kasteleyn

Printed by: ProefschriftMaken // www.proefschriftmaken.nl

Pulmonary Vascular Defects in Congenital Diaphragmatic Hernia

The quest for early factors and intervention

Pulmonale vasculaire defecten in congenitale hernia diafragmatica

De zoektocht naar vroege factoren en interventie

Proefschrift

ter verkrijging van de graad van doctor aan de
Erasmus Universiteit Rotterdam
op gezag van de
rector magnificus

Prof.dr. H.A.P. Pols

en volgens besluit van het College voor Promoties.
De openbare verdediging zal plaatsvinden op
donderdag 30 november 2017 om 11:30 uur

door

Daphne Stephanie Mous
geboren te Schiedam

Erasmus University Rotterdam

Erasmus

Promotiecommissie

Promotoren
Prof.dr. D. Tibboel
Prof.dr. R.M.H. Wijnen

Overige leden
Prof.dr. I.K.M. Reiss
Prof.dr. R. Morty
Prof.dr. K. Allegaert

Copromotor
Dr. R.J. Rottier

Paranimfen
Sabine Mous
Evelien Eenjes

Table of contents

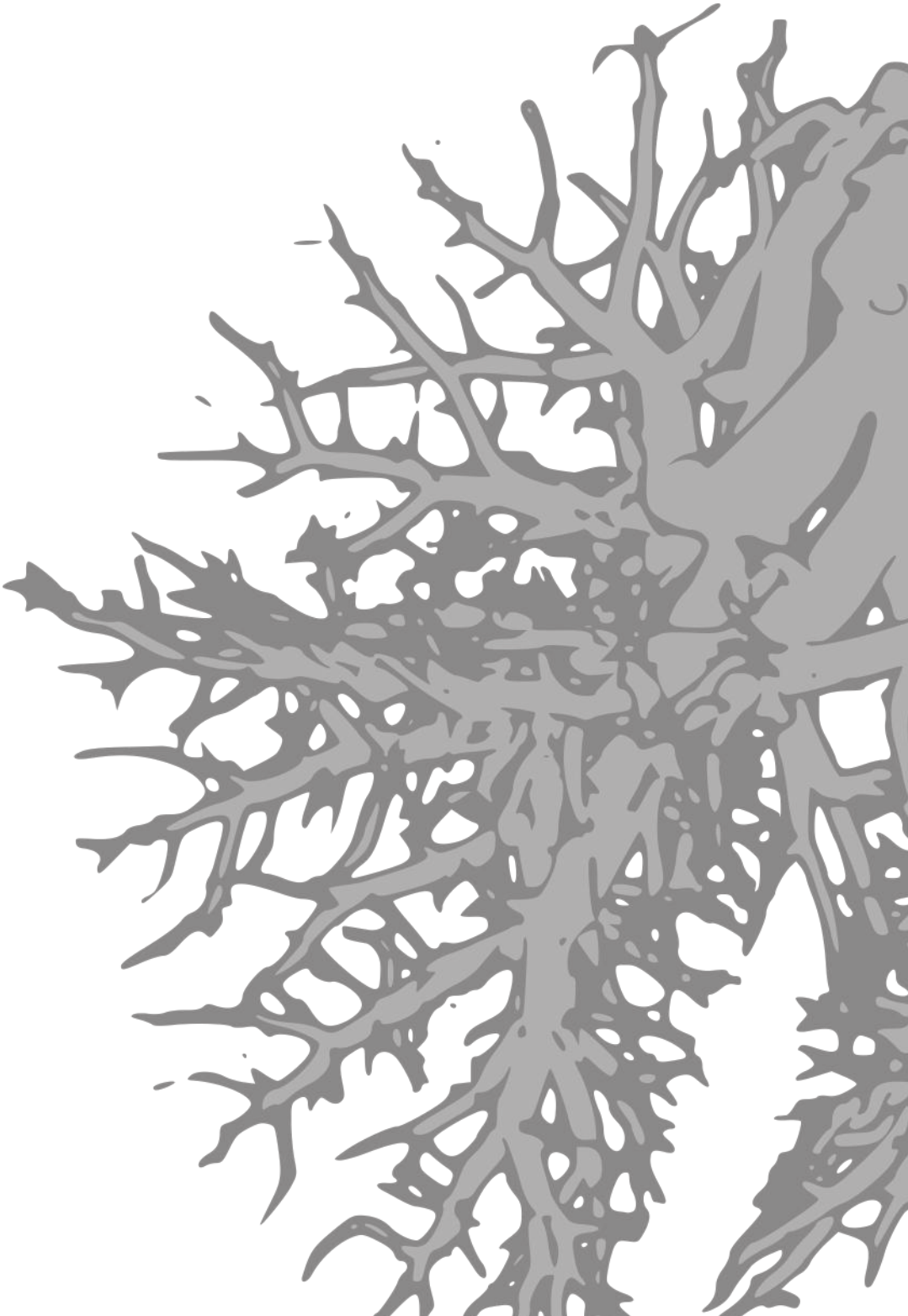

Chapter 1

General introduction

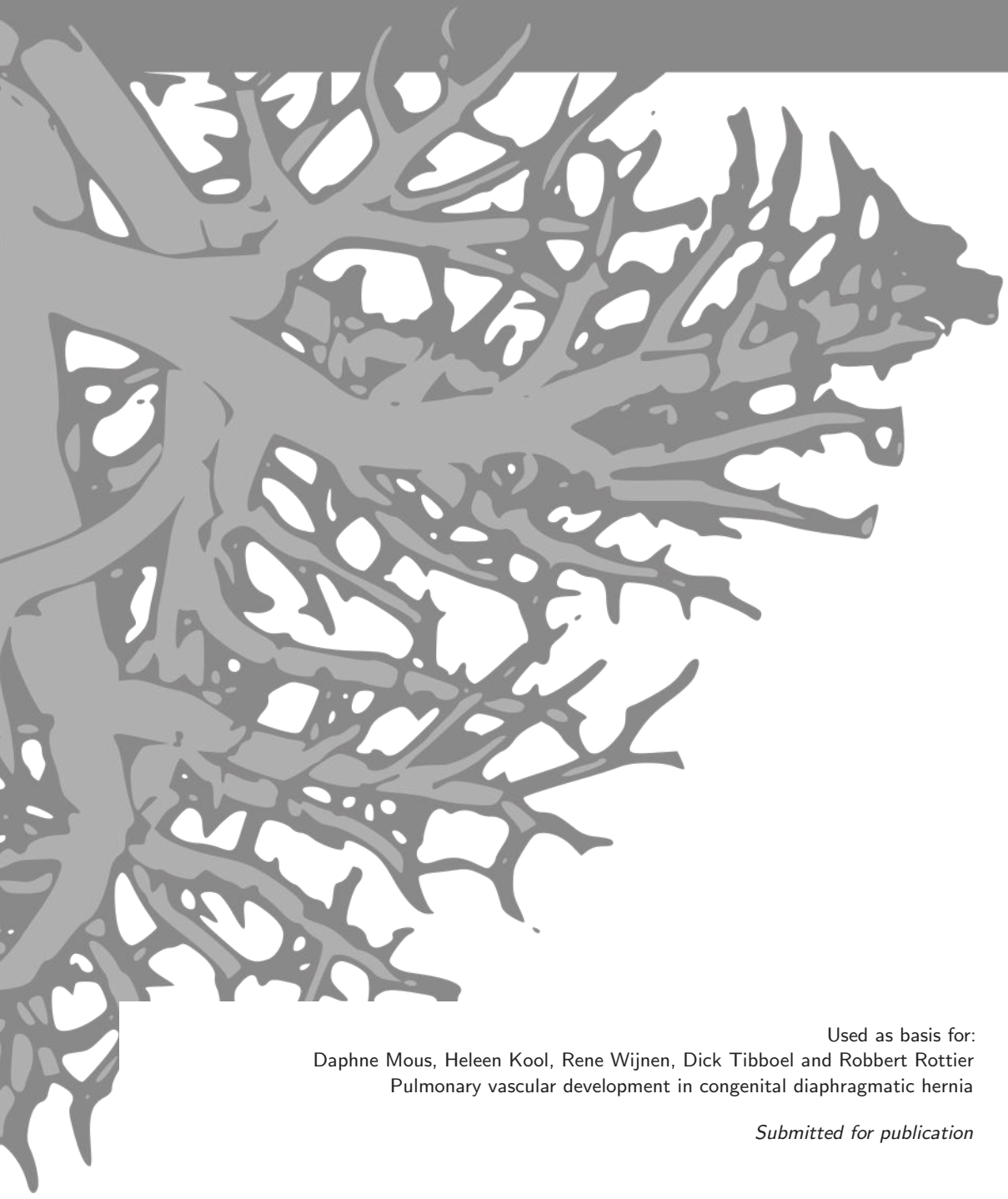

Used as basis for:
Daphne Mous, Heleen Kool, Rene Wijnen, Dick Tibboel and Robbert Rottier
Pulmonary vascular development in congenital diaphragmatic hernia

Submitted for publication

Congenital diaphragmatic hernia (CDH) is a rare congenital anomaly characterized by a diaphragmatic defect, pulmonary hypertension (PH) and lung hypoplasia (LH). It has a worldwide incidence of approximately 1 in 3000 live births [1, 2] and mortality varies from 20-40% [3], leading parents and treatment teams to termination of pregnancy or to consider ongoing therapy as futile. In some cases chromosomal aberrations have been found, but the etiology of CDH is largely unknown [4–6]. Approximately 60% of all cases are isolated, showing no additional congenital defects [6]. The high mortality and morbidity rates may depend on the presence of associated malformations and/or genetic abnormalities, but are mostly due to the concomitant PH. PH is the result of the altered development of the pulmonary vasculature, the unpredictable vascular reactivity and the disordered process of pulmonary vascular remodeling [7, 8]. Nowadays, at least in large parts of Europe and the USA, CDH is usually diagnosed at 20 weeks of gestation by ultrasound and/or Magnetic Resonance Imaging (MRI). Despite the significant improved management and survival in CDH over the last decade, potentially due to the release of and compliance to international guidelines initiated by the CDH EURO consortium [9, 10], PH in these patients remains a significant challenge.

Pulmonary development

Human lung development can be divided into different stages, starting with the embryonic stage at 4 weeks of gestation, followed by the pseudoglandular stage in which branching of the lung buds continues. During the canalicular stage, starting around 16 weeks of gestation, gas exchange regions will be formed. From 24 weeks of gestation until term, the saccular stage, airspaces will widen and alveoli are formed. During the alveolar stage, which persists into the postnatal period, maturation of the airways occurs [11]. In contrast to previous thoughts, our group and others showed that pulmonary vasculature develops in close relation with the airways already during the embryonic stage and might even be a rate limiting factor in the branching morphogenesis [12–14]. This implies that the pulmonary vasculature plays an important role in lung development. The formation of new blood vessels primarily occurs through distal angiogenesis where new capillaries are formed from preexisting vessels. This has been shown in lungs of mice with intact blood circulation to maintain vascular tone and integrity [14].

Normally, pulmonary vascular resistance is high during gestation and decreases rapidly after birth under the influence of both the increased ventilation and oxygenation and the release of different factors of the three major vasoactive pathways; the endothelin (ET), nitric oxide (NO) and prostacyclin (PGI_2) pathways [15–17] (Figure 1.1). Over the last decades research has shown changes in several molecular pathways involving the pulmonary vascular development in patients with PH. In different animal models abnormal retinoic acid (RA) signaling has been found to be involved in the etiology of CDH [18–21]. RA signaling has been shown to be important in lung development [22]. Active RA is formed from vitamin A through several enzymatic reactions. Subsequently it can form a complex with one of the retinoic acid receptors (RAR) which can bind to a retinoic acid responsive element (RARE) and can modulate transcription of target genes [23]. As described previously in a mouse model, lower levels of RA can cause an increase in Transforming Growth Factor β (TGFβ), which plays an important role in airway branching and muscularization of the pulmonary vasculature [24].

Important pathways involved in the etiology of pulmonary vascular defects in CDH

Current treatment of PH in CDH is based on targeting one of the three major vasoactive pathways involved in vasoconstriction and vasodilation of the pulmonary vasculature. The

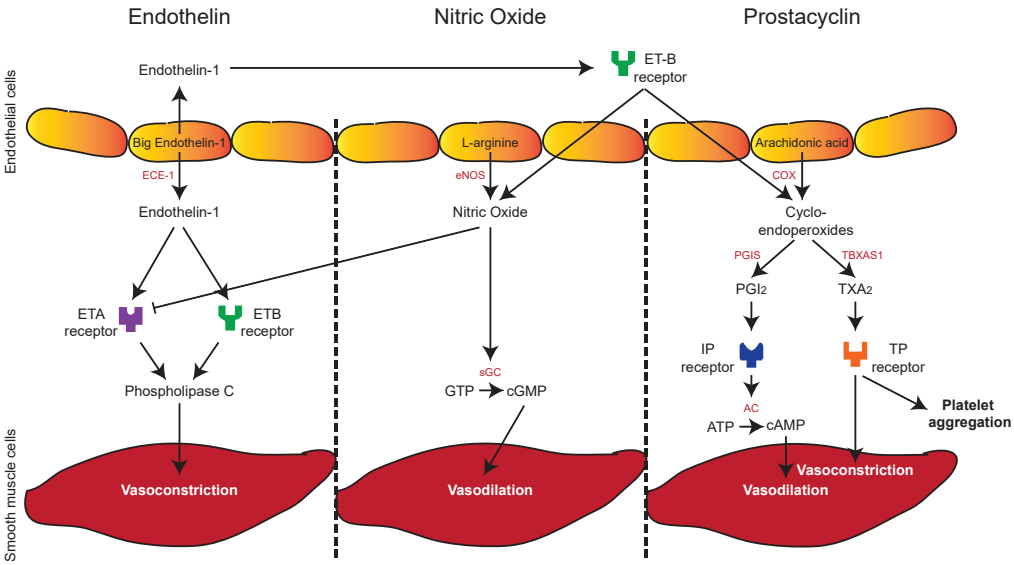

Figure 1.1: Overview of the vasoactive pathways. ECE-1 = endothelin converting enzyme 1, ETA = endothelin A, ETB = endothelin B, eNOS = endothelial nitric oxide synthase, sGC = soluble guanylate cyclase, COX = cyclooxygenase, PGIS = prostaglandin synthase, PGI_2 = prostaglandin I_2, AC = adenylate cyclase, TBXAS1 = thromboxane synthase, TXA_2 = thromboxane.

ET pathway is activated by three ligands: ET-1, ET-2 and ET-3, of which ET-1 is the most common isoform [25, 26]. The ET-1 precursor protein, Prepro-ET-1 is cleaved by furin into the Big-ET-1, which is subsequently processed to its active form by the endothelin converting enzyme (ECE-1) and binds and activates two different G-protein coupled receptors, ETA and ETB, with equal affinity. The ETA receptor is located at the cell surface of vascular smooth muscle cells and induces vasoconstriction and cell proliferation by activating phospholipase C, whereas the ETB receptor is located mainly in the cell membrane of the endothelium and induces vasodilation by regulating the release of NO and PGI_2 [27, 26]. Furthermore, ET-1 promotes cell growth, cell adhesion and thrombosis and is increased in lung tissue of patients with pulmonary hypertension. A negative feedback loop is triggered by NO that reduces the affinity of the ETA receptor for ET-1 and can therefore prevent ET-1 mediated signaling [27]. NO can be synthesized by one of three different NO synthases (NOS), of which endothelial NOS (eNOS) is the most important synthase involved in the regulation of the pulmonary vascular tone and is highly expressed in the endothelial cells [28]. NO can bind to its receptor, soluble guanylyl cyclase (sGC), which can synthesize the second messenger cyclic guanosine monophosphate (cGMP), thereby inducing vasodilation. The third important pathway involves prostaglandins and thromboxanes that act on prostanoid receptors which can be divided in receptors that cause relaxation (IP (PTGIR), EP2, EP4 and DP) or contraction (TP, EP1 and FP) of the vascular tone [29]. PGI_2 is an important mediator of vasodilation which binds and activates the prostaglandin-I_2 receptor (PTGIR) [30, 31]. This activation results in vasodilation through the release of cyclic adenosine monophosphate (cAMP).

The alveolar formation starts late in development and continues into the first years of life to expand the gas exchanging capacity of the lung. Concomitant with the expansion of the airways is the adaptation of the microvasculature to optimize the transport of oxygen and carbon dioxide from the blood to the airways and vice versa. This process is partly regulated by TGFβ.

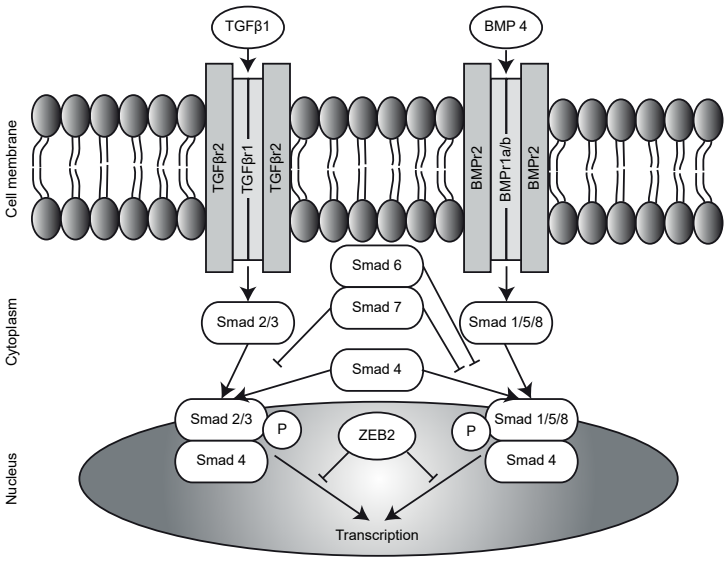

Figure 1.2: Overview of the TGFβ and BMP pathways. TGFβ = transforming growth factor β, BMP = bone morphogenetic protein, ZEB2 = zinc finger E-box binding homeobox 2, P = phosphorylation.

There are two main branches in the TGFβ superfamily; the TGFβ/activin family and the bone morphogenetic protein (BMP) family. All proteins of the TGFβ superfamily act through two classes of receptor serine/threonine kinases; type 1 and type 2. Active TGFβ or BMP can be bound to a specific type 2 receptor, which phosphorylates and activates a type 1 receptor. The activated type 1 receptor subsequently phosphorylates a set of receptor-regulated Smads, which form a complex with co-Smad (Smad4). TGFβ is responsible for the phosphorylation of Smad2 and Smad 3, where BMP phosphorylates Smad 1, 5 and 8. Eventually, the R-Smad/co-Smad complex modulates the transcription of target genes in the nucleus [32] (Figure 1.2). TGFβ is a negative regulator of airway branching in early lung development. However, TGFβ signaling is necessary in vascular and airway smooth muscle cells, and in alveolar and airway epithelial cells during late lung development [33]. Previous studies in rodents showed an arrest in alveolarization both in animals with upregulated TGFβ signaling [34] as well as after a complete blockade of TGFβ signaling [35], indicating the important differences in TGFβ signaling between early and late lung development.

Current treatment options of pulmonary hypertension pre- and postnatally

The significance of PH in the mortality and morbidity of patients with CDH has been increasingly recognized since 1971 [36, 37]. The first vasodilators used in these neonatal patients with PH, tolazoline [38], an α-adrenergic receptor antagonist, and prostacyclin [39], a prostaglandin-I_2 (PGI_2) agonist, resulted in variable results. Tolazoline infusion showed a response in 21 of 36 neonatal patients with lung disease, where systemic hypotension and bleeding tendency were seen as a side effect in several patients [38]. Treatment with PGI_2 improved pulmonary arterial pressure and oxygenation in 2 of 3 neonatal patients with idiopathic PH and PH caused by meconium aspiration. However, it had no beneficial effect in 2 patients with CDH, whereas

systemic hypotension was seen as a side effect in one of these patients [39]. Currently, patients with CDH still respond unpredictable to the available vasodilator therapy due to the lack of understanding of the underlying mechanisms which can be different in individual patients. Inhaled nitric oxide (iNO) is most commonly used, but studies have failed to show its efficacy in this specific group of patients [40–43]. Apart from iNO, sildenafil and some prostaglandin analogues are used as rescue therapy in a compassionate way in the most severe cases, but with variable results [44–48]. No appropriate trials have been performed on these drugs and, with a few exceptions, no data on pharmacokinetics are available for CDH neonates.

Currently, the only prenatal intervention used in CDH in the form of a clinical trial is Fetoscopic Endoluminal Tracheal Occlusion (FETO), where a small balloon will be inserted in the fetal trachea to temporarily block the airway for a period of 4-6 weeks (TOTAL; NCT02875860 (clinicaltrials.gov)) [49]. As a result, fluid will be trapped in the lungs, creating internal pressure which forces the lung to grow. This idea of blocking the airway emerged from the enlargement of the lungs seen in patients with congenital high airway obstruction syndrome (CHAOS) [50]. Previous research has shown that tracheal occlusion can indeed cause an increase in lung growth [51, 52] and removing the balloon before birth has shown to be necessary for a better maturation of the lung by decreasing the apoptosis of the alveolar type 2 cells which produce surfactant, an essential compound for lung function [53]. So far, FETO has shown to improve survival rate in high risk CDH patients but at the cost of increased morbidity and premature delivery [54–56]. As a consequence, the results of the FETO trial have to be awaited which will take another 1-2 years (personal communication J. Deprest).

At the moment treatment with vasodilators in patients with CDH is only used postnatally, where previous research has shown already major differences in the pulmonary vasculature early during development [57]. Over the last years some studies have been performed on the antenatal use of the phosphodiesterase-5 inhibitor sildenafil in different animal models of CDH, showing improvement in alveolarization and pulmonary vascular development [58–62]. However, treatment in these studies was already initiated very early during pregnancy, at the start of lung development and before CDH symptoms and pathology develop. At this time human CDH would not yet be detectable. Furthermore, pulmonary pathology in these treated animals was not totally reversed.

The absence of an integrated analysis of TGFβ signaling and of the pathways regulating vascular tone as well as the ineffective postnatal treatment in individual patients with CDH makes it essential to obtain more insight into these pathways during development to optimize targeting and timing of administration of these drugs. Furthermore, adequate prenatal treatment could be beneficial for the pulmonary development in CDH.

Experimental animal model

Different animal models have been developed to evaluate the abnormalities in CDH of which the nitrofen rat model is one of the best studied. In this model, pregnant Sprague-Dawley rats receive the herbicide nitrofen (2,4-dichlorophenyl-p-nitrophenyl ether) by gavage on gestational age day E9.5, which induces a developmental defect in the diaphragm of the fetuses and pathological signs of PH and LH. Nitrofen inhibits retinal dehydrogenase (RALDH-2), an enzyme that normally synthesizes RA, which, as described above, plays an important role in lung development [20, 63]. The first indication of abnormal RA signaling in CDH came from a study where 25-40% of pups born to rat dams with a vitamin A deficient diet had a diaphragmatic hernia [18]. Furthermore, administration of large amounts of vitamin A to nitrofen-treated animals has shown to reduce the incidence of CDH in the offspring [64]. These observations in animal models were strengthened by decreased retinol and retinol binding protein plasma levels in a small number of newborn CDH patients [65] and the discovery of

deregulated RA signaling genes in human CDH patients [66]. Additionally to the diaphragmatic defect, cardiovascular and skeletal defects, similar to those found in human CDH patients, have been seen in nitrofen-treated rat fetuses, which makes it a useful model for the research of the underlying pathology of this disease [63].

Aims and outline of this thesis

The aim of this thesis is to evaluate the expression of important factors in the different vasoactive pathways in CDH and to develop a potential prenatal intervention for the altered pulmonary vascular development.

In the first place important factors in the TGFβ pathway and the major vasoactive pathways, the endothelin, prostacyclin and nitric oxide pathways, were evaluated in human CDH patients and the well-established nitrofen rat model for CDH. Second, prenatal intervention using treatment with the phosphodiesterase-5 inhibitor sildenafil and/or prostaglandin-I_2 agonist NS-304 is implemented in this rat model.

Chapter 2 gives an overview of current knowledge on pulmonary vascular development in health and disease, describing aberrant expression of factors in both CDH and some other neonatal diseases. **Chapter 3** describes the alterations in the TGFβ pathway in CDH. In **Chapter 4** the three major vasoactive pathways are examined in exclusive material of human CDH patients and the well-established nitrofen rat model. **Chapter 5 and 6** describe two experimental animal studies on the antenatal use of the phosphodiesterase-5 inhibitor sildenafil and the prostaglandin-I_2 receptor agonist NS-304 in the nitrofen rat model. At last, in **Chapter 7** the results of these studies are placed in a broader perspective and future possibilities are discussed.

References

[1] Torfs CP, Curry CJ, et al. A population-based study of congenital diaphragmatic hernia. Teratology. 1992;46(6):555–65.

[2] McGivern MR, Best KE, et al. Epidemiology of congenital diaphragmatic hernia in Europe: a register-based study. Arch Dis Child Fetal Neonatal Ed. 2015;100(2):F137–44.

[3] Lally KP. Congenital diaphragmatic hernia - the past 25 (or so) years. J Pediatr Surg. 2016;51(5):695–8.

[4] Beurskens LW, Tibboel D, et al. Role of nutrition, lifestyle factors, and genes in the pathogenesis of congenital diaphragmatic hernia: human and animal studies. Nutr Rev. 2009;67(12):719–30.

[5] Veenma DC, de Klein A, et al. Developmental and genetic aspects of congenital diaphragmatic hernia. Pediatr Pulmonol. 2012;47(6):534–45.

[6] Donahoe PK, Longoni M, et al. Polygenic Causes of Congenital Diaphragmatic Hernia Produce Common Lung Pathologies. Am J Pathol. 2016;186(10):2532–43.

[7] Miniati D. Pulmonary vascular remodeling. Semin Pediatr Surg. 2007;16(2):80–7.

[8] Sluiter I, Reiss I, et al. Vascular abnormalities in human newborns with pulmonary hypertension. Expert Rev Respir Med. 2011;5(2):245–56.

[9] Reiss I, Schaible T, et al. Standardized postnatal management of infants with congenital diaphragmatic hernia in Europe: the CDH EURO Consortium consensus. Neonatology. 2010;98(4):354–64.

[10] Snoek KG, Reiss IK, et al. Standardized Postnatal Management of Infants with Congenital Diaphragmatic Hernia in Europe: The CDH EURO Consortium Consensus - 2015 Update. Neonatology. 2016;110(1):66–74.

[11] Warburton D, El-Hashash A, et al. Lung organogenesis. Curr Top Dev Biol. 2010;90:73–158.

[12] Schwarz MA, Zhang F, et al. Angiogenesis and morphogenesis of murine fetal distal lung in an allograft model. Am J Physiol Lung Cell Mol Physiol. 2000;278(5):L1000–7.

[13] van Tuyl M, Liu J, et al. Role of oxygen and vascular development in epithelial branching morphogenesis of the developing mouse lung. Am J Physiol Lung Cell Mol Physiol. 2005;288(1):L167–78.

[14] Parera MC, van Dooren M, et al. Distal angiogenesis: a new concept for lung vascular morphogenesis. Am J Physiol Lung Cell Mol Physiol. 2005;288(1):L141–9.

[15] Kraemer U, Cochius-den Otter S, et al. Pharmacodynamic considerations in the treatment of pulmonary hypertension in infants: challenges and future perspectives. Expert Opin Drug Metab Toxicol. 2016;12(1):1–19.

[16] Levy M, Maurey C, et al. Developmental expression of vasoactive and growth factors in human lung. Role in pulmonary vascular resistance adaptation at birth. Pediatr Res. 2005;57(5 Pt 2):21R–25R.

[17] Hillman NH, Kallapur SG, et al. Physiology of transition from intrauterine to extrauterine life. Clin Perinatol. 2012;39(4):769–83.

[18] Wilson JG, Roth CB, et al. An analysis of the syndrome of malformations induced by maternal vitamin A deficiency. Effects of restoration of vitamin A at various times during gestation. Am J Anat. 1953;92(2):189–217.

[19] Mendelsohn C, Lohnes D, et al. Function of the retinoic acid receptors (RARs) during development (II). Multiple abnormalities at various stages of organogenesis in RAR double mutants. Development. 1994;120(10):2749–71.

[20] Beurskens N, Klaassens M, et al. Linking animal models to human congenital diaphragmatic hernia. Birth Defects Res A Clin Mol Teratol. 2007;79(8):565–72.

[21] Greer JJ, Babiuk RP, et al. Etiology of congenital diaphragmatic hernia: the retinoid hypothesis. Pediatr Res. 2003;53(5):726–30.

[22] Malpel S, Mendelsohn C, et al. Regulation of retinoic acid signaling during lung morphogenesis. Development. 2000;127(14):3057–67.

[23] Kool H, Mous D, et al. Pulmonary vascular development goes awry in congenital lung abnormalities. Birth Defects Res C Embryo Today. 2014;102(4):343–58.

[24] Chen F, Desai TJ, et al. Inhibition of Tgf beta signaling by endogenous retinoic acid is essential for primary lung bud induction. Development. 2007;134(16):2969–79.

[25] Inoue A, Yanagisawa M, et al. The human endothelin family: three structurally and pharma-

cologically distinct isopeptides predicted by three separate genes. Proc Natl Acad Sci U S A. 1989;86(8):2863–7.

[26] Davenport AP, Hyndman KA, et al. Endothelin. Pharmacol Rev. 2016;68(2):357–418.

[27] Michael JR, Markewitz BA. Endothelins and the lung. Am J Respir Crit Care Med. 1996;154(3 Pt 1):555–81.

[28] Francis SH, Busch JL, et al. cGMP-dependent protein kinases and cGMP phosphodiesterases in nitric oxide and cGMP action. Pharmacol Rev. 2010;62(3):525–63.

[29] Mubarak KK. A review of prostaglandin analogs in the management of patients with pulmonary arterial hypertension. Respir Med. 2010;104(1):9–21.

[30] Weinberger B, Laskin DL, et al. The toxicology of inhaled nitric oxide. Toxicol Sci. 2001;59(1):5–16.

[31] Gao Y, Raj JU. Regulation of the pulmonary circulation in the fetus and newborn. Physiol Rev. 2010;90(4):1291–335.

[32] Weiss A, Attisano L. The TGFbeta superfamily signaling pathway. Wiley Interdiscip Rev Dev Biol. 2013;2(1):47–63.

[33] Alejandre-Alcazar MA, Michiels-Corsten M, et al. TGF-beta signaling is dynamically regulated during the alveolarization of rodent and human lungs. Dev Dyn. 2008;237(1):259–69.

[34] Alejandre-Alcazar MA, Kwapiszewska G, et al. Hyperoxia modulates TGF-beta/BMP signaling in a mouse model of bronchopulmonary dysplasia. Am J Physiol Lung Cell Mol Physiol. 2007;292(2):L537–49.

[35] Chen H, Sun J, et al. Abnormal mouse lung alveolarization caused by Smad3 deficiency is a developmental antecedent of centrilobular emphysema. Am J Physiol Lung Cell Mol Physiol. 2005;288(4):L683–91.

[36] Murdock AI, Burrington JB, et al. Alveolar to arterial oxygen tension difference and venous admixture in newly born infants with congenital diaphragmatic herniation through the foramen of Bochdalek. Biol Neonate. 1971;17(3):161–72.

[37] Rowe MI, Uribe FL. Diaphragmatic hernia in the newborn infant: blood gas and pH considerations. Surgery. 1971;70(5):758–61.

[38] Goetzman BW, Sunshine P, et al. Neonatal hypoxia and pulmonary vasospasm: response to tolazoline. J Pediatr. 1976;89(4):617–21.

[39] Kaapa P, Koivisto M, et al. Prostacyclin in the treatment of neonatal pulmonary hypertension. J Pediatr. 1985;107(6):951–3.

[40] Kinsella JP, Truog WE, et al. Randomized, multicenter trial of inhaled nitric oxide and high-frequency oscillatory ventilation in severe, persistent pulmonary hypertension of the newborn. J Pediatr. 1997;131(1 Pt 1):55–62.

[41] Inhaled nitric oxide and hypoxic respiratory failure in infants with congenital diaphragmatic hernia. The Neonatal Inhaled Nitric Oxide Study Group (NINOS). Pediatrics. 1997;99(6):838–45.

[42] Clark RH, Kueser TJ, et al. Low-dose nitric oxide therapy for persistent pulmonary hypertension of the newborn. Clinical Inhaled Nitric Oxide Research Group. N Engl J Med. 2000;342(7):469–74.

[43] Finer NN, Barrington KJ. Nitric oxide for respiratory failure in infants born at or near term. Cochrane Database Syst Rev. 2006;(4):CD000399.

[44] Olson E, Lusk LA, et al. Short-Term Treprostinil Use in Infants with Congenital Diaphragmatic Hernia following Repair. J Pediatr. 2015;167(3):762–4.

[45] Skarda DE, Yoder BA, et al. Epoprostenol Does Not Affect Mortality in Neonates with Congenital Diaphragmatic Hernia. Eur J Pediatr Surg. 2015;25(5):454–9.

[46] De Luca D, Zecca E, et al. Transient effect of epoprostenol and sildenafil combined with iNO for pulmonary hypertension in congenital diaphragmatic hernia. Paediatr Anaesth. 2006;16(5):597–8.

[47] Noori S, Friedlich P, et al. Cardiovascular effects of sildenafil in neonates and infants with congenital diaphragmatic hernia and pulmonary hypertension. Neonatology. 2007;91(2):92–100.

[48] Bialkowski A, Moenkemeyer F, et al. Intravenous sildenafil in the management of pulmonary hypertension associated with congenital diaphragmatic hernia. Eur J Pediatr Surg. 2015;25(2):171–6.

[49] Deprest J, Brady P, et al. Prenatal management of the fetus with isolated congenital diaphragmatic hernia in the era of the TOTAL trial. Semin Fetal Neonatal Med. 2014;19(6):338–48.

[50] Gupta A, Yadav C, et al. Chaos. J Obstet Gynaecol India. 2016;66(3):202–8.

[51] Hedrick MH, Estes JM, et al. Plug the lung until it grows (PLUG): a new method to treat congenital diaphragmatic hernia in utero. J Pediatr Surg. 1994;29(5):612–7.

[52] Harrison MR, Mychaliska GB, et al. Correction of congenital diaphragmatic hernia in utero IX: fetuses with poor prognosis (liver herniation and low lung-to-head ratio) can be saved by fetoscopic temporary tracheal occlusion. J Pediatr Surg. 1998;33(7):1017–22; discussion 1022–3.

[53] Flageole H, Evrard VA, et al. The plug-unplug sequence: an important step to achieve type II pneumocyte maturation in the fetal lamb model. J Pediatr Surg. 1998;33(2):299–303.

[54] Shan W, Wu Y, et al. Foetal endoscopic tracheal occlusion for severe congenital diaphragmatic hernia–a systemic review and meta-analysis of randomized controlled trials. J Pak Med Assoc. 2014;64(6):686–9.

[55] Ali K, Bendapudi P, et al. Congenital diaphragmatic hernia-influence of fetoscopic tracheal occlusion on outcomes and predictors of survival. Eur J Pediatr. 2016;175(8):1071–6.

[56] Al-Maary J, Eastwood MP, et al. Fetal Tracheal Occlusion for Severe Pulmonary Hypoplasia in Isolated Congenital Diaphragmatic Hernia: A Systematic Review and Meta-analysis of Survival. Ann Surg. 2016;264(6):929–933.

[57] Sluiter I, van der Horst I, et al. Premature differentiation of vascular smooth muscle cells in human congenital diaphragmatic hernia. Exp Mol Pathol. 2013;94(1):195–202.

[58] Luong C, Rey-Perra J, et al. Antenatal sildenafil treatment attenuates pulmonary hypertension in experimental congenital diaphragmatic hernia. Circulation. 2011;123(19):2120–31.

[59] Kattan J, Cespedes C, et al. Sildenafil stimulates and dexamethasone inhibits pulmonary vascular development in congenital diaphragmatic hernia rat lungs. Neonatology. 2014;106(1):74–80.

[60] Lemus-Varela Mde L, Soliz A, et al. Antenatal use of bosentan and/or sildenafil attenuates pulmonary features in rats with congenital diaphragmatic hernia. World J Pediatr. 2014;10(4):354–9.

[61] Makanga M, Maruyama H, et al. Prevention of pulmonary hypoplasia and pulmonary vascular remodeling by antenatal simvastatin treatment in nitrofen-induced congenital diaphragmatic hernia. Am J Physiol Lung Cell Mol Physiol. 2015;308(7):L672–82.

[62] Russo FM, Toelen J, et al. Transplacental sildenafil rescues lung abnormalities in the rabbit model of diaphragmatic hernia. Thorax. 2016;.

[63] Greer JJ, Allan DW, et al. Recent advances in understanding the pathogenesis of nitrofen-induced congenital diaphragmatic hernia. Pediatr Pulmonol. 2000;29(5):394–9.

[64] Thebaud B, Tibboel D, et al. Vitamin A decreases the incidence and severity of nitrofen-induced congenital diaphragmatic hernia in rats. Am J Physiol. 1999;277(2 Pt 1):L423–9.

[65] Major D, Cadenas M, et al. Retinol status of newborn infants with congenital diaphragmatic hernia. Pediatr Surg Int. 1998;13(8):547–9.

[66] Coste K, Beurskens LW, et al. Metabolic disturbances of the vitamin A pathway in human diaphragmatic hernia. Am J Physiol Lung Cell Mol Physiol. 2015;308(2):L147–57.

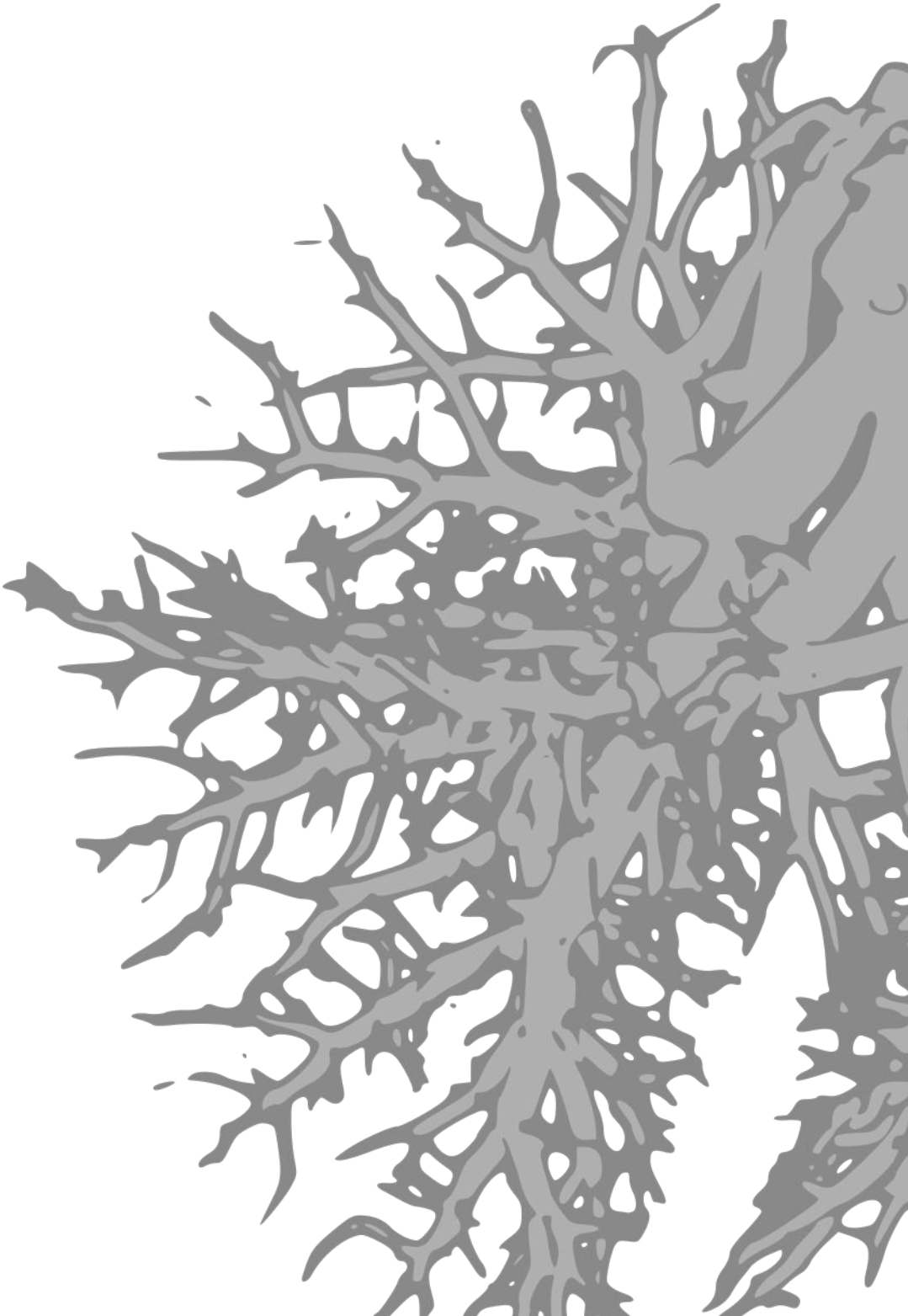

Chapter 2

Pulmonary vascular development goes awry in congenital lung abnormalities

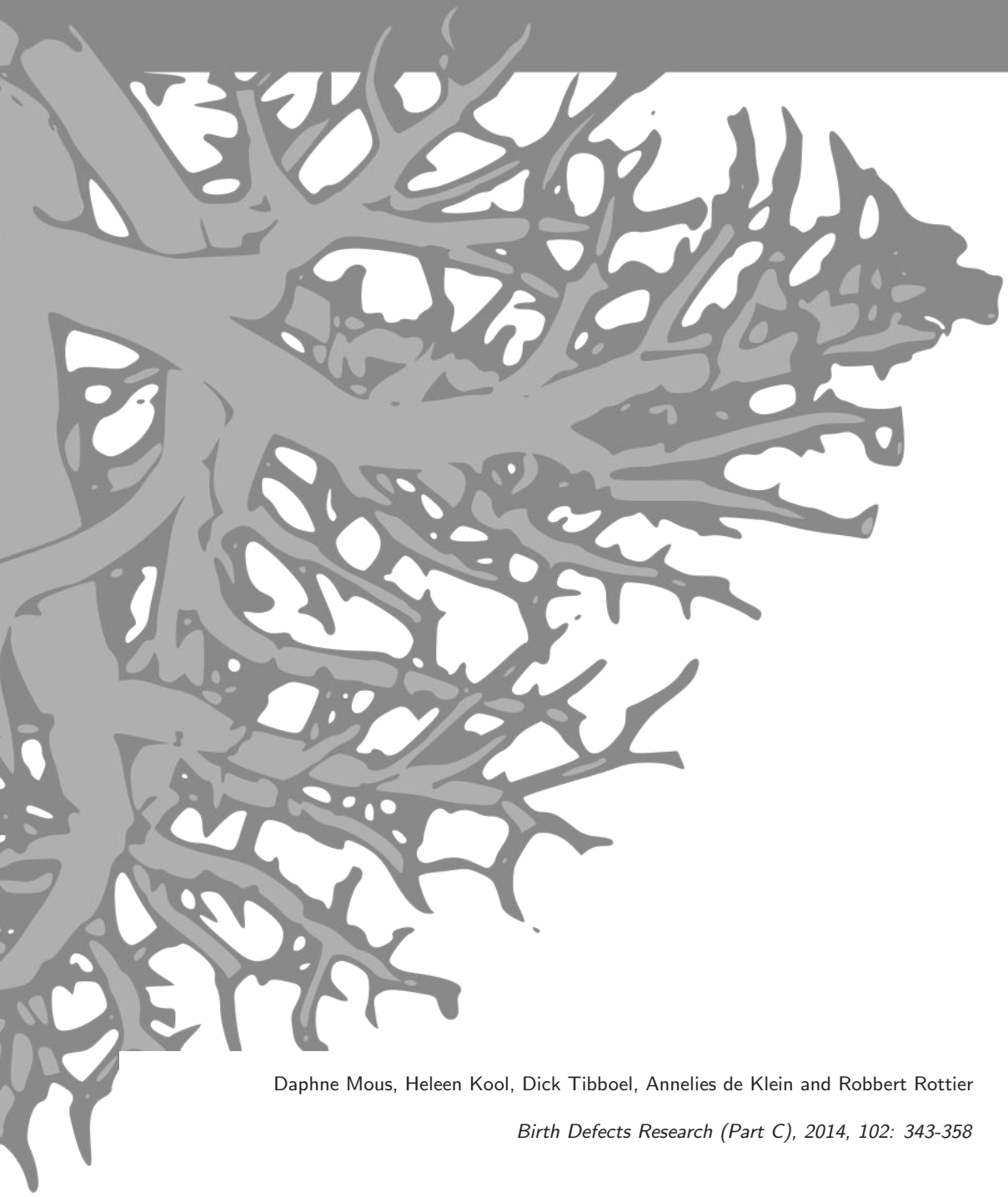

Daphne Mous, Heleen Kool, Dick Tibboel, Annelies de Klein and Robbert Rottier

Birth Defects Research (Part C), 2014, 102: 343-358

Abstract

Pulmonary vascular diseases of the newborn comprise a wide range of pathological conditions with developmental abnormalities in the pulmonary vasculature. Clinically, pulmonary arterial hypertension (PH) is characterized by persistent increased resistance of the vasculature and abnormal vascular response. The classification of PH is primarily based on clinical parameters instead of morphology and distinguishes five groups of PH. Congenital lung anomalies such as alveolar capillary dysplasia (ACD) and PH associated with congenital diaphragmatic hernia (CDH), but also bronchopulmonary dysplasia (BPD), are classified in group three.

Clearly, tight and correct regulation of pulmonary vascular development is crucial for normal lung development. Human and animal model systems have increased our knowledge and make it possible to identify and characterize affected pathways and study pivotal genes. Understanding of the normal development of the pulmonary vasculature will give new insights in the origin of the spectrum of rare diseases such as CDH, ACD and BPD, which render a significant clinical problem in neonatal intensive care units around the world.

In this review we will describe the normal pulmonary vascular development and we will focus on four diseases of the newborn in which abnormal pulmonary vascular development play a critical role in the morbidity and mortality. In the future perspective we indicate the lines of research that seems to be very promising for elucidating the molecular pathways involved in the origin of congenital pulmonary vascular disease.

The morphological development of pulmonary vasculature

In mammals, blood is transported through the cardiovascular system that can be divided in the systemic and the pulmonary circulation. These two types of circulations have histological similarities but differ in their physiological function and anatomic position to the heart. Oxygenated blood is transported and distributed throughout the body by the systemic circulation, whereas oxygen-depleted blood is transported to the lungs by the pulmonary circulation. The blood supply in the lung can be divided into the bronchial circulation and the pulmonary circulation. The bronchial circulation is mainly separated from the pulmonary circulation, although some overlap exists in the pre-capillary region. The bronchial circulation comprises arteries, which align with the bronchial tree. A third of the blood in the bronchial circulation returns to the right atrium through the bronchial vein. The pulmonary circulation transports oxygen-deprived blood to the gas exchange areas and oxygen-rich blood back to the left atrium. The bronchial circulation is part of the systemic circulation and delivers oxygen-rich blood to the cells of the lung at high systemic pressure.

The pulmonary vasculature comprises anatomically and functionally different compartments: the arterial tree, the capillary bed and the venular tree. The pulmonary arteries also support the intrapulmonary structure and ultimately regulate gas exchange via the capillary bed. Prenatally, the pulmonary circulation is characterized by high pulmonary vascular resistance (PVR) and low blood flow (compared to the ventricular output). The thick wall and high vasomotor tone contribute to the high PVR. The majority of the blood flow of the cardiac output is diverted to other organs than the lung through the foramen ovale and the ductus arteriosus. This process is facilitated by the relative high resistance in the pulmonary circulation compared to the systemic circulation. After birth, there is a large transition from relative hypoxic conditions to normoxic condition. This transition induces dramatic changes in the PVR leading to physiological adaptations in the lung. This adaption of the lung is required to exert its important function: exchange gas and oxygenate the blood.

The cellular composition of the pulmonary vascular wall varies depending on the functionality of the vessel. The outer layer of the pulmonary arteries, the adventitia, is a loosely organized structure consisting of an extracellular matrix with fibroblasts, vasa vasorum and a neuronal network [1, 2]. There is gradual change in structure from the proximal to distal end of the lung, which corresponds with the maturation of the developing airways. The large pulmonary arteries at the proximal end of the lung have a media consisting of a layer of smooth muscle cells in between the lamina elastic interna and externa. Towards the distal area of the lung, the arteries have a smaller lumen with a thinner smooth muscle cell layer and no lamina elastica. The smooth muscle cells in the tunica media form a heterogeneous population, ranging from cuboidal, synthetic cells to the characteristic elongated contractile cells. The contractile smooth muscle cells have more contractile fibers, have less proliferation and less migration activity compared to the synthetic phenotype [3, 4]. The pulmonary capillaries are the most distal compartment of the pulmonary vasculature and are the site where gas exchange takes place. Capillaries exist of a monolayer of endothelial cells, which are in direct contact with perivascular cells. The structure of the pulmonary veins is comparable to the structure of small arteries. Pulmonary veins consist of a thin intima, smooth muscle cell containing media in the larger veins and an adventitia containing a vaso vasorum, nerves and bundles of collagen and elastin fibers [2].

The development of the pulmonary vasculature

Understanding the process of normal pulmonary vascular development is a prerequisite to comprehend the origin of pulmonary hypertension (PH) and its associated diseases of the

Table 2.1: Overview of Stages in Lung Development in Mouse and Human

Stage	I Embryonic	II Pseudoglandular	III Canalicular	IV Saccular	V Alveolar
Mouse	E9–11.5	E11.5–16.5	E16.5–17.5	E17.5–PN5	PN5–30
Human	Wk 3–7	Wk 5–17	Wk 16–26	Wk 26–36	Wk 36–3 years

newborn. The pulmonary vasculature develops in close relation with the airways and has extensively been studied in rodent models. In mice, the first molecular sign of lung development is around embryonic day 8 (E8) when the expression of Nkx2-1 starts in the ventral wall of the anterior foregut (see table 2.1 for lung developmental stages of human and mouse). At E9.5 in the mouse, a primitive bud evaginates from the ventral side of the foregut and invades the surrounding mesenchyme [5]. This bud splits into two buds, which will form the right and left lung, but this embryonic phase is very short and rapidly turns into the pseudoglandular phase when the primary buds expand into the mesenchyme and start budding and branching until E16.5. After E16.5, when the bronchial tree is formed, development of the lung goes into a new stage, the canalicular phase. In mice it is very short (E16.5-E17.5) and during this period the terminal buds narrow. From E17.5 until postnatal day 5 (P5) lung development goes into the saccular stage and the precursors of the alveoli are formed. And finally from postnatal life onwards alveolarization starts and ends around P14. In humans, lung development follows a similar sequence of stages, but with a different timetable. Budding starts at 4 weeks of gestation, the pseudoglandular stage ends around week 6, followed by the canalicular (week 16-26), saccular (week 26-36) and alveolarisation (postnatal until 3 years of age) stages (Table 2.1).

The lung endoderm and mesoderm are interacting during all these developmental stages via multiple molecular pathways. These molecular pathways controlling these stages have been discussed in extensively in two recent reviews [6, 5]. In this review we focus on congenital diseases associated with pulmonary abnormalities and only describe the molecular players that have been associated with these diseases.

The past two decades new insights into the development of the pulmonary vasculature have been obtained. It was suggested that pulmonary vasculature in mice developed through two main mechanisms: the central vasculature through angiogenesis and the distal vasculature through vasculogenesis and either angioblasts from the mesenchyme or blood lakes would provide endothelial cells for vessel development [7]. These two structures would fuse around E13/E14 through a lytic process and circulation would start [8]. A histological and morphological study seemed to confirm this hypothesis and the same processes would underlie pulmonary vascular development in human [9]. The results from these studies were mainly obtained by histological analysis. However, fixation artifacts have led to inappropriate conclusion and analysis of lung development using transgenic mice expressing a lacZ reporter gene under the control of an early marker for endothelial cells (fetal liver kinase 1 (FLK1)) [10], showed that the proximal and distal pulmonary vasculature was already connected at E10.5 [11]. In addition, detailed analysis of lung samples of transgenic mice expressing the lacZ reporter under the control of the endothelium specific Tie2 promoter showed that already at day E9.5 the presence of a vascular network surrounded the primitive lung bud connected to the systemic circulation. This network mainly expands as the lung develops through angiogenesis, a process called distal angiogenesis [12]. It is still not completely understood how the pulmonary vasculature develops and where progenitor cells involved in angiogenesis in the lung come from. Lineage trace experiments, instrumental in deciphering the origin and the fate of early precursor cells in the lung, indicate that specific, cardiopulmonary, progenitor cells differentiate into both cardiac and pulmonary

mesenchymal cells. Moreover, these progenitor cells can differentiate into vascular smooth muscle cells and pericyte-like cells, but were only observed in the proximal end of the lung [13]. It remains unclear what the progenitors are for the perivascular cells and endothelial cells in the distal end of the lung. Proper lineage trace studies throughout pulmonary vascular development could serve to answer these questions.

Important molecular players in pulmonary vascular development

Normal pulmonary vascular development requires tight regulation of cell migration, proliferation and differentiation. The family of Vascular endothelial growth factors (VEGF), and their receptors Fetal liver kinase1 (KDL1 or VEGFr1) and Kinase domain receptor (Kdr or VEGFr2), are one of the most potent angiogenic factor signaling cascades and are required for vascular growth and endothelial cell proliferation [14, 15]. Early during lung development, VEGF is expressed by the epithelium and mesenchyme, but later its expression is restricted to the epithelium [16] where it is required for epithelial branching and morphogenesis [17]. In response to hypoxic conditions, as in the prenatal lung, VEGF expression is induced by Hypoxia-inducible transcription factor-1 and 2 (HIF1/HIF2). HIF1 and HIF2 are heterodimers existing of an oxygen-sensitive subunit, HIF1α or HIF2α, and a constitutive Arnt/HIF1β subunit. At normoxic conditions, specific prolyl hydroxylases (Phd) hydroxylate the HIFα subunit, which is subsequently ubiquitinated and targeted for degradation via the Von-Hippel-Lindau tumour suppressor protein pathway [18–20]. Under hypoxic conditions, the HIFα subunit is not hydroxylated and the HIFα/HIFβ complex translocates to the nucleus where it binds to hypoxic responsive elements in the regulatory unit of target genes to induce the transcription of these genes. Among the genes that are activated under hypoxic conditions are several angiogenic genes, such as VEGF, which results in the growth and expansion of the vasculature.

Vascular development consists of vasculogenesis and angiogenesis: vasculogenesis is the process where the vascular plexus is formed de novo from mesodermal progenitor cells [21], and angiogenesis is the process where endothelial cells sprout from preexisting vessels to form new tubes. There is constant competition between the leading cell, the tip cell, and the trailing cell, the stalk cell, to become or to stay on the tip of the sprout. Endothelial cells of the newly formed tubes recruit pericytes in a Platelet-derived growth factorβ (PDGFβ) depended manner (Figure 2.1). Pericytes wrap around the newly formed endothelial tubes and induce stabilization and maturation [22, 23] and the interaction between these two cells is crucial for normal vascular development. This interaction is regulated by different growth factors and their receptors, such as PDGF(r) and TGFβ(r) [24]. Tight regulation of this interaction is required for normal vascular development and disruption of this process may lead to pathological conditions. However, pericytes comprise a very heterogenic population in the lung and therefore they are rather difficult to identify. New, specific markers are required to better understand the interaction of pericytes and endothelial cells in both health and disease.

The specification of arteries and veins is one of the first events that take place in the development of the circulatory system. Arteries and veins can be distinguished from each other by the expression of members of a tyrosine kinase family Ephrin2 and Eph4 [25]. However, the specification of the pulmonary network occurs relatively late and the expression of Ephrin2 and Eph4 is not restricted to artery endothelial or vein endothelial cells, respectively until late in the pseudoglandular stage (Figure 2.1). In mice, at E13.5 endothelial cells still express both Ephrin2 and Eph4, but from E15.5 onwards the endothelial cells express either Ephrin2 or Eph4 when they become committed to arteries or veins, respectively. Furthermore, Ephrin expression in the lung is not restricted to endothelial cells but is also highly expressed by mural cells [26]. Modulation of the Notch pathway results in arterial defects and can lead, depending on

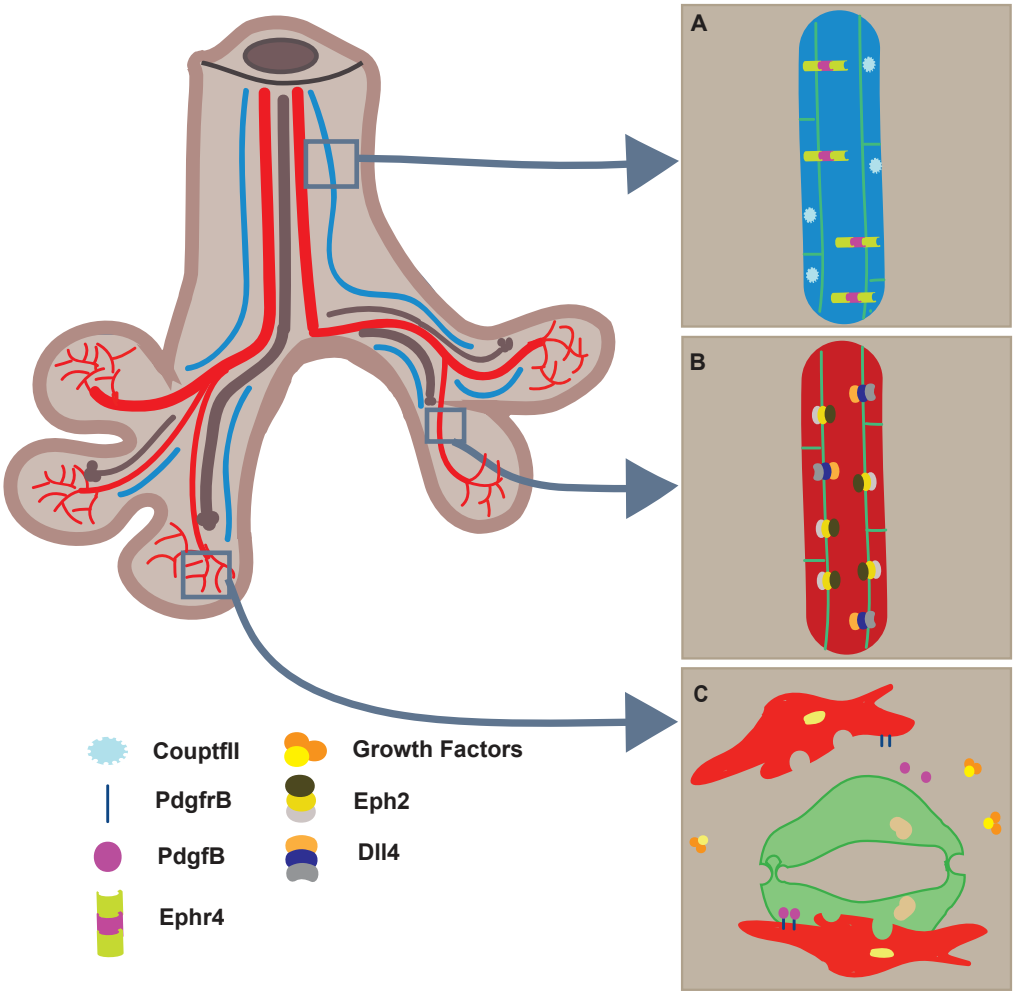

Figure 2.1: Simplified scheme of pulmonary vascular compartments. Schematic overview of pulmonary vasculature, with veins (**A**), arteries (**B**), and capillaries (**C**). Endothelial cells recruit pericytes in a PDGFβ dependent manner in the distal end of the lung (**C**). The pulmonary arteries are characterized by the expression of Eph2 and Notch family member Dll4 (**A**). Specification of the pulmonary veins includes expression of Ephrin4 and CouptfII (**B**).

which member of the pathway is affected, to early prenatal death. For example, heterozygous *Dll4* embryos suffer from remodeling defects in the yolk sac and have a smaller dorsal aorta [27] while the full *Dll4*-deficient embryos die due to early lethal loss of arterial identity at E9.5 [28]. To study the lung developmental phenotype, tissue specific inhibition of the Notch pathway is necessary and may give new insights in the specification of pulmonary arteries and veins. Specification of venous endothelium includes expression of the nuclear receptor Chicken ovalbumin upstream transcription factor II (CouptfII), which is expressed in venous and lymphatic endothelium (Figure 2.1). CouptfII is highly expressed in the foregut mesenchyme at the site where later in development the lung will be formed. CouptfII knock-out mice die at E10 from heart defects and loss of venous identity in the vasculature [29]. Lung-specific deficient CouptfII mice show a Bochdalek-type congenital diaphragmatic hernia (CDH) [30], lung hypoplasia associated with CDH indicates the importance of CouptfII in normal lung development.

Fibroblast growth factors (FGF) belong to a family of mitogens that are identified as regulators of lung development [31]. Early during lung development FGF10 is expressed in the mesoderm around the budding lung endoderm, which expresses its receptor FGFr2. Knockout mice of FGF10 [32] or FGFr2 [33] resulted in mice without lungs, indicating the crucial role for this signaling pathway in the development of the lung [34]. However, recently it was shown that FGF10 is not just inducing budding and branching of the lung during development, but that expression of FGF10 is also important for the maintenance of epithelial progenitor cells by preventing these cells to differentiate [35]. Another member of the fibroblast growth family, FGF9, is important for lung mesenchyme growth and proliferation [36]. More specific, FGF9 stimulates proliferation of mesenchymal cells and regulates mesenchymal Sonic hedgehog signaling (SHH) [37]. Furthermore, it is also shown that FGF9 and SHH regulate VEGFa expression what is required for capillary development in the distal end of the lung [17].

Retinoic acid (RA) signaling has been shown to be of high importance for lung development [38]. Vitamin A in the blood plasma is transported by Retinol binding protein 4 (RBP4), it binds to the extracellular receptor stimulated by retinoic acid 6 (STRA6) and then through several enzymatic reactions it is converted into its active form RA. Active RA is secreted and taken up by retinoic acid responsive cells. In the cytoplasm RA binds to one of the three Retinoic Acid Receptors (RAR), RARα, RARβ or RARγ [39]. These complexes bind to a Retinoic Acid active Responsive Element (RARE) in the regulatory elements of their target genes and modulate transcription of these genes [40, 41]. Targeted deletions of members of RAR and Rxr family have different effects. Double knockouts of RARα and RARβ result in failure to separate the esophagus and trachea and hypoplasia of the left and right lung. However, deletion of other members of the RAR and RXR family did not result in an obvious lung phenotype [42]. Binding of retinoic acid to its receptor directly affects the target genes either by inducing or repressing gene expression. Many genes regulated by the RA pathway are involved in embryogenesis [39]. However, it is possible that still many target genes have yet to be discovered. Tracing the activity of RARE's in embryonic development revealed high activity of the RA pathway in multiple developing organs, for example in heart, hindbrain and diaphragm [43, 44]. Activity of the retinoic acid receptors is important for proper lung development and at E9 in mice, when the first lung buds start to develop from the foregut, RA signaling is highly active [38]. Furthermore, in absence of retinoic acid, levels of FGF10 decrease and levels of TGFβ increase, and there is reduced budding and branching of the lung [45]. More specific, molecular processes required for formation of the lung primordium from the foregut are controlled by RA receptor activity. RA is a major regulator of Wnt signaling and the TGFβ pathway and thereby controls FGF10 expression, early in lung development [46]. The role of RA signaling in vascular development has so far only been shown in the development of the systemic blood circulation. In RA-deficient embryos endothelial cell growth and proliferation is uncontrolled, indicating a role for RA in suppression of endothelial cells

during vasculogenesis [47]. Although there is no direct evidence yet that the RA pathway is involved in the development of the pulmonary vasculature, it may be that this pathway is involved based on the intimate relation between the airways and the vasculature.

Abnormal pulmonary vascular development

Perturbations of the described molecular pathways in the pulmonary vascular development may cause congenital anomalies, like PH, in newborns, infants and children [48]. PH is characterized by persistent increased resistance of the vasculature and abnormal vascular tone, which is regulated by the contraction of smooth muscle cells. Five groups of PH can be distinguished: pulmonary arterial hypertension, PH due to left heart disease, PH due to lung diseases and/or hypoxia, chronic thromboembolic PH (CTEPH) and PH with unclear multifactorial mechanisms [49, 50] (Table 2.2). Normally the PVR is high antenatally and decreases immediately after birth, reaching levels that are comparable to adult values within 2 months after birth. PH has an incidence of approximately 63.7 per million children [51] and can be idiopathic or associated with other diseases. It can cause significant morbidity and mortality. In children, idiopathic pulmonary arterial hypertension (iPAH) and PH due to congenital heart disease comprise the majority of cases. Other important causes include persistent PH of the newborn (PPHN), bronchopulmonary dysplasia (BPD) and developmental lung diseases, like CDH, alveolar capillary dysplasia (ACD) and lung hypoplasia and surfactant protein abnormalities [48, 49]. Mutations in specific genes have been reported (Table 2.3), but PH in children can also be associated with genetic syndromes, like Down syndrome, DiGeorge syndrome, VACTERL syndrome, CHARGE syndrome and Noonan syndrome [52]. Perinatal care and prognosis in pediatric PH has improved over the last years, but despite the fact that there are significant differences in pulmonary vascularity between adults and children, most treatment is based on experimental research or trials in adults [53]. We will focus on iPAH, CDH, ACD and BPD which are all characterized by an abnormal pulmonary vascular development and in which PH plays an important role in the mortality and morbidity.

Idiopathic pulmonary arterial hypertension

iPAH is characterized by restricted blood flow through the pulmonary arterial circulation, elevated pulmonary vascular resistance and progressive right heart failure [66]. iPAH, previously known as primary PH, has an incidence of approximately 0.7 per million [49] with hypertensive vasculopathy exclusively in the pulmonary circulation without a demonstrable cause. Young children have a reduction in arterial number and a failure of the vasculature to relax, whereas in older children intimal hyperplasia, occlusive changes and plexiform lesions are found (Figure 2.2). In contrast to adults, children with iPAH have more pulmonary vascular medial hypertrophy and less intimal fibrosis and fewer plexiform lesions [67, 68]. Younger children have a more reactive pulmonary vascular bed with an increased prevalence of acute pulmonary hypertensive crises [69, 68]. Possible mechanisms that play a role in PAH development are endothelial cell dysfunction, smooth muscle cell migration and dysfunction, and abnormal apoptosis. In adult iPAH, in-vitro studies showed increased expression of endogenous vasoconstrictors and decreased expression of vasodilators [70–73]. The same vasoactive factors could play a role in pediatric iPAH. An increased expression of thromboxane and endothelin-1 (ET-1), both vasoconstrictive and proliferative mediators, are elevated in both adults and children [69, 74, 75]. However, besides these two factors, this might also be the case for other vasoactive factors.

Heritable forms of PH are caused by mutations in several genes. Point mutations and deletions in the bone morphogenetic protein receptor 2 (*BMPR2*) have been identified in approximately 10-40% of all patients with iPAH and are the major cause of heritable PAH [76]. Both pediatric and adult patients with *BMPR2* mutations appeared to have more severe disease compared to

Table 2.2: Classification of pulmonary hypertension

Pulmonary arterial hypertension
Idiopathic PAH (iPAH)
Heritable PAH
BMPR2
ALK-1, ENG, SMAD9, CAV1, KCNK3
Unknown
Drug- and toxin-induced
Associated with other diseases
Connective tissue disease
HIV infection
Portal hypertension
Congenital heart diseases
Schistosomiasis
Pulmonary veno-occlusive disease and/or pulmonary capillary hemangiomatosis
Persistent pulmonary hypertension of the newborn (PPHN)
Pulmonary hypertension due to left heart disease
Left ventricular systolic dysfunction
Left ventricular diastolic dysfunction
Valvular disease
Congenital/acquired left heart inflow/outflow tract obstruction and congenital cardiomyopathies
Pulmonary hypertension due to lung diseases and/or hypoxia
Chronic obstructive pulmonary disease (COPD)
Interstitial lung disease
Other pulmonary diseases with mixed restrictive and obstructive pattern
Sleep-disordered breathing
Alveolar hypoventilation disorders
Chronic exposure to high altitude
Developmental lung diseases
Congenital diaphragmatic hernia (CDH)
Bronchopulmonary dysplasia (BPD)
Alveolar capillary disease (ACD)
Lung hypoplasia
Surfactant protein abnormalities
Pulmonary interstitial glycogenosis
Pulmonary alveolar proteinosis
Pulmonary lymphangiectasia
Chronic thromboembolic pulmonary hypertension (CTEPH)
Pulmonary hypertension with unclear multifactorial mechanisms
Hematologic disorders: chronic hemolytic anemia, myeloproliferative disorders, splenectomy
Systemic disorders: sarcoidosis, pulmonary histiocytosis, lymphangioleiomyomatosis
Metabolic disorders: glycogen storage disease, Gaucher disease, thyroid disorders
Others: tumoral obstruction, fibrosing mediastinitis, chronic renal failure, segmental PH

Adapted from the updated Dana point classification [50]

Table 2.3: Genes involved in pulmonary hypertension in children

Disease	Gene	Chromosome	Reference
iPAH	BMPR2	2q33	[54–56]
	ACVRL1	12q13	[55, 56]
	ENG	9q34.11	[55]
	5HTT	17q11.2	[57]
	BMPR1B	4q22.3	[58]
CDH	FOG2	8q22.3–23.1	[59]
	COUP-TFII	15q26.1–26.2	[60]
	STRA6	15q23–25.1	[61]
	FREM1	9p22.3	[62]
	WT1	11p12–15.1	[63]
ACD	FOXF1	16q24.1	[64, 65]

iPAH = idiopathic pulmonary arterial hypertension, CDH = congenital diaphragmatic hernia, ACD = alveolar capillary dysplasia

those without this mutation [69]. Pfarr et al. found mutations in *BMPR2* and two receptors of the TGFβ/BMP pathway, activin receptor-like kinase 1 (*ACVRL1*) and endoglin (*ENG*), in 8/29 (27.6%) of the pediatric iPAH patients [55]. A genetic polymorphism detected in the serotonin 5-hydroxy tryptamine transporter (*5HTT*) gene is associated with iPAH in adults and might also play a role in iPAH in children. This polymorphism leads to elevated levels of 5HT and results in increased smooth muscle cell proliferation [57]. Most of the genetic mutations in iPAH are only studied in adults and in contrast to adults, PAH in children is often associated with genetic syndromes. However, not all patients with a mutation in the same gene will develop severe PAH, suggesting that modifiers and or epigenetic regulation of expression could also play a role.

Congenital diaphragmatic hernia

Congenital diaphragmatic hernia (CDH) has an incidence of approximately 1 in 2500-3000 live births. Beside a diaphragmatic defect, CDH is characterized by pulmonary hypoplasia and PH, which may be due to an altered development of the pulmonary vasculature and a disordered process of pulmonary vascular remodeling [77, 78]. Previous studies showed excessive muscularization of the pulmonary arteries and maladaptive pulmonary vascular remodeling in CDH patients [79, 77, 78, 4, 80] (Figure 2.2). In contrast to the positive effect of inhaled nitric oxide (iNO) in preterms with PH, the effectiveness of this treatment is only around 30-40% of patients with CDH.

Over the last years several factors involved in the abnormal pulmonary vascular development in CDH have been identified. Expression levels of these factors have been analyzed both in lung tissue of CDH patients and experimental animal models. We studied the role of the Von Hippel-Lindau protein (pVHL) and HIF1α and found a decrease of pVHL and HIF1α expression in the arterial endothelium and an elevated expression of pVHL in the pulmonary arterial media of human CDH cases compared to age-matched controls [81]. Shehata et al. showed increased VEGF expression in the bronchial epithelium and medial smooth muscle cells and positive VEGF staining in endothelial cells, which were negative in age-matched controls [82]. However, we have found lower expression of VEGF mRNA in the alveolar stage in CDH patients [83]. In the process of normal remodeling of the pulmonary vasculature, extracellular matrix membrane proteins (MMPs) are of fundamental importance. Altered expression of certain MMPs and

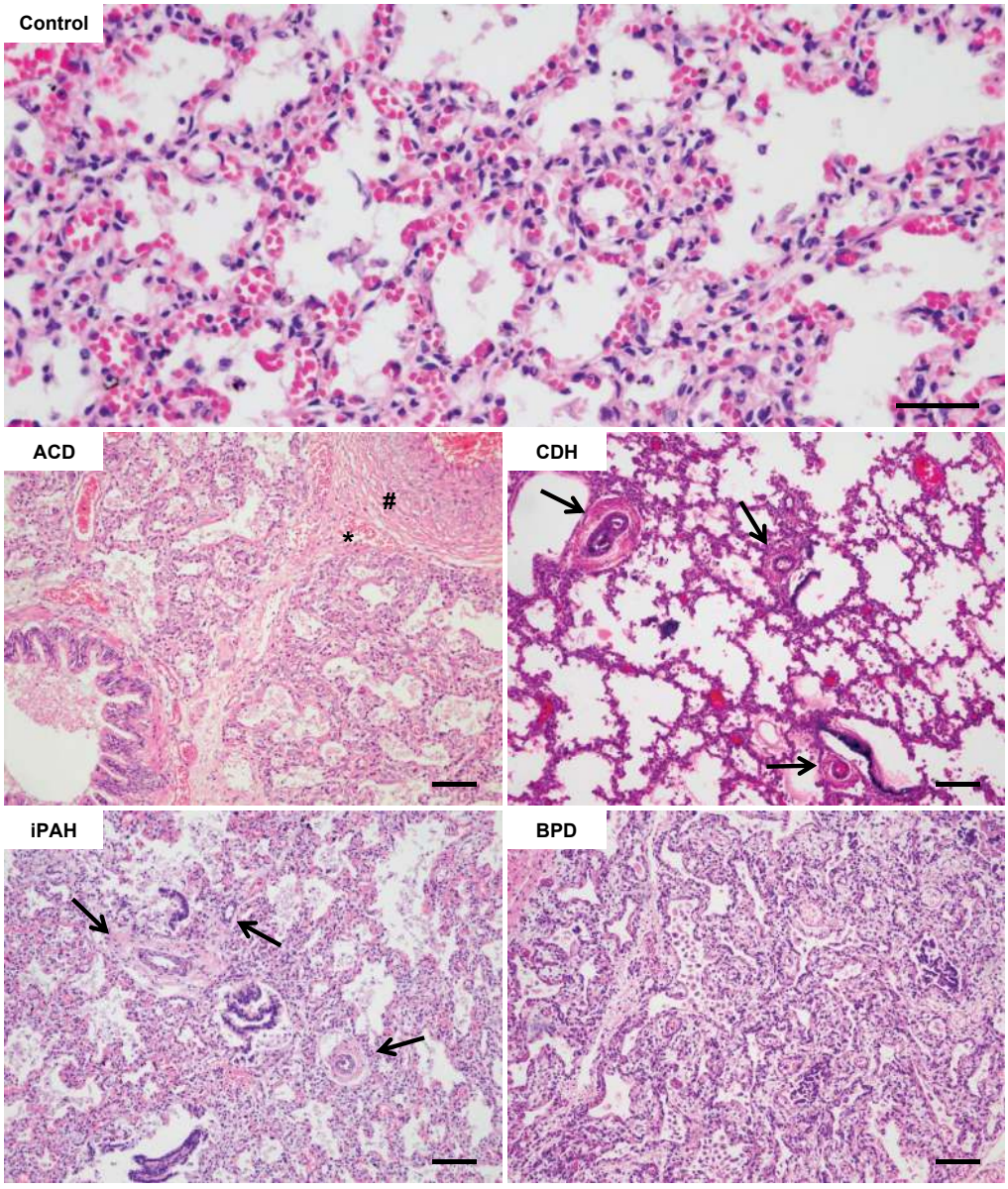

Figure 2.2: Characteristic histology of four pulmonary vascular disease samples. Hematoxylin- and eosin-staining of human lungs: control, alveolar capillary dysplasia (ACD), congenital diaphragmatic hernia (CDH), idiopathic pulmonary arterial hypertension (iPAH) and bronchopulmonary dysplasia (BPD). Scale bars 100 mm. ACD: medial hypertrophy and muscularization (#), malpositioning of the pulmonary veins (*) and central positioning of the capillaries in the alveolar septa, CDH: excessive muscularization of the arteries (arrows), iPAH: thickening of the arteries (arrows), BPD: fibrosis with widening of the alveolar septa.

tissue inhibitors of MMPs (TIMPs) was found in human CDH lungs compared to controls [84]. Decreased expression of VEGF and its receptors is also seen in the nitrofen rat model of CDH [85, 86]. In summary, an increase in pVHL may downregulate HIFα, leading to decreased expression of VEGF and a disturbance of vascular growth and endothelial cell proliferation during development. It would be interesting to investigate the oxygen concentration during the development of the (CDH) lung, to evaluate whether this may contribute, through HIFα, to the structural changes that contribute to PH.

Abnormal RA signaling contributes to the etiology of CDH, and the first evidence of its involvement in CDH came from observations of pups born to rat dams with vitamin A deficient diets. In 25-40% of these pups a diaphragmatic hernia was present [87]. This finding is supported by the development of a diaphragmatic defect, pulmonary hypoplasia and pulmonary vascular abnormalities after disruption of the retinoid signaling pathway by nitrofen [88]. Furthermore, RAR α/β double knock-out mice were found to have offspring with a diaphragmatic hernia [89]. In addition to the animal models, measurements of the levels of retinol and retinol-binding protein (RBP) in the first hours after birth in human CDH newborns showed a significant reduction compared to matched controls, independent of maternal retinol status [90, 91]. As described above, Chen et al. showed that lower levels of RA could cause an increase in TGFβ and a decrease in FGF10 [45]. Increased expression of TGFβ1 with immunostaining at the midpseudoglandular, late pseudoglandular and saccular stage of lung development is detected in the nitrofen rat model of CDH [92]. Also increased mRNA levels of TGFβ and TGFβRII are observed in the same model [93]. Teramoto et al. described a decrease in gene expression of FGF10 in the nitrofen rat model [94]. Since TGFβ plays a role in the airway branching and muscularization of the pulmonary vasculature and FGF10 was thought to regulate lung budding and branching, this might implicate that the neomuscularization and reduced branching in CDH may be caused by disturbances in the RA-TGFβ-FGF10 interactions.

Over 450 chromosomal aberrations have been reported in CDH [95]. Some of the recurrent genetic changes are found in retinoid-related genes. In autosomal recessive conditions as Matthew-Wood syndrome (Microophthalmia syndromic 9 (MCOPS9) or Donnai-Barrow syndrome; OMIM #222448 mutations in the *STRA6* and *LRP2* genes have been reported. STRA6 is the membrane receptor for retinol binding protein (RBP1) and mutations of the LRP2 gene lead to proteinuria with spillage of retinol-binding proteins. Deletions of *COUP-TFII* on chromosome 15q26.1-26.2 [60], and of *FOG2* (ZFPM2; chromosome 8q23.1) or SOX7 (8p23.1) lead to an autosomal dominant form of CDH with variable penetrance [96, 97]. Beck et al. showed that a deletion of the FRAS1-related extracellular matrix 1 (*FREM1*) gene, which encodes an extracellular matrix protein, can cause CDH in both human and mice [62].

Several CDH animal models have been developed, such as the surgical models in lambs and rabbits, several knockout models in mice and teratogenic models in rats [88, 98]. Surgical animal models are useful for the investigation of interventional therapies, but are less informative in studying the etiology and pathogenesis of CDH [98]. The nitrofen model is the most commonly used teratogenic model for CDH. When administered to pregnant rat dams at gestational day 9.5, the herbicide nitrofen (2,4-dichlorophenyl-*p*-nitrophenyl ether) causes diaphragmatic defects, lung hypoplasia and PH in pups, strikingly similar to the human condition [99, 98].

Alveolar capillary dysplasia

Alveolar capillary dysplasia (ACD) is a rare lethal developmental lung disorder with failure of alveolar capillary formation, often accompanied by misalignment of the pulmonary veins. This results in abnormal gas exchange, severe hypoxemia and PH. The prevalence and incidence is not known, but the mortality rate approaches 100%. ACD is characterized by premature growth arrest with immature lobular development, reduced capillary density, thickened alveolar septa, medial hypertrophy and muscularization of small pulmonary arteries and distal arterioles

and malposition of pulmonary veins (Figure 2.2). In 50-80% of patients, ACD is associated with other congenital anomalies. Although at the moment a definitive diagnose can only be obtained by histological examination of lung tissue [100], the detection of genetic changes of the Forkhead Box F1(*FOXF1*) locus on chromosome 16q24 can aid in the diagnosis of ACD.

Mutations of *FOXF1* and deletions of the 5' regulatory region of this transcription factor gene have been reported in most patients with ACD [65, 64]. FOXF1 deficiency is associated with reduced numbers of pulmonary capillaries in patients with ACD and similar observations have been made studying Foxf1 heterozygous knockout mice. Conditional deficient Foxf1 mouse models showed that loss of Foxf1 in the endothelial lineages resulted in an impaired angiogenesis, endothelial proliferation and VEGF signaling [101]. Involvement of the FOXF1 protein in SHH signaling has been shown both in vitro and in vivo in human and mice [100, 101, 65]. Mahlapuu et al. showed that SHH induces the transcriptional activation of Foxf1 [102]. This may imply that other genes from this pathway are involved in the etiology of ACD. In addition to the large phenotypic overlap between human ACD and the mouse Foxf1-mutant mice, overlapping expression profiles of lung specimens indicate that the Foxf1 mouse model is an excellent animal model for ACD.

In addition to the Foxf1 ACD mouse model other knock-out models show similarities to ACD and may potentially be used to study ACD. For example, the pulmonary phenotype and associated congenital defects observed in endothelial nitric oxide synthase (eNOS)-deficient mice are strikingly similar to the pathological features seen in ACD [103]. NO plays a role in the downstream signaling of angiogenic factors and the regulation of angiogenic gene expression in the developing lung. Furthermore, mice lacking the phosphatase and tensin homologue deleted from chromosome 10 (Pten) showed defects in the pulmonary microvasculature similar to those seen in ACD. Pten inactivation caused increased expression of FGF9, FGF10 and FGF7 and decreased expression of SHH, PTCH1 and GLI1. They also found a decreased expression of FOXF1 in these mice [104], which might indicate a role for Pten in the regulation of FOXF1.

As described above, FGF9 signaling, SHH signaling and VEGFa expression in lung mesenchyme are required for the pulmonary capillary formation. In an in vitro study in mice it was observed that FGF9 and SHH regulate each other and the expression of angiogenic factors such as VEGFa [17]. FGF9 and SHH might play a possible role in the development of ACD.

It is important to improve our knowledge of the pathology of ACD. The discovery of mutations in the FOXF1 gene locus has been a great improvement in the research on ACD. However not in all patients with ACD a mutation in this gene locus can be found, indicating that there might be other genetic or etiological factors involved in the genesis of this disease. Since the HIF1 and HIF2 complexes are involved in vascular expansion during development of the lung, alterations in HIF1/HIF2 may play a role in the premature growth arrest and vascular abnormalities in ACD. However, no altered expression of HIF1α in lungs of human ACD patients has been observed [105], but other genes in this pathway like HIF2α could play a role.

Bronchopulmonary dysplasia

Bronchopulmonary dysplasia (BPD) is a chronic lung disease associated with preterm newborns that weigh <1000g and receive respiratory support with mechanical ventilation and/or prolonged oxygenation [106]. More than 30% of preterm infants born before 30 weeks of gestation develop BPD and the incidence is still rising [107]. It is characterized by decreased or arrested alveolarization and pulmonary microvascular development (Figure 2.2). The definition of BPD changed over the past 50 years. It was last redefined in 2000 by the National Institute of Child Health and Human Development (NICHD) [108]. The current definition is graduated by the severity of the disease, where mild BPD is defined as the need for supplemental oxygen at $\geq$28 days but not at 36 weeks of gestation, moderate BPD as the need for supplemental oxygen at 28 days in addition to supplemental oxygen at $\leq$30% at 36 weeks of gestation, and severe

BPD as the need for supplemental oxygen at 28 days and the need for mechanical ventilation and/or oxygen >30% at 36 weeks of gestation [109]. Since the alveolar and distal vascular development in premature born infants are still in a crucial state, BPD results from the need for the lung to develop while continued injury and repair are occurring [109, 110]. The vascular pathology in BPD shows immature vessels with a dysmorphic structural configuration of the distal microvasculature and an abnormal distribution of alveolar capillaries with more distance from the air surface [111]. Just like in CDH, intrapulmonary shunting through precapillary arteriovenous anastomotic vessels was found in the lungs of patients with severe BPD [112]. This dysmorphic growth and impaired function of the pulmonary vasculature can be caused by various prenatal and postnatal factors and can result in PH [113].

Mechanical ventilation and oxygen therapy in preterm infants can result in impaired angiogenic signaling with an increased expression of antiangiogenic genes and a decreased expression of proangiogenic genes [113]. After short periods of ventilation fewer arteries and endothelial cells are seen, whereas longer periods of ventilation can cause decreased vessel branches and increased endothelial cell proliferation [114]. Changes in VEGF expression are observed in lungs of human BPD patients and in an experimental animal model. Where most of the in vitro studies in humans and animals showed a decrease in VEGF expression [115–117], one in vitro study in a baboon model of BPD showed an increase in VEGF protein [118]. Levels of soluble VEGFR1 (sVEGFR1), an endogenous antagonist of VEGF, were found to be elevated in amniotic fluid and maternal blood in preeclampsia and intra-amniotic administration of sVEGFR1 to pregnant rats resulted in pups with blunted alveolarization and reduced lung vessel density [119, 120]. This implicates a role for preeclampsia by perturbations in VEGF levels in the development of BPD. During fetal lung development, levels of HIF1α are high and are important for the expression of VEGF and other angiogenic factors. In premature born children, levels of HIFα decline rapidly [118], possibly because of the absence of a hypoxic environment or even because of the use of oxygen therapy. This may cause a decrease in angiogenic factors resulting in less vascular expansion. Also HIF2α is a regulator of VEGF and is critical for fetal lung maturation. However, it plays a more important role in the alveolar epithelial cells than in the vascular cells [121]. We showed earlier that HIF2α is a key regulator in the maturation of type II pneumocytes and that ectopic expression of an oxygen-insensitive, constitutive active form of HIF2α leads to a severe surfactant deficiency in the newborn [122], which is also seen in BPD patients. In contrast to the downregulated angiogenic factors found by others, Paepe et al. found an upregulation of endoglin mRNA and protein levels in ventilated preterm infants. Endoglin is a hypoxia-inducible TGFβ coreceptor and is an important regulator of angiogenesis. They speculated that there might be a shift in angiogenic regulators which contributes to the dysangiogenesis in BPD. Furthermore, the upregulated endoglin possibly modulates vascular permeability resulting in interstitial edema, which is a morphological feature of early BPD [123]. As such BPD forms an interesting model of postnatal injury and repair showing similarities in expression profiles of a number of transcription factors involved in normal development. This disease can thus be used to gain knowledge on these processes and can be implemented in our developmental studies.

Besides the angiogenic factors, there may be a possible role for the retinoid signaling pathway in the development of BPD. As already shown in CDH, a shortage in vitamin A can disrupt the retinoid signaling pathway. Preterm infants have low vitamin A levels at birth and supplementing very low birth weight infants with vitamin A was found to be associated with a reduction in incidence of BPD [124]. The shortage in vitamin A could possibly be a cause of impaired pulmonary vascular development and PH in BPD.

Many genes with a putative role in the development of BPD have been investigated in genotype association studies. These genes have been described in a recent review [125]. Many of these studies have tested polymorphisms in potential candidate genes such as surfactant proteins or cytokines but only weak associations implicating susceptibility to the disease have

been reported [126].

Over the last decades many animal models have been developed to study the impairments in lung development in BPD. These models are based on hyperoxia, mechanical ventilation and inflammation. Since newborn rodents are born during the saccular stage of lung development, they are well suited to model BPD. The hyperoxia animal model is most commonly used and results in acute lung injury, disrupted lung structure and impaired alveolarization and vascularization, resembling the pathology seen in BPD. However, in contrast to the used animal models, preterm infants normally receive lower concentrations of oxygen with a lot of fluctuations, possibly resulting in differences in molecular signaling. Over the last years animal models gave us a better insight in the pathogenesis of BPD and resulted in the development of new therapies [107]. Since HIF1α and its expression of angiogenic factors seem to play an important role in the development of BPD, this may be a good target for the treatment of BPD.

Conclusion and future perspectives

Over the past decades, human studies focusing on abnormal pulmonary vascular development have primarily been descriptive and molecular players have been investigated in archival and resection material. Human cell cultures have been instrumental in describing molecular pathways that may contribute to specific aspects of these congenital anomalies. Although these studies have been very valuable for generating hypotheses about the origin of congenital pulmonary diseases, the majority of the studies fail to identify the underlying mechanisms. Human studies linking molecular mechanisms to diseases remain rare, because the limited number and quality of human material prevents the initiation of large-scale studies. The combination of human studies with animal models facilitates the analysis of molecular mechanisms and pathways, although the different animal models only partly reflect and phenocopy the human pathology. For instance, the mouse model for BPD is induced by exposing mice to much higher levels of oxygen than the levels that are used in the clinical situation. The surgical CDH rabbit model is sufficient to explore surgical techniques, but cannot be used to study the etiology and pathogenesis of the disease.

The -omics era has opened new ways to generate and analyze large data sets, which facilitated discovery and characterization of specific chromosomal locations, SNPs, associated with specific diseases by Genome Wide Association Studies (GWAS). However, it remains unclear in the majority of cases how the identified loci or SNP are involved in the origin of diseases. In the near future, it will be interesting to investigate whether these SNPs harbor specific binding sites for transcription factors or other DNA associating proteins, like DNA methylases. Alterations in binding efficiency may have a huge impact on downstream processes, such as transcription, leading to changes in developmental processes. It may also be that these loci SNPs are involved in spatial and or temporal long-range chromosomal interactions, which may be investigated with specific techniques, such as 3C-Seq [127].

Another putative approach is to investigate the interaction network between proteins, which may identify specific partners that are involved in developmental processes. Searching for SOX2 binding partners in neural stem cells, we recently showed that SOX2 interacts with CHD7. Mutations in SOX2 cause Anophthalmia-Esophageal-Genital (AEG) syndrome and mutations in CDH7 are associated with CHARGE syndrome (Coloboma of the eye, Heart defects, Atresia of the nasal choanae, Retardation of growth and/or development, Genital and/or urinary abnormalities, and Ear abnormalities and deafness). AEG and CHARGE have overlapping clinical features, and disturbing the interaction between SOX2 and CHD7, or other members of this cascade, may cause a variety of clinical symptoms. Moreover, several genes that are implicated in related syndromes, like JAG1 (Alagille) and GLI3 (Pallister-Hall), were shown to be activated by SOX2/CHD7. In addition, we showed that the HMG domain of SOX2 and

SRY contains a binding site for the nuclear-cytoplasmic shuttling protein Exportin4. Several mutations have been described in the human SRY gene, which were shown to be involved in XY sex reversal. These mutations prevented SRY from associating with EXP4, leading to a block in its translocation to the nucleus and thus its transcriptional activity [128]. So, the study of protein-protein interactions may provide mechanistic insights in specific disease.

Aside from (familial) genetic studies, epigenetics has become a major field of interest, and encompasses three classes: chromatin modifications (DNA methylation), histone modifications (methylation, acetylation, phosphorylation) and noncoding RNA molecules (lncRNA, miRNA). Recently, microRNA-206 (miR-206) was found as a possible triggering factor of early stage hypoxia-induced PH by targeting the HIF-1α/Fhl-1 pathway [129]. Others have identified epigenetic changes in adult patients suffering from chronic obstructive pulmonary disease (COPD), asthma and interstitial lung disease (reviewed by Yang and Schwartz, 2011 [130]), and it would be interesting to analyze pulmonary vascular diseases with these whole genome epigenetics techniques to establish the full methyl-Cap-RNA Sequence, miRNA or lncRNA profiles of the congenital pulmonary vascular diseases.

Fetal lung explants have been studied for a long time, and have generated ample evidence for branching morphogenesis in the developing lung. Human lung explants have been used, but these cultures also suffer from technical limitations [131]. As human samples are very scarcely available, and mostly derived from end-stage disease, it is mandatory to investigate alternative ways of setting up culture systems beyond the classical cell culture. Currently, several emerging 3-D culture systems, such as tracheospheres [132], alveolar spheres [133], lung organoids [134], decellularized lungs [135], bioartificial lung [136] and lung on a chip [137, 138], are being employed to address specific developmental mechanisms or to optimize systems for regenerative medicine (for reviews, see Brouwer et al., 2013 [139]; Lancaster and Knoblich, 2014 [140]; Nichols et al., 2014 [141]). Moreover, the generation of hiPS cells has become a standard technique in most institutes, and the use of patient-specific cells in combination with protocols to differentiate these cells into cells representing the three germ layers has provided new ways to explore human (pulmonary vascular) diseases [142–147]. Especially the development and employment of bioartificial lungs, such as the lung on a chip and related cultures, with patient derived hiPS cells will contribute significantly to the understanding of how different cell layers interact during development and disease. We believe that the use of these systems in combination with patient-specific hiPS cells will also benefit the testing of putative therapeutic agents.

In summary, understanding lung development and the molecular pathways leading to the mature gas exchanging organ is necessary to decipher the underlying causes of congenital pulmonary vascular diseases. It is obvious from the above perspectives that the interaction between different scientific disciplines, such as development, cell science, genetics, bioengineering, bioinformatics, will be a prerequisite to take the next steps in this process.

References

[1] Ohtani O. Microvasculature of the rat lung as revealed by scanning electron microscopy of corrosion casts. Scan Electron Microsc. 1980;(3):349–56.

[2] Townsley MI. Structure and composition of pulmonary arteries, capillaries, and veins. Compr Physiol. 2012;2(1):675–709.

[3] Rensen SS, Doevendans PA, et al. Regulation and characteristics of vascular smooth muscle cell phenotypic diversity. Neth Heart J. 2007;15(3):100–8.

[4] Sluiter I, van der Horst I, et al. Premature differentiation of vascular smooth muscle cells in human congenital diaphragmatic hernia. Exp Mol Pathol. 2013;94(1):195–202.

[5] Morrisey EE, Hogan BL. Preparing for the first breath: genetic and cellular mechanisms in lung development. Dev Cell. 2010;18(1):8–23.

[6] Herriges M, Morrisey EE. Lung development: orchestrating the generation and regeneration of a complex organ. Development. 2014;141(3):502–13.

[7] Hall SM, Hislop AA, et al. Origin, differentiation, and maturation of human pulmonary veins. Am J Respir Cell Mol Biol. 2002;26(3):333–40.

[8] deMello DE, Sawyer D, et al. Early fetal development of lung vasculature. American Journal of Respiratory Cell and Molecular Biology. 1997;16(5):568–581.

[9] deMello DE, Reid LM. Embryonic and early fetal development of human lung vasculature and its functional implications. Pediatr Dev Pathol. 2000;3(5):439–49.

[10] Yamaguchi TP, Dumont DJ, et al. flk-1, an flt-related receptor tyrosine kinase is an early marker for endothelial cell precursors. Development. 1993;118(2):489–498.

[11] Schachtner SK, Wang Y, et al. Qualitative and quantitative analysis of embryonic pulmonary vessel formation. Am J Respir Cell Mol Biol. 2000;22(2):157–65.

[12] Parera MC, van Dooren M, et al. Distal angiogenesis: a new concept for lung vascular morphogenesis. Am J Physiol Lung Cell Mol Physiol. 2005;288(1):L141–9.

[13] Peng T, Morrisey EE. Development of the pulmonary vasculature: Current understanding and concepts for the future. Pulm Circ. 2013;3(1):176–8.

[14] Ferrara N, Carver-Moore K, et al. Heterozygous embryonic lethality induced by targeted inactivation of the VEGF gene. Nature. 1996;380(6573):439–42.

[15] Healy AM, Morgenthau L, et al. VEGF is deposited in the subepithelial matrix at the leading edge of branching airways and stimulates neovascularization in the murine embryonic lung. Dev Dyn. 2000;219(3):341–52.

[16] Voelkel NF, Vandivier RW, et al. Vascular endothelial growth factor in the lung. Am J Physiol Lung Cell Mol Physiol. 2006;290(2):L209–21.

[17] White AC, Lavine KJ, et al. FGF9 and SHH regulate mesenchymal Vegfa expression and development of the pulmonary capillary network. Development. 2007;134(20):3743–52.

[18] Ferrara N, Gerber HP, et al. The biology of VEGF and its receptors. Nat Med. 2003;9(6):669–76.

[19] Oettgen P. Transcriptional regulation of vascular development. Circ Res. 2001;89(5):380–8.

[20] Webb JD, Coleman ML, et al. Hypoxia, hypoxia-inducible factors (HIF), HIF hydroxylases and oxygen sensing. Cell Mol Life Sci. 2009 Nov;66(22):3539–3554.

[21] Risau W. Mechanisms of angiogenesis. Nature. 1997;386(6626):671–4.

[22] Carmeliet P. Angiogenesis in life, disease and medicine. 2005;438(7070):932–936.

[23] Herbert SP, Stainier DYR. Molecular control of endothelial cell behaviour during blood vessel morphogenesis. 2011;12(9):551–564.

[24] Armulik A, Abramsson A, et al. Endothelial/pericyte interactions. Circ Res. 2005;97(6):512–23.

[25] Coultas L, Chawengsaksophak K, et al. Endothelial cells and VEGF in vascular development. 2005;438(7070):937–945.

[26] Schwarz MA, Caldwell L, et al. Emerging pulmonary vasculature lacks fate specification. Am J Physiol Lung Cell Mol Physiol. 2009;296(1):L71–81.

[27] Krebs LT, Shutter JR, et al. Haploinsufficient lethality and formation of arteriovenous malformations in Notch pathway mutants. Genes Dev. 2004;18(20):2469–73.

[28] Duarte A, Hirashima M, et al. Dosage-sensitive requirement for mouse Dll4 in artery development.

Genes Dev. 2004;18(20):2474–8.

[29] Pereira FA, Qiu Y, et al. The orphan nuclear receptor COUP-TFII is required for angiogenesis and heart development. Genes Dev. 1999;13(8):1037–49.

[30] You LR, Takamoto N, et al. Mouse lacking COUP-TFII as an animal model of Bochdalek-type congenital diaphragmatic hernia. Proc Natl Acad Sci U S A. 2005;102(45):16351–6.

[31] Shannon JM, Hyatt BA. Epithelial-mesenchymal interactions in the developing lung. Annual Review of Physiology. 2004;66:625–645.

[32] Sekine K, Ohuchi H, et al. Fgf10 is essential for limb and lung formation. Nat Genet. 1999;21(1):138–41.

[33] Leach RE, Khalifa R, et al. Multiple roles for heparin-binding epidermal growth factor-like growth factor are suggested by its cell-specific expression during the human endometrial cycle and early placentation. J Clin Endocrinol Metab. 1999;84(9):3355–63.

[34] Cardoso WV, Lu J. Regulation of early lung morphogenesis: questions, facts and controversies. Development. 2006;133(9):1611–24.

[35] Volckaert T, Campbell A, et al. Localized Fgf10 expression is not required for lung branching morphogenesis but prevents differentiation of epithelial progenitors. Development. 2013;140(18):3731–42.

[36] Colvin JS, White AC, et al. Lung hypoplasia and neonatal death in Fgf9-null mice identify this gene as an essential regulator of lung mesenchyme. Development. 2001;128(11):2095–106.

[37] White AC, Xu J, et al. FGF9 and SHH signaling coordinate lung growth and development through regulation of distinct mesenchymal domains. Development. 2006;133(8):1507–1517.

[38] Malpel S, Mendelsohn C, et al. Regulation of retinoic acid signaling during lung morphogenesis. Development. 2000;127(14):3057–67.

[39] Duester G. Retinoic acid synthesis and signaling during early organogenesis. Cell. 2008;134(6):921–31.

[40] Mark M, Ghyselinck NB, et al. Function of retinoic acid receptors during embryonic development. Nucl Recept Signal. 2009;7:e002.

[41] Morriss-Kay GM, Ward SJ. Retinoids and mammalian development. Int Rev Cytol. 1999;188:73–131.

[42] Mollard R, Ghyselinck NB, et al. Stage-dependent responses of the developing lung to retinoic acid signaling. Int J Dev Biol. 2000;44(5):457–62.

[43] Dollé P, Fraulob V, et al. Fate of retinoic acidactivated embryonic cell lineages. Developmental Dynamics. 2010;239(12):3260–3274.

[44] Clugston RD, Zhang W, et al. Early development of the primordial mammalian diaphragm and cellular mechanisms of nitrofen-induced congenital diaphragmatic hernia. Birth Defects Res A Clin Mol Teratol. 2010;88(1):15–24.

[45] Chen F, Desai TJ, et al. Inhibition of Tgf beta signaling by endogenous retinoic acid is essential for primary lung bud induction. Development. 2007;134(16):2969–79.

[46] Chen F, Cao Y, et al. A retinoic acid-dependent network in the foregut controls formation of the mouse lung primordium. J Clin Invest. 2010;120(6):2040–8.

[47] Lai L, Bohnsack BL, et al. Retinoic acid regulates endothelial cell proliferation during vasculogenesis. Development. 2003;130(26):6465–74.

[48] Berger RM, Beghetti M, et al. Clinical features of paediatric pulmonary hypertension: a registry study. Lancet. 2012;379(9815):537–46.

[49] Ivy DD, Abman SH, et al. Pediatric pulmonary hypertension. J Am Coll Cardiol. 2013;62(25 Suppl):D117–26.

[50] Simonneau G, Gatzoulis MA, et al. Updated clinical classification of pulmonary hypertension. J Am Coll Cardiol. 2013;62(25 Suppl):D34–41.

[51] van Loon RL, Roofthooft MT, et al. Pediatric pulmonary hypertension in the Netherlands: epidemiology and characterization during the period 1991 to 2005. Circulation. 2011;124(16):1755–64.

[52] Ma L, Chung WK. The genetic basis of pulmonary arterial hypertension. Hum Genet. 2014;133(5):471–9.

[53] Berger RM, Bonnet D. Treatment options for paediatric pulmonary arterial hypertension. Eur Respir Rev. 2010;19(118):321–30.

[54] Aldred MA, Vijayakrishnan J, et al. BMPR2 gene rearrangements account for a significant proportion of mutations in familial and idiopathic pulmonary arterial hypertension. Hum Mutat. 2006;27(2):212–3.

[55] Pfarr N, Fischer C, et al. Hemodynamic and genetic analysis in children with idiopathic, heritable, and congenital heart disease associated pulmonary arterial hypertension. Respir Res. 2013;14:3.

[56] Fujiwara M, Yagi H, et al. Implications of mutations of activin receptor-like kinase 1 gene (ALK1) in addition to bone morphogenetic protein receptor II gene (BMPR2) in children with pulmonary arterial hypertension. Circ J. 2008;72(1):127–33.

[57] Vachharajani A, Saunders S. Allelic variation in the serotonin transporter (5HTT) gene contributes to idiopathic pulmonary hypertension in children. Biochem Biophys Res Commun. 2005;334(2):376–9.

[58] Chida A, Shintani M, et al. Missense mutations of the BMPR1B (ALK6) gene in childhood idiopathic pulmonary arterial hypertension. Circ J. 2012;76(6):1501–8.

[59] Longoni M, Russell MK, et al. Prevalence and penetrance of ZFPM2 mutations and deletions causing congenital diaphragmatic hernia. Clin Genet. 2014;.

[60] Klaassens M, van Dooren M, et al. Congenital diaphragmatic hernia and chromosome 15q26: determination of a candidate region by use of fluorescent in situ hybridization and array-based comparative genomic hybridization. Am J Hum Genet. 2005;76(5):877–82.

[61] Pasutto F, Sticht H, et al. Mutations in STRA6 cause a broad spectrum of malformations including anophthalmia, congenital heart defects, diaphragmatic hernia, alveolar capillary dysplasia, lung hypoplasia, and mental retardation. Am J Hum Genet. 2007;80(3):550–60.

[62] Beck TF, Veenma D, et al. Deficiency of FRAS1-related extracellular matrix 1 (FREM1) causes congenital diaphragmatic hernia in humans and mice. Hum Mol Genet. 2013;22(5):1026–38.

[63] Scott DA, Cooper ML, et al. Congenital diaphragmatic hernia in WAGR syndrome. Am J Med Genet A. 2005;134(4):430–3.

[64] Szafranski P, Dharmadhikari AV, et al. Small noncoding differentially methylated copy-number variants, including lncRNA genes, cause a lethal lung developmental disorder. Genome Res. 2013;23(1):23–33.

[65] Stankiewicz P, Sen P, et al. Genomic and genic deletions of the FOX gene cluster on 16q24.1 and inactivating mutations of FOXF1 cause alveolar capillary dysplasia and other malformations. Am J Hum Genet. 2009;84(6):780–91.

[66] Friedman D, Szmuszkovicz J, et al. Systemic endothelial dysfunction in children with idiopathic pulmonary arterial hypertension correlates with disease severity. J Heart Lung Transplant. 2012;31(6):642–7.

[67] Haworth SG. Pulmonary hypertension in the young. Heart. 2002;88(6):658–64.

[68] Widlitz A, Barst RJ. Pulmonary arterial hypertension in children. Eur Respir J. 2003;21(1):155–76.

[69] Barst RJ, Ertel SI, et al. Pulmonary arterial hypertension: a comparison between children and adults. Eur Respir J. 2011;37(3):665–77.

[70] Cella G, Bellotto F, et al. Plasma markers of endothelial dysfunction in pulmonary hypertension. Chest. 2001;120(4):1226–30.

[71] Mikhail G, Chester AH, et al. Role of vasoactive mediators in primary and secondary pulmonary hypertension. Am J Cardiol. 1998;82(2):254–5.

[72] Rubens C, Ewert R, et al. Big endothelin-1 and endothelin-1 plasma levels are correlated with the severity of primary pulmonary hypertension. Chest. 2001;120(5):1562–9.

[73] Stewart DJ, Levy RD, et al. Increased plasma endothelin-1 in pulmonary hypertension: marker or mediator of disease? Ann Intern Med. 1991;114(6):464–9.

[74] Mandegar M, Fung YC, et al. Cellular and molecular mechanisms of pulmonary vascular remodeling: role in the development of pulmonary hypertension. Microvasc Res. 2004;68(2):75–103.

[75] Saji T. Update on pediatric pulmonary arterial hypertension. Differences and similarities to adult disease. Circ J. 2013;77(11):2639–50.

[76] Best DH, Austin ED, et al. Genetics of pulmonary hypertension. Curr Opin Cardiol. 2014;.

[77] Miniati D. Pulmonary vascular remodeling. Semin Pediatr Surg. 2007;16(2):80–7.

[78] Sluiter I, Reiss I, et al. Vascular abnormalities in human newborns with pulmonary hypertension. Expert Rev Respir Med. 2011;5(2):245–56.

[79] Barghorn A, Koslowski M, et al. Alpha-smooth muscle actin distribution in the pulmonary vasculature comparing hypoplastic and normal fetal lungs. Pediatr Pathol Lab Med. 1998;18(1):5–22.

[80] Taira Y, Yamataka T, et al. Comparison of the pulmonary vasculature in newborns and stillborns with congenital diaphragmatic hernia. Pediatr Surg Int. 1998;14(1-2):30–5.

[81] de Rooij JD, Hosgor M, et al. Expression of angiogenesis-related factors in lungs of patients with congenital diaphragmatic hernia and pulmonary hypoplasia of other causes. Pediatr Dev Pathol. 2004;7(5):468–77.

[82] Shehata SM, Mooi WJ, et al. Enhanced expression of vascular endothelial growth factor in lungs of newborn infants with congenital diaphragmatic hernia and pulmonary hypertension. Thorax. 1999;54(5):427–31.

[83] van der Horst IW, Rajatapiti P, et al. Expression of hypoxia-inducible factors, regulators, and target genes in congenital diaphragmatic hernia patients. Pediatr Dev Pathol. 2011;14(5):384–90.

[84] Masumoto K, de Rooij JD, et al. The distribution of matrix metalloproteinases and tissue inhibitors of metalloproteinases in the lungs of congenital diaphragmatic hernia patients and age-matched controls. Histopathology. 2006;48(5):588–95.

[85] Muehlethaler V, Kunig AM, et al. Impaired VEGF and nitric oxide signaling after nitrofen exposure in rat fetal lung explants. Am J Physiol Lung Cell Mol Physiol. 2008;294(1):L110–20.

[86] Sbragia L, Nassr AC, et al. VEGF receptor expression decreases during lung development in congenital diaphragmatic hernia induced by nitrofen. Braz J Med Biol Res. 2014;47(2):171–8.

[87] Wilson JG, Roth CB, et al. An analysis of the syndrome of malformations induced by maternal vitamin A deficiency. Effects of restoration of vitamin A at various times during gestation. Am J Anat. 1953;92(2):189–217.

[88] Beurskens N, Klaassens M, et al. Linking animal models to human congenital diaphragmatic hernia. Birth Defects Res A Clin Mol Teratol. 2007;79(8):565–72.

[89] Mendelsohn C, Lohnes D, et al. Function of the retinoic acid receptors (RARs) during development (II). Multiple abnormalities at various stages of organogenesis in RAR double mutants. Development. 1994;120(10):2749–71.

[90] Beurskens LW, Tibboel D, et al. Retinol status of newborn infants is associated with congenital diaphragmatic hernia. Pediatrics. 2010;126(4):712–20.

[91] Major D, Cadenas M, et al. Retinol status of newborn infants with congenital diaphragmatic hernia. Pediatr Surg Int. 1998;13(8):547–9.

[92] Xu C, Liu W, et al. Effect of prenatal tetrandrine administration on transforming growth factor-beta1 level in the lung of nitrofen-induced congenital diaphragmatic hernia rat model. J Pediatr Surg. 2009;44(8):1611–20.

[93] Chen G, Qiao Y, et al. Effects of estrogen on lung development in a rat model of diaphragmatic hernia. J Pediatr Surg. 2010;45(12):2340–5.

[94] Teramoto H, Yoneda A, et al. Gene expression of fibroblast growth factors 10 and 7 is downregulated in the lung of nitrofen-induced diaphragmatic hernia in rats. J Pediatr Surg. 2003;38(7):1021–4.

[95] Holder AM, Klaassens M, et al. Genetic factors in congenital diaphragmatic hernia. Am J Hum Genet. 2007;80(5):825–45.

[96] Wat MJ, Beck TF, et al. Mouse model reveals the role of SOX7 in the development of congenital diaphragmatic hernia associated with recurrent deletions of 8p23.1. Hum Mol Genet. 2012;21(18):4115–25.

[97] Wat MJ, Veenma D, et al. Genomic alterations that contribute to the development of isolated and non-isolated congenital diaphragmatic hernia. J Med Genet. 2011;48(5):299–307.

[98] van Loenhout RB, Tibboel D, et al. Congenital diaphragmatic hernia: comparison of animal models and relevance to the human situation. Neonatology. 2009;96(3):137–49.

[99] Chiu PP. New Insights into Congenital Diaphragmatic Hernia - A Surgeon's Introduction to

CDH Animal Models. Front Pediatr. 2014;2:36.

[100] Bishop NB, Stankiewicz P, et al. Alveolar capillary dysplasia. Am J Respir Crit Care Med. 2011;184(2):172–9.

[101] Ren X, Ustiyan V, et al. FOXF1 Transcription Factor Is Required for Formation of Embryonic Vasculature by Regulating VEGF Signaling in Endothelial Cells. Circ Res. 2014;.

[102] Mahlapuu M, Enerback S, et al. Haploinsufficiency of the forkhead gene Foxf1, a target for sonic hedgehog signaling, causes lung and foregut malformations. Development. 2001;128(12):2397–406.

[103] Han RN, Babaei S, et al. Defective lung vascular development and fatal respiratory distress in endothelial NO synthase-deficient mice: a model of alveolar capillary dysplasia? Circ Res. 2004;94(8):1115–23.

[104] Tiozzo C, Carraro G, et al. Mesodermal Pten inactivation leads to alveolar capillary dysplasia-like phenotype. J Clin Invest. 2012;122(11):3862–72.

[105] Sen P, Choudhury T, et al. Expression of angiogenic and vasculogenic proteins in the lung in alveolar capillary dysplasia/misalignment of pulmonary veins: an immunohistochemical study. Pediatr Dev Pathol. 2010;13(5):354–61.

[106] Bancalari EH, Jobe AH. The respiratory course of extremely preterm infants: a dilemma for diagnosis and terminology. J Pediatr. 2012;161(4):585–8.

[107] Hilgendorff A, Reiss I, et al. Chronic lung disease in the preterm infant. Lessons learned from animal models. Am J Respir Cell Mol Biol. 2014;50(2):233–45.

[108] Jobe AH, Bancalari E. Bronchopulmonary dysplasia. Am J Respir Crit Care Med. 2001;163(7):1723–9.

[109] Ali Z, Schmidt P, et al. Bronchopulmonary dysplasia: a review. Arch Gynecol Obstet. 2013;288(2):325–33.

[110] Jobe AH. What is BPD in 2012 and what will BPD become? Early Hum Dev. 2012;88 Suppl 2:S27–8.

[111] Coalson JJ. Pathology of bronchopulmonary dysplasia. Semin Perinatol. 2006;30(4):179–84.

[112] Galambos C, Sims-Lucas S, et al. Histologic evidence of intrapulmonary anastomoses by three-dimensional reconstruction in severe bronchopulmonary dysplasia. Ann Am Thorac Soc. 2013;10(5):474–81.

[113] Baker CD, Abman SH, et al. Pulmonary Hypertension in Preterm Infants with Bronchopulmonary Dysplasia. Pediatr Allergy Immunol Pulmonol. 2014;27(1):8–16.

[114] Abman SH. The dysmorphic pulmonary circulation in bronchopulmonary dysplasia: a growing story. Am J Respir Crit Care Med. 2008;178(2):114–5.

[115] Bhatt AJ, Pryhuber GS, et al. Disrupted pulmonary vasculature and decreased vascular endothelial growth factor, Flt-1, and TIE-2 in human infants dying with bronchopulmonary dysplasia. Am J Respir Crit Care Med. 2001;164(10 Pt 1):1971–80.

[116] Lassus P, Turanlahti M, et al. Pulmonary vascular endothelial growth factor and Flt-1 in fetuses, in acute and chronic lung disease, and in persistent pulmonary hypertension of the newborn. Am J Respir Crit Care Med. 2001;164(10 Pt 1):1981–7.

[117] Maniscalco WM, Watkins RH, et al. Angiogenic factors and alveolar vasculature: development and alterations by injury in very premature baboons. Am J Physiol Lung Cell Mol Physiol. 2002;282(4):L811–23.

[118] Asikainen TM, Ahmad A, et al. Effect of preterm birth on hypoxia-inducible factors and vascular endothelial growth factor in primate lungs. Pediatr Pulmonol. 2005;40(6):538–46.

[119] Madurga A, Mizikova I, et al. Recent advances in late lung development and the pathogenesis of bronchopulmonary dysplasia. Am J Physiol Lung Cell Mol Physiol. 2013;305(12):L893–905.

[120] Tang JR, Karumanchi SA, et al. Excess soluble vascular endothelial growth factor receptor-1 in amniotic fluid impairs lung growth in rats: linking preeclampsia with bronchopulmonary dysplasia. Am J Physiol Lung Cell Mol Physiol. 2012;302(1):L36–46.

[121] Compernolle V, Brusselmans K, et al. Loss of HIF-2alpha and inhibition of VEGF impair fetal lung maturation, whereas treatment with VEGF prevents fatal respiratory distress in premature mice. Nat Med. 2002;8(7):702–10.

[122] Huang Y, Kempen MB, et al. Hypoxia-inducible factor 2alpha plays a critical role in the formation of alveoli and surfactant. Am J Respir Cell Mol Biol. 2012;46(2):224–32.

[123] De Paepe ME, Patel C, et al. Endoglin (CD105) up-regulation in pulmonary microvasculature of ventilated preterm infants. Am J Respir Crit Care Med. 2008;178(2):180–7.

[124] Darlow BA, Graham PJ. Vitamin A supplementation to prevent mortality and short and long-term morbidity in very low birthweight infants. Cochrane Database Syst Rev. 2007;(4):CD000501.

[125] Shaw GM, O'Brodovich HM. Progress in understanding the genetics of bronchopulmonary dysplasia. Semin Perinatol. 2013;37(2):85–93.

[126] Somaschini M, Castiglioni E, et al. Genetic susceptibility to neonatal lung diseases. Acta Biomed. 2012;83 Suppl 1:10–4.

[127] de Wit E, de Laat W. A decade of 3C technologies: insights into nuclear organization. Genes Dev. 2012 Jan;26(1):11–24.

[128] Gontan C, Güttler T, et al. Exportin 4 mediates a novel nuclear import pathway for Sox family transcription factors. J Cell Biol. 2009 Apr;185(1):27–34.

[129] Yue J, Guan J, et al. MicroRNA-206 is involved in hypoxia-induced pulmonary hypertension through targeting of the HIF-1alpha/Fhl-1 pathway. Lab Invest. 2013;93(7):748–59.

[130] Yang IV, Schwartz DA. Epigenetic control of gene expression in the lung. Am J Respir Crit Care Med. 2011 May;183(10):1295–1301.

[131] Rajatapiti P, de Rooij JD, et al. Effect of oxygen on the expression of hypoxia-inducible factors in human fetal lung explants. Neonatology. 2010 Jun;97(4):346–354.

[132] Rock JR, Onaitis MW, et al. Basal cells as stem cells of the mouse trachea and human airway epithelium. Proc Natl Acad Sci U S A. 2009 Aug;106(31):12771–12775.

[133] Barkauskas CE, Cronce MJ, et al. Type 2 alveolar cells are stem cells in adult lung. J Clin Invest. 2013 Jul;123(7):3025–3036.

[134] Hynds RE, Giangreco A. Concise review: the relevance of human stem cell-derived organoid models for epithelial translational medicine. Stem Cells. 2013 Mar;31(3):417–422.

[135] Crapo PM, Gilbert TW, et al. An overview of tissue and whole organ decellularization processes. Biomaterials. 2011 Apr;32(12):3233–3243.

[136] Lemon G, Lim ML, et al. The development of the bioartificial lung. Br Med Bull. 2014 Jun;110(1):35–45.

[137] Harink B, Le Gac S, et al. Regeneration-on-a-chip? The perspectives on use of microfluidics in regenerative medicine. Lab Chip. 2013 Sep;13(18):3512–3528.

[138] Huh D, Hamilton GA, et al. From 3D cell culture to organs-on-chips. Trends Cell Biol. 2011;21(12):745–54.

[139] Brouwer KM, Hoogenkamp HR, et al. Regenerative medicine for the respiratory system: distant future or tomorrow's treatment? Am J Respir Crit Care Med. 2013 Mar;187(5):468–475.

[140] Lancaster MA, Knoblich JA. Organogenesis in a dish: modeling development and disease using organoid technologies. Science. 2014 Jul;345(6194):1247125.

[141] Nichols JE, Niles JA, et al. Modeling the lung: Design and development of tissue engineered macro- and micro-physiologic lung models for research use. Exp Biol Med (Maywood). 2014 Sep;239(9):1135–1169.

[142] Firth AL, Dargitz CT, et al. Generation of multiciliated cells in functional airway epithelia from human induced pluripotent stem cells. Proc Natl Acad Sci U S A. 2014 Apr;111(17):E1723–E1730.

[143] Green MD, Chen A, et al. Generation of anterior foregut endoderm from human embryonic and induced pluripotent stem cells. Nat Biotechnol. 2011 Mar;29(3):267–272.

[144] Huang SXL, Islam MN, et al. Efficient generation of lung and airway epithelial cells from human pluripotent stem cells. Nat Biotechnol. 2014 Jan;32(1):84–91.

[145] Longmire TA, Ikonomou L, et al. Efficient derivation of purified lung and thyroid progenitors from embryonic stem cells. Cell Stem Cell. 2012 Apr;10(4):398–411.

[146] Mou H, Zhao R, et al. Generation of multipotent lung and airway progenitors from mouse ESCs and patient-specific cystic fibrosis iPSCs. Cell Stem Cell. 2012 Apr;10(4):385–397.

[147] Wong AP, Bear CE, et al. Directed differentiation of human pluripotent stem cells into mature airway epithelia expressing functional CFTR protein. Nat Biotechnol. 2012 Sep;30(9):876–882.

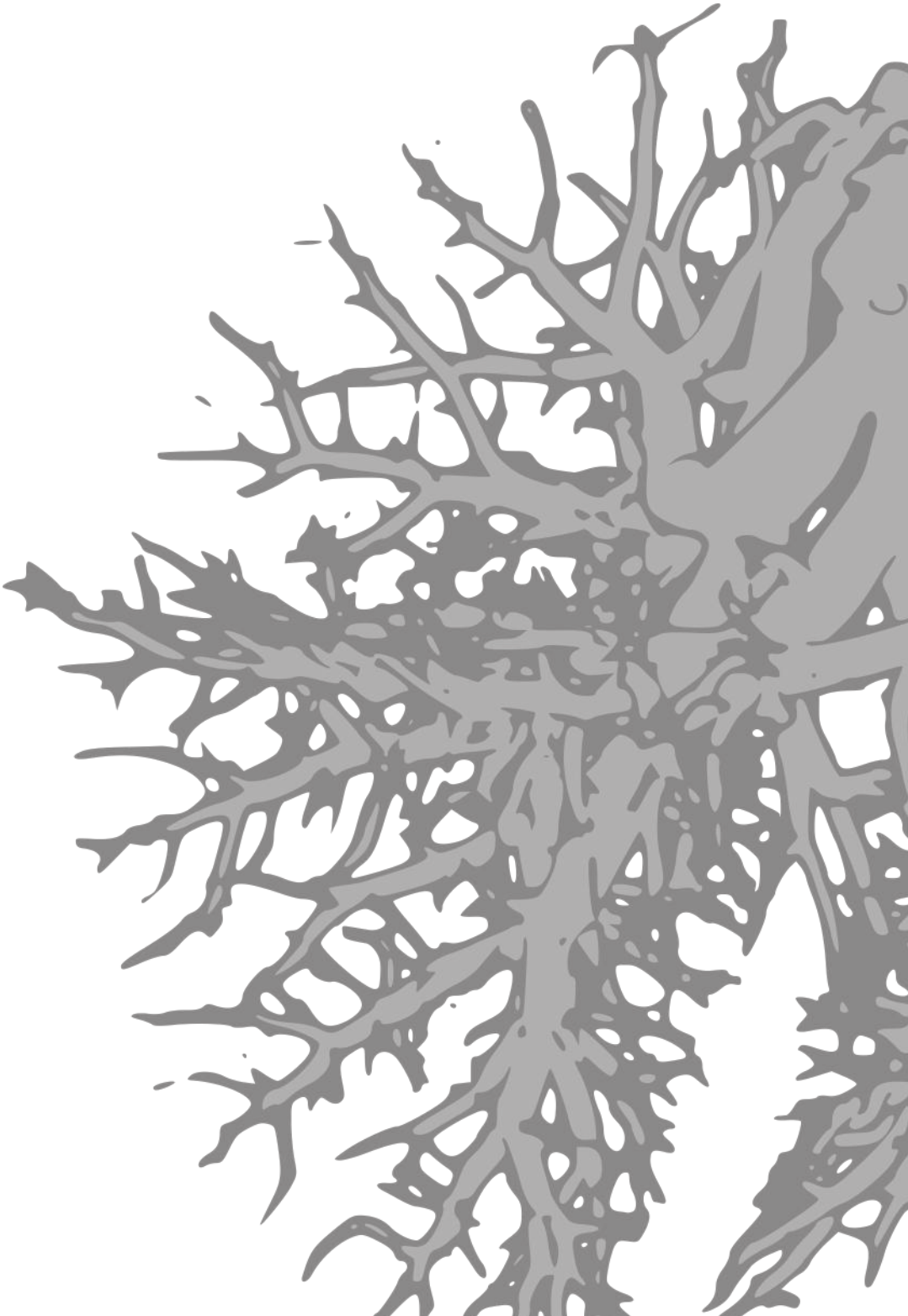

Chapter 3

Opposite effects of TGFβ and BMP in the pulmonary vasculature of congenital diaphragmatic hernia

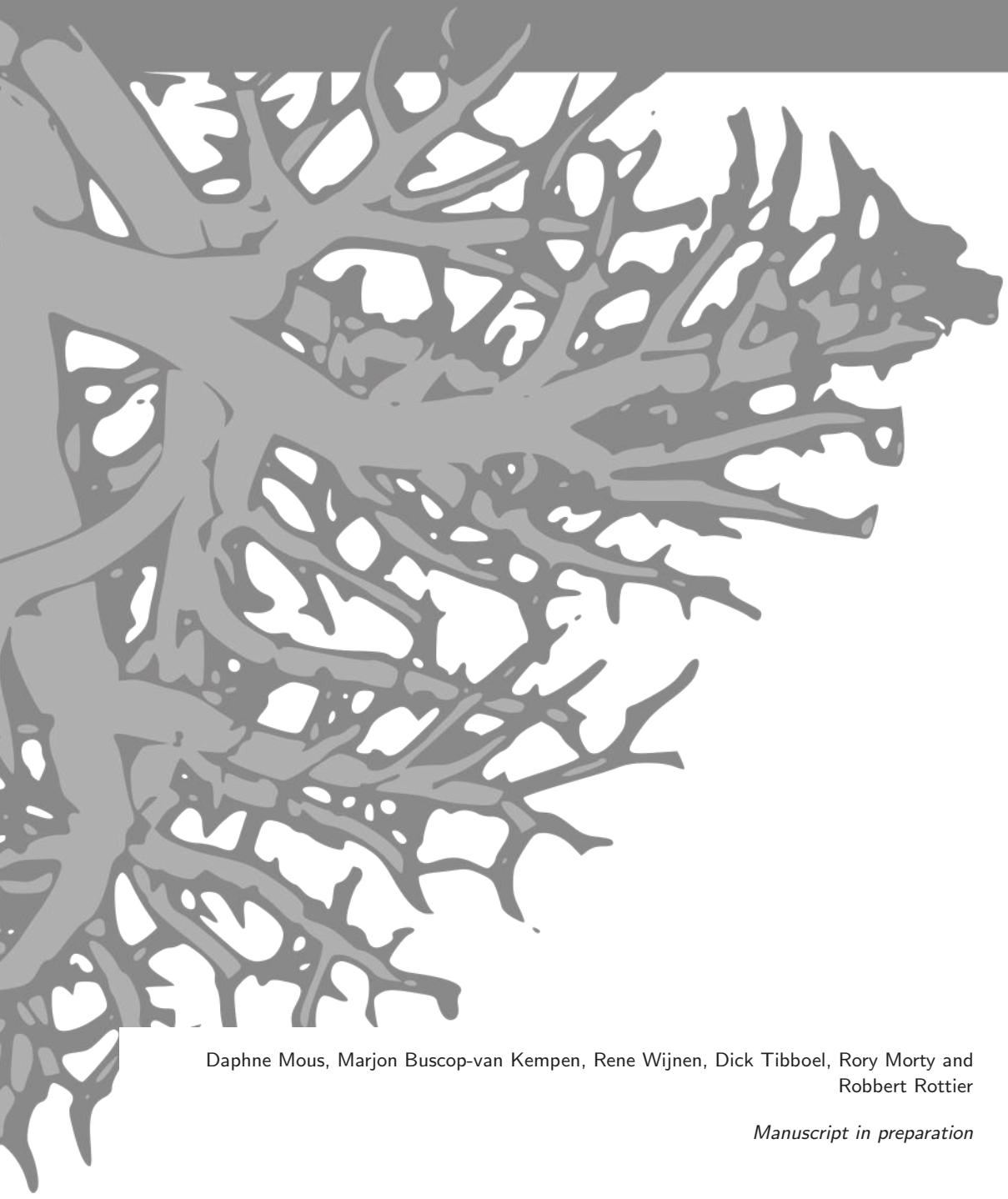

Daphne Mous, Marjon Buscop-van Kempen, Rene Wijnen, Dick Tibboel, Rory Morty and Robbert Rottier

Manuscript in preparation

Abstract

Background: Pulmonary hypertension is the major cause of mortality and morbidity in congenital diaphragmatic hernia (CDH). Mutations in different genes of the transforming growth factor β (TGFβ) and bone morphogenetic protein (BMP) pathways have previously been described in both adult and pediatric patients with different forms of pulmonary hypertension. Since studies on the activation of these pathways in CDH are scarce and show inconsistent results, we analyzed the downstream activity of both pathways in the nitrofen-CDH rat model.

Methods and results: Pregnant Sprague-Dawley rats were treated with nitrofen at day 9.5 of gestation (E9.5) to induce CDH in the offspring. At E21 the whole lungs were analyzed at RNA and protein level for the expression of important factors of both pathways. Subsequently, we focused on the pulmonary vasculature, which showed increased phosphorylation of the receptor-regulated Smad2 and decreased phosphorylation of Smad5 in the muscular wall of the small pulmonary vessels using immunostaining. This was accompanied by increased proliferation of the smooth muscle layer of these vessels.

Conclusions: We showed increased activation of the TGFβ pathway and decreased activation of the BMP pathway in combination with increased proliferation in the pulmonary vasculature of CDH rats, possibly indicating an important role of these pathways in the development of pulmonary hypertension in this disease.

Introduction

Congenital diaphragmatic hernia (CDH) is a severe developmental anomaly characterized by a diaphragmatic defect and a variable extent of bilateral pulmonary hypoplasia and pulmonary hypertension (PH). The concomitant PH can cause major problems in the newborn and is responsible for the high mortality and morbidity in these patients. Although the morphology of the pulmonary vessels is well described and consist of increased muscularization of the pulmonary vessels in CDH [1], the molecular mechanisms and pathways involved in PH in these patients are still largely unknown. Mutations in different genes involved in the transforming growth factor β (TGFβ) and bone morphogenetic protein (BMP) pathways have been described in both adult and pediatric patients with familial, heritable and idiopathic pulmonary arterial hypertension (PAH). Of these genes the BMP receptor 2 (BMPr2) is most commonly affected [2].

TGFβ is a negative regulator of airway branching in early lung development. However, TGFβ signaling is also active in the vascular and airway smooth muscle and alveolar and airway epithelium during late lung development. Both up- and down-regulation of TGFβ signaling impairs the alveolarization process [3, 4], depending on a time dependent manner. Both TGFβ and BMP have shown to influence proliferation of endothelial and smooth muscle cells and control apoptosis and extracellular matrix secretion and deposition [5]. Studies on the TGFβ pathway in CDH failed to show consistent results. Decreased expression of TGFβ1 was found at mRNA level in the hearts of the nitrofen-CDH rat pups [6], where increased expression of this factor was shown on immunostaining of the lung in the same animal model [7]. Others even showed no differences at all in TGFβ and its activity on the phosphorylation of Smad2/3 in both human samples and the nitrofen-CDH rat model [8]. A study performed in pregnant women carrying CDH fetuses showed decreased TGFβ in the amniotic fluid, but no differences in expression of this factor in the lungs of these children after birth [9]. Both the TGFβ receptor (TGFβr) 1 and 2 as well as endoglin, an auxiliary receptor of TGFβ, were found to be decreased in nitrofen-CDH rat pups [10].

In contrast to the TGFβ pathway, results on factors of the BMP pathway in CDH seem to be more consistent. Reduced expression of BMPr2 [11, 12] and BMP4 [13, 12] were found in the lungs of different animal models of CDH. Furthermore, apelin, a target gene of BMPr2 which can have a hypotensive effect, has shown to be decreased in nitrofen-CDH rat pups [14] and activin receptor-like kinase 1 (ALK1), another receptor in this pathway, was upregulated in the same animal model [15]. However, others did not find any differences in signaling downstream of the BMPr [16] and so far no mutations were found in the BMPr2 gene in human CDH patients [17]. Literature data on the TGFβ and BMP pathways in CDH is summarized in Table 3.1 and an overview of both pathways is displayed in Figure 3.1.

Since most of the research has been done on the receptors in both pathways and not much is known about the actual activation of these pathways, we analyzed the effect of downstream signaling in the well-established nitrofen-CDH rat model.

Methods

Animal Model

Pregnant Sprague-Dawley rats received either 100 mg nitrofen dissolved in 1 ml olive oil or just 1 ml olive oil by gavage on gestational age day E9.5. Nitrofen induces CDH in approximately 70% of the offspring, while all pups have pulmonary hypertension [18]. At day E21 pups were delivered by caesarean section and euthanized by lethal injection of pentobarbital.

All animal experiments were approved by an independent animal ethical committee and according to national guidelines.

Table 3.1: Overview of studies in TGFβ in CDH

Factor	Animal	Human
TGFβ	Decreased [6] Increased [7] No difference [8]	Decreased [9] No difference [8]
TGFβ receptor	Decreased [10]	
BMPr2	Decreased [12] Decreased [11]	No difference [17]
BMP4	Decreased [13] Decreased [12]	
ALK1	Increased [15]	
pSmad 1/5/8	No difference [16]	
Apelin	Decreased [14]	

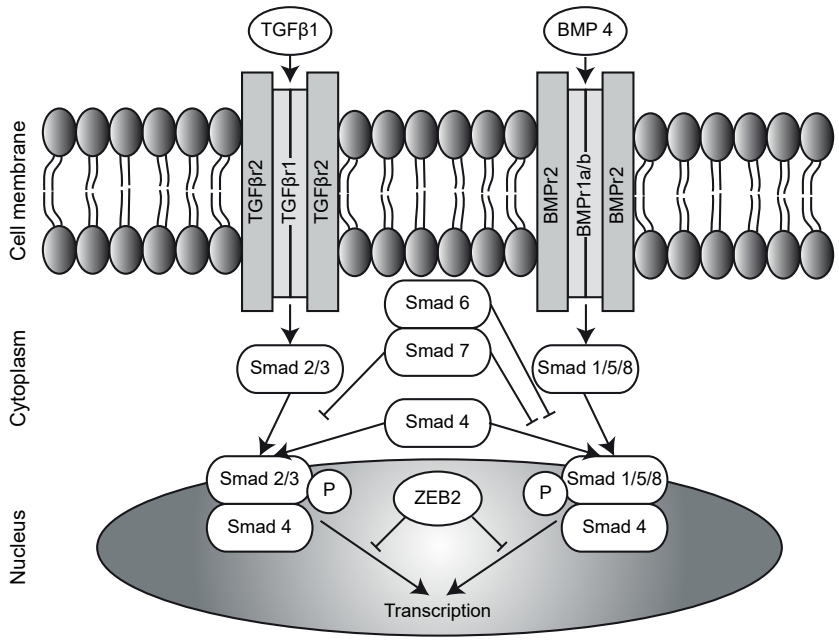

Figure 3.1: Overview of the TGFβ and BMP pathways. TGFβ = transforming growth factor β, BMP = bone morphogenetic protein, ZEB2 = zinc finger E-box binding homeobox 2, P = phosphorylation.

Table 3.2: Primer sequences

Gene	Sequence (forward 5'- 3')	Sequence (reverse 5'- 3')
Tgfβ1	AACCAAGGAGACGGAATACAG	GACTGATCCCATTGATTTCCA
Tgfβr1	CCATTGGCGGAATCCACGAAGAC	CGCAAAGCTGTCAGCCTAGCTG
Tgfβr2	CGTGACACTGTCCACTTGTGAC	GACGCACGTGGGAGAAGTGGCATC
Bmp4	CCATCACGAAGAACATCTGG	GGATGCTGCTGAGGTTAAAGA
Bmpr1b	ATGTGTTTCTGGAGGTATAGTGG	CTCATGTCCTCATAAGAAGGGTC
Bmpr2	ATTGAGGGTGGGGTGGTAGT	GTGAAACAAGGGTGCTGGTC
Alk1	GTCAAGAAGCCTCCAGCAAC	CTCAACTCAGGCTTCGGG
Smad1	TCAATAGAGGAGATGTTCAAGCAGT	GAAACCATCCACCAACACGC
Smad2	AGAATACCGGAGGCAGACAG	GTTAATACTTTGTCCAACCACTGC
Smad3	GCTGTCTACCAGTTGACTCG	TCACTGTCTGTCTCCTGTACTC
Smad4	TCATCCTGCTCCTGAATATTGGT	AGTTACAATAGGACAGCTTGAAGG
Smad5	CAATAACAAGAGCCGCTTCTG	ATAGATGGACACCTTTCCCG
Smad6	GTCCGATTCTACATTGTCTTACAC	TGCTGGCATCTGAGAATTCAC
Smad7	AAACCAACTGCAGACTGTCC	AGAAGAAGTTGGGAATCTGAAAGC
Zeb2	CCTATACCTACCCAACGGGA	AGCAATTCTCCCTGAAATCCT
Actb	AGATGACCCAGATCATGTTTGAG	GTACGACCAGAGGCATACAG

Quantitative Real-Time Polymerase Chain Reaction (qPCR)

RNA isolation, cDNA synthesis and subsequent qPCR analysis was performed as previously [19]. The gene-specific primers used are listed in 6.2.

Immunohistochemistry and Immunofluorescence Staining

Immunohistochemistry (IHC) was performed on 5 μm paraffin sections of lungs of both rats and humans according to standard protocols, using the Envision^{TM} detection system (Dako Cytomatic, Glostrup, Denmark) [19]. Primary antibody used for IHC was ZEB2 (Sip1; 1:400, [20]). Primary antibodies used for IF were smooth muscle actin (α-SMA; MS-113-P1; 1:500, Thermo Scientific, Fremont, CA, USA), phosphorylated SMAD 2 (pSMAD2; 1:250, Cell Signaling, Danvers, MA, USA), phosphorylated SMAD 1/5/8 (pSMAD1/5/8; 1:500, Kerafast, Boston, MA, USA) and Ki-67 (1:100, Abcam, Cambridge, UK). Secondary antibodies against mouse (α-SMA) and rabbit (pSMAD2, pSMAD1/5/8 and Ki-67) were used. Negative controls were performed by omitting the primary antibody. Antigen retrieval with Citric Acid buffer (pH 6.0) was used. Negative controls were performed by omitting the primary antibody.

Immunoblotting

Snap frozen lungs were homogenized on ice in Carin buffer, containing protease inhibitor Complete (Roche, Basel, Switzerland). Samples were centrifuged at 14.200 RPM for 15 min and protein concentration in the supernatant was measured using the Bradford method. Subsequently 50 microgram of protein per lane was loaded on SDS-PAGE and transferred to nitrocellulose membranes using wetblotting. Blots were labeled with TGFβ (1:1000, Abcam), pSMAD2 (1:1000, Cell Signaling), SMAD2 (1:1000, Cell Signaling), pSMAD5 (1:1000, Abcam), SMAD5 (1:1000, Cell Signaling) and Sip1 (1:1000, [20]). Cofilin (1:400, Abcam) and β-actin (1:1000, Cell Signaling) were used for loading control.

Statistical Analyses

Data are presented as percentages, means (SD) for normally distributed variables. Univariate analyses were performed using independent samples t-tests for normally distributed variables. The analyses were performed using SPSS 21.0 for Windows (Armonk, NY, USA: IBM Corp.). All statistical tests were two-sided and used a significance level of 0.05.

Results

TGFβ activation is upregulated in CDH

We first checked the expression of important factors in the TGFβ pathway in whole lung homogenates at mRNA level, which showed an increase in both the Tgfβr1 and Tgfβr2, but no differences in the ligand Tgfβ1. Both the receptor-activated Smads, Smad2 and Smad3, as well as the co-Smad, Smad4, which form together an important complex for the translocation into the cell nucleus, were increased in CDH (Figure 3.2A). No differences were found in expression of the ligand Tgfβ1 at protein level (Figure 3.2B). For the activation of this pathway, receptor-activated Smads are phosphorylated. The amount of phosphorylation of Smad2 was not different in whole lung homogenates of CDH pups compared to control (Figure 3.2C). Since the major problems in CDH are based on abnormalities in the pulmonary vasculature, we focused on changes in the small pulmonary vessels (25-50 μm) using immunofluorescence staining. This showed an increased number of SMA positive cells in the small vessels of CDH pups expressing phosphorylated Smad2 (pSmad2), which points to an increased activation of this pathway in the pulmonary vasculature (Figure 3.2D).

BMP activation is reduced in CDH

In contrast to the TGFβ receptors, we found a decrease in Bmpr1b in CDH and no differences in the well-studied Bmpr2 between both groups at mRNA level in whole lung homogenates. Activin receptor-like kinase 1 (Alk1), another receptor in the BMP/TGFβ pathway, was slightly increased in CDH. Bmp4, one of the important ligands in this pathway, and the receptor-activated Smad1 and Smad5 showed an increase in CDH (Figure 3.3A). Western blot on whole lung homogenates showed a decreased expression of Smad5 in CDH with no differences in relative phosphorylation (Figure 3.3B). However, when focusing on the pulmonary vasculature in detail, the number of SMA positive cells expressing phosphorylated Smad1/5/8 (pSmad158)

Figure 3.2 (following page): TGFβ activation is upregulated in CDH. (**A**) Quantitative PCR shows a significant increase in *Tgfβr1* and *Tgfβr2* in CDH (respectively $p < 0.001$ and $p = 0.033$), but no difference in *Tgfβ1*. Smad2, Smad3 and Smad4 are all significantly higher in CDH (respectively $p = 0.001$, $p = 0.002$ and $p = 0.002$). $N = 6$ for both groups. (**B**) Western blot on whole lung homogenates shows no differences in Tgfβ1 between control and CDH when corrected for total protein amount, using β-actin as a loading control. $N = 5$ for both groups. (**C**) pSmad2 protein expression related to the total Smad2 protein expression is not different between control and CDH in whole lung homogenates. Cofilin was used as a loading control. $N = 5$ for both groups. (**D**) Representative images of immunofluorescence staining show an increase of pSmad2/Sma double positive cells in small pulmonary vessels in CDH ($p = 0.049$). $N = 3$ samples for both groups. Per sample 6 vessels were counted. Scale bars represent 10 μm.
*$p < 0.05$, **$p < 0.01$, ***$p < 0.001$. Error bars represent SD.

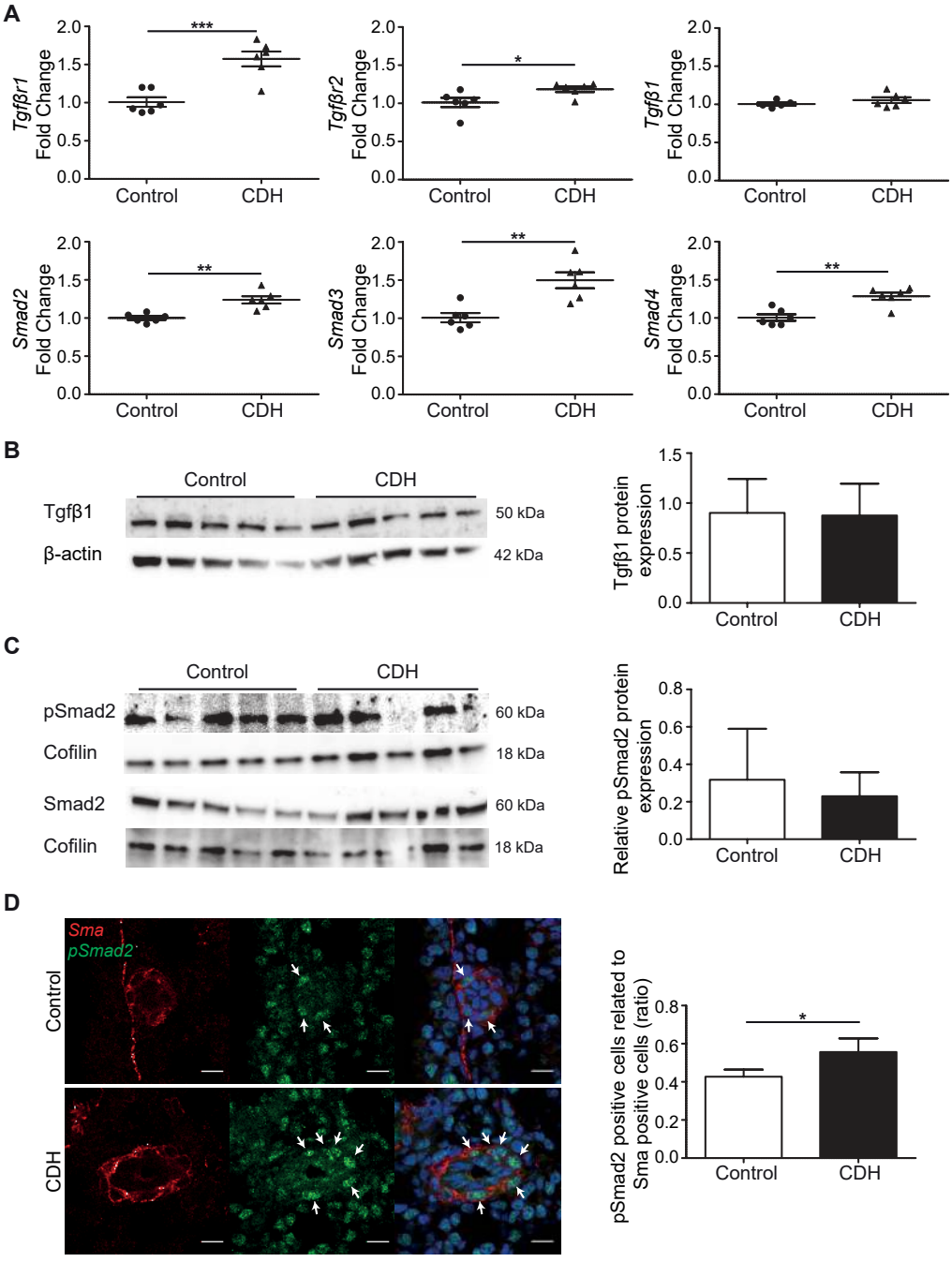
A
Tgfβr1 Fold Change
Tgfβr2 Fold Change
Tgfβ1 Fold Change
Smad2 Fold Change
Smad3 Fold Change
Smad4 Fold Change
Control
CDH
B
Control
CDH
Tgfβ1
β-actin
50 kDa
42 kDa
Tgfβ1 protein expression
C
pSmad2
Cofilin
Smad2
60 kDa
18 kDa
Relative pSmad2 protein expression
D
Sma
pSmad2
pSmad2 positive cells related to Sma positive cells (ratio)

was reduced in CDH on immunofluorescence staining, indicating decreased activation of this pathway in the pulmonary vasculature (Figure 3.3C).

Downstream effects of TGFβ and BMP signaling

Both the TGFβ and BMP pathways can be inhibited by the inhibitory Smads, Smad6 and Smad7. These proteins compete with Smad4 in the formation of complexes and can therefore prevent transcription of genes. We found no differences in expression of Smad6 at mRNA level, but Smad7 was slightly increased in CDH. Zeb2, a transcriptional corepressor of the activated pathway, showed an increase in CDH at mRNA level (Figure 3.4A). However, no significant differences in protein level of ZEB2 were found on western blot using whole lung homogenates (Figure 3.4B) and no clear changes were seen in expression in the small vessels with immunohistochemistry staining (Figure 3.4C). Since increased activation of the TGFβ pathway can induce proliferation of pulmonary artery smooth muscle cells, we checked the expression of Ki-67, a marker for proliferation. In small pulmonary vessels in CDH more SMA positive cells expressed Ki-67 (Figure 3.5A,B).

Discussion

In this paper we show the upregulated activation of the TGFβ pathway and downregulated activation of the BMP pathway in small pulmonary vessels in the nitrofen-CDH rat model.

No differences were observed in the amount of phosphorylation of the ligand TGFβ1 and both Smad2 and Smad5 at protein level in whole lung homogenates. Striking is that the total amount of Smad5 and pSmad5 were both less expressed at protein level in whole lung homogenates of CDH pups, but no changes were present in the relative phosphorylation in the total lung. However, the important pulmonary vessels of nitrofen-CDH pups showed increased expression of pSmad2 and decreased expression of pSmad1/5/8 in the smooth muscle layer specifically. Phosphorylation of the receptor-activated Smads is necessary for the activation of downstream mediators and plays therefore an important role in this pathway. The increased expression of the inhibitory Smad7 and corepressor Zeb2 at mRNA level might point to increased production of these inhibitors in order to inhibit the increased activity of the TGFβ pathway. The absence of changes in Smad6, which only inhibits the BMP pathway, strengthens this idea. However, the expression of ZEB2 at protein level in whole lungs only showed a trend to increase and no clear differences were seen on immunostaining of the pulmonary vessels. Both TGFβ and BMP can regulate proliferation of the vascular cells and previous studies have shown increased proliferation of pulmonary artery vascular smooth muscle cells from patients with PAH without CDH in response to TGFβ1 [21, 22]. We showed increased proliferation of the smooth muscle layer of small pulmonary vessels in the nitrofen-CDH pups as well, which might indicate an abnormal response of these cells to the increased TGFβ activity.

TGFβ has found to be a target candidate of retinoic acid (RA) [23]. Increased activity of the TGFβ pathway with higher levels of pSmad2 has been described in RA deficient foreguts and a mouse model with RA deficiency. In that study lung agenesis was observed both by decreasing RA levels as well as by increasing TGFβ levels, indicating the interaction between both pathways early in development [24]. Furthermore, a study in rats with alveolar hypoplasia caused by caloric restriction showed improvement of the alveolar formation after treatment with RA, accompanied by a decrease in TGFβ activity at postnatal day 21 [25]. These findings strengthen our results of increased TGFβ activity in the nitrofen treated rat model, where nitrofen has been shown to disrupt the retinoid signaling pathway [26]. Since a reduction in retinol and retinol binding protein (RBP) has been found in human newborns with CDH as well [27, 28], the increased activity of the TGFβ pathway might play an important role

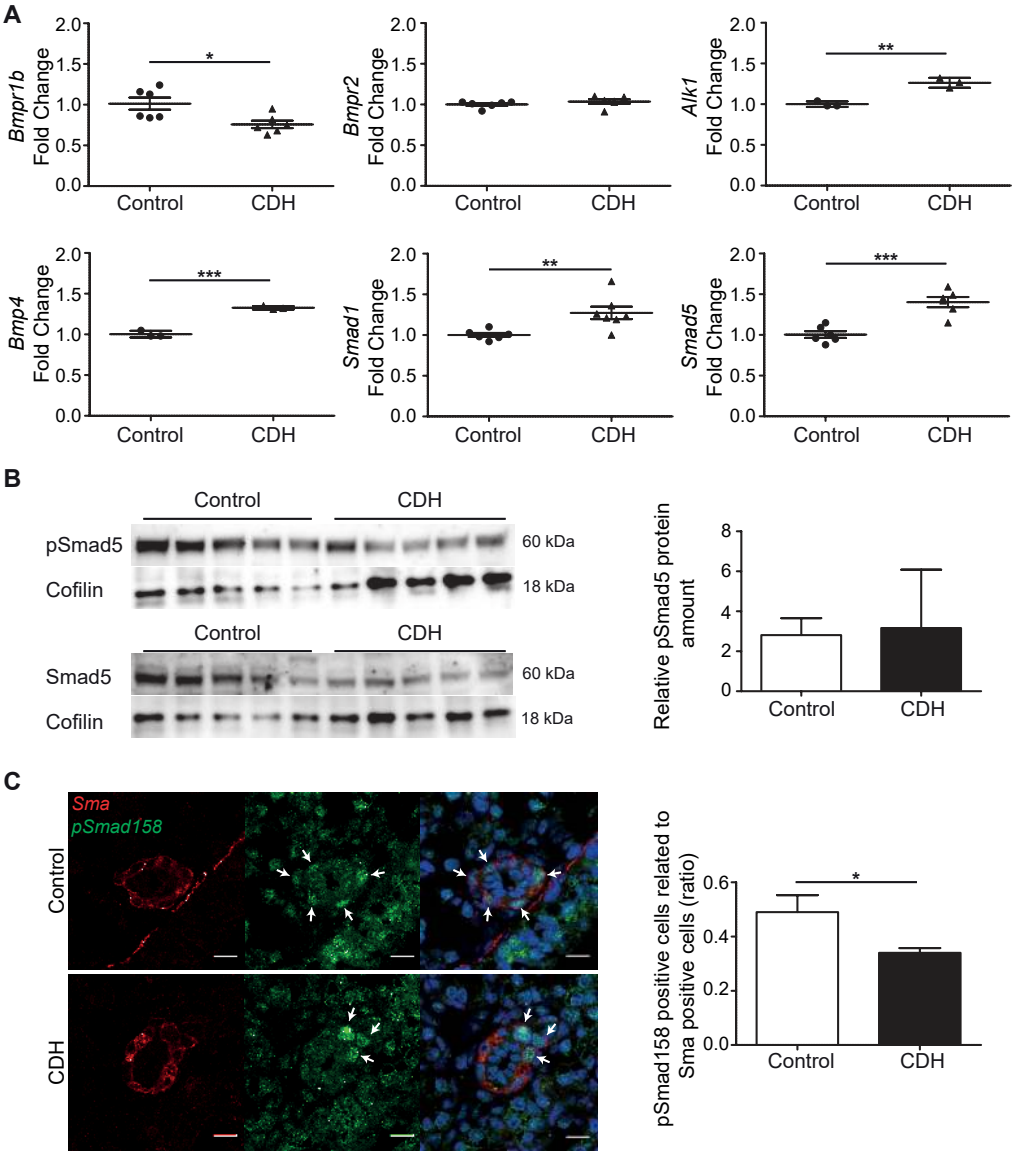

Figure 3.3: BMP activation is reduced in CDH. (**A**) Quantitative PCR shows a significantly decreased expression of Bmpr1b ($p = 0.016$), no differences in Bmpr2 and an increased expression of Alk1 ($p = 0.003$) in CDH. Bmp4, Smad1 and Smad5 are all significantly higher in CDH (respectively $p < 0.001$, $p = 0.009$ and $p < 0.001$). $N = 3$ (Alk1 and Bmp4) or 6 (rest) for both groups. (**B**) pSmad5 protein expression related to the total Smad5 protein expression is not different between control and CDH in whole lung homogenates. Cofilin was used as a loading control. $N = 5$ for both groups. (**C**) Representative images of immunofluorescence staining show a decrease of pSmd158/Sma double positive cells in small pulmonary vessels in CDH ($p = 0.016$). $N = 3$ samples for both groups. Per sample 6 vessels were counted. Scale bars represent 10 μm. *$p < 0.05$, **$p < 0.01$, ***$p < 0.001$. Error bars represent SD.

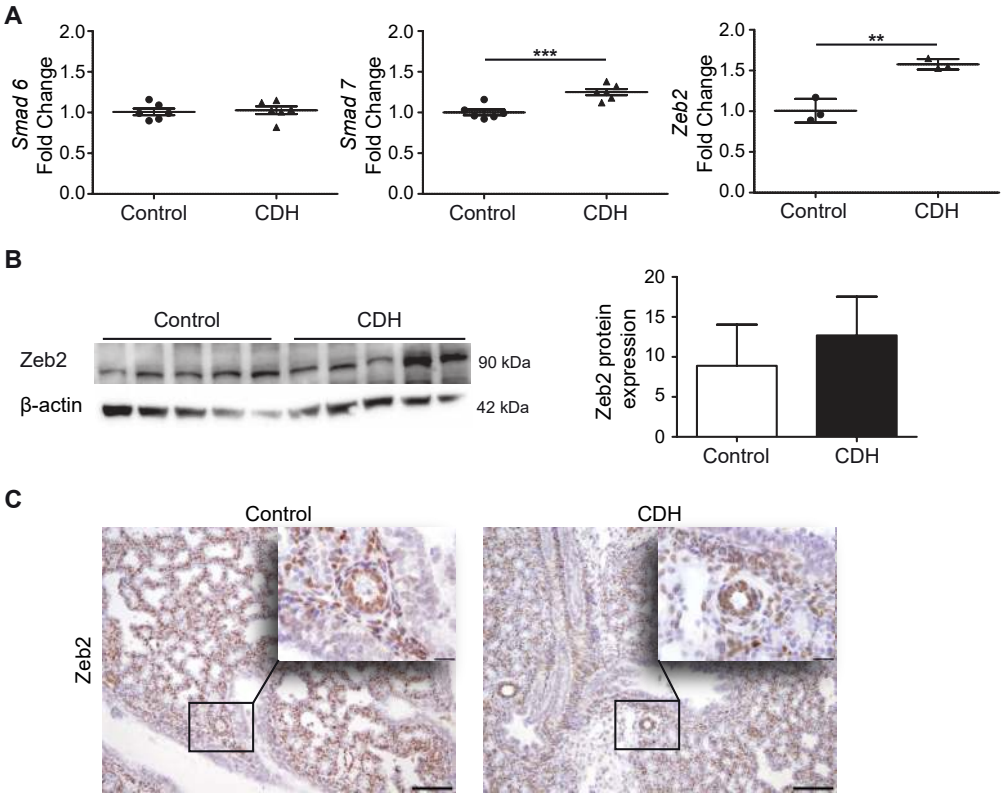

Figure 3.4: No clear differences in inhibitors of TGFβ in CDH (**A**) Quantitative PCR shows no difference in the inhibitory Smad6, but increased expression of inhibitory Smad7 and Zeb2 (respectively $p < 0.001$ and $p = 0.003$). $N = 3$ (Zeb2) or 6 (rest) per group. (**B**) Western blot of whole lung homogenates shows no differences of Zeb2 between both groups. β-actin was used as a loading control. $N = 5$ for both groups. (**C**) Representative images of immunohistochemistry staining show no differences in expression of Zeb2 in the small vessels of all lungs. $N = 3$ samples for both groups. Scale bars represent $100\mu m$ (low power) and $20\mu m$ (high power).
**$p < 0.01$, ***$p < 0.001$. Error bars represent SD.

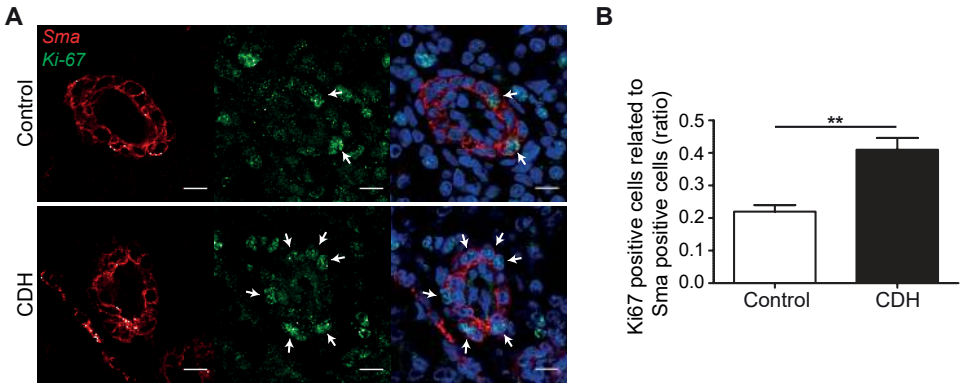

Figure 3.5: Increased proliferation of the muscular cells in the vessel wall in CDH. Representative images of immunofluorescence staining show an increase in Ki-67/Sma double positive cells in small pulmonary vessels in CDH ($p = 0.001$). $N = 3$ samples for both groups. Per sample 4 vessels were counted. Scale bars represent $10\mu m$.
*$p < 0.05$, **$p < 0.01$, ***$p < 0.001$. Error bars represent SD.

in this disease. The previous described involvement of TGFβ and BMP in the proliferation of pulmonary vascular cells [21, 22] in combination with our results on the relation between proliferation and TGFβ/BMP activation in the pulmonary vasculature possibly indicate a role of these pathways in the development of the pulmonary vasculature and pulmonary hypertension in particular.

The inconsistent results found in the literature on the expression of different factors in this pathway might possibly be explained by the large differences during gestation. In this study we found some variability between samples as well, showing that only small differences in age might already have large consequences.

In conclusion, we found increased phosphorylation of Smad2 and decreased phosphorylation of Smad5 in the vessel wall of small pulmonary vessels of nitrofen-CDH pups, indicating an increased activation of the TGFβ pathway and a decreased activation of the BMP pathway in the pulmonary vasculature of these animals at day 21 of gestation, possibly leading to increased proliferation of the muscularized vessel wall. Since the different factors in these pathways are differently expressed during gestation and might differ from the human situation, further research has to be done at different developmental stages and most importantly in material of human patients.

References

[1] Sluiter I, van der Horst I, et al. Premature differentiation of vascular smooth muscle cells in human congenital diaphragmatic hernia. Exp Mol Pathol. 2013;94(1):195–202.

[2] Ma L, Chung WK. The role of genetics in pulmonary arterial hypertension. J Pathol. 2017;241(2):273–280.

[3] Alejandre-Alcazar MA, Michiels-Corsten M, et al. TGF-beta signaling is dynamically regulated during the alveolarization of rodent and human lungs. Dev Dyn. 2008;237(1):259–69.

[4] Chen H, Sun J, et al. Abnormal mouse lung alveolarization caused by Smad3 deficiency is a developmental antecedent of centrilobular emphysema. Am J Physiol Lung Cell Mol Physiol. 2005;288(4):L683–91.

[5] Eickelberg O, Morty RE. Transforming growth factor beta/bone morphogenic protein signaling in pulmonary arterial hypertension: remodeling revisited. Trends Cardiovasc Med. 2007;17(8):263–9.

[6] Teramoto H, Shinkai M, et al. Altered expression of angiotensin II receptor subtypes and transforming growth factor-beta in the heart of nitrofen-induced diaphragmatic hernia in rats. Pediatr Surg Int. 2005;21(3):148–52.

[7] Xu C, Liu W, et al. Effect of prenatal tetrandrine administration on transforming growth factor-beta1 level in the lung of nitrofen-induced congenital diaphragmatic hernia rat model. J Pediatr Surg. 2009;44(8):1611–20.

[8] Vuckovic A, Herber-Jonat S, et al. Increased TGF-beta: a drawback of tracheal occlusion in human and experimental congenital diaphragmatic hernia? Am J Physiol Lung Cell Mol Physiol. 2016;310(4):L311–27.

[9] Candilera V, Bouche C, et al. Lung growth factors in the amniotic fluid of normal pregnancies and with congenital diaphragmatic hernia. J Matern Fetal Neonatal Med. 2016;29(13):2104–8.

[10] Zimmer J, Takahashi T, et al. Decreased Endoglin expression in the pulmonary vasculature of nitrofen-induced congenital diaphragmatic hernia rat model. Pediatr Surg Int. 2017;33(2):263–268.

[11] Gosemann JH, Friedmacher F, et al. Disruption of the bone morphogenetic protein receptor 2 pathway in nitrofen-induced congenital diaphragmatic hernia. Birth Defects Res B Dev Reprod Toxicol. 2013;98(4):304–9.

[12] Makanga M, Dewachter C, et al. Downregulated bone morphogenetic protein signaling in nitrofen-induced congenital diaphragmatic hernia. Pediatr Surg Int. 2013;29(8):823–34.

[13] Emmerton-Coughlin HM, Martin KK, et al. BMP4 and LGL1 are Down Regulated in an Ovine Model of Congenital Diaphragmatic Hernia. Front Surg. 2014;1:44.

[14] Hofmann A, Gosemann JH, et al. Imbalance of caveolin-1 and eNOS expression in the pulmonary vasculature of experimental diaphragmatic hernia. Birth Defects Res B Dev Reprod Toxicol. 2014;101(4):341–6.

[15] Hofmann AD, Zimmer J, et al. The Role of Activin Receptor-Like Kinase 1 Signaling in the Pulmonary Vasculature of Experimental Diaphragmatic Hernia. Eur J Pediatr Surg. 2016;26(1):106–11.

[16] Corbett HJ, Connell MG, et al. ANG-1 TIE-2 and BMPR signalling defects are not seen in the nitrofen model of pulmonary hypertension and congenital diaphragmatic hernia. PLoS One. 2012;7(4):e35364.

[17] Chiu JS, Ma L, et al. Mutations in BMPR2 are not present in patients with pulmonary hypertension associated with congenital diaphragmatic hernia. J Pediatr Surg. 2017;.

[18] Greer JJ, Allan DW, et al. Recent advances in understanding the pathogenesis of nitrofen-induced congenital diaphragmatic hernia. Pediatr Pulmonol. 2000;29(5):394–9.

[19] Rajatapiti P, van der Horst IW, et al. Expression of hypoxia-inducible factors in normal human lung development. Pediatr Dev Pathol. 2008;11(3):193–9.

[20] Seuntjens E, Nityanandam A, et al. Sip1 regulates sequential fate decisions by feedback signaling from postmitotic neurons to progenitors. Nat Neurosci. 2009;12(11):1373–80.

[21] Morrell NW, Yang X, et al. Altered growth responses of pulmonary artery smooth muscle cells from patients with primary pulmonary hypertension to transforming growth factor-beta(1) and bone morphogenetic proteins. Circulation. 2001;104(7):790–5.

[22] Thomas M, Docx C, et al. Activin-like kinase 5 (ALK5) mediates abnormal proliferation of vascular

smooth muscle cells from patients with familial pulmonary arterial hypertension and is involved in the progression of experimental pulmonary arterial hypertension induced by monocrotaline. Am J Pathol. 2009;174(2):380–9.

[23] Balmer JE, Blomhoff R. Gene expression regulation by retinoic acid. J Lipid Res. 2002;43(11):1773–808.

[24] Chen F, Desai TJ, et al. Inhibition of Tgf beta signaling by endogenous retinoic acid is essential for primary lung bud induction. Development. 2007;134(16):2969–79.

[25] Londhe VA, Maisonet TM, et al. Retinoic acid rescues alveolar hypoplasia in the calorie-restricted developing rat lung. Am J Respir Cell Mol Biol. 2013;48(2):179–87.

[26] Beurskens N, Klaassens M, et al. Linking animal models to human congenital diaphragmatic hernia. Birth Defects Res A Clin Mol Teratol. 2007;79(8):565–72.

[27] Beurskens LW, Tibboel D, et al. Retinol status of newborn infants is associated with congenital diaphragmatic hernia. Pediatrics. 2010;126(4):712–20.

[28] Major D, Cadenas M, et al. Retinol status of newborn infants with congenital diaphragmatic hernia. Pediatr Surg Int. 1998;13(8):547–9.

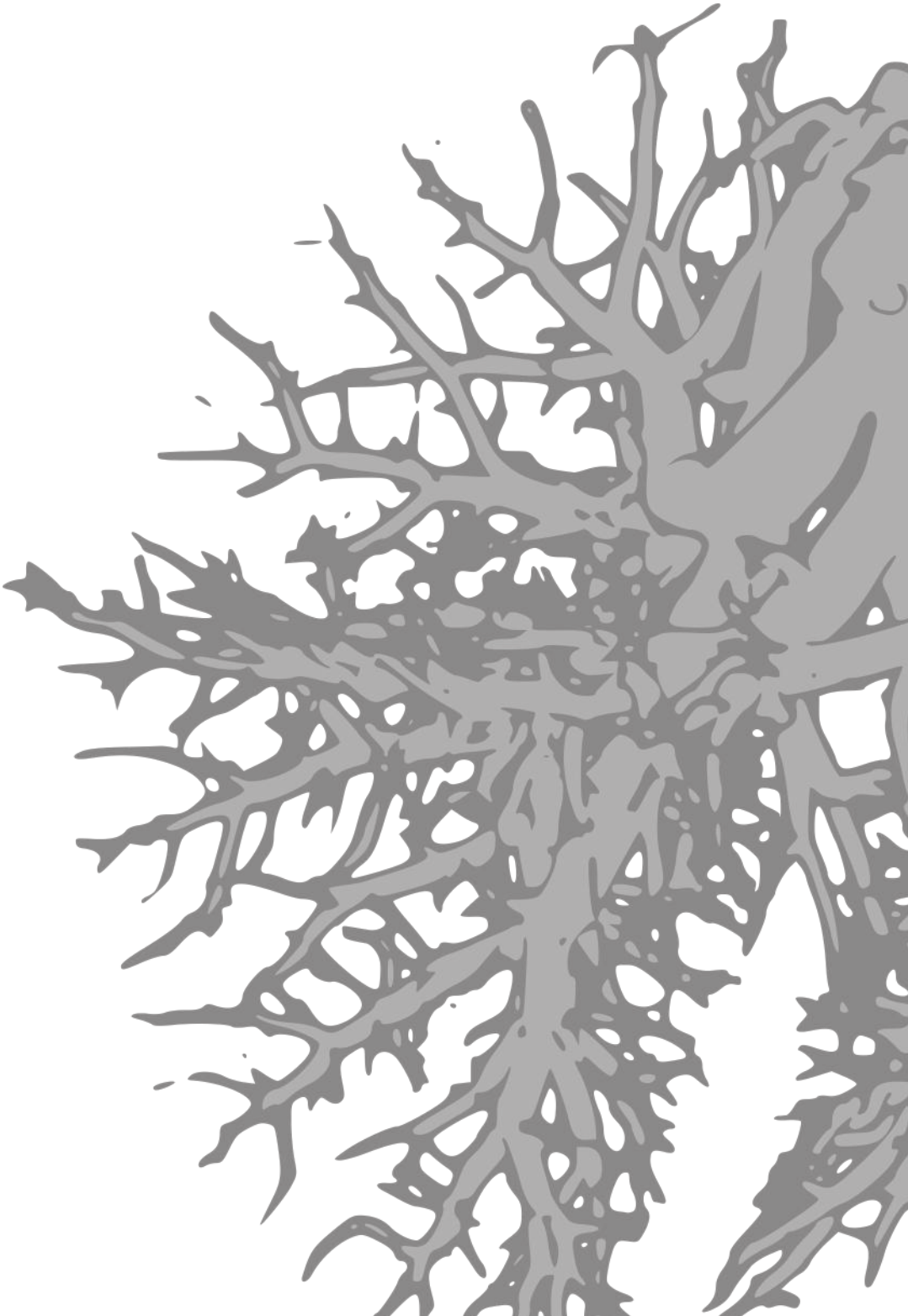

Chapter 4

Changes in vasoactive pathways in congenital diaphragmatic hernia associated pulmonary hypertension explain unresponsiveness to pharmacotherapy

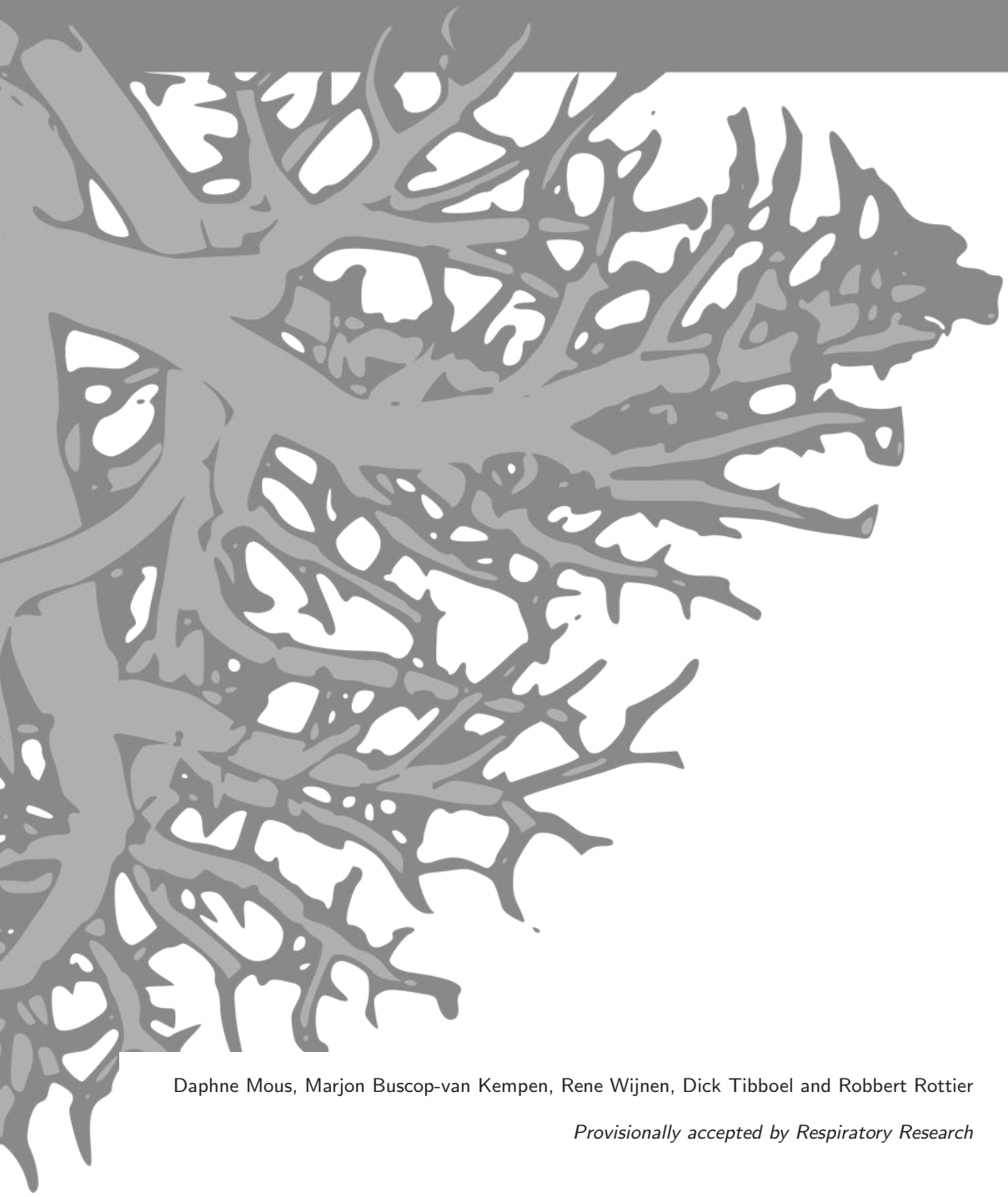

Daphne Mous, Marjon Buscop-van Kempen, Rene Wijnen, Dick Tibboel and Robbert Rottier

Provisionally accepted by Respiratory Research

Abstract

Background: Patients with congenital diaphragmatic hernia (CDH) have structural and functional different pulmonary vessels, leading to pulmonary hypertension. They often fail to respond to standard vasodilator therapy targeting the major vasoactive pathways, causing a high morbidity and mortality. We analyzed whether the expression of crucial members of these vasoactive pathways could explain the lack of responsiveness to therapy in CDH patients.

Methods: The expression of direct targets of current vasodilator therapy in the endothelin and prostacyclin pathway was analyzed in human lung specimens of control and CDH patients.

Results: CDH lungs showed increased expression of both ETA and ETB endothelin receptors and the rate-limiting Endothelin Converting Enzyme (ECE-1), and a decreased expression of the prostaglandin-I_2 receptor (PTGIR). These data were supported by increased expression of both endothelin receptors and ECE-1, endothelial nitric oxide synthase and PTGIR in the well-established nitrofen-CDH rodent model.

Conclusions: Together, these data demonstrate aberrant expression of targeted receptors in the endothelin and prostacyclin pathway in CDH already early during development. The analysis of this unique patient material may explain why a significant number of patients do not respond to vasodilator therapy. This knowledge could have important implications for the choice of drugs and the design of future clinical trials internationally.

Background

Pulmonary hypertension (PH) is the leading cause of morbidity and mortality in patients with congenital diaphragmatic hernia (CDH) [1]. The altered development of the pulmonary vasculature and the disordered pulmonary vascular remodeling [2] in combination with the imbalance of vasoactive mediators caused by endothelial dysfunction result in the arrest of pulmonary vascular growth in these patients. Current treatment of CDH patients is not evidence based [3] and is derived from studies in adults, leading mainly to off-label and unlicensed use of drugs. Current knowledge is based on compassionate use and case reports, while some patients with CDH were included in trials that were underpowered for definitive conclusions. Even international therapy guidelines are based on consensus only (level 3 evidence) [4]. In 2012, experts evaluated the current antenatal and postnatal management of CDH and emphasized the importance of optimal management of PH in these patients [5]. Worldwide, PH treatment is mainly directed against the receptors of the endothelin (ET) and prostacyclin (PGI_2) pathways or the conversion of cyclic guanosine monophosphate (cGMP) in the nitric oxide (NO) pathway (Figure 4.1A). In spite of these targeted treatments, it is still largely unknown how the different components of these pathways are expressed in lungs of unaffected individuals and CDH patients.

Previous studies reported increased levels of both the endothelin A (ETA) and B (ETB) receptors in human CDH as well as in the nitrofen rat model [6, 7]. Endothelin-1 (ET-1) is a potent vasoconstrictor [8] and is increased in lung tissue of patients with pulmonary hypertension. Moreover, high plasma levels of circulating ET-1 associated with the severity of PH in human CDH [9]. NO reduces the affinity of the ETA receptor for ET-1 and may therefore terminate the ET-1 mediated signaling [10]. NO is synthesized by different NO synthases (NOS), of which endothelial NOS (eNOS) was decreased in some human and rat CDH studies [11–13]. However, we and others showed no differences or even an increased expression of eNOS in both human and rat CDH [14–17]. PGI_2 is an important mediator of vasodilation, acting through the prostaglandin-I_2 receptor (PTGIR) [18]. Several prostacyclin receptor agonists have been used in the treatment of persistent pulmonary hypertension of the newborn with variable effects [19–21]. Limited data are available about the use of these drugs in patients with CDH, but the few case reports show contrasting results [22–24]. An overview of the current data for human and the rat model is provided (Table 4.1 and 4.2).

Since CDH patients respond poorly to current treatment strategies, we analyzed for the first time the expression of the direct targets of the most commonly used vasodilator drugs, as well as some of the important members of all three major pathways. Using unique patient lung material, we show an increased expression of both endothelin receptors and the rate-limiting endothelin converting enzyme (ECE-1), as well as a decreased expression of the prostaglandin-I_2 receptor in human CDH. Moreover, we found changes in the expression of these and other important factors of the pathways in rat CDH (Figure 4.1B).

Methods

Human Lung Samples

Human lung samples were retrieved from the archives of the Department of Pathology of the Erasmus Medical Center, Rotterdam. In our high-volume, leading center of the EURO consortium [4], approximately 15 to 20 CDH patients a year are born, which ensures a large experience in the treatment of this disease. Paraffin-embedded lung samples, which did not show severe hemorrhage or necrosis, were selected of control and CDH patients and of patients with lung hypoplasia or pulmonary hypertension with other cause than CDH. Only the most extreme cases of left-sided CDH with a survival of less than 7 hours were selected to prevent secondary sequelae. Patient characteristics are described in Table 4.3.

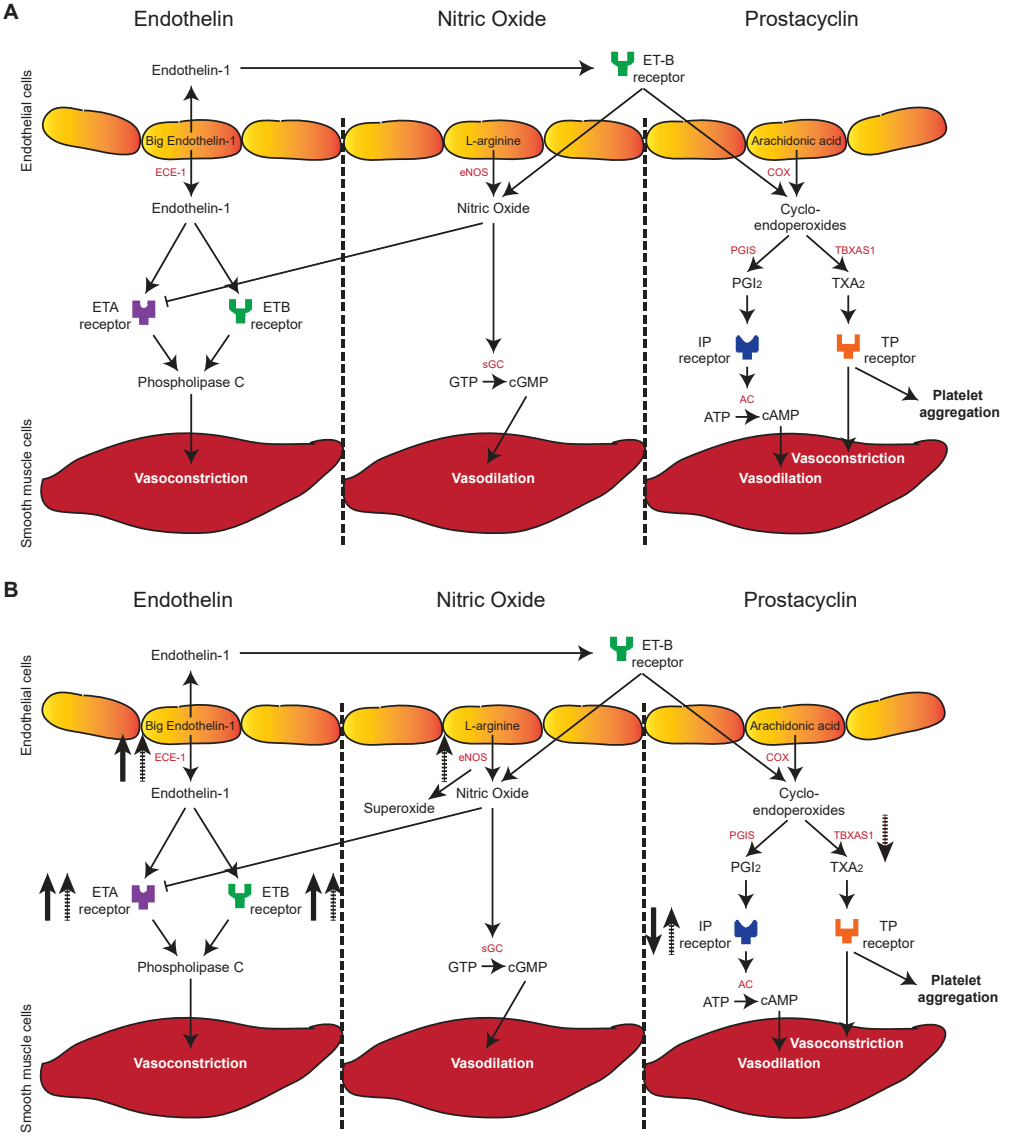

Figure 4.1: Pathways in vasodilation and vasoconstriction Overview of the major pathways involved in vasodilation and vasoconstriction (**A**) and the aberrant expression in both human and rat congenital diaphragmatic hernia (CDH) (**B**).
Solid arrows represent up- or downregulation in human CDH, dashed arrows represent up- or downregulation in rat CDH. ECE-1 = endothelin converting enzyme 1, ETA = endothelin A, ETB = endothelin B, eNOS = endothelial nitric oxide synthase, sGC = soluble guanylate cyclase, COX = cyclooxygenase, PGIS = prostaglandin synthase, PGI_2 = prostaglandin-I_2, AC = adenylate cyclase, TBXAS1 = thromboxane synthase, TXA_2 = thromboxane.

Table 4.1: Overview of studies in human CDH

Our group	Others
Increased expression of ETA and ETB (protein level), Increased expression of ECE-1 (protein level)	Increased ET-1 (plasma levels and protein level) [25], Increased ET-1 (plasma levels) [9], Increased expression of ETA and ETB (RNA and protein level) [6]
No differences in eNOS expression [15]	Increased expression of eNOS in arteriolar endothelium and alveolar epithelium (protein level) [16], No differences in eNOS expression (protein level) [12], Decreased expression of eNOS (protein and RNA level) [13]
Decreased expression of Ptgir (protein level)	No information about prostaglandin-I_2

Table 4.2: Overview of studies in experimental rat CDH

Our group	Others
Increased expression of ETA (RNA and protein level) and ETB (RNA level), Increased expression of ECE-1 (RNA level)	Increased expression of ETA and ETB (RNA and protein level) [7], Increased expression of ET-1 after 1 and 6 hours of ventilation (RNA level) [17], Increased response of arterioles to ET-1 [26]
Increased expression of eNOS (RNA and protein level)	Increased expression of eNOS (RNA and protein level) [14], Increased expression of eNOS after 1 hour of ventilation (RNA level) [17], Decreased expression of eNOS (RNA and protein level) [11]
Increased expression of Ptgir (RNA level) and decreased expression of Tbxas1 (RNA level)	Increased levels of prostaglandin-I_2 and an increased ratio of prostaglandin-I_2 and thromboxane (protein level) [27]

Table 4.3: Patient characteristics

Disease	GA	Sex	Age of death	Cause of death
Control	18+0	Male	-	Abortion
	24+6	Female	Minutes	Prematurity
	26+5	Female	1 hour	Prematurity
	33+0	Male	Minutes	Developmental delay
	38+3	Male	Minutes	Asphyxia
	38+5	Male	1.5 hours	Anencephaly
	40+0	Female	18 hours	Asphyxia
CDH	17+6	Male	-	Abortion
	21+4	Male	-	Abortion
	36+2	Male	Some hours	Respiratory failure
	36+2	Female	Some hours	Respiratory failure
	37+2	Male	7 hours	Respiratory failure
	38+0	Male	2 hours	Respiratory failure
	40+0	Female	Some hours	Respiratory failure
LH	22+3	Male	-	Abortion
	28+5	Female	15 minutes	Respiratory failure
	41+0	Male	30 minutes	Respiratory failure
PH	34+3	Female	4 days	PPHN
	37+1	Male	4 days	Respiratory failure

GA = gestational age (weeks + days), CDH = congenital diaphragmatic hernia, LH = lung hypoplasia, PH = pulmonary hypertension, PPHN = persistent pulmonary hypertension of the newborn.

Animal Model

The well-established animal model was used, where in short pregnant Sprague-Dawley rats received either 100 mg nitrofen dissolved in 1 ml olive oil or just 1 ml olive oil by gavage on gestational age day E9.5. Nitrofen induces left-sided CDH in approximately 70% of the offspring, while all pups have pulmonary hypertension. At day E21 pups were delivered by caesarean section and euthanized by lethal injection of pentobarbital.

All animal experiments were approved by an independent animal ethical committee and according to national guidelines.

Immunohistochemistry and Immunofluorescence Staining

Immunohistochemistry (IHC) was performed on 5 μm paraffin sections of lungs of both rats and humans according to standard protocols, using the Envision^{TM} detection system (Dako Cytomatic, Glostrup, Denmark) [28]. Primary antibodies used for IHC were Endothelin receptor A (ETA; 1:5000 (rat) 1:100 (human); Alamone, Jerusalem, Israel), Endothelin receptor B (ETB; 1:2500 (rat) 1:500 (human); Alamone), Endothelin Converting Enzyme (ECE-1; 1:500 (human); Abcam, Cambridge, MA, USA), endothelial nitric oxide synthase (eNOS; 1:400 (rat); Thermo Fisher Scientific, Waltham, MA, USA) and prostaglandin-I_2 receptor (Ptgir; 1:1000 (rat) 1:500 (human); Cayman Chemical, Ann Arbor, Michigan, USA). Antigen retrieval with Tris-EDTA buffer (pH 9.0) was used. Negative controls were performed by omitting the primary antibody.

Table 4.4: Primer sequences

Gene	Sequence (forward 5'- 3')	Sequence (reverse 5'- 3')
Eta	AACCTGGCAACCATGAACTC	ATGAGGCTTTTGGACTGGTG
Etb	CAGGATTCTGAAGCTCACCCTTT	TCCAAAACCAGCAAAAAACTCA
Et-1	TGTGCTCACCAAAAAGACAAGAA	GGTACTTTGGGCTCGGAGTTC
Ece-1	GCAAGAACATAGCCAGCGAG	CTCCGAGTATCTTCATCCATCC
eNos	CATACTTGAGGATGTGGCTG	CCACGTTAATTTCCACTGCT
Sma	TGACCCAGATTATGTTTGAGAC	AGAGTCCAGCACAATACCAG
Ptgis	CATCAAACAGTTTGTGGTCCT	CAAAGCCATATCTGCTAAGGT
Ptgir	CACGAGAGGATGAAGTTTACCA	AATCCTCTGATCGTGAGAGGC
Tbxas1	AGACTCAGGTTCCACTTCAG	TCACACCTGCCTTCTATGTC
Tbxa2r	ACTGTGAGGTGGAGATGATGG	CAGGATGAAGACCAGCAAGG
Actb	AGATGACCCAGATCATGTTTGAG	GTACGACCAGAGGCATACAG

Quantitative Real-Time Polymerase Chain Reaction (qPCR)

RNA isolation of whole lungs of rat pups, cDNA synthesis and subsequent qPCR analysis was performed as previously described [28]. The gene-specific primers used are listed in Table 4.4. *Actb* was used as housekeeping gene.

Statistical Analyses

Data are presented as percentages, means (SD) for normally distributed variables. Univariate analyses were performed using independent samples t-tests for normally distributed variables. The analyses were performed using SPSS 21.0 for Windows (Armonk, NY, USA: IBM Corp.). All statistical tests were two-sided and used a significance level of 0.05.

Results

In order to identify a possible explanation for the unresponsiveness of CDH patients to different vasodilator therapies, the expression of receptors which are currently targeted during treatment as well as other critical factors of the different vasoactive pathways were analyzed. Therefore, a unique set of lungs from CDH patients were used and these data were verified using the more dynamical nitrofen rat model.

Human

Since current treatment is, besides the use of inhaled NO (iNO), based on targeting the receptors in both the prostacyclin and endothelin pathway, we started by analyzing the expression of the critical proteins of both pathways in human lungs of control and CDH patients. Previously, we and others already showed no apparent differences in the NO pathway [12, 15]. Immunohistochemistry was used to determine the expression pattern of the receptors in lung samples of CDH patients and age-matched controls. Human control lung samples showed little expression of the main target of the prostacyclin therapy, the important prostacyclin receptor PTGIR, in the fetal period, which sharply increased later during gestation at the preterm and term age (Figure 4.2A). However this significant increase was absent in CDH (Figure 4.2B). The ETA receptor, which induces vasoconstriction and cell proliferation, was expressed in the small (25-50 μm) and larger ($> 50\mu m$) vessels as well as in the very small capillaries $< 25\mu m$) in CDH, contrasting the control lungs in which only the small and larger

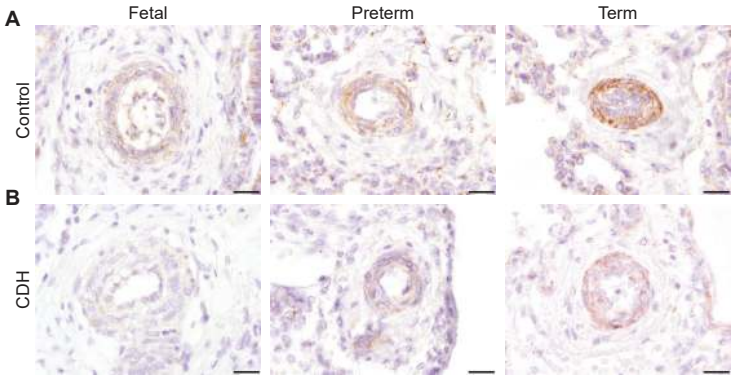

Figure 4.2: Suppressed progression of prostaglandin-I_2 receptors during gestation in human CDH
Representative images show progressive expression of PTGIR in the vessels during gestation in human control patients (**A**). In human CDH patients there is only progression to a lesser extent (**B**).
Scale bars represent $20\mu m$. Patients: GA 18+0, 33+0 and 38+0 (control), GA 21+4, 36+2 and 37+2 (CDH).

vessels expressed this receptor (Arrowheads in Figure 4.3A,B). The ETB receptor, involved in vasodilation through the release of NO and PGI_2 (Figure 4.1), was expressed both in the bronchial epithelium and in some of the larger vessels ($> 50\mu m$) in CDH (Arrowheads in Figure 4.3A,B), whereas in control lungs expression of ETB was found only in the bronchial epithelium (Figure 4.3B). Since ECE-1, a membrane-bound metalloprotease that converts big-endothelin into the biologically active compound, is the rate-limiting factor in the ET pathway, we analyzed this enzyme as well in the human samples. Early during gestation, in the fetal period, ECE-1 is minimally expressed in the vessels of the human control lung samples, with an increase at preterm and term age (Figure 4.3C). Increased expression of this enzyme at both fetal, preterm and term age was observed in CDH (Figure 4.3D), indicating a potential increased bio-availability of active ET-1.

To exclude that the differences in expression patterns of the crucial prostacyclin and endothelin receptors and the rate-limiting factor ECE-1 was solely an effect of lung hypoplasia (LH) or PH, we performed immunohistochemistry on lungs of patients with LH and PH with other cause than CDH. The PTGIR receptor expression was reduced in both LH and PH (Figure 4.4A). Increased expression of ETA was detected in the smallest vessels in lungs of both LH and PH (Arrowheads in Figure 4.4B), whereas increased expression of ETB was only observed in both small and very small vessels of lungs of PH patients (Arrowheads in Figure 4.4C). ECE-1 was not expressed differently in both LH and PH lung samples (Figure 4.4D).

Rat

In order to validate these interesting human data, we evaluated the expression patterns of the proteins of these three pathways in the nitrofen rat model, which was supplemented with RNA and protein expression analysis of related factors. Real-time qPCR showed that the mRNA expression of both the *Eta* and *Etb* receptors was significantly higher in lungs of E21 pups with CDH compared to those of control pups. We also analyzed the expression of the ETA and ETB ligand, *Et-1*, but no significant differences were found between the groups. However, the mRNA encoding the rate-limiting factor *Ece-1* was significantly increased in CDH compared to control, confirming the human data (Figure 4.5A). Next, we analyzed the protein expression pattern of the ET receptors with immunohistochemistry. The ETA receptor was expressed

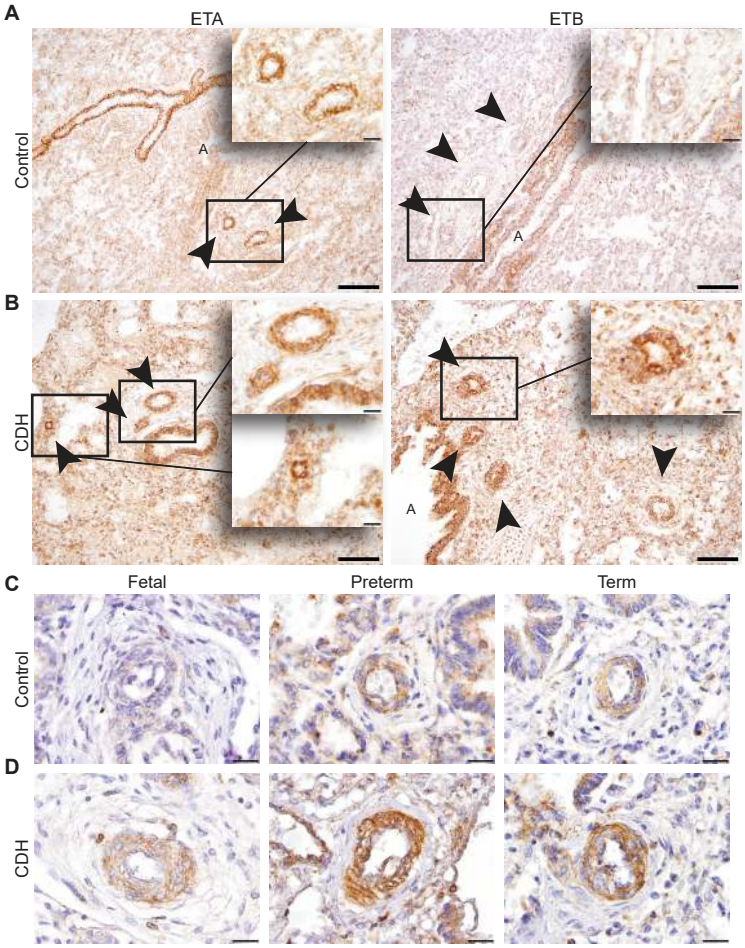

Figure 4.3: Increased expression of both the ETA and ETB receptor and endothelin converting enzyme in human CDH. Representative images show expression of the ETA receptor in the larger vessels and no expression of ETB in control (**A**), where there is increased expression of ETA in the smaller vessels in CDH patients and expression of the ETB receptor in some of the vessels in CDH (**B**). ECE-1 is progressively expressed in the vessels in human control patients during gestation (**C**), where this expression is decreased in CDH patients at both fetal, preterm and term age (**D**).
Arrows indicate vessels, A indicates airways. Scale bars represent 100 μm (low power) and 20 μm (high power). Patients: GA 38+3 (control), GA 38+0 and 37+2 (CDH) (A+B). Patients: GA 18+0, 26+5 and 38+0 (control), GA 21+4, 36+2 and 37+2 (CDH) (C+D).

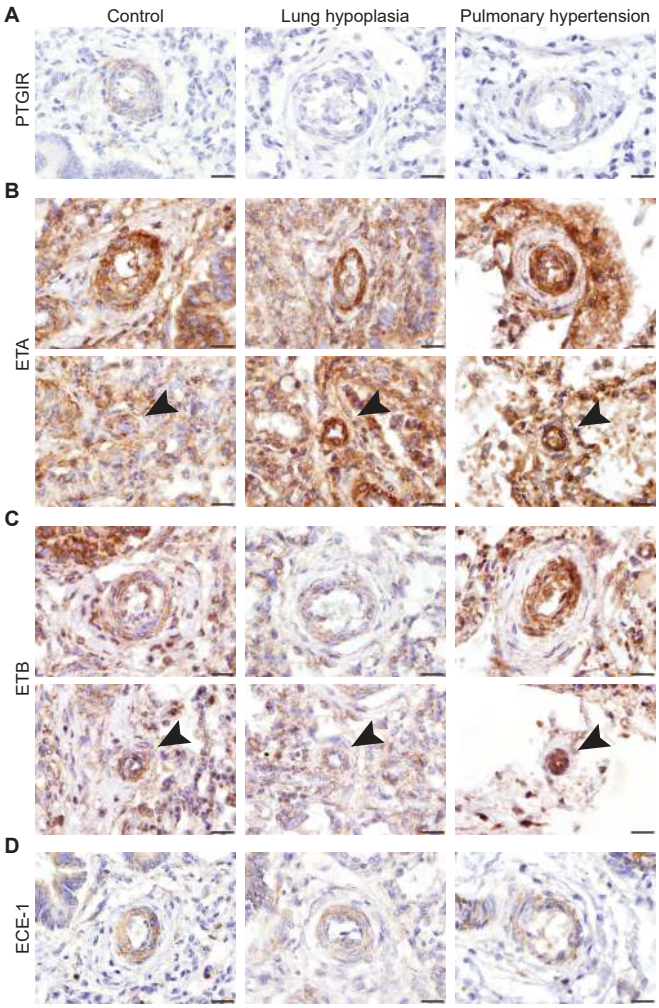

Figure 4.4: Expression of prostaglandin and endothelin factors in human LH and PH patients Representative images show decreased expression of PTGIR in both patients with LH and PH (**A**). The expression of ETA is increased in the smaller vessels of patients with lung hypoplasia (LH) and pulmonary hypertension (PH) with other cause than CDH (**B**) and the expression of ETB is only increased in the vessels of patients with PH (**C**). ECE-1 is not differently expressed in the vessels both LH and PH lung samples (**D**).
Scale bars represent 20 μm. Arrows indicate very small vessels. Patients: GA 38+3 (control), GA 41+0 (LH), GA 34+3 (PH).

in the small capillaries of both groups at E15 until E21 with a stronger expression level in CDH (Figure 4.5B). At E21 only CDH lungs showed expression of the ETA receptor in the larger vessels ($> 50\mu m$) (Arrowheads in Figure 4.5C). The ETB receptor was expressed in the bronchial epithelium of all lungs without significant differences between control and CDH at all ages (Figure 4.5D-E). There was a significant higher mRNA expression of *eNos* in CDH rats compared to control in relation to all cells as well as in relation to only the smooth muscles cells (Figure 4.6A) or endothelial cells (data not shown). This increased expression was clearly detectable with immunostaining in the larger and smaller ($< 50\mu m$) vessels at E21 (Arrowheads in Figure 4.6B). However, no obvious differences were noted earlier during development (E15 till E19) (Figure 4.6C). Although there was no difference in expression of prostaglandin-I_2 synthase (*Ptgis*) between control and CDH rat pups, there was a slight increase in the expression of *Ptgir* and the prostaglandin-E1 receptor (*Ptger1*) in CDH at the mRNA level in both the whole lung as well as compared to the number of smooth muscle cells. In contrast, thromboxane synthase (*Tbxas1*), a contractile ligand in the prostanoid pathway, was clearly lower expressed in CDH, whereas the thromboxane receptor (*Tbxa2r*) did not show significant differences (Figure 4.7A). However immunostaining showed no clear differences in the vessels between both groups (Arrowheads in Figure 4.7B).

Discussion

This is the first study showing the aberrant expression of different important factors in the endothelin, NO and PGI_2 pathways all combined together in CDH patients (Figure 4.1B) and human patients with LH or PH with other cause, possibly explaining why a large number of patients do not respond to the current vasodilator therapy. We focused our research on direct targets of the most frequent used drugs to investigate the effectiveness of the current approach and combined this with the analysis of some key factors of the different pathways.

Since our unique human CDH material is scarce and a limiting factor, because only specimens of newborns who lived for a short period were analyzed to prevent secondary morphological changes, supplemental analyses were done on lung tissue of the dynamical nitrofen rat model.

In line with previous results in both human and rat studies, we found a significant increased expression of the ETA and ETB receptor, important targets of vasodilator therapy, in human CDH patients and the nitrofen rat model [6, 7, 29]. However, we are the first to show an increased expression of the crucial ECE-1 enzyme in both human pulmonary vessels of CDH patients and whole lung homogenates of nitrofen treated rat pups. ECE-1 converts big ET-1 into the active form of ET-1 and is the rate-limiting step in the production of ET-1 [30]. Although there was no apparent difference in total ET-1 in CDH pups, the higher expression of ECE-1 in lungs of CDH pups may lead to an increase in the active form of ET-1.

In contrast to other studies [11–13, 29], we found an increased expression of eNOS in CDH rats. The increased eNOS expression in CDH may be explained by activation of eNOS because of the decreased NO availability, or the process of eNOS uncoupling. In case of decreased bioavailability of the cofactor tetrahydrobiopterin (BH4), eNOS produces superoxide instead of NO [31]. This superoxide leads to oxidative stress, which has been observed in vessels of patients with PH [32]. The enhanced activation of the ETA receptor might lead to the increase in superoxide production through the induction of reactive oxygen species (ROS) and can thereby induce SMC proliferation and vasoconstriction. Thus, eNOS uncoupling leads to a reduction in NO bioavailability without a necessary change in the amount of eNOS [31]. Previously, we showed a slight increase in expression of the cGMP-specific phosphodiesterase 5 (Pde5) in nitrofen treated rat pups. However, no differences were found in its phosphorylation or its downstream targets, protein kinase G1 (Prkg1) and Prkg2 [33].

The increased expression of PTGIR in control lungs during gestation could be expected since

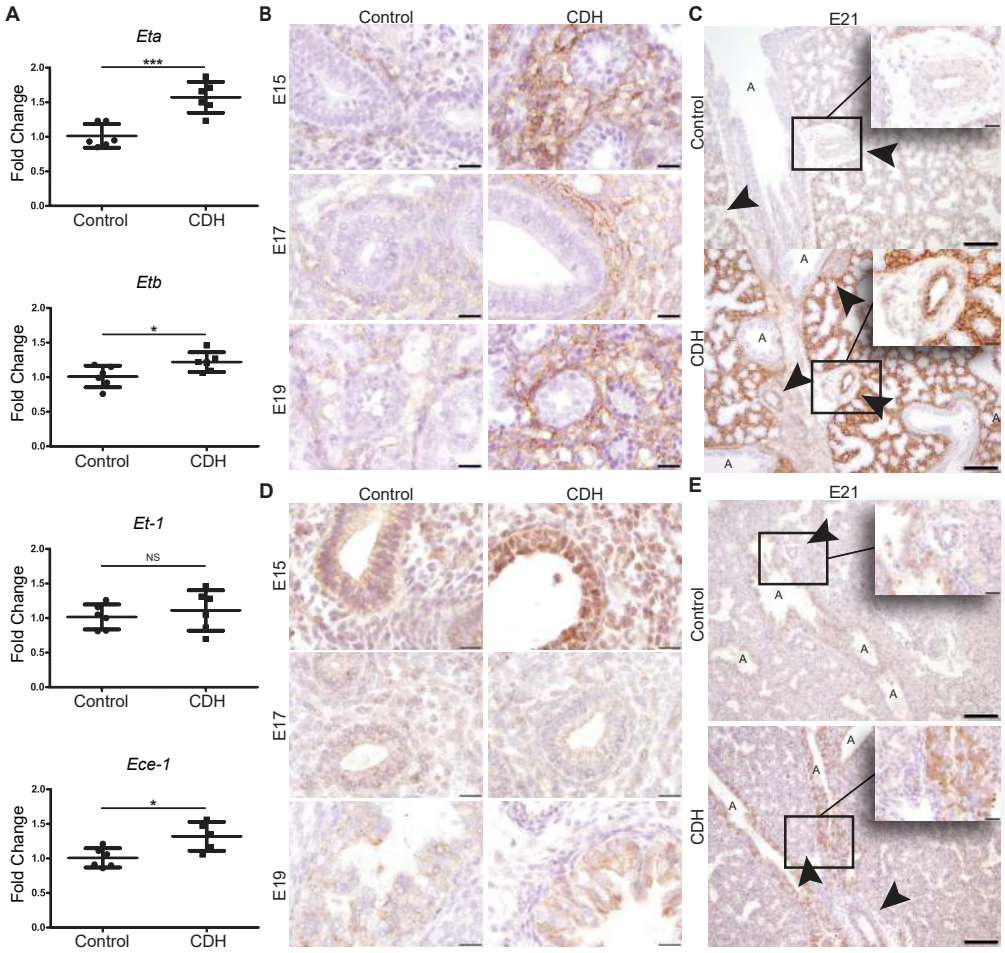

Figure 4.5: Upregulation of ET-receptors in CDH rat pups. RNA expression of the ETA receptor (*Eta*) and ETB receptor (*Etb*) shows a significant increase in rat CDH pups ($p < 0.001$ and $p < 0.05$, respectively). RNA expression of *ET-1* shows no differences between control and CDH, where *Ece-1* is significantly increased ($p < 0.05$) (**A**). Representative images show increased expression of the ETA receptor in the parenchyma of CDH pups at all ages during development (E15-E21) (**B**) and in the larger vessels at E21 (**C**). Representative images show expression of the ETB receptor in only the bronchial epithelium in both control and CDH pups at all ages during development (E15-E21) (**D**,**E**).
*$p < 0.05$, ***$p < 0.001$. Error bars represent SD. Arrows indicate vessels, A indicates airways. Scale bars represent $100\mu m$ (low power) and $20\mu m$ (high power).

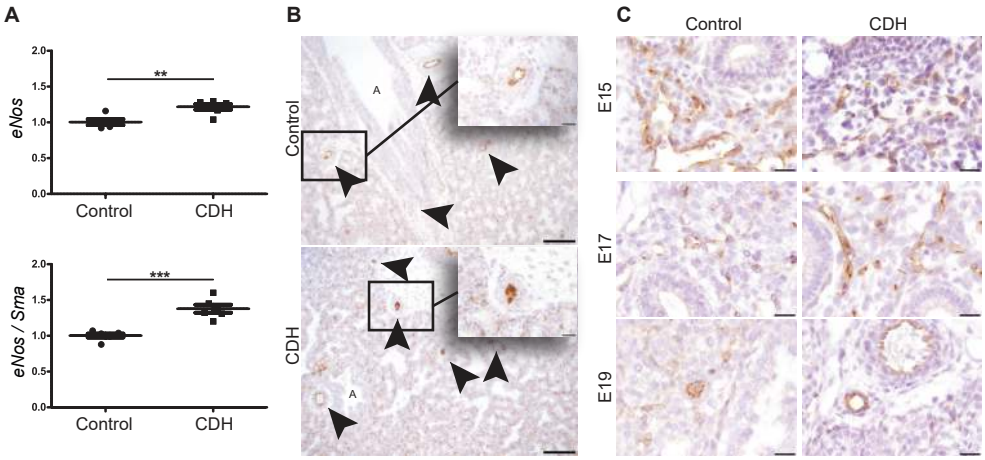

Figure 4.6: eNOS expression is increased at the end of gestation in CDH rat pups. RNA expression of *eNOS* is increased in rat CDH in all cells ($p < 0.01$) and in the smooth muscle cells (*Sma*) only ($p < 0.001$) (**A**). Representative images show increased expression of eNOS in the vessels of CDH pups at E21 (**B**), but not at other ages during gestation (**C**).
$^{**}p < 0.01$, $^{***}p < 0.001$. Error bars represent SD. Arrows indicate vessels, A indicates airways. Scale bars represent $100\mu m$ (low power) and $20\mu m$ (high power) (B) and $50\mu m$ (C).

it has been shown that the placental PGI_2 increases gradually toward term [34]. The decreased expression in CDH could be a sign of less activation of this pathway. In contrast to our human results, we found no differences in the expression of Ptgir in CDH rat pups and an increase of this receptor on mRNA level. Since PGI_2 is a potent vasodilator and thromboxane A2 (TXA_2) a potent vasoconstrictor, the increased expression of Ptgir and decreased expression of Tbxas1 was unexpected. However, this aberrant balance between PGI_2 and TXA_2 in CDH was already previously described by our group [27]. We showed an increased level of 6-keto-$PGF_1\alpha$, the stable metabolite of PGI_2, and an increased ratio of 6-keto-$PGF_1\alpha$ and TXA_2 in both lung homogenates and broncho-alveolar lavage (BAL) fluid of nitrofen treated rat pups. The discrepancy between the increased mRNA expression of *Ptgir* in CDH lungs and the absence of differences at the protein level, may be explained by a negative feedback because of a decreased activation of downstream targets of prostacyclin signaling. This may lead to an enhanced degradation of the Ptgir, or a decreased translation of the mRNA.

Current treatment of CDH patients with PH is not evidence based [3] and most patients respond poorly to the used medication. Inhaled NO (iNO) is most commonly used as a first line drug, but its use varies significantly among different centers internationally [35]. In contrast to the promising results of iNO in patients with persistent pulmonary hypertension of the newborn [36], in CDH studies have failed to show its efficacy [35, 37], as no trials have been performed to evaluate the potential role of iNO specifically in CDH patients. Apart from iNO therapy there are some case reports on the use of sildenafil and prostacyclins in CDH patients with variable results [23, 24, 38, 39]. However, administration of enteral sildenafil in neonates leads to highly variable plasma concentrations because of variable gut absorption and/or limited hepatic clearance [40]. The recent availability of intravenous sildenafil may change its application [41], but solid pharmacokinetic data on optimal dosage are still to be published. Treatment with endothelin receptor antagonists is even a bigger problem since these drugs are only available in oral form, while data of its use in newborns are virtually absent concerning dosage absorption and safety. The fact that the current therapy should be considered mainly as "trial and error" and is effective in the minority of patients with CDH strengthens our results that there are

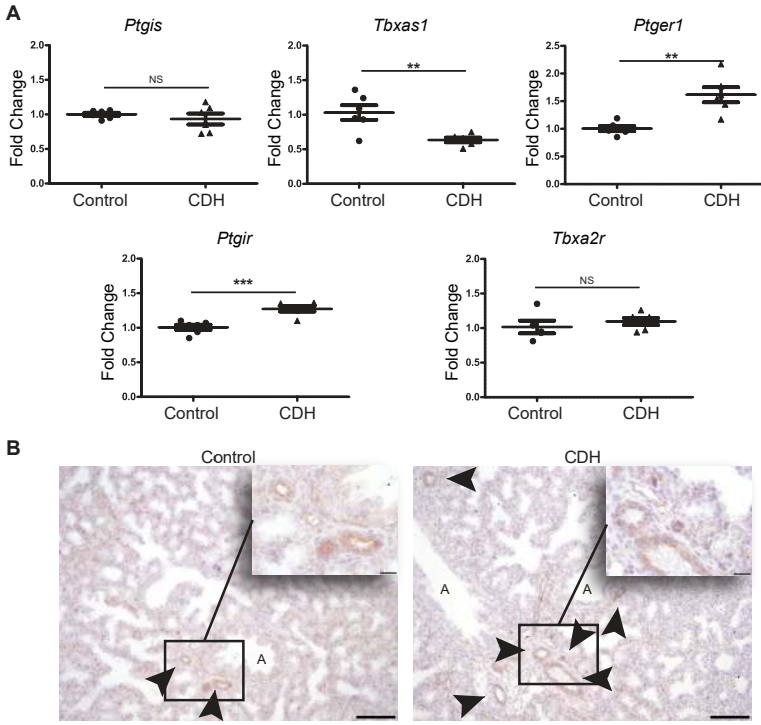

Figure 4.7: Prostacyclin expression in rat pups. RNA expression of the prostaglandin-I synthase (*Ptgis*) did not show any differences between control and CDH rat pups, but there was a significant increased expression of the prostaglandin-I_2 receptor (*Ptgir*) ($p < 0.001$) and the prostaglandin-E1 receptor (*Ptger1*) ($p < 0.01$) in CDH rat pups. In contrast, thromboxane synthase (*Tbxas1*) was significantly decreased in CDH ($p < 0.01$) with no differences in the thromboxane receptor (*Tbxa2r*) (**A**). Representative images do not show clear differences of PTGIR expression in the pulmonary vessels between both groups (**B**).
**$p < 0.01$, ***$p < 0.001$. Error bars represent SD. Arrows indicate vessels, A indicates airways. Scale bars represent $100\mu m$ (low power) and $20\mu m$ (high power).

more pathways affected. Furthermore, the severity of PH in CDH patients has been known as an important predictor of the outcome and further evaluation of current therapies has been recommended by experts in the field [5]. Future treatment should become more personalized in this group of patients using pathway directed clinical trials and risk stratification [42].

Ideally, we would like to be able to directly correlate the findings of aberrant expression of the different vasoactive pathways with the individual response of patients to specific vasoactive drugs. However, given the overall limitations of these types of studies and the lack of material of patients who did respond to one of the three therapies, this remains impossible as repeated lung biopsies would be needed to accomplish this. This approach is unethical for obvious reasons and no IRB would ever approve such an approach.

In conclusion, our study shows the aberrant expression of specific vasodilator drug targets and crucial, rate-limiting factors in human CDH and the nitrofen rat model in both the endothelin, NO and PGI_2 pathway already early during development. Since PH is still a major problem and the most important cause of morbidity and mortality in CDH patients nowadays while current treatment strategies are disappointing, a good insight in these pathways is needed for specific and patient directed targeting of pharmacotherapy.

Acknowledgements

This study was supported in part by the Sophia Foundation for Medical Research grant number 678.

References

[1] Lally KP. Congenital diaphragmatic hernia - the past 25 (or so) years. J Pediatr Surg. 2016;51(5):695–8.

[2] Sluiter I, Reiss I, et al. Vascular abnormalities in human newborns with pulmonary hypertension. Expert Rev Respir Med. 2011;5(2):245–56.

[3] Puligandla PS, Grabowski J, et al. Management of congenital diaphragmatic hernia: A systematic review from the APSA outcomes and evidence based practice committee. J Pediatr Surg. 2015;50(11):1958–70.

[4] Snoek KG, Reiss IK, et al. Standardized Postnatal Management of Infants with Congenital Diaphragmatic Hernia in Europe: The CDH EURO Consortium Consensus - 2015 Update. Neonatology. 2016;110(1):66–74.

[5] Kotecha S, Barbato A, et al. Congenital diaphragmatic hernia. Eur Respir J. 2012;39(4):820–9.

[6] de Lagausie P, de Buys-Roessingh A, et al. Endothelin receptor expression in human lungs of newborns with congenital diaphragmatic hernia. J Pathol. 2005;205(1):112–8.

[7] Dingemann J, Doi T, et al. Upregulation of endothelin receptors A and B in the nitrofen induced hypoplastic lung occurs early in gestation. Pediatr Surg Int. 2010;26(1):65–9.

[8] Davenport AP, Hyndman KA, et al. Endothelin. Pharmacol Rev. 2016;68(2):357–418.

[9] Keller RL, Tacy TA, et al. Congenital diaphragmatic hernia: endothelin-1, pulmonary hypertension, and disease severity. Am J Respir Crit Care Med. 2010;182(4):555–61.

[10] Michael JR, Markewitz BA. Endothelins and the lung. Am J Respir Crit Care Med. 1996;154(3 Pt 1):555–81.

[11] North AJ, Moya FR, et al. Pulmonary endothelial nitric oxide synthase gene expression is decreased in a rat model of congenital diaphragmatic hernia. Am J Respir Cell Mol Biol. 1995;13(6):676–82.

[12] Shehata SM, Sharma HS, et al. Pulmonary hypertension in human newborns with congenital diaphragmatic hernia is associated with decreased vascular expression of nitric-oxide synthase. Cell Biochem Biophys. 2006;44(1):147–55.

[13] Solari V, Piotrowska AP, et al. Expression of heme oxygenase-1 and endothelial nitric oxide synthase in the lung of newborns with congenital diaphragmatic hernia and persistent pulmonary hypertension. J Pediatr Surg. 2003;38(5):808–13.

[14] Hofmann A, Gosemann JH, et al. Imbalance of caveolin-1 and eNOS expression in the pulmonary vasculature of experimental diaphragmatic hernia. Birth Defects Res B Dev Reprod Toxicol. 2014;101(4):341–6.

[15] de Rooij JD, Hosgor M, et al. Expression of angiogenesis-related factors in lungs of patients with congenital diaphragmatic hernia and pulmonary hypoplasia of other causes. Pediatr Dev Pathol. 2004;7(5):468–77.

[16] Sood BG, Wykes S, et al. Expression of eNOS in the lungs of neonates with pulmonary hypertension. Exp Mol Pathol. 2011;90(1):9–12.

[17] Shinkai T, Shima H, et al. Expression of vasoactive mediators during mechanical ventilation in nitrofen-induced diaphragmatic hernia in rats. Pediatr Surg Int. 2005;21(3):143–7.

[18] Gao Y, Raj JU. Regulation of the pulmonary circulation in the fetus and newborn. Physiol Rev. 2010;90(4):1291–335.

[19] De Jaegere AP, van den Anker JN. Endotracheal instillation of prostacyclin in preterm infants with persistent pulmonary hypertension. Eur Respir J. 1998;12(4):932–4.

[20] Kelly LK, Porta NF, et al. Inhaled prostacyclin for term infants with persistent pulmonary hypertension refractory to inhaled nitric oxide. J Pediatr. 2002;141(6):830–2.

[21] Sood BG, Delaney-Black V, et al. Aerosolized PGE1: a selective pulmonary vasodilator in neonatal hypoxemic respiratory failure results of a Phase I/II open label clinical trial. Pediatr Res. 2004;56(4):579–85.

[22] De Luca D, Zecca E, et al. Transient effect of epoprostenol and sildenafil combined with iNO for pulmonary hypertension in congenital diaphragmatic hernia. Paediatr Anaesth. 2006;16(5):597–8.

[23] Olson E, Lusk LA, et al. Short-Term Treprostinil Use in Infants with Congenital Diaphragmatic Hernia following Repair. J Pediatr. 2015;167(3):762–4.

[24] Skarda DE, Yoder BA, et al. Epoprostenol Does Not Affect Mortality in Neonates with Congenital

Diaphragmatic Hernia. Eur J Pediatr Surg. 2015;25(5):454–9.

[25] Kobayashi H, Puri P. Plasma endothelin levels in congenital diaphragmatic hernia. J Pediatr Surg. 1994;29(9):1258–61.

[26] Coppola CP, Au-Fliegner M, et al. Endothelin-1 pulmonary vasoconstriction in rats with diaphragmatic hernia. J Surg Res. 1998;76(1):74–8.

[27] Ijsselstijn H, Zijlstra FJ, et al. Lung eicosanoids in perinatal rats with congenital diaphragmatic hernia. Mediators Inflamm. 1997;6(1):39–45.

[28] Rajatapiti P, van der Horst IW, et al. Expression of hypoxia-inducible factors in normal human lung development. Pediatr Dev Pathol. 2008;11(3):193–9.

[29] Makanga M, Maruyama H, et al. Prevention of pulmonary hypoplasia and pulmonary vascular remodeling by antenatal simvastatin treatment in nitrofen-induced congenital diaphragmatic hernia. Am J Physiol Lung Cell Mol Physiol. 2015;308(7):L672–82.

[30] Kuruppu S, Smith AI. Endothelin Converting Enzyme-1 phosphorylation and trafficking. FEBS Lett. 2012;586(16):2212–7.

[31] Roe ND, Ren J. Nitric oxide synthase uncoupling: a therapeutic target in cardiovascular diseases. Vascul Pharmacol. 2012;57(5-6):168–72.

[32] Bowers R, Cool C, et al. Oxidative stress in severe pulmonary hypertension. Am J Respir Crit Care Med. 2004;169(6):764–9.

[33] Mous DS, Kool HM, et al. Clinically relevant timing of antenatal sildenafil treatment reduces pulmonary vascular remodeling in congenital diaphragmatic hernia. Am J Physiol Lung Cell Mol Physiol. 2016;311(4):L734–L742.

[34] Walsh SW. Eicosanoids in preeclampsia. Prostaglandins Leukot Essent Fatty Acids. 2004;70(2):223–32.

[35] Putnam LR, Tsao K, et al. Evaluation of Variability in Inhaled Nitric Oxide Use and Pulmonary Hypertension in Patients With Congenital Diaphragmatic Hernia. JAMA Pediatr. 2016;.

[36] Roberts J J D, Fineman JR, et al. Inhaled nitric oxide and persistent pulmonary hypertension of the newborn. The Inhaled Nitric Oxide Study Group. N Engl J Med. 1997;336(9):605–10.

[37] Inhaled nitric oxide and hypoxic respiratory failure in infants with congenital diaphragmatic hernia. The Neonatal Inhaled Nitric Oxide Study Group (NINOS). Pediatrics. 1997;99(6):838–45.

[38] Bialkowski A, Moenkemeyer F, et al. Intravenous sildenafil in the management of pulmonary hypertension associated with congenital diaphragmatic hernia. Eur J Pediatr Surg. 2015;25(2):171–6.

[39] Noori S, Friedlich P, et al. Cardiovascular effects of sildenafil in neonates and infants with congenital diaphragmatic hernia and pulmonary hypertension. Neonatology. 2007;91(2):92–100.

[40] Ahsman MJ, Witjes BC, et al. Sildenafil exposure in neonates with pulmonary hypertension after administration via a nasogastric tube. Arch Dis Child Fetal Neonatal Ed. 2010;95(2):F109–14.

[41] Steinhorn RH, Kinsella JP, et al. Intravenous sildenafil in the treatment of neonates with persistent pulmonary hypertension. J Pediatr. 2009;155(6):841–847 e1.

[42] Akinkuotu AC, Cruz SM, et al. Risk-stratification of severity for infants with CDH: Prenatal versus postnatal predictors of outcome. J Pediatr Surg. 2016;51(1):44–8.

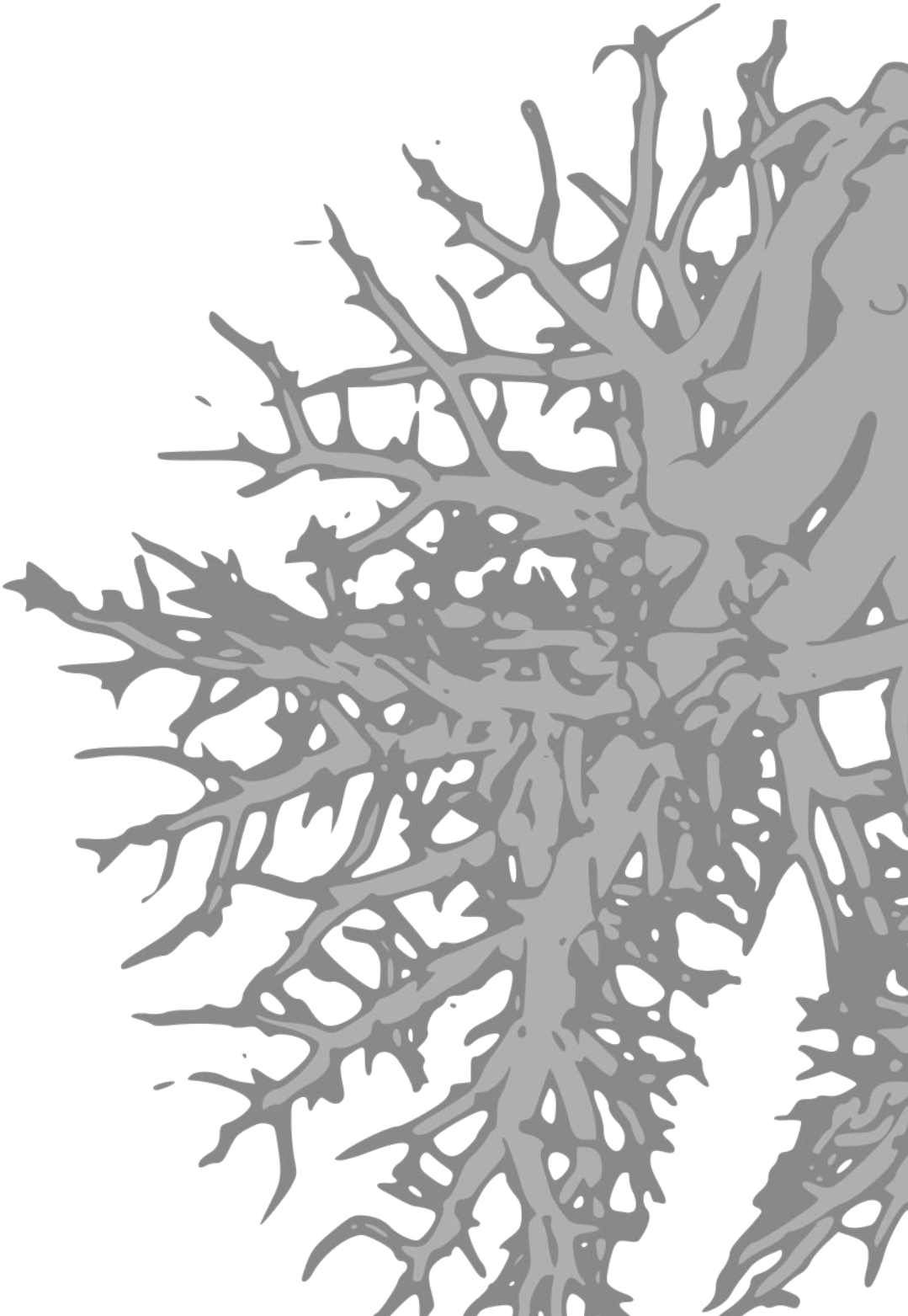

Chapter 5

Clinical relevant timing of antenatal sildenafil treatment reduces pulmonary vascular remodeling in congenital diaphragmatic hernia

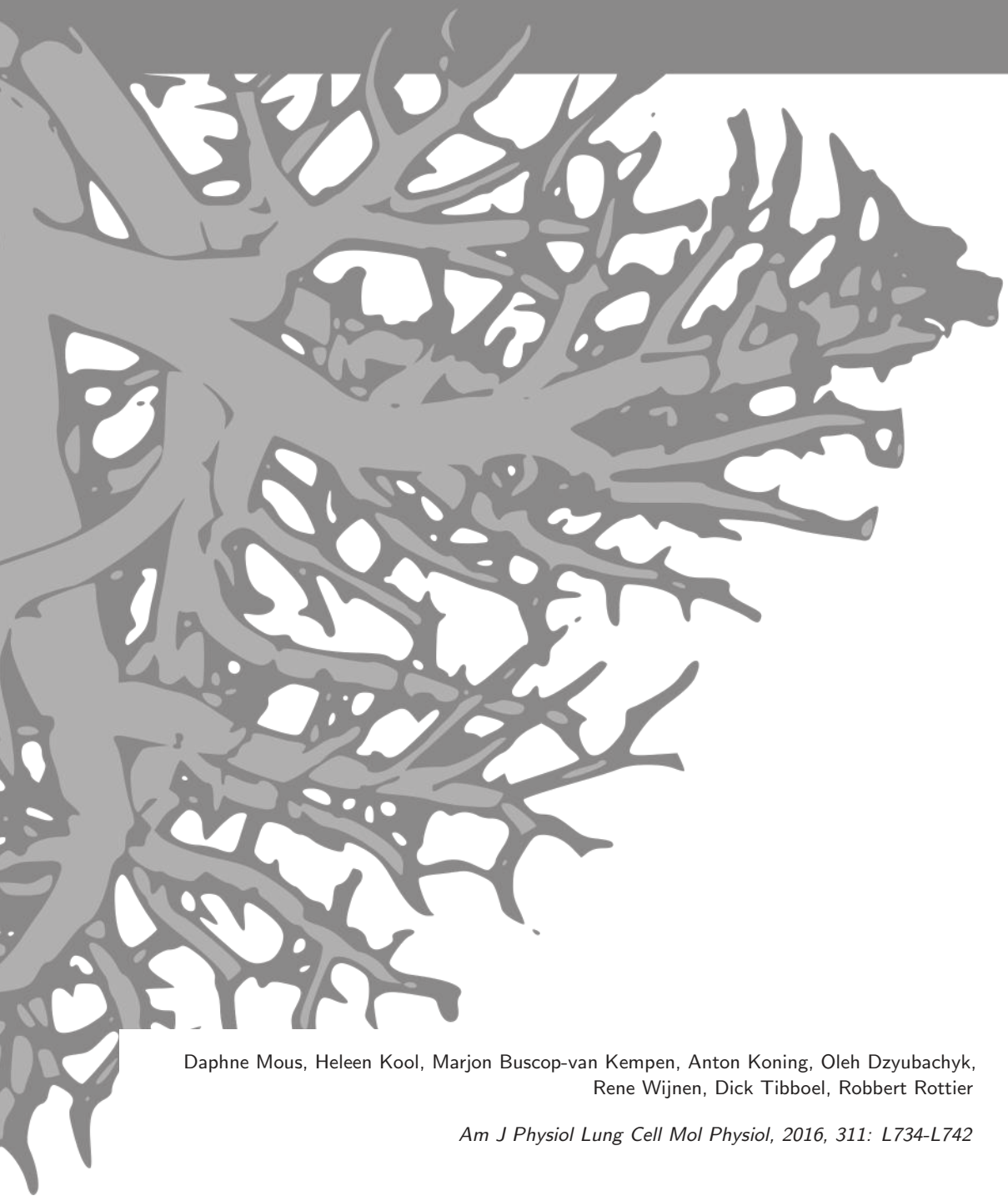

Daphne Mous, Heleen Kool, Marjon Buscop-van Kempen, Anton Koning, Oleh Dzyubachyk, Rene Wijnen, Dick Tibboel, Robbert Rottier

Am J Physiol Lung Cell Mol Physiol, 2016, 311: L734-L742

Abstract

Patients with congenital diaphragmatic hernia (CDH) suffer from severe pulmonary hypertension due to altered development of the pulmonary vasculature, which is often resistant to vasodilator therapy. Current treatment starts postnatally even though significant differences in the pulmonary vasculature are already present early during pregnancy. We examined the effects of prenatal treatment with the phosphodiesterase-5 inhibitor sildenafil on pulmonary vascular development in experimental CDH starting at a clinical relevant time. The well-established, nitrofen induced CDH rodent model was treated daily with 100 mg/kg sildenafil from day 17.5 until day 20.5 of gestation (E17.5-20.5). Importantly, this timing perfectly corresponds to the developmental stage of the lung at 20 weeks of human gestation, when CDH is detectable by 2D-ultrasonography and/or MRI. At E21.5 pups were delivered by caesarean section and euthanized by lethal injection of pentobarbital. The lungs were isolated and subsequently analyzed using immunostaining, real-time PCR and volume measurements. Prenatal treatment with sildenafil improved lung morphology and attenuated vascular remodeling with reduced muscularization of the smaller vessels. Pulmonary vascular volume was not affected by sildenafil treatment. We show that prenatal treatment with sildenafil within a clinically relevant period improves pulmonary vascular development in an experimental CDH model. This may have important implications for the management of this disease and related pulmonary vascular diseases in human.

Introduction

Congenital diaphragmatic hernia (CDH) is a developmental defect characterized by an incomplete diaphragm and lung hypoplasia [1]. CDH patients have a high risk of mortality and morbidity due to the associated pulmonary hypertension, which is the result of altered development of the pulmonary vasculature and disordered pulmonary vascular remodeling [2–4]. Advancement in medicine has resulted in early detection of CDH by ultrasonography at 20 weeks of gestation, but the severity of clinical symptoms postnatally remains poorly predictable at this stage due to significant differences in pulmonary vascular resistance and flow after birth. In addition, the pulmonary hypertension in CDH is often unaffected by standard vasodilator therapy and the lack of randomized controlled trials prevents the implementation of alternative drugs. Trials with Nitric Oxide (NO), one of the most commonly used drugs in newborns, failed to show consistently positive effects in CDH patients [5]. The impaired responsiveness to NO may be due to rapid degradation of the intracellular messenger cyclic guanosine monophosphate (cGMP) by phosphodiesterase-5 (PDE5) [6]. Binding of cGMP to PDE5 stimulates the phosphorylation and activation of PDE5 by cGMP dependent protein kinase G (PKG), which results in the conversion of cGMP into GMP [7]. Sildenafil is a potent PDE5 inhibitor, leading to an accumulation of cGMP and thus the continuous activation of PKG. PKG has several physiological substrates, which are involved in smooth muscle cell (SMC) relaxation by lowering intracellular calcium [8, 9]. Sildenafil also reduces inflammation, improves early postnatal survival and prevents pulmonary vascular remodeling in different experimental animal models of pulmonary hypertension without CDH [10–12] and prolongs survival and improves lung structure in a neonatal hyperoxia rat model [13]. It has been successfully used in the postnatal treatment of persistent pulmonary hypertension of the newborn (PPHN) [14–19] and pulmonary hypertension in patients with congenital heart disease [20]. There are no randomized controlled trials of sildenafil in CDH patients, but there are case reports showing positive effects after postnatal treatment [21, 22]. Previously, we showed thickening of the smooth muscle cell layer in arterioles, neomuscularization of small capillaries and phenotypic changes of the smooth muscle cells in the vascular wall in lungs of CDH patients at 30 weeks of gestation, indicating that significant differences in vascular structure are already present in unborn children that will develop PH after birth [23]. The premature differentiation of vascular smooth muscle cells and the early structural changes in pulmonary vascular development suggest that antenatal treatment of CDH patients could be beneficial. Recently, Luong et al. showed a reduced pathology in experimental CDH after prolonged antenatal treatment with sildenafil [24]. However, they started the daily treatment with sildenafil already at day 10.5 of gestation, when the lung bud is just emerging from the primitive foregut. At this embryonic phase of lung development there are no signs of CDH pathology, yet. Therefore, it is unclear whether the prophylactic treatment prevented the development of pathological features, or that the sildenafil indeed regressed the clinical signs. Since human CDH can be diagnosed at 20 weeks of gestation, the canalicular phase of lung development, we analyzed the therapeutic effects of sildenafil in the nitrofen induced rat CDH model starting at the corresponding gestational age (E17.5). In rat, the CDH pathology is already noticeable from E13.5 on with a defective diaphragm and affected lungs [25–29]. We show that starting the treatment of the CDH rat model with sildenafil at the clinical relevant time point improved lung morphology and attenuated or reversed the vascular remodeling of the smaller vessels. These findings may directly be valuable for future treatment modalities of severe CDH patients.

Methods

Animal Model

Pregnant Sprague-Dawley rats received either 100 mg nitrofen dissolved in 1 ml olive oil or just 1 ml olive oil by gavage on gestational age day E9.5. Nitrofen induces CDH in approximately 70% of the offspring, while all pups have pulmonary hypertension. Administration of nitrofen at exactly this time point results in mainly left sided hernias [30]. Pregnant rats were divided into 4 groups: control, nitrofen (CDH), control+sildenafil and nitrofen+sildenafil (CDH + sildenafil). Sildenafil (100 mg/kg/day, Pfizer, New York, USA) dissolved in water was administered via oral gavage for 4 consecutive days from day E17.5 to day E20.5. At day E21 pups were delivered by caesarean section and euthanized by lethal injection of pentobarbital. All animal experiments were approved by an independent animal ethical committee and according to national guidelines.

Plasma Sildenafil Concentration

Maternal and fetal rat blood samples were collected directly after caesarian section. Fetal blood samples were pooled, and plasma (50 μl) from 6 maternal and 9 fetal samples was isolated by centrifugation (10.000 RPM, 15 minutes) and sildenafil and its metabolite N-desmethyl-sildenafil (DMS) concentrations were analyzed using ultra-performance liquid chromatography with tandem mass spectrometry (UPLC-MS/MS).

Lung Morphology

Fetal rat lungs were isolated, fixed overnight in 4% PFA and embedded in paraffin. Serial 5 μm thick sections were made through the middle of the left lobe and stained with haematoxylin and eosin (HE). Sections were imaged at 40x magnification using a BX41 research stereomicroscope system (Olympus; Tokyo, Japan). Four non-overlapping images in different parts of each lung were acquired. Major airways and vessels were excluded from the analysis. The airspace size was automatically quantified using an index (D2-score) that is based on the alveolar airspace diameter and takes into account the first three central moments of the airspace size distribution. This measurement is designed to account for airspaces of different sizes by assigning them different weights. Compared to the well-known mean linear intercept (Lm), this method is more reliable in the presence of a large variability in airspace sizes [31, 32].

Immunohistochemistry and Immunofluorescence Staining

Immunohistochemistry (IHC) was performed on 5 μm paraffin sections of the lungs according to standard protocols, using the Envision detection system (Dako Cytomatic, Glostrup, Denmark) [33]. Primary antibodies used for IHC were smooth muscle actin (α-SMA; MS-113-P1; 1:1200, Thermo Scientific, Fremont, CA, USA), phosphodiesterase-5 (PDE5A; PD5A-101AP; 1:300, Fabgennix, Frisco, TX, USA) and phosphorylated phosphodiesterase-5 (phospho-PDE5; PPD5-140AP; 1:100, Fabgennix). Antigen retrieval with Tris-EDTA buffer (pH 9.0) was used for α-SMA. Primary antibodies used for immunofluorescence (IF) staining on 5 μm paraffin sections were smooth muscle actin (α-SMA; MS-113-P1; 1:500, Thermo Scientific), smooth muscle actin (clone 1a4) (α-SMA direct labelled FITC; 1:200, Sigma, The Netherlands) and platelet derived growth factor β (PDGFrβ; 1:100). Secondary antibodies against mouse (α-SMA) and rabbit (PDGFrβ) were used. Negative controls were performed by omitting the primary antibody.

Table 5.1: Primer sequences

Gene	Sequence (forward 5'–3')	Sequence (reverse 5'–3')
Pde5	TCAACAACGGATAGCAGAACTC	CCCTGTTCATTAGATCAGCGG
Prkg1	AACTATGCAGGGACAACCCA	CCTTCCCAGTTAAAGCCCTC
Prkg2	ACTAGGCATTATCTACAGAGACC	TCCAAAGTCAACCAACTTAAGG
Sma	TGACCCAGATTATGTTTGAGAC	AGAGTCCAGCACAATACCAG
Pdgfr-β	AACGACCAGTTCTACAATGCC	CATGATCTCATAGATCTCGTCGG
Pecam-1	GCAGTCCCACTTCTGAACTC	GTTCTGGGAGTCGTAATGGC
Actb	AGATGACCCAGATCATGTTTGAG	GTACGACCAGAGGCATACAG
Hprt	AGACTGAAGAGCTACTGTAATGAC	CAACAATCAAGACGTTCTTTCCAG

Quantitative Real-Time Polymerase Chain Reaction (qPCR)

RNA isolation, cDNA synthesis and subsequent qPCR analysis was performed as previously described [33]. The gene-specific primers were custom designed using PerlPrimer 1.1.21 [34] and all sequences were blasted using Ensembl (RLS 84) [35]. The primer combinations for the qPCR reactions are listed in Table 6.2. Both Actb and Hprt were used as housekeeping genes and all represented data are based on Actb.

Volume Measurements Pulmonary Vascularity

Lungs of pups were perfused through the right ventricle with Microfil contrast agent (Microfil, Flow Tech; Carver, MA, USA) and imaged with a micro Computed Tomography (micro-CT) scanner (Quantum FX, PerkinElmer; Waltham, MA, USA; pixel size 10-295 μm). Subsequently, the images were analyzed with the I-Space (Barco, Kortrijk, Belgium), a CAVETM-like Virtual Reality system in which 3D holograms can be viewed with depth perception by wearing a pair of stereo glasses with polarizing lenses. Volumes were calculated by semi-automatic region growing using the V-Scope volume-rendering software (Department of Bioinformatics, Erasmus MC, Rotterdam, The Netherlands) as previously described [36, 37]. Volume of the pulmonary vasculature was measured in relation to the total lung volume. Results obtained with the I-Space were validated using Analyze Direct software (Kansas City, US).

Statistical Analyses

Data are presented as percentages, means (SD) and univariate analyses were performed using two-way ANOVA tests for normally distributed variables. The analyses were performed using SPSS 21.0 for Windows (Armonk, NY, USA: IBM Corp.). All statistical tests were two-sided and used a significance level of 0.05.

Results

Sildenafil Effectively Crosses the Placental Barrier

In order to investigate potential effects of oral sildenafil on fetuses, we first analyzed the levels of sildenafil and its major metabolite N-desmethyl-sildenafil (DMS) in blood plasma of the mothers and pups approximately 24 hours after the last dose of sildenafil. These measurements showed that the oral application facilitated efficient uptake of sildenafil in the bloodstream and subsequent passage through the placental barrier into the fetal circulation (Table 5.2, Figure 5.1A).

Table 5.2: Plasma level of sildenafil and N-desmehtyl-sildenafil (DMS)

Mothers		Pups	
Sildenafil (ng/ml)	**DMS (ng/ml)**	**Sildenafil (ng/ml)**	**DMS (ng/ml)**
7.00	14.30	15.00	1.80
1.60	4.40	19.80	1.60
1.30	2.70	4.60	1.50
2.70	3.70	4.70	1.90
0.90	2.80	13.20	1.40
1.30	10.80	7.70	0.90
		5.00	1.20
		6.70	3.10
		5.20	1.70

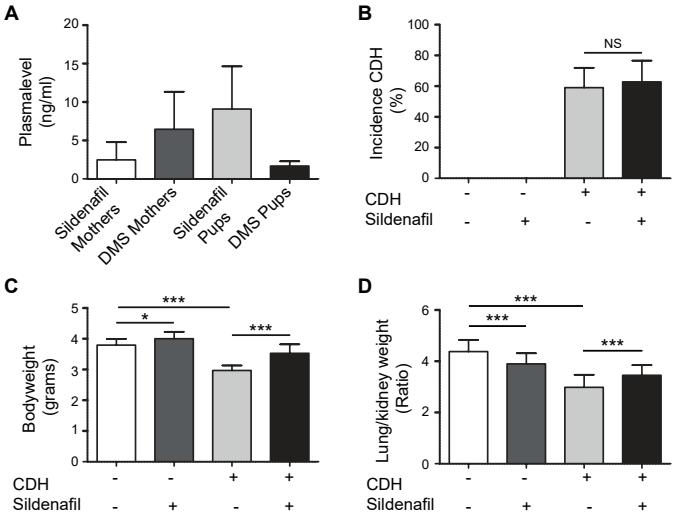

Figure 5.1: Effects of maternal sildenafil on pups. (**A**) Levels of sildenafil and its metabolite desmethyl-sildenafil (DMS) measured in plasma of mother rats and her fetuses indicate effective placental passage of sildenafil, median (IQR), $n = 6$ (mothers), $n = 9$ (pups). (**B**) The incidence of CDH is not affected by sildenafil treatment (63% vs 59%, $p = 0.665$); $n = 5$ for all groups. (**C**) Bodyweight is decreased in pups with CDH (3.0 gr vs 3.8 gr, $p < 0.001$), which is reversed by treatment with sildenafil (3.5 gr, $p < 0.001$). Sildenafil also caused an increase in bodyweight in control pups (4.0 gr, $p < 0.05$); $n = 13$ (control), $n = 23$ (CDH), $n = 16$ (control + sildenafil), $n = 24$ (CDH + sildenafil). (**D**) LW/KW is decreased in CDH (3.0 vs 4.4, $p < 0.001$), and slightly improves after sildenafil treatment in CDH (3.5, $p < 0.001$). Sildenafil caused a decrease in the ratio in controls (3.9, $p < 0.001$); $n = 33$ (control), $n = 38$ (CDH), $n = 23$ (control + sildenafil), $n = 28$ (CDH + sildenafil).
*$p < 0.05$, **$p < 0.01$, ***$p < 0.001$. Error bars represent standard error (SD). LW Lung Weight, KW Kidney Weight.

Since the administration of sildenafil to the rats was started late in gestation after the development of the diaphragm, we did not observe a reduction in the incidence of CDH after treatment (Figure 5.1B). The effect of sildenafil on the general development of the fetuses was analyzed by assessing the body weight. Fetuses of nitrofen treated mothers (CDH) had a significantly lower body weight compared to control at E21.5, but antenatal treatment with sildenafil resulted in a significant increase in body weight in control and CDH fetuses (Figure 5.1C). The lung weight-to-kidney weight ratio (LW/KW) was used as an indicator for lung hypoplasia, since the kidney weight is less affected by treatment with sildenafil than the body weight. This LW/KW ratio was significantly reduced in CDH fetuses compared to control, indicating severe lung hypoplasia in the CDH fetuses. Antenatal sildenafil treatment reduced the hypoplasia as indicated by the significant improvement of the LW/KW ratio in CDH fetuses. However, sildenafil induced a mild hypoplasia in control fetuses (Figure 5.1D).

Sildenafil inhibits PDE5, so we analyzed if sildenafil had an effect on the expression of its target. RNA expression of Pde5 was increased in fetal CDH lungs, but sildenafil did not reduce this elevated expression. In addition, the downstream targets of Pde5, Prkg1 and Prkg2, were not affected in any of the groups (Figure 5.2A). Since we did not find differences in expression level, we analyzed the distribution of Pde5 in the lungs of the fetuses. The expression pattern of Pde5 was primarily in the very large ($> 100\mu m$) vessels in some of the control samples, but this pattern was expanded in the CDH lungs to a number of small ($< 50\mu m$) and larger ($50-100\mu m$) vessels (Figure 5.2B). Remarkably, treatment with sildenafil resulted in a reduction of the number of Pde5 positive vessels in CDH, and the staining pattern was comparable to control lungs, being primarily around some of the larger vessels. The activated, phosphorylated Pde5 was detected in part of both small and larger vessels of all samples with no clear differences between all groups.

Sildenafil Improves Lung Morphology and Attenuates Pulmonary Vascular Remodeling in CDH

We analyzed the histology of the lungs of the different treated pups, which clearly showed differences in cellular density of the lung structure, with thicker septa and smaller alveolar airspaces in CDH (Figure 5.3A). The alveolar airspace diameter (D2-score) was used to quantify the alveolar airspaces. Both alveolar density and the number of alveoli were significantly increased in CDH rats compared to control and returned to normal after treatment with sildenafil (Figure 5.3B,C).

We and others have previously shown that the nitrofen rat model phenocopies the vascular defects observed in human CDH patients with increased muscularization of the arterioles [23]. To analyze whether nitrofen and/or sildenafil would affect the development of the vascular tree, we measured the total pulmonary vascular volume. Three dimensional volume measurements done in the I-Space showed a significant decrease in total lung volume (LV), in pulmonary vascular volume (PVV) and in the ratio of PVV to LV in CDH fetuses compared to controls. We observed no significant improvement of the vascular volume in CDH fetuses treated with sildenafil, but antenatal sildenafil decreased pulmonary vascular volume and PVV/LV in control fetuses (Table 5.3, Figure 5.4A,B). This indicates that starting sildenafil treatment at a clinical relevant time point did not improve the vascular tree.

Previously, we showed a thickening of the smooth muscle cell layer in small capillaries in rats with PH [38], and a more extensive peripheral distribution of contractile vascular smooth muscle cells in human CDH [23]. Based on these results, we analyzed gene and protein expression of several vascular-associated markers to study the effects of sildenafil treatment on vascular remodeling. Gene expression analysis of α-Smooth Muscle Actin (α-Sma) and Platelet-Derived Growth Factor receptor β (Pdgfr-β, pericyte marker) in relation to endothelial cells (Pecam-1/CD31) showed a significant increase of Pdgfr-β in CDH lungs compared to control, indicative

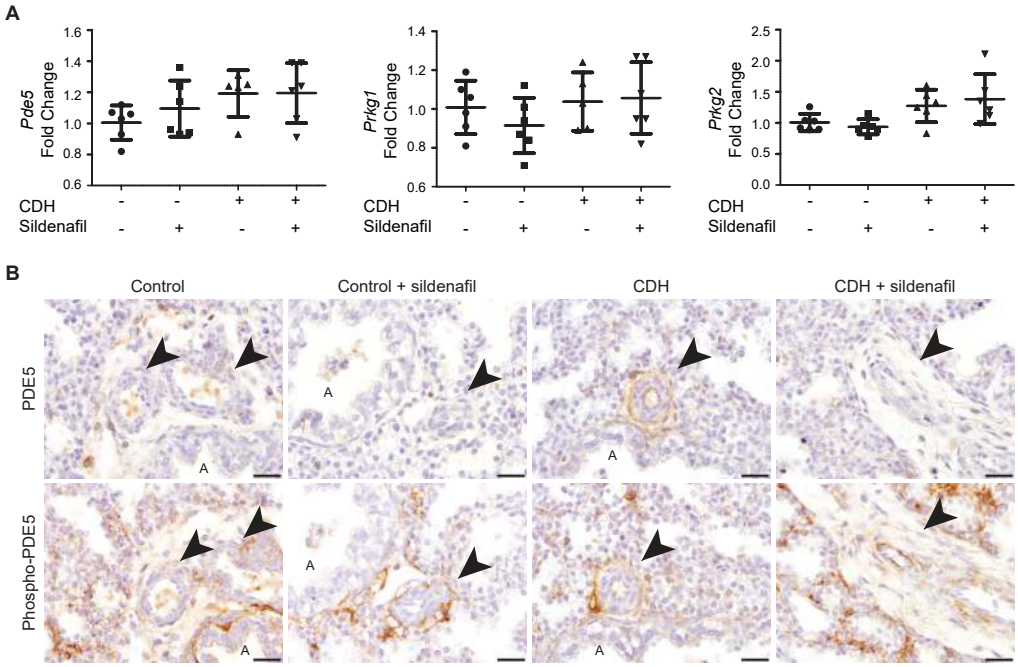

Figure 5.2: Expression of phosphodiesterase-5 (Pde5) in the lungs of rat fetuses. (**A**) Expression of Pde5, Prkg1 and Prkg2 RNA show no significant differences. For all groups 6 independent lung samples were used. Error bars represent SE. (**B**) Representative images of immunohistochemistry staining show expression of Pde5 around the vessels of CDH lungs (top) and phosphorylated Pde5around the vessels in all groups (bottom). Arrows indicate vessels, A indicates airways. Scale bars represent 20 μm. For all groups 3 independent lung samples were used.

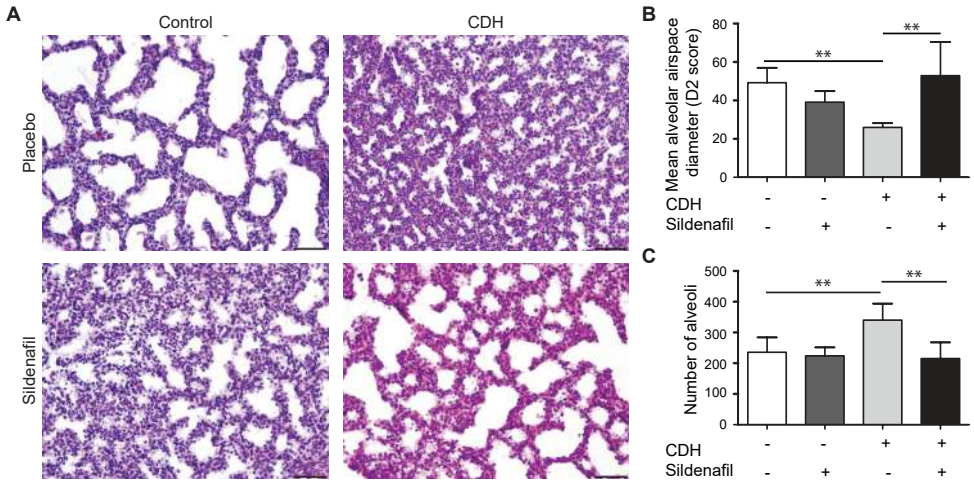

Figure 5.3: Prenatal sildenafil improves alveolar development in CDH. (**A**) Representative images of HE stained sections show a significant decreased mean alveolar airspace diameter in CDH rats compared to control. Scale bars represent $50\mu m$. (**B**) Quantification of alveolar development in control and CDH using the D2-score ($49.3\mu m$ (7.8) and 25.9 μm (2.2), respectively, $p = 0.002$). Sildenafil clearly showed an increase in alveolar airspace diameter in CDH ($52.9\mu m$ (17.6), $p = 0.001$), taking into account the D2-score (in μm) that incorporates the first three central moments of airspace distribution. (**C**) The number of alveoli is significantly increased in CDH ($p = 0.003$), while treatment with sildenafil reverted the alveolar abnormality to normal ($p = 0.001$). For all groups 4 non-overlapping images were used of 5 independent lung samples. *$p < 0.05$, **$p < 0.01$, ***$p < 0.001$. Error bars represent SD.

for an increase of differentiating perivascular cells in the CDH lungs. Treatment with sildenafil significantly reduced these markers, suggesting a restoration of normal pulmonary vascular development. However, the expression of Pdgfr-β did not revert completely to the control levels (Figure 5.5A,B). Analysis of the distribution pattern showed an increased thickening of the α-Sma+ smooth muscle cell layer in small pulmonary vessels ($< 50\mu m$) in CDH fetuses. Sildenafil treatment reduced this thickening of the media in CDH lungs, corresponding with the RNA expression data. Remarkably, sildenafil slightly increased the media in control rats (Figure 5.5C,D).

Immunofluorescence staining of control lungs showed expression of α-Sma almost exclusively in the media of the large vessels and in the subepithelial layer of the airways, and a peripheral, parenchymal staining of Pdgfr-β (Figure 5.6). Interestingly, α-Sma and Pdgfr-β co-localized around the smallest vessels in CDH lungs, most likely staining differentiating perivascular cells. Thus, in contrast to control lungs, the small capillaries are muscularized in CDH fetuses.

Table 5.3: Pulmonary vasculature volume in rat fetuses

	Control ($n = 7$)	**CDH ($n = 5$)**	**Control + sildenafil ($n = 9$)**	**CDH + sildenafil ($n = 8$)**
Lung volume mm^3 (SD)	134.0 (22.8)	95.2 (22.3)*	110.4 (22.8)	93.4 (8.3)***
Vasculature volume mm^3 (SD)	11.3 (3.3)	4.8 (2.3)**	6.9 (3.1)*	3.6 (0.5)***
Ratio vasculature/lung	0.084 (0.019)	0.048 (0.019)**	0.060 (0.017)*	0.039 (0.005)***

Results are shown as mean (SD). * $p < 0.05$, ** $p < 0.01$, *** $p < 0.001$ compared to control.

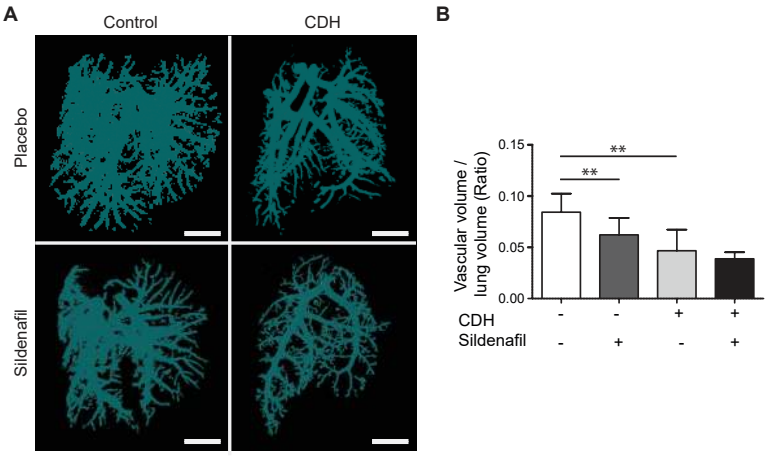

Figure 5.4: Sildenafil does not affect vasculature volume. (**A**) Representative images of computed tomography scans of microfil-injected pulmonary vessels analyzed with the I-Space. Scale bars represent 2 mm. (**B**) The ratio of the pulmonary vasculature volume to total lung volume is significantly decreased in CDH rats (0.048 vs 0.084, $p = 0.001$) and control rats treated with sildenafil (0.060, $p = 0.005$); $n = 7$ (control), $n = 5$ (CDH), $n = 9$ (control + sildenafil), $n = 8$ (CDH + sildenafil).
*$p < 0.05$, **$p < 0.01$, ***$p < 0.001$. Error bars represent SD.

Sildenafil treatment of CDH fetuses resulted in a reversion of the staining pattern of α-Sma and Pdgfr-β to the control situation, indicating that sildenafil may reduce the pulmonary hypertension. This would suggest a beneficial effect of sildenafil on reducing the pulmonary hypertension at the cellular level (Figure 5.6).

Discussion

Our study shows that antenatal treatment of CDH pups with the PDE5 inhibitor sildenafil starting at the clinical relevant time point results in reduced lung hypoplasia and reduced vascular abnormalities. Administration of sildenafil was started at the canalicular stage of lung development in the rat, which corresponds with the time point when human CDH can be detected by routine ultrasound at 20 weeks of gestation. The diaphragm of the rat is already formed and the major pulmonary vessels are already developed at the time the administration of sildenafil was started. Therefore we did not observe a reduction in the incidence of CDH or an improvement of the pulmonary vascular volume in the major branches of the vascular tree. However, sildenafil improved the body weight and LW/KW ratio, indicating a better lung growth development compared to untreated CDH pups. Furthermore, the alveolar airspaces increased in diameter, which could be related to the formation of the primary and secondary septa later in prenatal lung development. Moreover, sildenafil reduced the thickening of the smooth muscle cell layer in arterioles normally present in CDH, and prevented the frequently observed aberrant differentiation of pericytes in CDH as indicated by the loss of the co-localization of α-Sma and Pdgfr-β in capillaries [23, 38].

In this study we proved the placental crossing of sildenafil into the fetal circulation with higher levels of plasma sildenafil and lower levels of plasma DMS in the pups compared to the mother. Sildenafil is known to be catalyzed by hepatic CYP3A4 and CYP2C9. Prenatal and early postnatal CYP-mediated N-demethylation is less prominent compared to adults, which causes less clearance of sildenafil. This reduced clearance in fetuses results in a longer terminal

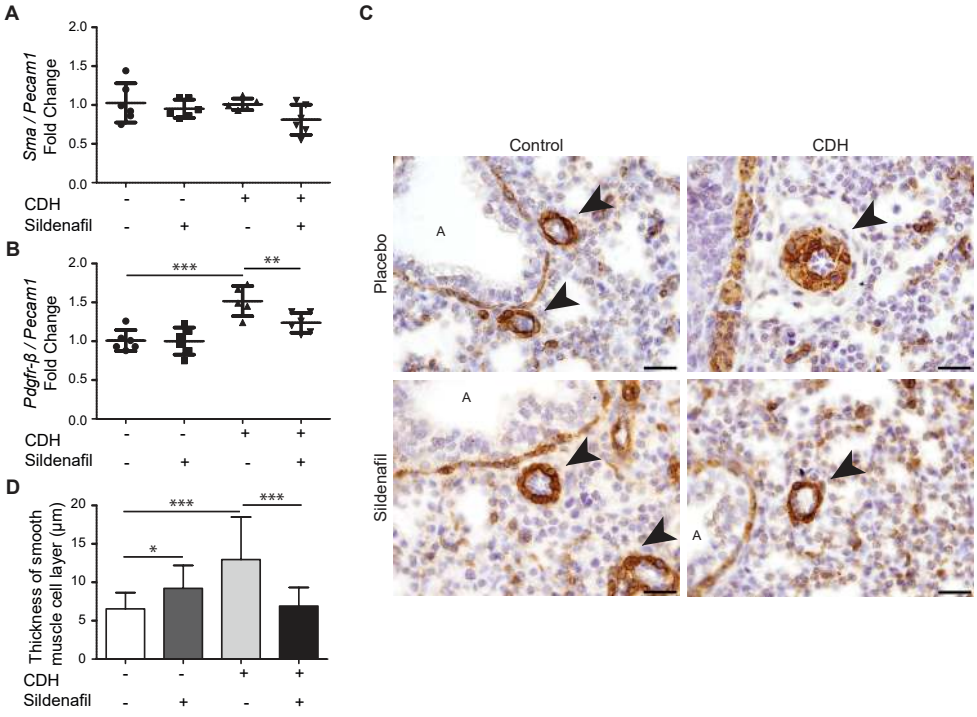

Figure 5.5: Sildenafil decreases pathological muscularization in CDH. (**A**) RNA expression of smooth muscle actin (Sma) in relation to platelet endothelial cell adhesion molecule (Pecam1) shows no significant changes between the groups. (**B**) RNA expression of platelet derived growth factor β (Pdgfr-β) in relation to Pecam1 shows a significant increase in CDH ($p < 0.001$), which is slightly improved after treatment with sildenafil ($p = 0.009$). (**C**,**D**) Representative images of immunohistochemistry staining (C) and quantitation (D) show increased expression of Sma and a significant thickening of the vessel wall of small pulmonary vessels (<50 μm) in CDH (12.96 μm vs 6.55 μm, $p < 0.001$), which is completely reversed by antenatal treatment with sildenafil in CDH (6.91 μm, $p < 0.001$) and thickened in control (9.21 μm, $p = 0.030$). Arrows indicate vessels, A indicates airways. Scale bars represent 20 μm. For all groups 15 to 20 vessels of 3 independent lung samples were measured.
*$p < 0.05$, **$p < 0.01$, ***$p < 0.001$. Error bars represent SD.

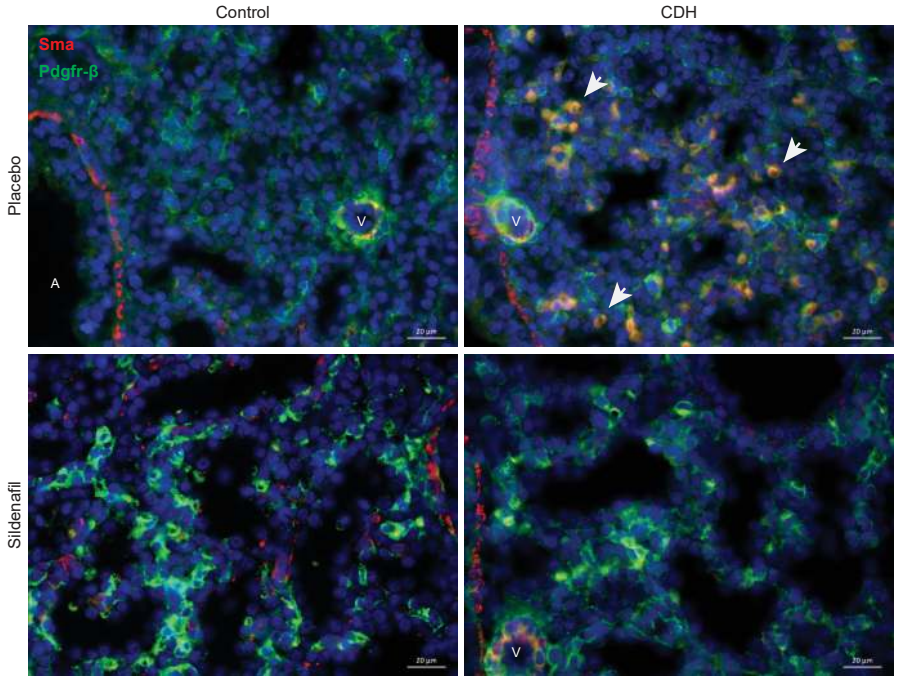

Figure 5.6: Abnormal smooth muscle cells surround arterioles in CDH. Representative immunofluorescence staining images of all 4 groups show colocalization of Sma (red) and platelet derived growth factor β (Pdgfr-β; green) in the parenchyma of CDH lungs. Arrowheads indicate examples of capillaries with colocalization, A indicates airways, V indicates vessels. Scale bars represent 20 μm.

half-life [39]. The dose of sildenafil chosen for this study was 100 mg/kg/d, which was based on a previous study on the pharmacokinetics of sildenafil in rats. Since the metabolism in rats is tremendously faster than in human, this dose is a lot higher than the normal dose used in the clinical setting. Although the oral bioavailability of sildenafil in female rats is only 44%, which is comparable to humans (38%), it remains the preferred method over other methods keeping in mind the potential translation to a clinical application [40].

Luong et al had previously shown that antenatal sildenafil crosses the placenta without affecting the PDE5-expressing organs of the pups in the nitrofen-rat model. Consistent with our study, they show improvement in lung structure in the nitrofen-induced rat model after antenatal sildenafil. However, Luong et al treated rats for 10 days, starting already at day 10.5 of gestation, which is only one day after the start of lung development in rats and can therefore be seen as prophylactic [24]. Furthermore, an increase in the number of arterioles [41], a decrease in vascular remodeling [42], a decrease in medial wall thickness and improvement in alveolar density [43] and improvement in pulmonary vascular response and lung growth [44] were shown after antenatal treatment with sildenafil of different duration in the nitrofen rat model. Improvement in parenchymal and lung abnormalities after antenatal sildenafil was shown in a rabbit model of CDH [45] and in a lamb model, downregulation of eNOS was shown to be normalized after antenatal treatment with tadalafil, another PDE-5 inhibitor [46]. However, the treatment strategies in all these studies were already initiated very early during pregnancy, at a time when human CDH would not yet be detectable and before CDH symptoms and pathology develop. A summary of the relevant sildenafil studies in the nitrofen rat model is shown in Table 5.4.

We found that sildenafil caused a decreased LW/KW ratio, increased muscularization of the arterioles and decreased pulmonary vascular volume in healthy control rats, contrasting the earlier results of Luong et al. This difference may be caused by several different aspects. First of all, the oral treatment may provide a sudden increase of sildenafil in the plasma, which is not achieved by the more steady delivery by subcutaneous treatment. Secondly, our treatment may be more efficient than the treatment by Luong et al. Thirdly, the long treatment of animals with sildenafil may induce some kind of adaptation to sildenafil which reduces its effects. Differences in lung structure in control rats and rabbits treated with sildenafil were also reported by Luong et al [24] and Russo et al [45]. The pathophysiology of these side-effects is still not clear, but might involve the increase in cGMP after PDE-5 inhibition, since increased cGMP can also lead to toxicity and interfere with normal cellular proliferation [47]. Extreme vasodilation caused by increased cGMP might also have a deleterious effect on the development of the pulmonary vasculature. However, sildenafil has been used as a treatment for preeclampsia in pregnant women with no significant adverse effects in both mother and fetus during follow up of 30 days post-delivery [48]. Furthermore, recently a trial has started for the antenatal use of sildenafil in pregnancies complicated by early-onset extreme fetal growth restriction (STRIDER; NCT02277132 (clinicaltrials.gov)) [49].

In the present study we focused on pulmonary vascular development, since pulmonary hypertension in CDH is the major cause of morbidity and mortality. The major strength of this study is the timing of the sildenafil treatment at day 17.5 of gestation, which corresponds to 20 weeks of gestation in human pregnancy, when CDH is detectable by routine ultrasound in many countries. Sildenafil has never been tested in a clinical trial as an antenatal treatment to target the pulmonary vascular growth. However, the possibility of prenatal diagnosis of CDH offers a unique opportunity to treat fetuses antenatally. So far, sildenafil is only used postnatally as a treatment for severe pulmonary hypertension and in some of the most severe CDH patients who are resistant to current therapies, in an attempt to prevent extracorporeal membrane oxygenation (ECMO). Therefore, it is not possible to directly compare the pathological changes seen in these patients with the effects of the antenatal sildenafil treatment in the CDH rat model.

Table 5.4: Overview of studies with antenatal sildenafil treatment in the nitrofen rat model

		Our study	**Luong et al [24]**	**Kattan et al [41]**	**Lemus-Varela et al [42]**	**Yamamoto et al [44]**
		100 mg/kg oral 24h E17.5 – E20.5	100 mg/kg subcutaneous 24h E10.5 – E20.5	45 mg/kg oral 12h E14 – E22	100 mg/kg oral 24h E16 – E20	100 mg/kg subcutaneous 24h E11.5 – E20.5
Fetal body weight	CDH	significantly decreased	significantly decreased			
	CDHsil	significant improvement	no improvement			
Lung weight	CDH	decreased lung/kidney weight	decreased lung/body weight			decreased lung/body weight
	CDHsil	significant improvement	no improvement			significant improvement
	Cosil	decreased lung/kidney weight	no significant differences			
Morphology	CDH	decreased alveolar airspaces	increased mean linear intercept		decreased alveolar airspaces	decreased alveolar airspaces
	CDHsil	significant improvement	significant improvement		no improvement	significant improvement
	Cosil	No significant differences	no significant differences			
Vasculature	CDH	decreased vascular volume	less pulmonary vessels	less arterioles		
	CDHsil	No improvement	significant improvement	significant improvement		
	Cosil	decreased vascular volume	less pulmonary vessels			
Vessel wall	CDH	increased SMC[§] layer	no significant differences		increased SMC[§] layer	
	CDHsil	significant improvement	no significant differences		significant improvement	
	Cosil	increased SMC[§] layer	no significant differences			

[§] SMC = smooth muscle cell

The potential to treat CDH already antenatally might be a big improvement in the management of this disease in humans. So far the approach for antenatal modulation of the severity of pulmonary hypoplasia is through mechanical interference with pulmonary fluid drainage. To this effect antenatal tracheal plugging has been advocated [50, 51]. An alternative approach can be the provision of antenatal sildenafil in selected high risk prenatally diagnosed CDH fetuses. However, even for postnatal sildenafil no solid safety data are available [52]. Even more for antenatal sildenafil (STRIDER; NCT02277132 (clinicaltrials.gov)) questions remain on safety, dosage as well as repeated prescription and optimal timing of the drug.

In conclusion, our study demonstrates that antenatal treatment with sildenafil started at a clinical relevant time point improves bodyweight, decreases lung hypoplasia and attenuates vascular remodeling in nitrofen-induced CDH in rats. Antenatal use of sildenafil might improve morbidity and mortality in CDH patients by improving lung structure. However, it is important to determine the optimum dosage for this therapy in a potential phase I trial.

Acknowledgements

The authors like to acknowledge the Clinical Pharmacy and Toxicology Laboratory at the Erasmus MC (Rotterdam) for analysis of the plasma levels of sildenafil and its metabolite.

This study was supported in part by the Sophia Foundation for Medical Research grant number 678.

References

[1] Rottier R, Tibboel D. Fetal lung and diaphragm development in congenital diaphragmatic hernia. Semin Perinatol. 2005;29(2):86–93.

[2] Miniati D. Pulmonary vascular remodeling. Semin Pediatr Surg. 2007;16(2):80–7.

[3] Sluiter I, Reiss I, et al. Vascular abnormalities in human newborns with pulmonary hypertension. Expert Rev Respir Med. 2011;5(2):245–56.

[4] Kool H, Mous D, et al. Pulmonary vascular development goes awry in congenital lung abnormalities. Birth Defects Res C Embryo Today. 2014;102(4):343–58.

[5] Inhaled nitric oxide and hypoxic respiratory failure in infants with congenital diaphragmatic hernia. The Neonatal Inhaled Nitric Oxide Study Group (NINOS). Pediatrics. 1997;99(6):838–45.

[6] Vukcevic Z, Coppola CP, et al. Nitrovasodilator responses in pulmonary arterioles from rats with nitrofen-induced congenital diaphragmatic hernia. J Pediatr Surg. 2005;40(11):1706–11.

[7] Corbin JD, Turko IV, et al. Phosphorylation of phosphodiesterase-5 by cyclic nucleotide-dependent protein kinase alters its catalytic and allosteric cGMP-binding activities. Eur J Biochem. 2000;267(9):2760–7.

[8] Rybalkin SD, Yan C, et al. Cyclic GMP phosphodiesterases and regulation of smooth muscle function. Circ Res. 2003;93(4):280–91.

[9] Francis SH, Busch JL, et al. cGMP-dependent protein kinases and cGMP phosphodiesterases in nitric oxide and cGMP action. Pharmacol Rev. 2010;62(3):525–63.

[10] Yin J, Kukucka M, et al. Sildenafil preserves lung endothelial function and prevents pulmonary vascular remodeling in a rat model of diastolic heart failure. Circ Heart Fail. 2011;4(2):198–206.

[11] Bogdan S, Seferian A, et al. Sildenafil Reduces Inflammation and Prevents Pulmonary Arterial Remodeling of the Monocrotaline - induced Disease in the Wistar Rats. Maedica (Buchar). 2012;7(2):109–16.

[12] Shekerdemian LS, Ravn HB, et al. Intravenous sildenafil lowers pulmonary vascular resistance in a model of neonatal pulmonary hypertension. Am J Respir Crit Care Med. 2002;165(8):1098–102.

[13] de Visser YP, Walther FJ, et al. Sildenafil attenuates pulmonary inflammation and fibrin deposition, mortality and right ventricular hypertrophy in neonatal hyperoxic lung injury. Respir Res. 2009;10:30.

[14] Shah PS, Ohlsson A. Sildenafil for pulmonary hypertension in neonates. Cochrane Database Syst Rev. 2011;(8):CD005494.

[15] Baquero H, Soliz A, et al. Oral sildenafil in infants with persistent pulmonary hypertension of the newborn: a pilot randomized blinded study. Pediatrics. 2006;117(4):1077–83.

[16] Juliana AE, Abbad FC. Severe persistent pulmonary hypertension of the newborn in a setting where limited resources exclude the use of inhaled nitric oxide: successful treatment with sildenafil. Eur J Pediatr. 2005;164(10):626–9.

[17] Yaseen H, Darwich M, et al. Is sildenafil an effective therapy in the management of persistent pulmonary hypertension? J Clin Neonatol. 2012;1(4):171–5.

[18] Vargas-Origel A, Gomez-Rodriguez G, et al. The use of sildenafil in persistent pulmonary hypertension of the newborn. Am J Perinatol. 2010;27(3):225–30.

[19] Perez KM, Laughon M. Sildenafil in Term and Premature Infants: A Systematic Review. Clin Ther. 2015;37(11):2598–2607 e1.

[20] Uhm JY, Jhang WK, et al. Postoperative use of oral sildenafil in pediatric patients with congenital heart disease. Pediatr Cardiol. 2010;31(4):515–20.

[21] Bialkowski A, Moenkemeyer F, et al. Intravenous sildenafil in the management of pulmonary hypertension associated with congenital diaphragmatic hernia. Eur J Pediatr Surg. 2015;25(2):171–6.

[22] Noori S, Friedlich P, et al. Cardiovascular effects of sildenafil in neonates and infants with congenital diaphragmatic hernia and pulmonary hypertension. Neonatology. 2007;91(2):92–100.

[23] Sluiter I, van der Horst I, et al. Premature differentiation of vascular smooth muscle cells in human congenital diaphragmatic hernia. Exp Mol Pathol. 2013;94(1):195–202.

[24] Luong C, Rey-Perra J, et al. Antenatal sildenafil treatment attenuates pulmonary hypertension in experimental congenital diaphragmatic hernia. Circulation. 2011;123(19):2120–31.

[25] Clugston RD, Zhang W, et al. Early development of the primordial mammalian diaphragm and cellular mechanisms of nitrofen-induced congenital diaphragmatic hernia. Birth Defects Res A Clin Mol Teratol. 2010;88(1):15–24.

[26] Clugston RD, Zhang W, et al. Understanding abnormal retinoid signaling as a causative mechanism in congenital diaphragmatic hernia. Am J Respir Cell Mol Biol. 2010;42(3):276–85.

[27] Greer JJ, Allan DW, et al. Recent advances in understanding the pathogenesis of nitrofen-induced congenital diaphragmatic hernia. Pediatr Pulmonol. 2000;29(5):394–9.

[28] Santos M, Bastos P, et al. Ghrelin expression in human and rat fetal lungs and the effect of ghrelin administration in nitrofen-induced congenital diaphragmatic hernia. Pediatr Res. 2006;59(4 Pt 1):531–7.

[29] Takahashi T, Friedmacher F, et al. Kif7 expression is decreased in the diaphragmatic and pulmonary mesenchyme of nitrofen-induced congenital diaphragmatic hernia. J Pediatr Surg. 2015;50(6):904–7.

[30] Kluth D, Kangah R, et al. Nitrofen-induced diaphragmatic hernias in rats: an animal model. J Pediatr Surg. 1990;25(8):850–4.

[31] Parameswaran H, Majumdar A, et al. Quantitative characterization of airspace enlargement in emphysema. J Appl Physiol (1985). 2006;100(1):186–93.

[32] Jacob RE, Carson JP, et al. Comparison of two quantitative methods of discerning airspace enlargement in smoke-exposed mice. PLoS One. 2009;4(8):e6670.

[33] Rajatapiti P, van der Horst IW, et al. Expression of hypoxia-inducible factors in normal human lung development. Pediatr Dev Pathol. 2008;11(3):193–9.

[34] Marshall OJ. PerlPrimer: cross-platform, graphical primer design for standard, bisulphite and real-time PCR. Bioinformatics. 2004;20(15):2471–2.

[35] Yates A, Akanni W, et al. Ensembl 2016. Nucleic Acids Res. 2016;44(D1):D710–6.

[36] Koning AH, Rousian M, et al. V-scope: design and implementation of an immersive and desktop virtual reality volume visualization system. Stud Health Technol Inform. 2009;142:136–8.

[37] van Oppenraaij RH, Koning AH, et al. Vasculogenesis and angiogenesis in the first trimester human placenta: an innovative 3D study using an immersive Virtual Reality system. Placenta. 2009;30(3):220–2.

[38] Sluiter I, Veenma D, et al. Etiological and pathogenic factors in congenital diaphragmatic hernia. Eur J Pediatr Surg. 2012;22(5):345–54.

[39] Mukherjee A, Dombi T, et al. Population pharmacokinetics of sildenafil in term neonates: evidence of rapid maturation of metabolic clearance in the early postnatal period. Clin Pharmacol Ther. 2009;85(1):56–63.

[40] Walker DK, Ackland MJ, et al. Pharmacokinetics and metabolism of sildenafil in mouse, rat, rabbit, dog and man. Xenobiotica. 1999;29(3):297–310.

[41] Kattan J, Cespedes C, et al. Sildenafil stimulates and dexamethasone inhibits pulmonary vascular development in congenital diaphragmatic hernia rat lungs. Neonatology. 2014;106(1):74–80.

[42] Lemus-Varela Mde L, Soliz A, et al. Antenatal use of bosentan and/or sildenafil attenuates pulmonary features in rats with congenital diaphragmatic hernia. World J Pediatr. 2014;10(4):354–9.

[43] Makanga M, Maruyama H, et al. Prevention of pulmonary hypoplasia and pulmonary vascular remodeling by antenatal simvastatin treatment in nitrofen-induced congenital diaphragmatic hernia. Am J Physiol Lung Cell Mol Physiol. 2015;308(7):L672–82.

[44] Yamamoto Y, Thebaud B, et al. Doppler parameters of fetal lung hypoplasia and impact of sildenafil. Am J Obstet Gynecol. 2014;211(3):263 e1–8.

[45] Russo FM, Toelen J, et al. Transplacental sildenafil rescues lung abnormalities in the rabbit model of diaphragmatic hernia. Thorax. 2016;.

[46] Shue EH, Schecter SC, et al. Antenatal maternally-administered phosphodiesterase type 5 inhibitors normalize eNOS expression in the fetal lamb model of congenital diaphragmatic hernia. J Pediatr Surg. 2014;49(1):39–45; discussion 45.

[47] Weinberger B, Laskin DL, et al. The toxicology of inhaled nitric oxide. Toxicol Sci. 2001;59(1):5–16.

[48] Samangaya RA, Mires G, et al. A randomised, double-blinded, placebo-controlled study of the phosphodiesterase type 5 inhibitor sildenafil for the treatment of preeclampsia. Hypertens

Pregnancy. 2009;28(4):369–82.

[49] Ganzevoort W, Alfirevic Z, et al. STRIDER: Sildenafil Therapy In Dismal prognosis Early-onset intrauterine growth Restriction–a protocol for a systematic review with individual participant data and aggregate data meta-analysis and trial sequential analysis. Syst Rev. 2014;3:23.

[50] Flageole H, Evrard VA, et al. Tracheoscopic endotracheal occlusion in the ovine model: technique and pulmonary effects. J Pediatr Surg. 1997;32(9):1328–31.

[51] Deprest J, De Coppi P. Antenatal management of isolated congenital diaphragmatic hernia today and tomorrow: ongoing collaborative research and development. Journal of Pediatric Surgery Lecture. J Pediatr Surg. 2012;47(2):282–90.

[52] Samiee-Zafarghandy S, Smith PB, et al. Safety of sildenafil in infants*. Pediatr Crit Care Med. 2014;15(4):362–8.

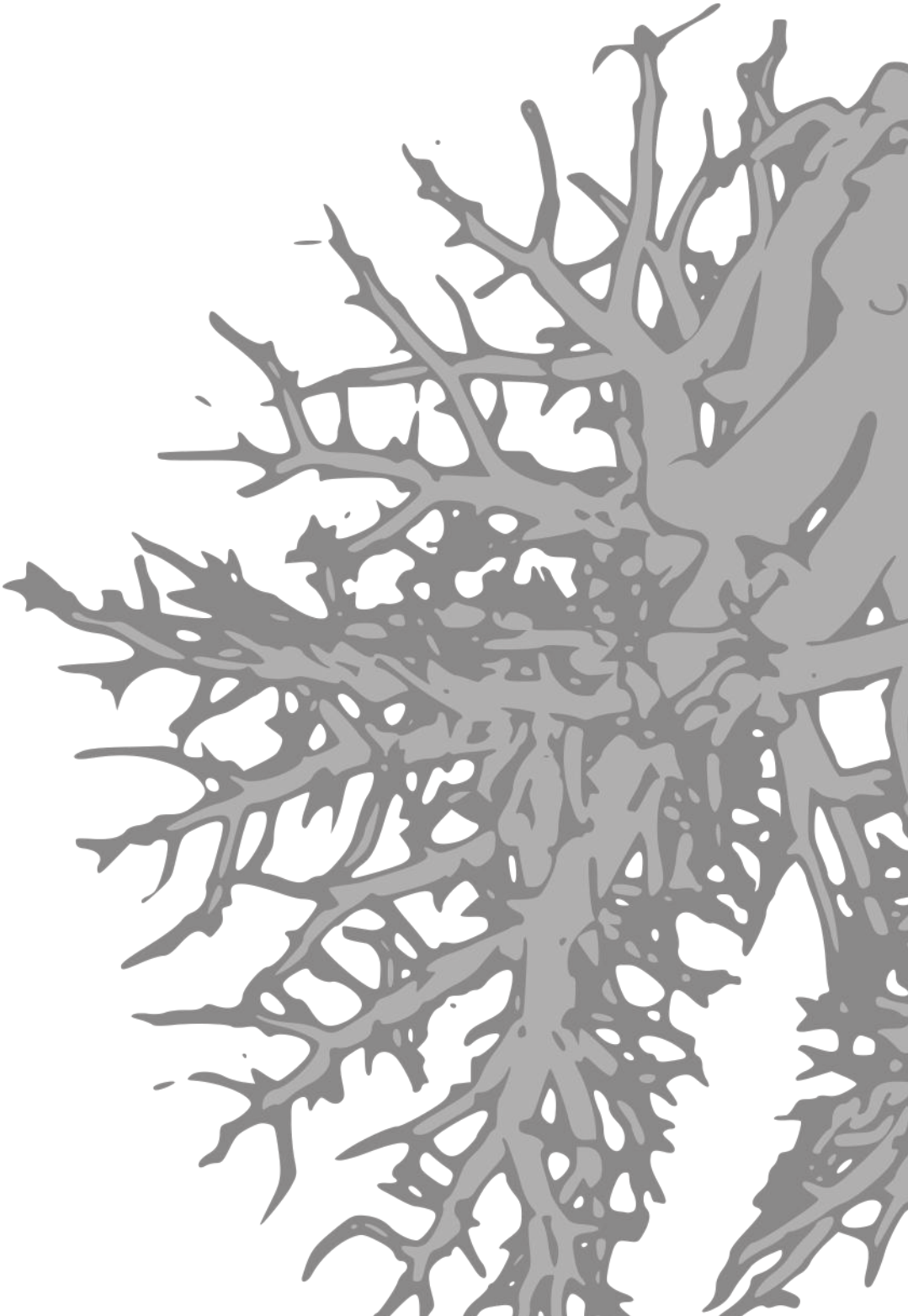

Chapter 6

Prenatal sildenafil and selexipag improve pulmonary vascularity in congenital diaphragmatic hernia

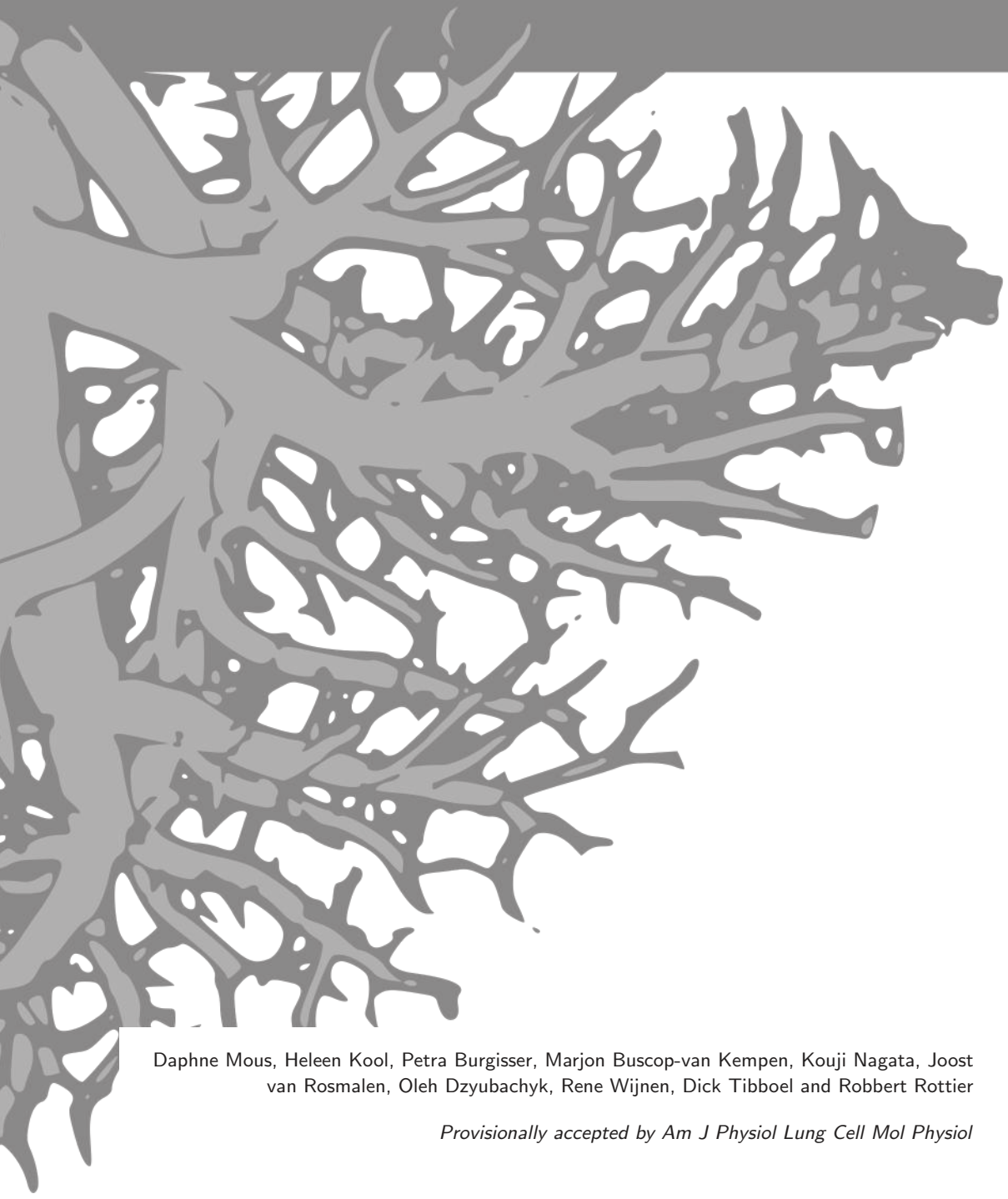

Daphne Mous, Heleen Kool, Petra Burgisser, Marjon Buscop-van Kempen, Kouji Nagata, Joost van Rosmalen, Oleh Dzyubachyk, Rene Wijnen, Dick Tibboel and Robbert Rottier

Provisionally accepted by Am J Physiol Lung Cell Mol Physiol

Abstract

Rationale: Patients with congenital diaphragmatic hernia (CDH) often suffer from severe pulmonary hypertension and the choice of current vasodilator therapy is based on trial and error.

Objectives: Since pulmonary vascular alterations are already present early during development, we performed a study to modulate the pulmonary vascular abnormalities at an early stage during gestation.

Methods: Pregnant Sprague-Dawley rats were treated with nitrofen at day 9.5 of gestation (E9.5) to induce CDH in the offspring and subsequently the phosphodiesterase-5 inhibitor sildenafil and/or the novel prostaglandin-I receptor agonist selexipag (NS-304) were administered at E17.5 until E20.5. This time point of start of treatment corresponds to week 20 of gestation in human, when CDH is usually detected, making it clinically relevant.

Measurements and main results: CDH pups showed increased density of air saccules which was reverted after the use of sildenafil solely. The pulmonary vascular wall was thickened and right ventricular hypertrophy was present in the CDH group and improved both after treatment with sildenafil and selexipag alone, where combination therapy with both compounds did not have additive value.

Conclusions: In conclusion, antenatal treatment with sildenafil improved airway morphogenesis and pulmonary vascular development, while selexipag only acted positively on pulmonary vascular development. The combination of both compounds did not act synergistically, probably because of a decreased efficiency of both compounds caused by CYP interaction. These new insights create important possibilities for future treatment of pulmonary vascular abnormalities in CDH patients already in the antenatal period of life.

Introduction

Congenital diaphragmatic hernia (CDH) is a rare developmental anomaly characterized by an incomplete diaphragm, lung hypoplasia and pulmonary hypertension (PH), which is often unresponsive to current vasodilator therapy [1]. Although the postnatal therapeutic approach is highly protocolized nowadays [2] the pharmacotherapy of PH in CDH is mainly trial and error and is based on the modulation of three major vasoactive pathways: the nitric oxide (NO), endothelin (ET) and prostacyclin (PGI_2) pathways. Inhaled NO (iNO) is the most frequently used drug followed by (i.v.) sildenafil, a phosphodiesterase-5 (PDE5) inhibitor acting on the same pathway by inhibiting the conversion of cyclic guanosine monophosphate (cGMP). Currently drugs acting on the PGI_2 pathway are used only in a compassionate way, showing contradicting results [3–5]. Although the ET pathway has shown to be affected in patients with CDH [6, 7], targeting this pathway is even more challenging because of the clinical availability of oral formulation only. A recent Cochrane review showed no improvement in patients with CDH after iNO treatment [8]. However, properly designed trials are lacking while no systematic research has been performed into the different pathways involved. An overview of all studies performed in humans using postnatal vasodilator therapy in CDH is presented in Table 6.1. Furthermore, changes in the pulmonary vasculature, leading to PH, have previously been shown to be present already early during gestation [9], while treatment is only offered postnatally. Over the last years we and others showed improvement in lung development after antenatal treatment with sildenafil in different animal models of CDH [10–12]. However, the pulmonary pathology in these animals was not totally reversed. Since CDH-associated abnormalities may not be limited to only one pathway, antenatal targeting of more pathways could possibly provide new approaches for therapeutic strategies. Antenatal use of all endothelin receptor antagonists have shown to be teratogenic [13, 14]. However, prenatal monotherapy with a slow-release synthetic prostacyclin agonist in a rat model of CDH showed improvement of the diminished development of alveolar and capillary networks [15]. Until recently most available prostacyclin analogues could only be administered by continuous intravenous infusion or inhalation, and had limited stability and a very short half-life [16]. Selexipag is a novel highly selective long-acting oral PGI_2 receptor agonist that has recently been approved for the treatment of PH in adults. The active compound of selexipag, NS-304, is hydrolyzed by the liver to its active metabolite ACT-333679, which has an even higher affinity for the PGI_2 receptor [17, 18].

Table 6.1: Studies on vasodilatory drugs in CDH

Compound	Pathway	Patients	Effect	Reference
Inhaled NO	Nitric Oxide	34	No effect	[19]
		53	No effect in mortality and ECMO	[20]
		31	No effect in mortality and ECMO	[21]
		84	No effect in mortality and ECMO	[22]
Sildenafil	Nitric Oxide	9	Improved oxygenation index	[23]
		7	Improved cardiac output, Reduced PVR	[24]
Milrinone	Prostacyclin	6	Improved RV function, Improved oxygenation index, No effect on PVR	[25]
Prostacyclin	Prostacyclin	9	Improved oxygenation index	[26]
Bosentan	Endothelin		No studies performed	

ECMO = extracorporeal membrane oxygenation, PVR = pulmonary vascular resistance, RV = right ventricle.

Here, we analyzed for the first time the effects of antenatal treatment targeting both the NO pathway and the PGI_2 pathway in the nitrofen-CDH rat model, starting at a clinically relevant time point.

Methods

Animal Model

Pregnant Sprague-Dawley rats received either 100 mg nitrofen dissolved in 1 ml olive oil or just olive oil by gavage on gestational age day E9.5. Administration of nitrofen at exactly this time point induces mainly left sided CDH in approximately 70% of the offspring, while all pups have PH [27]. This study included only pups with an observable diaphragmatic defect. Pregnant rats were divided into 8 groups: control, nitrofen (CDH), control+sildenafil, nitrofen+sildenafil (CDH+sildenafil), control+NS-304, nitrofen+NS-304 (CDH+NS-304), control+sildenafil/NS-304 and nitrofen+sildenafil/NS-304 (CDH+sildenafil/NS-304). Sildenafil (100 mg/kg/day, Pfizer, New York, NY, USA) and NS-304 (1 mg/kg/day, MedChem Express, Monmouth Junction, NJ, USA) were dissolved in 0.8% ethanol in water and administered via oral gavage for 4 consecutive days from E17.5 to E20.5. At E21 pups were delivered by caesarean section and euthanized by lethal injection of pentobarbital (Figure 6.1).

All animal experiments were approved by an independent animal ethical committee and according to national guidelines.

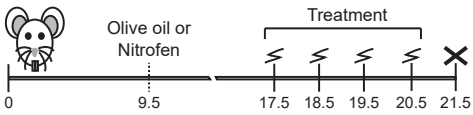

Figure 6.1: Schematic overview of the study design Overview of study design showing interventions at different time points. X-axis shows days during gestation. Flashes indicate time point of intervention, cross indicates time point of termination. The different treatments are placebo, sildenafil, NS-304 and sildenafil + NS-304. $n = 2$ litters for control and nitrofen with placebo ($n = 26$ and 24 pups, respectively) or sildenafil ($n = 15$ and 24 pups, respectively), $n = 3$ litters for control and nitrofen with NS-304 ($n = 35$ and 37 pups, respectively) or sildenafil+NS-304 ($n = 36$ and 37 pups, respectively).

Lung Morphology

Fetal rat lungs were isolated, fixed overnight in 4% PFA and embedded in paraffin. Serial 5 μm thick sections were made through the middle of the left lobe and stained with haematoxylin and eosin (HE). Sections were imaged at 40x magnification using a BX41 research stereomicroscope system (Olympus; Tokyo, Japan). Four non-overlapping images in three different sections of each lung were acquired. Major airways and vessels were excluded from analysis. The airspace size was automatically quantified using the two following measures: the D_2-score, as previously described [10], and the mean linear intercept L_m. Approximate value of the latter was calculated as proposed by Muñoz-Barrutia et al. [28], using both horizontal and vertical test lines. However, previous comparisons between both methods have shown a higher accuracy of the D_2-score [29].

Immunohistochemistry and Immunofluorescence Staining

Immunohistochemistry (IHC) was performed on 5 μm paraffin sections of lungs according to standard protocols, using the Envision^{TM} detection system (Dako Cytomatic, Glostrup,

Table 6.2: Primer sequences

Gene	Sequence (forward 5'- 3')	Sequence (reverse 5'- 3')
Ptgir	CACGAGAGGATGAAGTTTACCA	AATCCTCTGATCGTGAGAGGC
Ptgis	CATCAAACAGTTTGTGGTCCT	CAAAGCCATATCTGCTAAGGT
eNos	CATACTTGAGGATGTGGCTG	CCACGTTAATTTCCACTGCT
Pde3	CCAGCAACCGAATATTGACCA	AATCTGAAAGTTCCAGTTGCTC
Pde5	TCAACAACGGATAGCAGAACTC	CCCTGTTCATTAGATCAGCGG
Prkg2	ACTAGGCATTATCTACAGAGACC	TCCAAAGTCAACCAACTTAAGG
Sma	TGACCCAGATTATGTTTGAGAC	AGAGTCCAGCACAATACCAG
Pdgfr-β	AACGACCAGTTCTACAATGCC	CATGATCTCATAGATCTCGTCGG
Actb	AGATGACCCAGATCATGTTTGAG	GTACGACCAGAGGCATACAG

Denmark) [30]. Primary antibody used for IHC was smooth muscle actin (α-SMA; MS-113-P1; 1:1200, Thermo Scientific, Fremont, CA, USA). Antigen retrieval with Tris-EDTA buffer (10 mmol Tris, 1 mmol EDTA; pH 9.0) was used.

Primary antibodies used for immunofluorescence staining were smooth muscle actin (α-SMA; MS-113-P1; 1:500, Thermo Scientific) and Ki-67 (1:100, Abcam, Cambridge, UK). Secondary antibodies against mouse (α-SMA) and rabbit (Ki-67) were used. Negative controls were performed by omitting the primary antibody. Antigen retrieval with Citric Acid buffer (11.2 mmol; pH 6.0) was used.

Quantitative Real-Time Polymerase Chain Reaction (qPCR)

RNA isolation of whole lungs, cDNA synthesis and subsequent qPCR analysis were performed as previously described [30]. Primer combinations for the qPCR reactions are listed in Table 6.2. *Actb* was used as housekeeping gene.

Cardiovascular measurements

Lungs and heart of pups were perfused through the right ventricle with Microfil contrast agent (Microfil, Flow Tech; Carver, MA, USA) and imaged with a micro Computed Tomography (micro-CT) scanner (Quantum FX, PerkinElmer; Waltham, MA, USA; pixel size 10-295 μm). Subsequently, images of the hearts were analyzed with Dataviewer (Skyscan, Bruker, BioSpin, Ettlingen, Germany).

Statistical Analyses

Data are presented as means (SD). For the results of the dose study, one-way analysis of variance (ANOVA) was applied to compare bodyweight and lung-to-kidney weight ratio (LW/KW) between dose levels (placebo, 0.1, 1 and 10 mg/kg), followed by Tukey's method for post-hoc multiple comparisons. For the data of the intervention study, two-way ANOVA with factors disease (control versus CDH) and treatment (placebo, sildenafil, NS-304 and combination of sildenafil and NS-304) was used to compare the results of the experiments between groups. The interaction effect of disease and treatment was included in the model in case this effect was statistically significant. The normality assumption of the ANOVA models was assessed by creating histograms of the model residuals. The analyses were performed using SPSS 21.0 for Windows (Armonk, NY, USA: IBM Corp.). All statistical tests were two-sided and used a significance level of 0.05.

Results

Dose study

We first established an effective antenatal dose of NS-304 by analyzing the effects on the pups and monitoring possible side-effects of this compound. Therefore we started a dose study in control rat pups using 3 different dosages based on previous studies in adult rats [31, 32].

Pups of mothers treated with NS-304 did not show any malformations of face, palate, limbs or other organs. Bodyweight was increased in pups treated with 1 and 10 mg/kg/day and LW/KW was increased in all treated pups (Figure 6.2A). No differences in histology were observed in both lungs and kidneys between all dose levels (Figure 6.2B). The livers of all pups showed steatosis, which was resolved after adjusting the percentage of ethanol in which the compound was dissolved from 8 to 0.8% (Figure 6.2C). Based on this dose study the optimal dosage of NS-304 was found to be 1 mg/kg/day. The dosage of sildenafil was based on our previous study [10].

Lung morphology

In accordance with our previous study [10], CDH pups had a decreased bodyweight, which increased after treatment with sildenafil. Lung weight was also reduced in CDH pups, but this did not improve after treatment with sildenafil, NS-304 or the combination of sildenafil and NS-304 (Figure 6.3A,B). Both lung-to-bodyweight ratio (LW/BW) and LW/KW were significantly reduced in CDH pups. LW/BW increased only after treatment with NS-304, where LW/KW increased in all three groups receiving treatment (Figure 6.3C,D)

In correspondence with our previous results [10], the density of the air saccules was increased in lungs of CDH pups (Figure 6.4A). Statistical analyses showed a significant positive correlation between disease and treatment for both the D_2-score, the L_m and the number of air saccules ($p = 0.005$, $p = 0.024$ and $p < 0.001$, respectively). The lower D_2-score and L_m in CDH were significantly higher in the pups treated with sildenafil, while NS-304 alone or the combination of sildenafil and NS-304 were not significantly different (Figure 6.4B,C). The number of air saccules was increased in CDH and diminished after treatment with sildenafil or the combination of sildenafil and NS-304 (Figure 6.4D). Combined, these results show a therapeutic effect on the formation of air saccules after antenatal targeting mainly by sildenafil.

Since NS-304 acts on the IP-receptor (Ptgir), we checked the expression of this receptor and its synthase at mRNA level. We found an increase in *Ptgir* and a decrease in *Ptgis* in CDH with only a trend to improvement after treatment in case of *Ptgir* (Figure 6.5A,B). The expression of endothelial NO synthase (*eNos*), an important enzyme in the production of vasoactive NO, was increased in CDH and did not change after treatment (Figure 6.5C). Phosphodiesterase-3 (*Pde3*), which hydrolyses and thus inactivates the secondary messengers cyclic adenosine monophosphate (cAMP) and cGMP, was not differently expressed in control and CDH, but was decreased after treatment with NS-304 in both control and CDH (Figure 6.5D). Phosphodiesterase-5 (*Pde5*), the enzyme which hydrolyses cGMP and is inhibited by sildenafil, and its downstream target protein kinase G2 (*Prkg2*) were both increased in CDH. Prkg2 was decreased in CDH in all treatment groups (Figure 6.5E,F). All these changes in the expression of these factors in both therapeutic pathways confirm the importance of these pathways in CDH.

Pulmonary vasculature

Next, we analyzed the pulmonary vascular development by whole mount imaging after infusion of a contrast agent (Figure 6.6A). This revealed a decrease in the vascular branching and

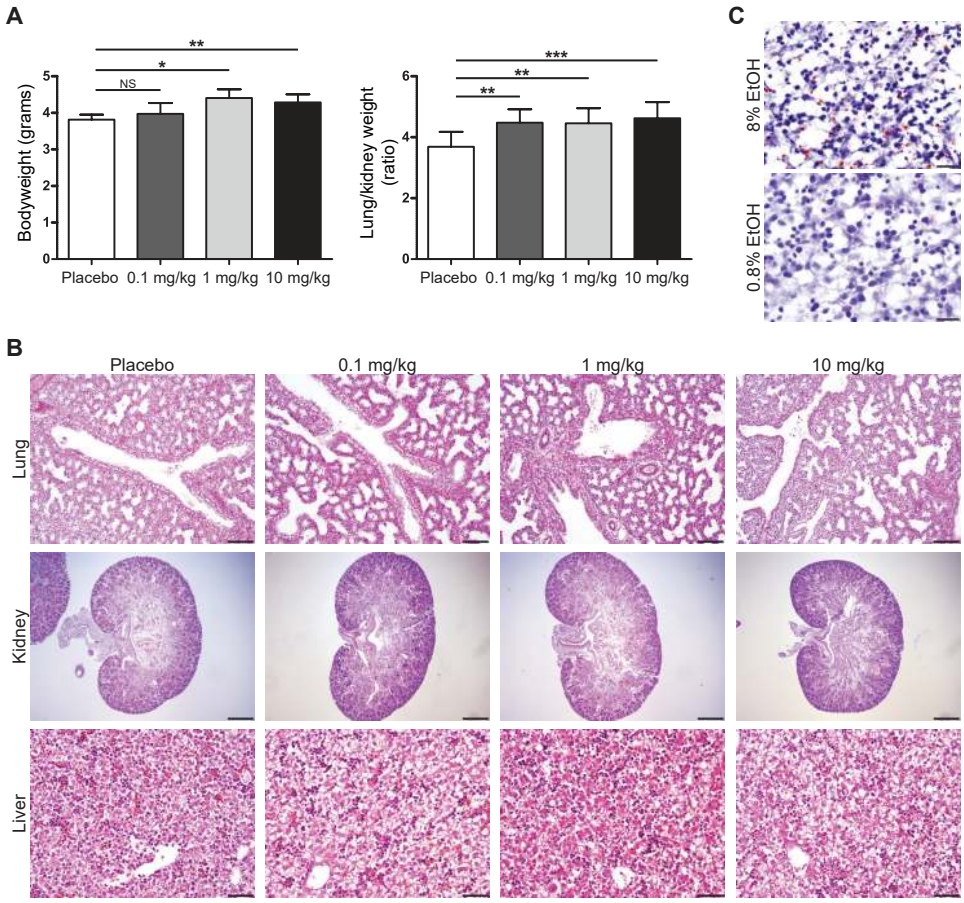

Figure 6.2: Dose study of NS-304 (**A**) Bodyweight is significantly increased after treatment with NS-304 at 1 mg/kg ($p = 0.036$) and 10 mg/kg ($p = 0.009$) ($n = 12$, 13, 10 and 14, respectively). Lung-to-kidney weight ratio is significantly increased in all treated groups ($p = 0.001$, $p = 0.005$ and $p < 0.001$, respectively) ($n = 13$, 14, 11 and 15, respectively). (**B**) Representative images of H&E staining on lung and kidney show no abnormalities in all groups. Representative images of the liver show vacuoles in all samples. Scale bars represent $200\mu m$ (lung), $500\mu m$ (kidney) and $50\mu m$ (liver). (**C**) Representative images of Oil-Red-O (ORO)-staining showing steatosis of the liver after use of 8% EtOH, but not after use of 0.8% EtOH. Scale bars represent $20\mu m$. *$p < 0.05$, ** $p < 0.01$, *** $p < 0.001$. Bars represent means (SD).

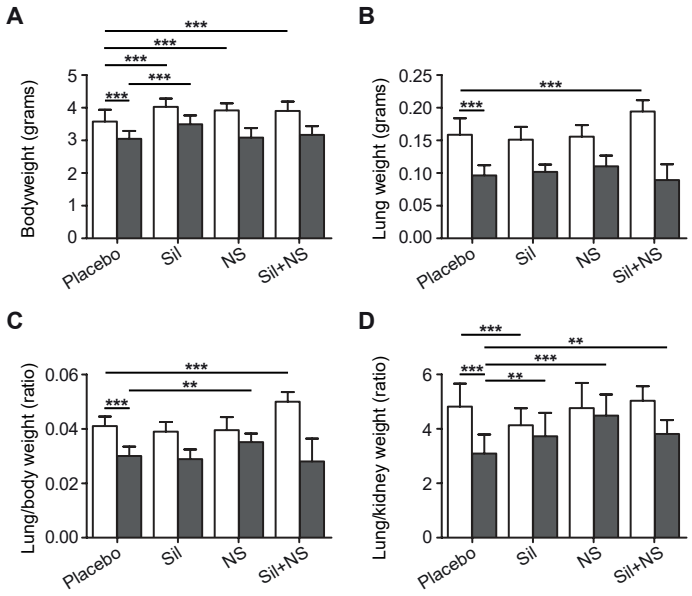

Figure 6.3: Body and lung weight (**A**) Bodyweight is decreased in pups with CDH ($p < 0.001$). Sildenafil increases bodyweight significantly in both control and CDH pups (both $p < 0.001$), where NS-304 and the combination of both compounds only increases bodyweight in control pups (both $p < 0.001$). $n = 39$, 37, 35 and 36 in the control groups and 19, 31, 14 and 21 in the nitrofen groups, respectively. (**B**) Lung weight is significantly decreased in CDH pups ($p < 0.001$) with no difference after treatment. $N = 53$, 50, 26 and 27 in the control groups and 24, 32, 10 and 16 in the nitrofen groups, respectively. (**C**) The lung-to-body weight ratio is significantly decreased in CDH ($p < 0.001$) with improvement only after NS-304 ($p = 0.003$). $n = 33$, 35, 26 and 27 in the control groups and 17, 28, 10 and 16 in the nitrofen groups, respectively. (**D**) Lung-to-kidney weight ratio is significantly decreased in CDH ($p < 0.001$) and improved in all treatment groups ($p = 0.002$, $p < 0.001$ and $p = 0.004$, respectively). $n = 44$, 50, 24 and 27 in the control groups and 23, 32, 10 and 15 in the nitrofen groups, respectively. Weights of pups from our previous experiment [10] were included to enlarge the data.
* $p < 0.05$, ** $p < 0.01$, *** $p < 0.001$. Bars represent means (SD). White bars represent control pups, grey bars represent CDH pups. Sil means sildenafil, NS means NS-304.

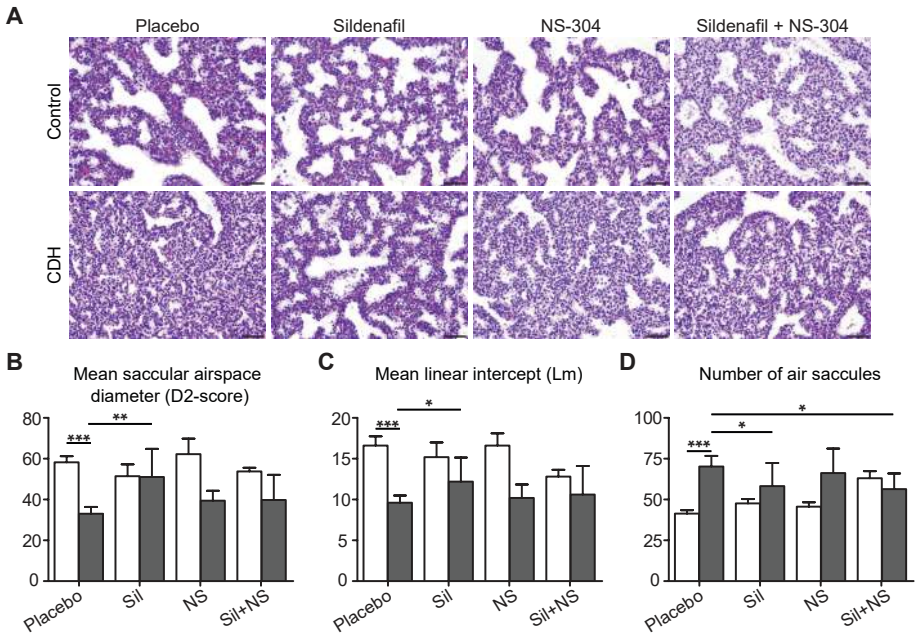

Figure 6.4: Disrupted lung morphogenesis is partly resolved after sildenafil treatment (**A**) Representative images of H&E stained lungs. Scale bars represent $50\mu m$. (**B**) Mean saccular airspace diameter (D2-score) is significantly decreased in CDH ($p < 0.001$), with a significant increase after treatment with sildenafil only ($p = 0.001$). (**C**) The mean linear intercept (Lm) is significantly decreased in CDH ($p < 0.001$), with a significant increase after treatment with sildenafil only ($p = 0.048$). (**D**) The average number of air saccules in 1 image per lung was increased in CDH ($p < 0.001$) and decreased after sildenafil ($p = 0.036$) and combination therapy ($p = 0.017$). For each group, 4 non-overlapping images on 3 different sections for 5 different animals were used.
*$p < 0.05$, **$p < 0.01$, ***$p < 0.001$. Bars represent means (SD). White bars represent control pups, grey bars represent CDH pups. Sil means sildenafil, NS means NS-304.

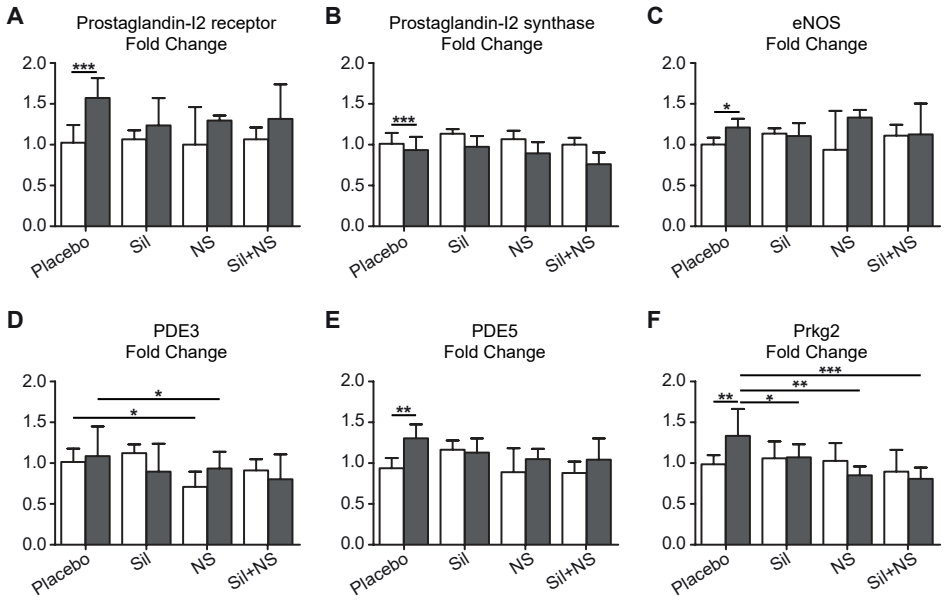

Figure 6.5: RNA expression levels of relevant factors in the NO and PGI2 pathways (**A**) Quantitative PCR shows a significant increase in *Ptgir* in CDH ($p < 0.001$) with no differences after treatment. (**B**) *Ptgis* is decreased in CDH ($p < 0.001$) with no improvement after treatment. (**C**) *eNos* expression is increased in CDH ($p = 0.041$) and shows no improvement after treatment. (**D**) No differences were found in *Pde3* between control and CDH pups, but treatment with NS-304 decreased *Pde3* expression in both control and CDH (both $p = 0.030$). (**E**) *Pde5* is increased in CDH ($p = 0.007$) with no improvement after treatment. (**F**) *Prkg2* is increased in CDH ($p = 0.013$) and decreased after treatment with sildenafil, NS-304 and the combination of both ($p = 0.045$, $p = 0.002$ and $p < 0.001$, respectively). $n = 6$ for all groups.
* $p < 0.05$, ** $p < 0.01$, *** $p < 0.001$. Bars represent means (SD). White bars represent control pups, grey bars represent CDH pups. Sil means sildenafil, NS means NS-304. No interaction model was used for *Ptgir*, *Ptgis*, *eNos*, *Pde3* and *Pde5*.

total vasculature volume in CDH. None of the applied treatment modalities showed significant improvement (Figure 6.6B), as we previously reported after prenatal sildenafil monotherapy [10]. However, histological analysis of the lungs revealed an increased thickening of the smooth muscle layer of the small pulmonary vessels ($25 - 50\mu m$) in CDH pups, comparable to our previous results [10]. This augmented thickness of the vascular wall was significantly reduced after treatment with sildenafil as well as with NS-304 alone or the combination of both. Remarkably, all treated control groups showed an increase in thickness of the medial smooth muscle layer (Figure 6.6C,D). Immunofluorescence staining showed an increase in Ki67/Sma double-positive cells in the small pulmonary vessels in CDH pups, which was reversed to normal in all three treatment groups, indicating reduced proliferation of these cells after treatment (Figure 6.6E,F).

Since we found reduced muscularization of the pulmonary vasculature in CDH lungs after antenatal vasodilator therapy, we checked the effect of the treatment on the heart. Since right ventricular hypertrophy is an indication for pulmonary hypertension postnatally [33], we measured the myocardium of the right ventricle in relation to the total diameter of the heart. This showed a significant increase in CDH with reversion to normal after treatment in all 3 groups (Figure 6.7A,B) showing a potential effect of treatment on the already higher pulmonary vascular resistance before birth.

Discussion

In this paper we show that antenatal treatment with sildenafil, starting at a clinically relevant time point, results in a partial reversal of the abnormal development of the lung morphology and pulmonary vasculature in the nitrofen-induced CDH rat model, whereas the novel PGI_2 receptor agonist selexipag only improves the pulmonary vasculature. Combination therapy with both compounds did not have a synergistic effect. This is the first study combining therapies targeting both the NO and PGI_2 pathway for antenatal use in CDH.

In accordance with our previous work [10], sildenafil increased bodyweight and LW/KW ratio and improved the lung morphogenesis in CDH pups. LW/KW ratio was even reversed to normal after treatment with selexipag, but sildenafil did not have a synergistic effect when combined with selexipag. This may be explained by a combined inducing effect of sildenafil and selexipag on the activation of CYP3A4. This enzyme is involved in the clearance of both compounds, and, therefore, the combination of these drugs may result in an increased clearance of both compounds, thereby reducing their window of activity. This is supported by a phase 3 study on selexipag, which predicted a 30% lower exposure to the active metabolite ACT-333679 when used in combination with a PDE-5 inhibitor [34]. The saccular airspaces did not increase after the use of selexipag and, when added together with sildenafil, it only seemed to reverse the positive effects of sildenafil, suggesting the enhanced clearance of both compounds. In contrast to the lung morphology, selexipag caused a decrease in muscularization and proliferation of the smooth muscle layer and a reduced myocardial thickness of the right ventricular wall. These effects were also observed after the use of sildenafil as well as the combined sildenafil/selexipag therapy. The increased proliferation of Sma positive cells in CDH might relate to the pulmonary hypertension in these pups and was previously shown by others as well [15]. Hypertrophy of the right ventricular wall has been known to be an early sign of PH postnatally followed by right ventricular dilatation and eventually heart failure [33]. Normally, early during gestation the right and left cardiac ventricles are approximately identical in size, whereas later in pregnancy the right ventricle becomes slightly more dilated [35]. However, in case of right ventricular outlet obstruction the myocardial mass can already increase antenatally [36]. A previous study in adult rats with monocrotaline-induced PH showed reduced hypertrophy of the pulmonary arterial wall and less thickening of the right ventricle after the use of selexipag postnatally [31]. These combined results indicate a potential effect of this drug on the severity of the PH. Reduced

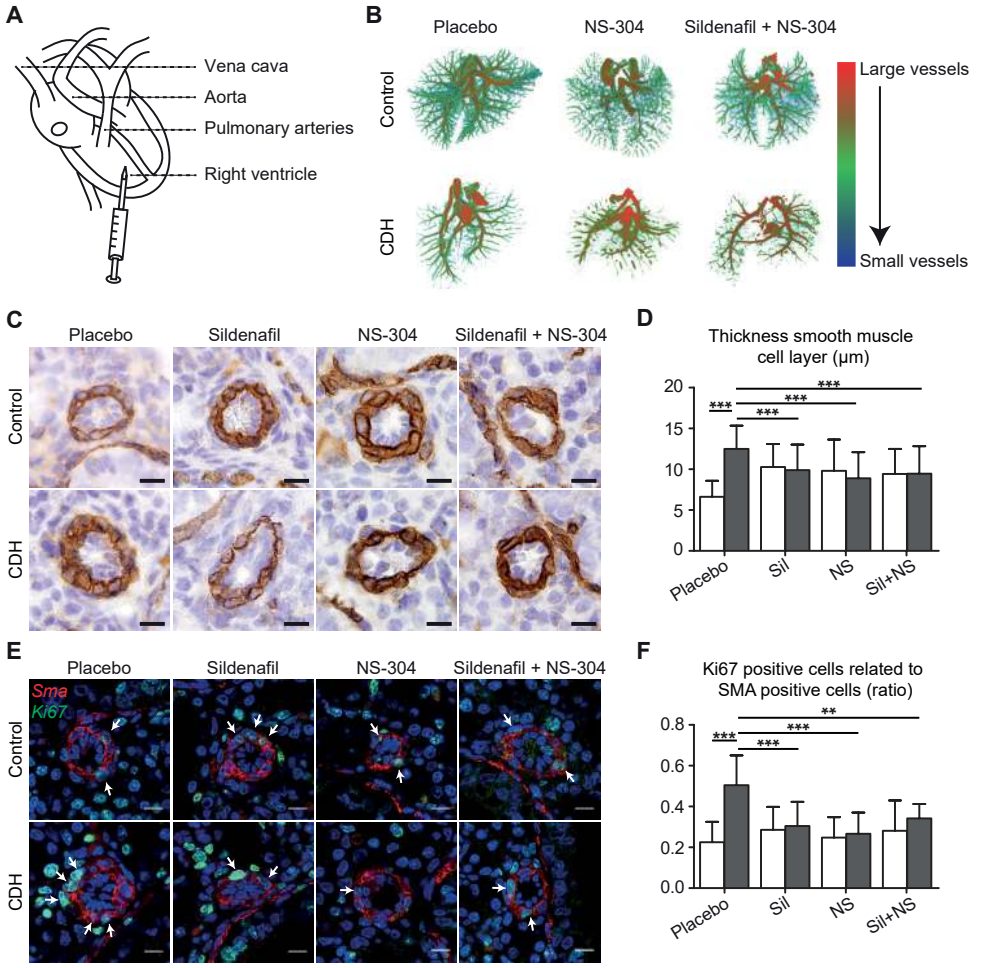

Figure 6.6: Both sildenafil and NS-304 reduce muscularization defects in CDH (**A**) Schematic image of injection through the right ventricle. (**B**) Representative images of Microfil-injected pulmonary vessels show decreased branching and volume in CDH with no improvement after treatment with NS-304 or the combination of sildenafil and NS-304. (**C**+**D**) Representative images of immunohistochemistry staining show increased expression of Sma and an increased thickening of the vascular wall of small pulmonary vessels ($25 - 50\mu m$) in CDH ($p < 0.001$) and control lungs treated with all compounds (all $p < 0.001$). In CDH this thickening is decreased after all treatments (all $p < 0.001$). $n = 34$, 30, 33 and 34 in the control groups and 32, 33, 38 and 33 in the nitrofen groups, respectively. (**E**+**F**) Representative images of immunofluorescence staining show an increase in Ki-67/Sma double-positive cells in small pulmonary vessels in CDH ($p < 0.001$) with improvement to normal in all treated groups ($p < 0.001$, $p < 0.001$ and $p = 0.001$, respectively). $n = 12$ for all groups. Scale bars represent $10\mu m$.
** $p < 0.01$, *** $p < 0.001$. Bars represent means (SD).

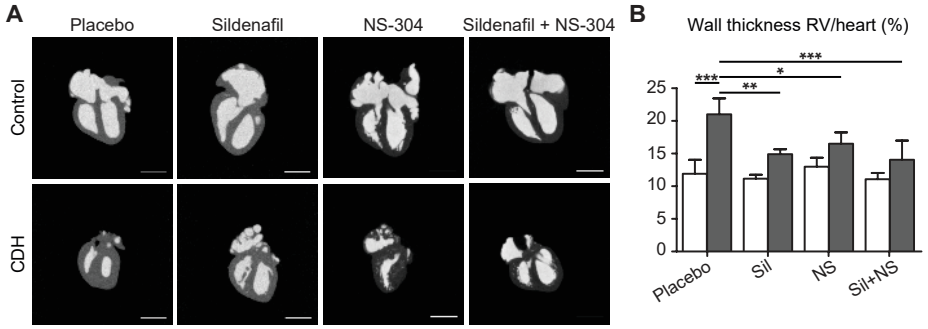

Figure 6.7: Prenatal treatment improves cardiovascular defects Representative images of with Microfil filled hearts show increased thickness of the right ventricle wall in relation to the total diameter of the heart ($p < 0.001$). This thickening improved after treatment with sildenafil, NS-304 and the combination of both ($p = 0.001$, $p = 0.023$, $p < 0.001$, respectively). Scale bars represent 2 mm. $n = 5$, 3, 5 and 4 in the control groups and 2, 3, 2 and 4 in the nitrofen groups, respectively.
* $p < 0.05$, ** $p < 0.01$, *** $p < 0.001$. Bars represent means (SD).

pulmonary vascular pathology was also observed in a prophylactic study by Umeda et al., who applied a prostacyclin agonist antenatally in CDH [15]. They showed an increased LW/BW ratio and reduced thickening of the medial wall of pulmonary arteries, as we show as well. In contrast to our results, they found an improvement of the alveolar and capillary networks with an increased mean linear intercept at E21. These differences can possibly be explained by the thromboxane inhibitory activity of their compound or the early start of treatment at day E9.5, when development is still at an earlier stage and deviations in lung development have not yet started. The major advantage of our approach is the start of our treatment at E17.5, a phase of lung development comparable to 20 weeks of gestation in human when CDH can be detected, which makes it potentially more clinically relevant. Furthermore, we used an orally available approved medicine for our treatment, which could be extrapolated easier to clinical use. As previously described by our group [10], pulmonary vascular volume is decreased in CDH. Apart from sildenafil, selexipag and combination therapy with both compounds did not increase vascular volume and branching. This may well be expected since the majority of the pulmonary vessels is already developed at the start of treatment and treatment will therefore mostly affect the vascular remodeling.

Confirming the results previously shown by us and others [10–12], sildenafil caused unanticipated differences in lung structure in healthy controls, with a thickening of the smooth muscle layer in the pulmonary vessels. However, selexipag induced similar effects in healthy subjects, which strengthens the idea that inducing vasodilation in already healthy vessels might be deleterious for the development of the pulmonary vasculature [10].

The possibility of early detection of CDH by ultrasound makes this disease suitable for antenatal therapies. Some studies have already been performed in the nitrofen rat model on the antenatal use of sildenafil alone [10, 11] or in combination with steroids [37, 38] or the endothelin antagonist bosentan [39]. However, the combination with a prostacyclin agonist, which can safely be used antenatally, has never been studied in this disease. Although antenatal treatment with selexipag or the combination of selexipag and sildenafil did not seem advantageous over monotherapy, at least in the nitrofen rat model, the addition of a second drug might still be of interest because of the variable response to vasodilator therapy of CDH patients in the clinical setting [1] (Table 6.1). The variability between patients and the altered expression of different vasoactive factors in CDH strengthens the need for ongoing evaluation of the developmental

sequences of the pathways involved and subsequently, a more precision medicine approach.

We analyzed for the first time the feasibility and effects of antenatal use of the novel PGI_2-receptor agonist selexipag in the nitrofen-induced CDH rat model. The positive effects on the pulmonary vasculature show that the compound successfully entered the fetal circulation. Embryotoxicity studies in rats and rabbits have shown no malformations, irregularities or neurological differences after the use of selexipag during pregnancy [34, 40]. Indeed, no malformations or abnormalities in histology were seen in different organs in our study.

In conclusion, this study demonstrates improvement of lung morphogenesis after antenatal treatment with sildenafil monotherapy and a reduction in vascular remodeling after antenatal treatment with both sildenafil and selexipag monotherapy, where no synergistic effect was present after combination of both compounds. This knowledge creates important possibilities in the therapy of pulmonary hypertension in CDH patients. Ideally, future research has to reveal antenatal differences in expression of vasoactive factors in specific individual CDH patients before clinical trials on precision medicine with these compounds can be performed.

Acknowledgements

The authors would like to thank Rob Verdijk for his advice on histology and Kim Moerkerke and colleagues for the treatment of the rats.

This study was supported in part by the Sophia Foundation for Medical Research grant number 678 (HMK) and S15-11 (PMB).

References

[1] Puligandla PS, Grabowski J, et al. Management of congenital diaphragmatic hernia: A systematic review from the APSA outcomes and evidence based practice committee. J Pediatr Surg. 2015;50(11):1958–70.

[2] Snoek KG, Reiss IK, et al. Standardized Postnatal Management of Infants with Congenital Diaphragmatic Hernia in Europe: The CDH EURO Consortium Consensus - 2015 Update. Neonatology. 2016;110(1):66–74.

[3] De Luca D, Zecca E, et al. Transient effect of epoprostenol and sildenafil combined with iNO for pulmonary hypertension in congenital diaphragmatic hernia. Paediatr Anaesth. 2006;16(5):597–8.

[4] Olson E, Lusk LA, et al. Short-Term Treprostinil Use in Infants with Congenital Diaphragmatic Hernia following Repair. J Pediatr. 2015;167(3):762–4.

[5] Skarda DE, Yoder BA, et al. Epoprostenol Does Not Affect Mortality in Neonates with Congenital Diaphragmatic Hernia. Eur J Pediatr Surg. 2015;25(5):454–9.

[6] de Lagausie P, de Buys-Roessingh A, et al. Endothelin receptor expression in human lungs of newborns with congenital diaphragmatic hernia. J Pathol. 2005;205(1):112–8.

[7] Dingemann J, Doi T, et al. Upregulation of endothelin receptors A and B in the nitrofen induced hypoplastic lung occurs early in gestation. Pediatr Surg Int. 2010;26(1):65–9.

[8] Barrington KJ, Finer N, et al. Nitric oxide for respiratory failure in infants born at or near term. Cochrane Database Syst Rev. 2017;1:CD000399.

[9] Sluiter I, van der Horst I, et al. Premature differentiation of vascular smooth muscle cells in human congenital diaphragmatic hernia. Exp Mol Pathol. 2013;94(1):195–202.

[10] Mous DS, Kool HM, et al. Clinically relevant timing of antenatal sildenafil treatment reduces pulmonary vascular remodeling in congenital diaphragmatic hernia. Am J Physiol Lung Cell Mol Physiol. 2016;311(4):L734–L742.

[11] Luong C, Rey-Perra J, et al. Antenatal sildenafil treatment attenuates pulmonary hypertension in experimental congenital diaphragmatic hernia. Circulation. 2011;123(19):2120–31.

[12] Russo FM, Toelen J, et al. Transplacental sildenafil rescues lung abnormalities in the rabbit model of diaphragmatic hernia. Thorax. 2016;.

[13] Spence S, Anderson C, et al. Teratogenic effects of the endothelin receptor antagonist L-753,037 in the rat. Reprod Toxicol. 1999;13(1):15–29.

[14] de Raaf MA, Beekhuijzen M, et al. Endothelin-1 receptor antagonists in fetal development and pulmonary arterial hypertension. Reprod Toxicol. 2015;56:45–51.

[15] Umeda S, Miyagawa S, et al. Enhanced Pulmonary Vascular and Alveolar Development via Prenatal Administration of a Slow-Release Synthetic Prostacyclin Agonist in Rat Fetal Lung Hypoplasia. PLoS One. 2016;11(8):e0161334.

[16] Asaki T, Kuwano K, et al. Selexipag: An Oral and Selective IP Prostacyclin Receptor Agonist for the Treatment of Pulmonary Arterial Hypertension. J Med Chem. 2015;58(18):7128–37.

[17] Kaufmann P, Cruz HG, et al. Pharmacokinetics of the novel oral prostacyclin receptor agonist selexipag in subjects with hepatic or renal impairment. Br J Clin Pharmacol. 2016;82(2):369–79.

[18] Sardana M, Moll M, et al. Pharmacokinetic drug evaluation of selexipag for the treatment of pulmonary arterial hypertension. Expert Opin Drug Metab Toxicol. 2016;12(12):1513–1520.

[19] Kinsella JP, Truog WE, et al. Randomized, multicenter trial of inhaled nitric oxide and high-frequency oscillatory ventilation in severe, persistent pulmonary hypertension of the newborn. J Pediatr. 1997;131(1 Pt 1):55–62.

[20] Inhaled nitric oxide and hypoxic respiratory failure in infants with congenital diaphragmatic hernia. The Neonatal Inhaled Nitric Oxide Study Group (NINOS). Pediatrics. 1997;99(6):838–45.

[21] Clark RH, Kueser TJ, et al. Low-dose nitric oxide therapy for persistent pulmonary hypertension of the newborn. Clinical Inhaled Nitric Oxide Research Group. N Engl J Med. 2000;342(7):469–74.

[22] Finer NN, Barrington KJ. Nitric oxide for respiratory failure in infants born at or near term. Cochrane Database Syst Rev. 2006;(4):CD000399.

[23] Bialkowski A, Moenkemeyer F, et al. Intravenous sildenafil in the management of pulmonary hypertension associated with congenital diaphragmatic hernia. Eur J Pediatr Surg. 2015;25(2):171–6.

[24] Noori S, Friedlich P, et al. Cardiovascular effects of sildenafil in neonates and infants with congenital diaphragmatic hernia and pulmonary hypertension. Neonatology. 2007;91(2):92–100.

[25] Patel N. Use of milrinone to treat cardiac dysfunction in infants with pulmonary hypertension secondary to congenital diaphragmatic hernia: a review of six patients. Neonatology. 2012;102(2):130–6.

[26] Bos AP, Tibboel D, et al. Persistent pulmonary hypertension in high-risk congenital diaphragmatic hernia patients: incidence and vasodilator therapy. J Pediatr Surg. 1993;28(11):1463–5.

[27] Kluth D, Kangah R, et al. Nitrofen-induced diaphragmatic hernias in rats: an animal model. J Pediatr Surg. 1990;25(8):850–4.

[28] Munoz-Barrutia A, Ceresa M, et al. Quantification of lung damage in an elastase-induced mouse model of emphysema. Int J Biomed Imaging. 2012;2012:734734.

[29] Jacob RE, Carson JP, et al. Comparison of two quantitative methods of discerning airspace enlargement in smoke-exposed mice. PLoS One. 2009;4(8):e6670.

[30] Rajatapiti P, van der Horst IW, et al. Expression of hypoxia-inducible factors in normal human lung development. Pediatr Dev Pathol. 2008;11(3):193–9.

[31] Kuwano K, Hashino A, et al. 2-[4-[(5,6-diphenylpyrazin-2-yl)(isopropyl)amino]butoxy]-N-(methylsulfonyl)acetam ide (NS-304), an orally available and long-acting prostacyclin receptor agonist prodrug. J Pharmacol Exp Ther. 2007;322(3):1181–8.

[32] Kuwano K, Hashino A, et al. A long-acting and highly selective prostacyclin receptor agonist prodrug, 2-4-[(5,6-diphenylpyrazin-2-yl)(isopropyl)amino]butoxy-N-(methylsulfonyl)acetam ide (NS-304), ameliorates rat pulmonary hypertension with unique relaxant responses of its active form, 4-[(5,6-diphenylpyrazin-2-yl)(isopropyl)amino]butoxyacetic acid (MRE-269), on rat pulmonary artery. J Pharmacol Exp Ther. 2008;326(3):691–9.

[33] Bogaard HJ, Abe K, et al. The right ventricle under pressure: cellular and molecular mechanisms of right-heart failure in pulmonary hypertension. Chest. 2009;135(3):794–804.

[34] EMA. Public assessment report; selexipag. 2016;Procedure No. EMEA/H/C/003774/0000.

[35] Sharland GK, Allan LD. Normal fetal cardiac measurements derived by cross-sectional echocardiography. Ultrasound Obstet Gynecol. 1992;2(3):175–81.

[36] Rudolph AM. Myocardial growth before and after birth: clinical implications. Acta Paediatr. 2000;89(2):129–33.

[37] Kattan J, Cespedes C, et al. Sildenafil stimulates and dexamethasone inhibits pulmonary vascular development in congenital diaphragmatic hernia rat lungs. Neonatology. 2014;106(1):74–80.

[38] Burgos CM, Pearson EG, et al. Improved pulmonary function in the nitrofen model of congenital diaphragmatic hernia following prenatal maternal dexamethasone and/or sildenafil. Pediatr Res. 2016;80(4):577–85.

[39] Lemus-Varela Mde L, Soliz A, et al. Antenatal use of bosentan and/or sildenafil attenuates pulmonary features in rats with congenital diaphragmatic hernia. World J Pediatr. 2014;10(4):354–9.

[40] FDA. Pharmacology reviews; selexipag. 2014;Application number 207947Orig1s000.

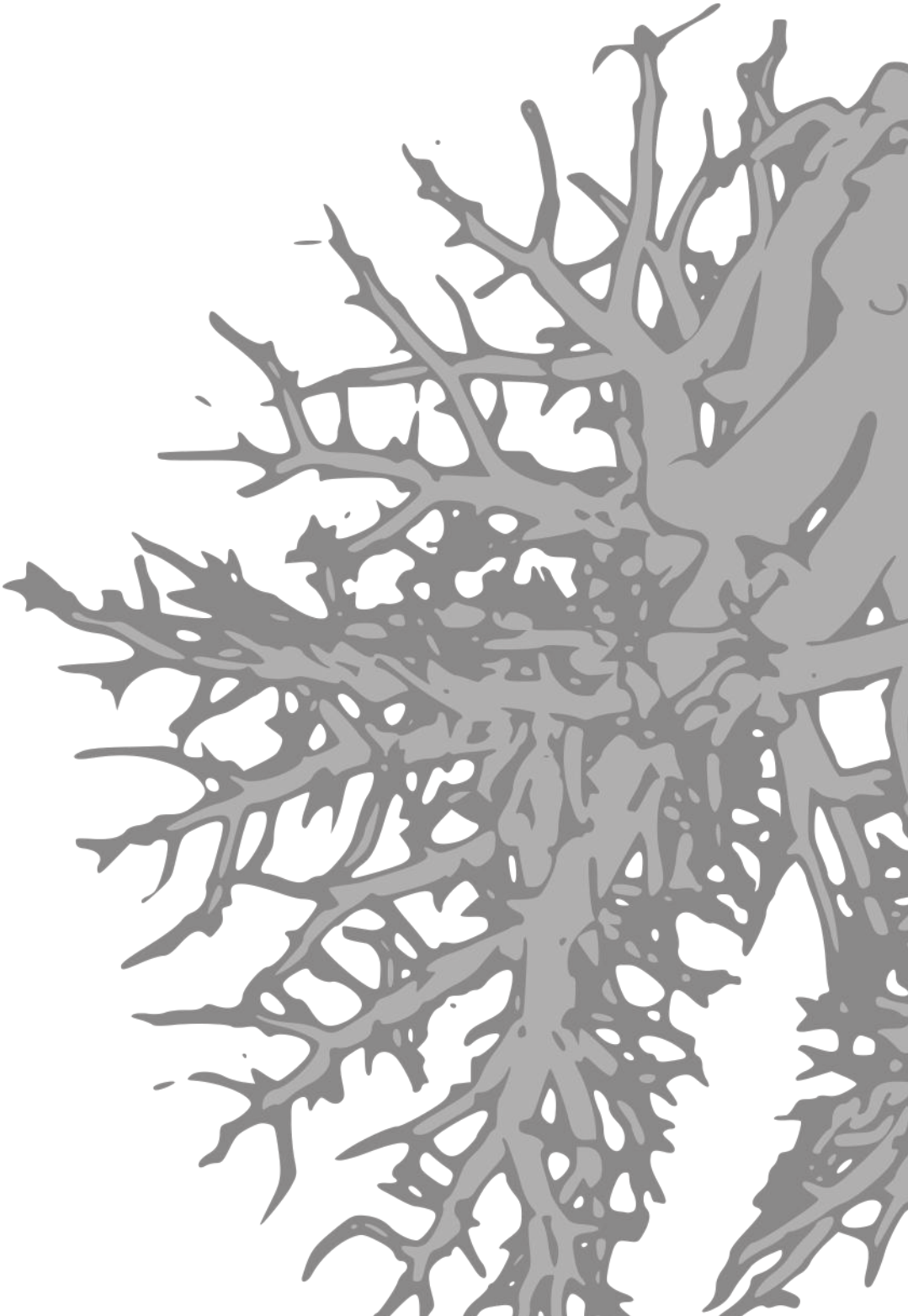

Chapter 7

General discussion

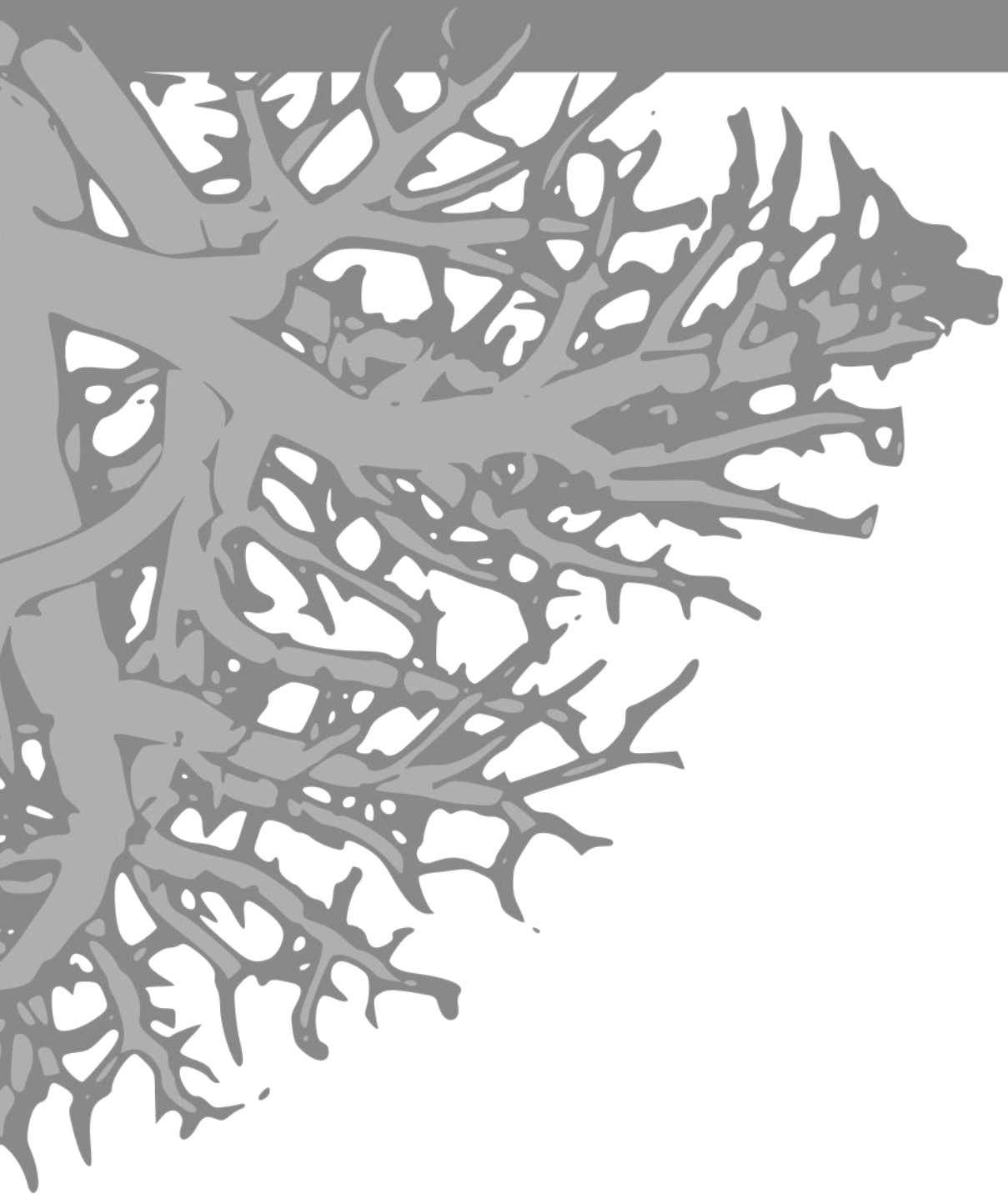

This thesis describes the role of important pathways in the normal and aberrant pulmonary vascular development in patients with Congenital Diaphragmatic Hernia (CDH) and the feasibility of antenatal treatment with vasodilator therapy in these patients. Most studies were performed using the well-established nitrofen-treated rat model for CDH [1], supplemented by research on exclusive human material of CDH patients. In this chapter the main findings will be highlighted in relation to the current clinical standard of protocolized care [2, 3] and future implications.

Pulmonary hypertension

A large group of patients with CDH suffer from severe pulmonary hypertension due to altered vasoreactivity in combination with pulmonary vascular remodeling. Consequences of pulmonary hypertension and pulmonary hypoplasia play a significant role in the high morbidity and mortality of these patients [4]. Management of pulmonary hypertension in CDH patients is still challenging. Current therapy strategies in pulmonary hypertension treatment are mostly based on targeting the major vasoactive pathways; the Endothelin (ET), Nitric Oxide (NO) and Prostacyclin (PGI_2) pathways. However, in contrast to the promising results in patients with persistent pulmonary hypertension of the newborn (PPHN) [5], CDH patients are often unresponsive to current vasodilator therapy. Inhaled Nitric Oxide (iNO) is most commonly used in the treatment of patients with CDH, but showed no benefit in risk of death or the use of extracorporeal membrane oxygenation (ECMO) [6–9]. Sildenafil, an inhibitor of phosphodiesterase-5 (PDE5) which normally converts cyclic guanosine monophosphate (cGMP) into GMP causing an increase in vasoconstriction, has shown to decrease mortality in patients with PPHN [10–15]. In CDH, some case reports on the use of sildenafil showed positive effects on the oxygenation index and pulmonary vascular resistance [16, 17], but contained only a small number of patients ($n = 9$ and $n = 7$, respectively). Other case reports on drugs targeting the prostacyclin pathway, prostacyclin and the PDE3 inhibitor milrinone, also showed an improvement of the oxygenation index, but were equally underpowered ($n = 6$ and $n = 9$, respectively) [18, 19]. No information is available on the use of the endothelin receptor antagonist bosentan in the early stage of treatment of CDH. Bosentan is available only orally, limiting its application in critically ill patients taking into account the abnormal position of the stomach and unpredictable absorption rate. Apart from these scarce case reports and some patients included in other trials, large randomized controlled trials for the treatment of pulmonary hypertension in CDH are still lacking. Over the last years, several factors involved in the abnormal development of the pulmonary vasculature in CDH have been identified, including mutations in some retinoid related genes, such as *STRA6*, *COUP-TFII* and *FOG2* [20–22]. However, almost no overlap can be found in genes expressed in CDH and other forms of pulmonary hypertension. Where patients with idiopathic pulmonary arterial hypertension (iPAH) show mainly mutations in genes involved in the TGFβ/BMP pathways, like the well-studied *BMPr2* mutation [23], these mutations could not be found in CDH patients. However, mutations in *STRA6*, the membrane receptor for retinol binding protein (RBP1) have been found as well in CDH as in some isolated cases of alveolar capillary dysplasia (ACD) [20], indicating a possible genetic overlap between both rare diseases.

TGFβ/BMP pathways

Although almost no mutations in genes of the TGFβ pathway are found in CDH patients, mutations in the retinoic acid (RA) pathway can influence TGFβ signaling. RA is a negative regulator of TGFβ and the absence of RA has been shown to inhibit lung bud formation through increased TGFβ activity [24]. Furthermore, rats with alveolar hypoplasia caused by

caloric restriction showed both improvement of the alveolar formation and decreased TGFβ activity after treatment with RA [25], indicating an interaction between RA and TGFβ in the development of the lung morphology. RA deficiency has also been shown to play a role in the vasculature by affecting the vasculogenesis of the systemic circulation [26]. Some studies have shown deviations of both the TGFβ and BMP receptors in an animal model of CDH [27–34], but the results are inconsistent and not much is known about the downstream activity of this pathway and especially its role in the pulmonary vasculature. We showed increased activation of the TGFβ pathway and decreased activation of the BMP pathway in the pulmonary vasculature of nitrofen-CDH pups, as described in Chapter 3, which might indeed be caused by a relative RA deficiency at organ level in this animal model, since nitrofen has been shown to disrupt the retinoid signaling pathway [35]. Furthermore, we found increased proliferation of the smooth muscle cells in pulmonary vessels, indicating a possible aberrant response to the increased TGFβ activity. The combination of increased TGFβ activity and increased proliferation in the same cell layer of the vessel wall, might partly explain the already known increased muscularization of the pulmonary vasculature in CDH.

Vasoactive pathways

Even though patients with CDH are often unresponsive to vasodilator therapy, almost no information is available on the possible aberrant expression of the targeted molecules of current drugs in this group of patients. The different genetic background combined with the unresponsiveness to therapy strengthens the idea that different factors might be affected in pulmonary hypertension in CDH compared to, for instance, patients with so-called idiopathic pulmonary hypertension. We investigated for the first time important factors in all 3 major vasoactive pathways in both human and rat CDH, as described in Chapter 4. This study showed an increased expression of both the endothelin A (ETA) and B (ETB) receptors and the endothelin converting enzyme (ECE-1) in human and rat CDH. ECE-1 is a key molecule in the endothelin pathway which converts endothelin-1 (ET-1) into its active form. Although some previous studies have shown the increased expression of ETA and ETB in both human and rat tissue as well [36, 37], the important ECE-1 has never been analyzed before. Apart from the important increase in receptors and the converting enzyme, increased plasma levels of ET-1 have been described in patients with CDH and documented PH [38, 39] and an increased response of arterioles to ET-1 was found in the nitrofen rat model [40]. Overall these results point to an increased activation and sensitivity of the endothelin mediated vasoconstriction.

Alterations in the NO pathway, currently the most targeted pathway in the treatment of pulmonary hypertension, have shown contradictory results over the years. Endothelial Nitric Oxide Synthase (eNOS), an important enzyme that produces NO, has previously been found decreased, increased or not changed at all in patients with CDH [41–44]. This is probably due to the investigations performed at autopsy of patients all dying under hypoxia due to therapy resistant PH. Even animal studies could not provide a decisive answer to this indistinctness [45, 33, 46]. This variability in results might indicate a less important role of NO in the pathophysiology of pulmonary hypertension in CDH than expected and could be the reason of the reduced response to iNO in these patients.

Although prostacyclin agonists are used as compassionate treatment of pulmonary hypertension in CDH, no studies in these patients have been performed on this pathway at all. A previous study performed by our group showed increased levels of PGI_2 and an increased ratio of PGI_2 and thromboxane in the nitrofen rat model [47]. These observations in rat were complemented by us, showing an increase in expression of the PGI_2-receptor at RNA level, as described in Chapter 4. We showed a gradually increase in the PGI_2-receptor in human control lungs over time which was decreased in CDH patients at both the fetal, preterm and term

phase of lung development. This decreased expression of the important PGI_2-receptor possibly indicates a reduced activity of this pathway, making it a potential target in the treatment of pulmonary hypertension in CDH.

All these differences in expression of important factors in the sporadically targeted prostacyclin and endothelin pathways point to the need for well-organized randomized controlled trials in this group of patients. However, although the ET pathway has shown to be affected in CDH, the use of endothelin receptor antagonists in these newborn patients is complicated by the clinical availability of oral formulation only. Recently the COdiNOS trial, where iNO versus intravenous sildenafil will be tested, has been approved by the IRB at the Erasmus MC Rotterdam in the Netherlands. This study will be conducted within the frame work of the CDH-EURO Consortium.

Potential antenatal treatment modalities

In general, current treatment of pulmonary hypertension in CDH only starts postnatally. However, as described in Chapter 4 and previously by our group [48], abnormalities in the pulmonary vasculature and the major vasoactive pathways already develop earlier during development. Fetoscopic Endoluminal Tracheal Occlusion (FETO), an antenatal procedure where a small balloon device is inserted to temporarily occlude the trachea to increase lung growth, is currently the only clinically used antenatal intervention in an international randomized controlled trial (NCT 02875860; clinicaltrials.gov). Until now, FETO has shown to improve survival rate in high risk CDH patients but at the cost of increased morbidity and premature delivery as the most important and unwanted side effects [49–52]. Apart from FETO, corticosteroids can be used as an antenatal therapy for lung hypoplasia in CDH. However, no clear differences were seen in perinatal mortality, duration of ventilation and hospital stay in the clinical setting [53] and different animal studies showed no increase in lung to bodyweight ratio after antenatal corticosteroids, but some reported improvement in airway histology [54]. In the past the proposed trial on the use of antenatal corticosteroids was stopped prematurely due to the lack of inclusion.

Antenatal use of vasodilators is not yet approved for clinical use and these drugs are therefore only tested in various animal models of CDH. As described in Chapter 4, enhanced activation of the endothelin pathway is present in the lungs of patients with CDH. However, both selective and dual endothelin receptor antagonists have shown to be teratogenic, causing craniofacial and cardiovascular malformations in the unborn fetus [55, 56] and are therefore not eligible for antenatal therapy. On the other hand, antenatal targeting of the nitric oxide or prostacyclin pathway are not known to induce abnormal development. We conducted a study using antenatal sildenafil and the novel orally available prostacyclin receptor agonist selexipag (NS-304), as described in Chapters 5 and 6. We showed improvement in lung histology, with enlargement of the decreased alveolar airspaces, and pulmonary vascular development, with less muscularization of the thickened pulmonary vessel wall, in nitrofen-treated rats after the use of antenatal sildenafil. Like us, other research on the antenatal use of sildenafil in both rat and rabbit studies has shown improvement in lung development [57–61]. However, we were the first to show positive effects after starting the treatment at a clinically relevant time point at day 17.5 of gestation, corresponding with 20 weeks of gestation in human when CDH is usually detected. Apart from sildenafil, targeting of the prostacyclin pathway using selexipag (NS-304) showed improvement in the aberrant cardio and pulmonary vascularity. These results correspond with the positive effects seen on the pulmonary vasculature in the only other available study using an antenatal prostacyclin agonist [62]. However, again their treatment was started early during development when deviations in lung development have not yet started. Furthermore, the oral form and clinical availability of our compound makes it more clinically relevant. Combination therapy of

sildenafil and NS-304, targeting both the NO and prostacyclin pathway, did not have added value to both compounds solely, probably because of increased clearance of the active metabolites by inducement of the same CYP enzyme.

Although positive effects on pulmonary vascular development have now been shown after antenatal therapies in several animal studies, clinical trials have to be conducted to test the eligibility of this approach. To date antenatal sildenafil is administered to pregnant mothers in a trial of severe intrauterine growth restriction to modulate vascular tone and improve growth of the fetus [STRIDER; NCT02277132 (clinicaltrials.gov)]. The possibility to target different pathways in the treatment of pulmonary hypertension in patients with CDH might provide added value in the future implementation of a precision medicine approach.

Clinical implications

Since human material of CDH patients is scarce and animal models of this disease are only comparable to the clinical situation to a limited extent, it is difficult to draw clear conclusions from current research. However, our studies may have a considerable effect in identifying new or better targets for pharmacological therapies and may lead eventually to a more precision medicine approach in which antenatal targeting could even play a potential role. Currently, clinical postnatal treatment of patients with CDH is mainly trial and error and no properly designed studies on all used drugs have been performed in this specific group of patients. The choice of combination therapy for individual patients is another important step to be made to enhance the treatment results in the most severely affected patients unresponsive to the current approaches including ECMO. Vasodilator therapy is mostly based on the major vasoactive pathways in adults or at best on some trials in neonatal patients with persistent pulmonary hypertension due to other causes [63]. However, the underlying pathophysiology of pulmonary vascular defects is most likely different in CDH patients, given the poor response to current therapies. Systematic research on the different targeted pathways in these patients is lacking, making it difficult to use specific directed treatment. Representative material of CDH patients is scarce, since age and therapies could cause secondary morphological changes while the patients usually die under severe hypoxic conditions and the time to harvest material after death is not standardized either. Therefore, our study on the expression of important target-directed factors of all major pathways in human material of CDH patients, described in Chapter 4, could be of great importance to future therapy. Although some studies have been performed previously on only a few components of these pathways, we are the first to combine this important research in all pathways in both human material and the well-established nitrofen rat model, obtaining a clear insight of existing alterations in the pulmonary vasculature. Over the last years antenatal treatment of congenital anomalies has become an upcoming interest in CDH research. The possibility of early detection at 20 weeks of gestation by ultrasound, makes this disease suitable for an antenatal approach of therapy. Our studies, described in Chapter 5 and 6, show the feasibility of antenatal treatment with the phosphodiesterase-5 inhibitor sildenafil and the novel prostaglandin-I2 receptor agonist selexipag (NS-304) in the nitrofen rat model. Although further studies are needed to prove safety and efficacy in clinical use, our research might add to a potential start of a new era in the treatment of CDH with the aim to correct or modulate the pulmonary vasculature at an earlier stage of abnormal development instead of “damage control”.

Future research

Before the suggested antenatal therapies can be implemented in the clinical setting, clinical trials should be initiated to test safety and efficacy of different forms of antenatal vasodilator therapy

in patients with CDH and the optimum dosage should be determined. Ideally, antenatal testing of the expression of factors that can be targeted would be of great value for the implementation of a precision medicine approach.

Furthermore, research should become more focused on the actual changes in the aberrant pulmonary development between different diseases of the newborn. Patients with CDH often develop neonatal chronic lung disease (nCLD), because of their high susceptibility for oxygen and ventilation damage, indicating an overlap in the pathophysiology of both diseases. And although the genetic mutations found in CDH differ from those in PPHN, both in CDH and nCLD as well as in PPHN multiple developmental signaling pathways are affected, of which for instance TGFβ seems to be a common factor. In Chapter 3 we described the upregulated activation of TGFβ in the nitrofen rat model, which corresponds to the effects seen on PDGF-Rα in a mouse model of nCLD, as described in the Appendix. Furthermore, some overlap might exist between CDH and ACD, which are both developmental diseases associated with severe pulmonary hypertension mostly unresponsive to current therapies. Further research in both diseases could have important implications in the approach of treatment in both patient groups.

Conclusions

In conclusion, our work shows important alterations already early during development in the TGFβ pathway and all three major vasoactive pathways in both human CDH and the well-established nitrofen rat model. Furthermore, it shows the feasibility of antenatal treatment of pulmonary vascular defects in this disease with two different vasodilators acting on the NO and PGI_2 pathway. These results indicate the importance of a precision medicine approach, potentially even already starting antenatally. As the mortality of CDH has significantly decreased in the last decade, still around 20-25% of patients die due to a lack of insight in the optimal therapy for this high risk patient population so far.

References

[1] Greer JJ, Allan DW, et al. Recent advances in understanding the pathogenesis of nitrofen-induced congenital diaphragmatic hernia. Pediatr Pulmonol. 2000;29(5):394–9.

[2] Reiss I, Schaible T, et al. Standardized postnatal management of infants with congenital diaphragmatic hernia in Europe: the CDH EURO Consortium consensus. Neonatology. 2010;98(4):354–64.

[3] Snoek KG, Reiss IK, et al. Standardized Postnatal Management of Infants with Congenital Diaphragmatic Hernia in Europe: The CDH EURO Consortium Consensus - 2015 Update. Neonatology. 2016;110(1):66–74.

[4] Lally KP. Congenital diaphragmatic hernia - the past 25 (or so) years. J Pediatr Surg. 2016;51(5):695–8.

[5] Roberts J J D, Fineman JR, et al. Inhaled nitric oxide and persistent pulmonary hypertension of the newborn. The Inhaled Nitric Oxide Study Group. N Engl J Med. 1997;336(9):605–10.

[6] Inhaled nitric oxide and hypoxic respiratory failure in infants with congenital diaphragmatic hernia. The Neonatal Inhaled Nitric Oxide Study Group (NINOS). Pediatrics. 1997;99(6):838–45.

[7] Kinsella JP, Truog WE, et al. Randomized, multicenter trial of inhaled nitric oxide and high-frequency oscillatory ventilation in severe, persistent pulmonary hypertension of the newborn. J Pediatr. 1997;131(1 Pt 1):55–62.

[8] Clark RH, Kueser TJ, et al. Low-dose nitric oxide therapy for persistent pulmonary hypertension of the newborn. Clinical Inhaled Nitric Oxide Research Group. N Engl J Med. 2000;342(7):469–74.

[9] Finer NN, Barrington KJ. Nitric oxide for respiratory failure in infants born at or near term. Cochrane Database Syst Rev. 2006;(4):CD000399.

[10] Baquero H, Soliz A, et al. Oral sildenafil in infants with persistent pulmonary hypertension of the newborn: a pilot randomized blinded study. Pediatrics. 2006;117(4):1077–83.

[11] Juliana AE, Abbad FC. Severe persistent pulmonary hypertension of the newborn in a setting where limited resources exclude the use of inhaled nitric oxide: successful treatment with sildenafil. Eur J Pediatr. 2005;164(10):626–9.

[12] Perez KM, Laughon M. Sildenafil in Term and Premature Infants: A Systematic Review. Clin Ther. 2015;37(11):2598–2607 e1.

[13] Vargas-Origel A, Gomez-Rodriguez G, et al. The use of sildenafil in persistent pulmonary hypertension of the newborn. Am J Perinatol. 2010;27(3):225–30.

[14] Yaseen H, Darwich M, et al. Is sildenafil an effective therapy in the management of persistent pulmonary hypertension? J Clin Neonatol. 2012;1(4):171–5.

[15] Shah PS, Ohlsson A. Sildenafil for pulmonary hypertension in neonates. Cochrane Database Syst Rev. 2011;(8):CD005494.

[16] Bialkowski A, Moenkemeyer F, et al. Intravenous sildenafil in the management of pulmonary hypertension associated with congenital diaphragmatic hernia. Eur J Pediatr Surg. 2015;25(2):171–6.

[17] Noori S, Friedlich P, et al. Cardiovascular effects of sildenafil in neonates and infants with congenital diaphragmatic hernia and pulmonary hypertension. Neonatology. 2007;91(2):92–100.

[18] Patel N. Use of milrinone to treat cardiac dysfunction in infants with pulmonary hypertension secondary to congenital diaphragmatic hernia: a review of six patients. Neonatology. 2012;102(2):130–6.

[19] Bos AP, Tibboel D, et al. Persistent pulmonary hypertension in high-risk congenital diaphragmatic hernia patients: incidence and vasodilator therapy. J Pediatr Surg. 1993;28(11):1463–5.

[20] Pasutto F, Sticht H, et al. Mutations in STRA6 cause a broad spectrum of malformations including anophthalmia, congenital heart defects, diaphragmatic hernia, alveolar capillary dysplasia, lung hypoplasia, and mental retardation. Am J Hum Genet. 2007;80(3):550–60.

[21] Klaassens M, van Dooren M, et al. Congenital diaphragmatic hernia and chromosome 15q26: determination of a candidate region by use of fluorescent in situ hybridization and array-based comparative genomic hybridization. Am J Hum Genet. 2005;76(5):877–82.

[22] Longoni M, Russell MK, et al. Prevalence and penetrance of ZFPM2 mutations and deletions causing congenital diaphragmatic hernia. Clin Genet. 2014;.

[23] Ma L, Chung WK. The role of genetics in pulmonary arterial hypertension. J Pathol.

2017;241(2):273–280.

[24] Chen F, Desai TJ, et al. Inhibition of Tgf beta signaling by endogenous retinoic acid is essential for primary lung bud induction. Development. 2007;134(16):2969–79.

[25] Londhe VA, Maisonet TM, et al. Retinoic acid rescues alveolar hypoplasia in the calorie-restricted developing rat lung. Am J Respir Cell Mol Biol. 2013;48(2):179–87.

[26] Lai L, Bohnsack BL, et al. Retinoic acid regulates endothelial cell proliferation during vasculogenesis. Development. 2003;130(26):6465–74.

[27] Teramoto H, Shinkai M, et al. Altered expression of angiotensin II receptor subtypes and transforming growth factor-beta in the heart of nitrofen-induced diaphragmatic hernia in rats. Pediatr Surg Int. 2005;21(3):148–52.

[28] Xu C, Liu W, et al. Effect of prenatal tetrandrine administration on transforming growth factor-beta1 level in the lung of nitrofen-induced congenital diaphragmatic hernia rat model. J Pediatr Surg. 2009;44(8):1611–20.

[29] Zimmer J, Takahashi T, et al. Decreased Endoglin expression in the pulmonary vasculature of nitrofen-induced congenital diaphragmatic hernia rat model. Pediatr Surg Int. 2017;33(2):263–268.

[30] Gosemann JH, Friedmacher F, et al. Disruption of the bone morphogenetic protein receptor 2 pathway in nitrofen-induced congenital diaphragmatic hernia. Birth Defects Res B Dev Reprod Toxicol. 2013;98(4):304–9.

[31] Makanga M, Dewachter C, et al. Downregulated bone morphogenetic protein signaling in nitrofen-induced congenital diaphragmatic hernia. Pediatr Surg Int. 2013;29(8):823–34.

[32] Emmerton-Coughlin HM, Martin KK, et al. BMP4 and LGL1 are Down Regulated in an Ovine Model of Congenital Diaphragmatic Hernia. Front Surg. 2014;1:44.

[33] Hofmann A, Gosemann JH, et al. Imbalance of caveolin-1 and eNOS expression in the pulmonary vasculature of experimental diaphragmatic hernia. Birth Defects Res B Dev Reprod Toxicol. 2014;101(4):341–6.

[34] Hofmann AD, Zimmer J, et al. The Role of Activin Receptor-Like Kinase 1 Signaling in the Pulmonary Vasculature of Experimental Diaphragmatic Hernia. Eur J Pediatr Surg. 2016;26(1):106–11.

[35] Beurskens LW, Tibboel D, et al. Retinol status of newborn infants is associated with congenital diaphragmatic hernia. Pediatrics. 2010;126(4):712–20.

[36] de Lagausie P, de Buys-Roessingh A, et al. Endothelin receptor expression in human lungs of newborns with congenital diaphragmatic hernia. J Pathol. 2005;205(1):112–8.

[37] Dingemann J, Doi T, et al. Upregulation of endothelin receptors A and B in the nitrofen induced hypoplastic lung occurs early in gestation. Pediatr Surg Int. 2010;26(1):65–9.

[38] Kobayashi H, Puri P. Plasma endothelin levels in congenital diaphragmatic hernia. J Pediatr Surg. 1994;29(9):1258–61.

[39] Keller RL, Tacy TA, et al. Congenital diaphragmatic hernia: endothelin-1, pulmonary hypertension, and disease severity. Am J Respir Crit Care Med. 2010;182(4):555–61.

[40] Coppola CP, Au-Fliegner M, et al. Endothelin-1 pulmonary vasoconstriction in rats with diaphragmatic hernia. J Surg Res. 1998;76(1):74–8.

[41] Sood BG, Wykes S, et al. Expression of eNOS in the lungs of neonates with pulmonary hypertension. Exp Mol Pathol. 2011;90(1):9–12.

[42] Shehata SM, Sharma HS, et al. Pulmonary hypertension in human newborns with congenital diaphragmatic hernia is associated with decreased vascular expression of nitric-oxide synthase. Cell Biochem Biophys. 2006;44(1):147–55.

[43] Solari V, Piotrowska AP, et al. Expression of heme oxygenase-1 and endothelial nitric oxide synthase in the lung of newborns with congenital diaphragmatic hernia and persistent pulmonary hypertension. J Pediatr Surg. 2003;38(5):808–13.

[44] de Rooij JD, Hosgor M, et al. Expression of angiogenesis-related factors in lungs of patients with congenital diaphragmatic hernia and pulmonary hypoplasia of other causes. Pediatr Dev Pathol. 2004;7(5):468–77.

[45] North AJ, Moya FR, et al. Pulmonary endothelial nitric oxide synthase gene expression is decreased in a rat model of congenital diaphragmatic hernia. Am J Respir Cell Mol Biol. 1995;13(6):676–82.

[46] Shinkai T, Shima H, et al. Expression of vasoactive mediators during mechanical ventilation in

nitrofen-induced diaphragmatic hernia in rats. Pediatr Surg Int. 2005;21(3):143–7.

[47] Ijsselstijn H, Zijlstra FJ, et al. Lung eicosanoids in perinatal rats with congenital diaphragmatic hernia. Mediators Inflamm. 1997;6(1):39–45.

[48] Sluiter I, Reiss I, et al. Vascular abnormalities in human newborns with pulmonary hypertension. Expert Rev Respir Med. 2011;5(2):245–56.

[49] Shan W, Wu Y, et al. Foetal endoscopic tracheal occlusion for severe congenital diaphragmatic hernia–a systemic review and meta-analysis of randomized controlled trials. J Pak Med Assoc. 2014;64(6):686–9.

[50] Ali K, Bendapudi P, et al. Congenital diaphragmatic hernia-influence of fetoscopic tracheal occlusion on outcomes and predictors of survival. Eur J Pediatr. 2016;175(8):1071–6.

[51] Al-Maary J, Eastwood MP, et al. Fetal Tracheal Occlusion for Severe Pulmonary Hypoplasia in Isolated Congenital Diaphragmatic Hernia: A Systematic Review and Meta-analysis of Survival. Ann Surg. 2016;264(6):929–933.

[52] Persico N, Fabietti I, et al. Fetoscopic Endoluminal Tracheal Occlusion in Fetuses with Severe Diaphragmatic Hernia: A Three-Year Single-Center Experience. Fetal Diagn Ther. 2016;.

[53] Lally KP, Bagolan P, et al. Corticosteroids for fetuses with congenital diaphragmatic hernia: can we show benefit? J Pediatr Surg. 2006;41(4):668–74; discussion 668–74.

[54] Eastwood MP, Russo FM, et al. Medical interventions to reverse pulmonary hypoplasia in the animal model of congenital diaphragmatic hernia: A systematic review. Pediatr Pulmonol. 2015;50(8):820–38.

[55] de Raaf MA, Beekhuijzen M, et al. Endothelin-1 receptor antagonists in fetal development and pulmonary arterial hypertension. Reprod Toxicol. 2015;56:45–51.

[56] Spence S, Anderson C, et al. Teratogenic effects of the endothelin receptor antagonist L-753,037 in the rat. Reprod Toxicol. 1999;13(1):15–29.

[57] Luong C, Rey-Perra J, et al. Antenatal sildenafil treatment attenuates pulmonary hypertension in experimental congenital diaphragmatic hernia. Circulation. 2011;123(19):2120–31.

[58] Lemus-Varela Mde L, Soliz A, et al. Antenatal use of bosentan and/or sildenafil attenuates pulmonary features in rats with congenital diaphragmatic hernia. World J Pediatr. 2014;10(4):354–9.

[59] Kattan J, Cespedes C, et al. Sildenafil stimulates and dexamethasone inhibits pulmonary vascular development in congenital diaphragmatic hernia rat lungs. Neonatology. 2014;106(1):74–80.

[60] Yamamoto Y, Thebaud B, et al. Doppler parameters of fetal lung hypoplasia and impact of sildenafil. Am J Obstet Gynecol. 2014;211(3):263 e1–8.

[61] Russo FM, Toelen J, et al. Transplacental sildenafil rescues lung abnormalities in the rabbit model of diaphragmatic hernia. Thorax. 2016;.

[62] Umeda S, Miyagawa S, et al. Enhanced Pulmonary Vascular and Alveolar Development via Prenatal Administration of a Slow-Release Synthetic Prostacyclin Agonist in Rat Fetal Lung Hypoplasia. PLoS One. 2016;11(8):e0161334.

[63] Kraemer U, Cochius-den Otter S, et al. Pharmacodynamic considerations in the treatment of pulmonary hypertension in infants: challenges and future perspectives. Expert Opin Drug Metab Toxicol. 2016;12(1):1–19.

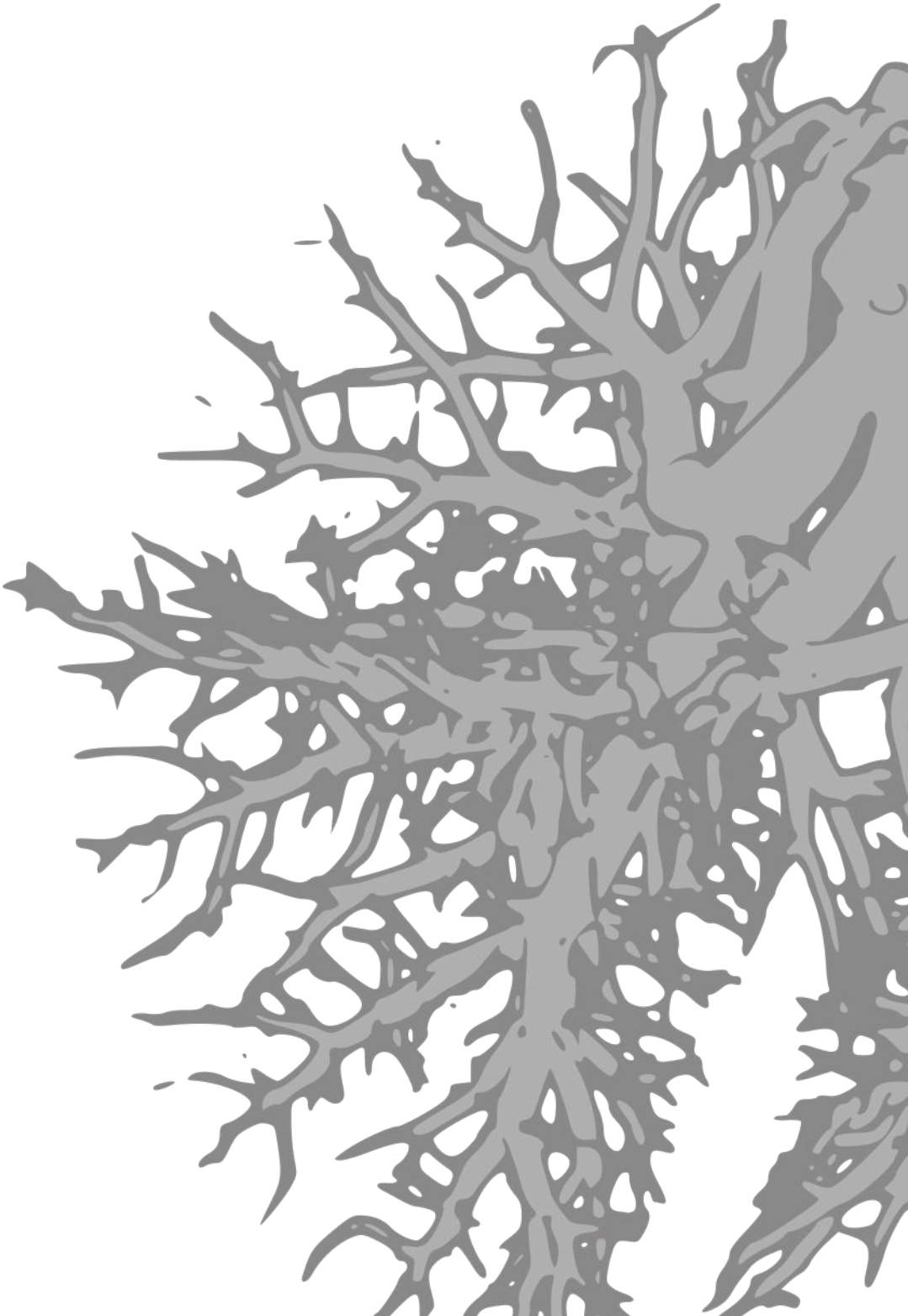

Appendix

Attenuated PDGF signaling drives alveolar and microvascular defects in neonatal chronic lung disease

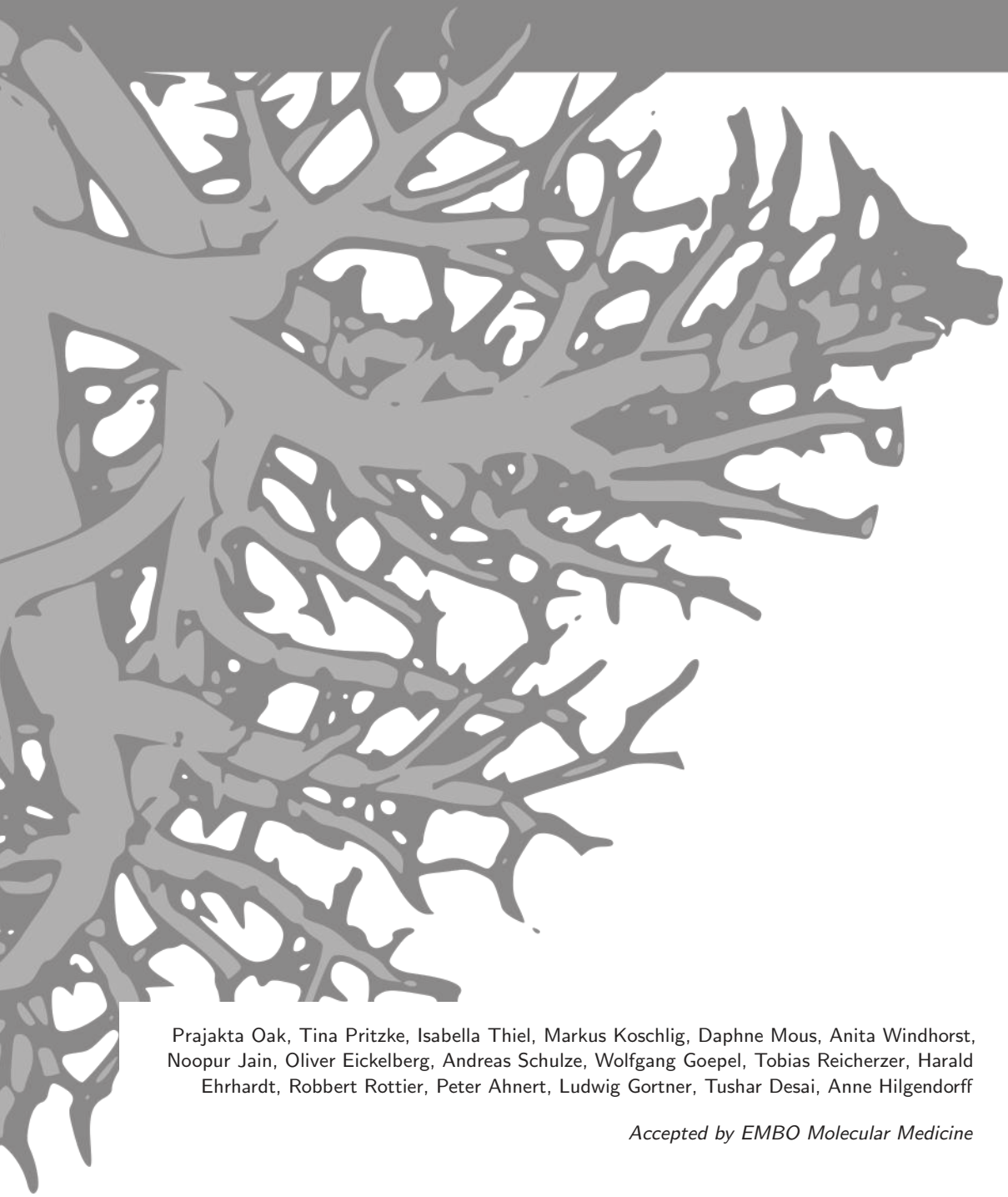

Prajakta Oak, Tina Pritzke, Isabella Thiel, Markus Koschlig, Daphne Mous, Anita Windhorst, Noopur Jain, Oliver Eickelberg, Andreas Schulze, Wolfgang Goepel, Tobias Reicherzer, Harald Ehrhardt, Robbert Rottier, Peter Ahnert, Ludwig Gortner, Tushar Desai, Anne Hilgendorff

Accepted by EMBO Molecular Medicine

Abstract

Neonatal chronic lung disease (nCLD) affects a significant number of neonates receiving mechanical ventilation with oxygen-rich gas (MV-O_2). Regardless, the primary molecular driver of the disease remains elusive. We discover significant enrichment for SNPs in the PDGF-Rα gene in preterms with nCLD and directly test the effect of PDGF-Rα haploinsufficiency on the development of nCLD using a preclinical mouse model of MV-O_2. In the context of MV-O_2, attenuated PDGF signaling independently contributes to defective septation and endothelial cell apoptosis stemming from a PDGF-Rα dependant reduction in lung VEGF-A. TGF-β contributes to the PDGF-Rα dependant decrease in myofibroblast function. Remarkably, endotracheal treatment with exogenous PDGF-A rescued both the lung defects in haploinsufficient mice undergoing MV-O_2. Overall, our results establish attenuated PDGF signaling as an important driver of nCLD pathology with provision of PDGF-A as a protective strategy for newborns undergoing MV-O_2.

Introduction

Positive pressure mechanical ventilation with O_2-rich gas (MV-O_2) offers life-saving treatment for respiratory failure due to lung immaturity and insufficient respiratory drive in preterm infants. Unfortunately, this therapy significantly increases the risk for an important number of preterm and a subset of newborns to develop neonatal chronic lung disease (nCLD), i.e. Bronchopulmonary Dysplasia (BPD) [1–4]. Characterized by defective alveolar septation and impaired vascularization, nCLD remains the most common complication of preterm birth [2] and is associated with poor pulmonary and neurological long-term outcomes in affected infants [5, 6]. The adverse effects of positive pressure MV-O_2 on pulmonary development have been reproduced in experimental models of the disease [7, 6, 8–10], manifesting as increased lung apoptosis and disordered matrix elastin characteristic of nCLD. Because a myriad of developmental signals are perturbed in the setting of active disease, it is difficult to distinguish primary drivers of pathology from secondary effectors or compensatory responses. Yet, if a defect in a specific signaling pathway underlies the susceptibility to developing nCLD and orchestrates the multiple processes that execute disease pathology, it would be critical to identify this potential therapeutic target.

An essential role for platelet-derived growth factor (PDGF) signaling in alveolar development was established by the discovery that lungs of 'knockout' mice lacking PDGF-A failed to form alveoli, with animals that survived infancy demonstrating an emphysema-like phenotype of enlarged distal air sacs [11, 12]. This lung pathology was attributed to failure of migration of PDGF-Rα positive alveolar smooth muscle progenitor cells (also known as myofibroblasts) into the distal embryonic lung. Because myofibroblasts are believed to drive normal subdivision of primitive air sacs into mature alveoli ('secondary septation'), their absence presumably resulted in abnormally large distal air sacs due to a failure to execute this process. Deletion of the cognate receptor, PDGF-Rα, resulted in death in mid-gestation before air sac morphogenesis initiated [13], but transgenic rescue of the profound craniofacial abnormalities and spina bifida enabled survival through birth. Distal lungs in these mutants also lacked myofibroblasts and failed to undergo secondary septation [14].

When the PDGF signaling pathway was examined in the lungs of animal models of nCLD employing mechanical ventilation (MV-O_2), reduced abundance of PDGF-A and PDGF-Rα proteins or mRNA was observed [15, 7, 16], similar to the lungs of neonatal rats exposed to hyperoxia [17] and preterm infants developing nCLD [18]. These findings suggest that reduced PDGF signaling may be involved in the air sac morphogenesis defect of nCLD, but a causal role has not yet been demonstrated. Furthermore, since microvascular defects were not reported in the lungs of PDGF mouse mutants that failed to undergo secondary septation, the position of this pathway in the hierarchy of perturbed signaling in nCLD is uncertain. Here, in a case-control study of infants with nCLD, we discover significant enrichment for SNPs in the PDGF-Rα gene associated with reduced PDGF-R levels and diminished migration of lung fibroblasts suggesting that impairment of this pathway might be a primary driver of disease. We confirm this model using gene-targeted mice haploinsufficient for PDGF-Rα, showing an interaction with an established model of MV-O_2 that reproduces the multiple pathologies of nCLD, all of which are ameliorated by exogenous administration of PDGF-A protein during MV-O_2. We also dissect the molecular crosstalk that mediate nCLD pathology, showing that attenuated PDGF-Rα signaling results in a reduction of VEGF-A expression, likely responsible for the vasculature phenotype through increased endothelial cell apoptosis. We also find that increased TGF-β and mechanical stretch, driving lung injury in the newborn lung, to act in concert to reduce PDGF-Rα signaling, exacerbating the underlying basal reduction in PDGF-Rα to a level sufficient to result in disease. Our work implicating attenuated PDGF signaling as driving the air sac and vasculature defects of nCLD, along with our demonstration that both pathologies can be ameliorated by exogenous PDGF-A protein, provide a strong rationale

for pursuing augmentation of PDGF signaling as a potential targeted therapy for this serious disease.

Materials and methods

All the antibodies used in the manuscript could be found in 1DegreeBio database. Study design for the manuscript experiments is described in Supplemental methods.

Human studies

Patient characteristics

Two study cohorts comprising of 1061 preterm infants at or less than 32 weeks of gestational age (GA) with and without nCLD, i.e. BPD grade 2 or 3 according to Jobe et al. [19] (Pneumonia Research Network on Genetic Resistance and Susceptibility for the Evolution of Severe Sepsis (PROGRESS); German Neonatal Network (GNN)) were included in the SNP analysis (Ethics Approval #65/07, Homburg, University of Saarland; #145-07, Munich, Ludwig Maximillians University of Munich and #File 79/01, Giessen, University of Giessen, Germany). Detailed patient characteristics are in Supplemental methods. 9 patients out of this cohort were subjected to PDGF-Rα transcriptome analysis in association with presence of single nucleotide polymorphism (SNPs). Patient characteristics of this cohort are in Supplemental Table A.3A. A separate study cohort was obtained from Perinatal Center of the Ludwig-Maximilians-University, Campus Grosshadern (Ethics Approval #195-07, Munich, Ludwig Maximillians University of Munich, Germany) for SNP and protein analysis uring SOMAscan ($n = 13$). The patient characteristics are in Supplemental Table A.3B. Tracheal aspirates of few patients from this patient cohort were used to isolate primary fibroblasts ($n = 6$). Patient characteristics of this cohort are in Supplemental Table A.3C. Sections from human lung were available through the Department of Pediatric Surgery at the Erasmus Medical Center. Lung samples were retrieved from the archives of the Department of Pathology of the Erasmus MC, Rotterdam, following approval by the Erasmus MC Medical Ethical Committee. Patient characteristics of this cohort are in Supplemental Table A.3D. According to Dutch law following consent to perform autopsy, no separate consent is needed from the parents to perform additional staining of tissues. A group of 20 preterm infants from Giessen was subjected to microarray analysis (Ethics Approval #File 79/01, Giessen, University of Giessen, Germany). The clinical course of all infants was comprehensively monitored. Approval of the local ethics committee and written informed parental consent was obtained for all samples studied. All the experiments conformed to the principles set out in the WMA declaration of Helsinki and Department of Health and Human Services Belmount Report. The limitation of human material to be tested in case of neonatal chronic lung disease is well known hence, analysis was performed with samples available in maximum capacity. Samples were collected from patients randomly. Our datasets were obtained from subjects who have consented to the use of their individual genetic data for biomedical research, but not for unlimited public data release. Therefore, we submitted it to the European Genome-phenome Archive (accession number- EGAS00001002586, study unique name- ena-STUDY-IMI-24-07- 2017-10:03:30:362-576), through which researchers can apply for access of the raw data.

SNP and protein analysis

Cord blood samples of 1061 preterm infants at or below 32 weeks of gestational age ($n = 492$ BPD cases) were collected in Ethylenediaminetetraacetic acid (EDTA) neonatal collection tubes. Genotypes of this patient cohort for PDGF-Rα SNPs (single nucleotide polymorphisms) were

determined using Affymetrix Axiom microarrays based on the Axiom CEU array supplemented with some custom content. Matched controls were selected according to gender, GA, birth weight $< 10th$ percentile, and country of maternal origin. Case-control analysis adjusted for relatedness. 117 SNPs were measured in or near the PDGF-Rα. Whole blood samples collected from a separate patient cohort ($n = 13$) that were analyzed for 3 significant SNPs by Eurofins Geomics was subjected to proteomic screening for PDGF-R and VEGF-A (SOMAscan ^{TM}, SomaLogic, Boulder, USA). For a detailed description please refer to Supplemental methods.

Human primary lung fibroblasts

Human primary lung fibroblasts were extracted from serial tracheal aspirate samples obtained from ventilated preterm infants (mean GA 24.9±1 weeks, $n = 6$) later developing nCLD, at 4.7±1 and 21.7±8 day of life (Ethics Approval #195-07, Munich, Ludwig Maximillians university of Munich, Germany). Human lung fibroblasts were cultured until 80% confluency in DMEM medium with 2mM L-glutamine, Pen/Strep and 20% FCS (PAN Biotech GmbH). Purity of cell cultures was $> 95\%$ and FACS verified expression of CD11b ($< 3\%$) (eBiosciences #48-0112-80), CD11c ($< 3\%$) (BD Biosciences #557401), CD14 ($< 5\%$) (BD Biosciences #09475A), CD45 ($< 5\%$) (BD Biosciences #552848), CD90 ($> 95\%$) (eBiosciences #48-0900-80), and CD105 ($> 95\%$) (Miltenyi Biolabs #130-092-930), differences between patient samples were $< 5\%$ (Supplemental Figure A.13A). All fibroblast cultures expressed α-SMA as detected in cytosolic cell lysates by immunoblot analysis. This section is further described in Supplemental methods.

Gene expression microarray analysis

$250 - 300\mu l$ of whole cord blood was obtained from 20 preterm infants 72 hours after birth and directly transferred to $750 - 900\mu l$ of the PAXgene Blood RNA System (PreAnalytiX, Heidelberg, Germany). RNA was isolated using PAXgene Blood RNA System (PreAnalytiX, Heidelberg, Germany) and was subjected to CodeLink Human Whole Genome Bioarrays (GE Healthcare). PDGF-Rα gene expression in GWAS patient cohort was measured by the expression of NM_006206 on the human whole genome bioarray and human 10 k I bioarray by Codelink. For details of blood sampling and RNA analysis please refer to Supplemental methods.

Human lung slides

Human slides were obtained from paraformaldehyde fixed and paraffin embedded autopsy lungs from preterm infants with different BPD grades ($n = 7$) and an infant that died from a non-pulmonary cause. Tissue sections were stained for PDGF-Rα, and TGF-β for further quantification. Please refer to Supplemental methods for details of patient characteristics.

In vivo studies

All the studies were performed as per ARRIVE guidelines.

Gene-targeted mice

Gene-targeted mice (B6.129S4-Pdgfra$^{tm11(EGFP)Sor}$/J) referred to in manuscript as PDGF-R$\alpha^{+/-}$ or PDGF-Rα haploinsufficient mice, were purchased from Jackson laboratories (Bar Harbor, Maine, USA). Heterozygous mice are healthy and viable and reported to have no lung abnormalities [8]. Co-staining for PDGF-Rα and α-SMA showed a reduction in myofibroblasts (double-positive), and mRNA and immunoblot analysis confirmed the reduced abundance of pulmonary PDGF-Rα expression in unventilated PDGF-R$\alpha^{+/-}$ mice when compared to WT

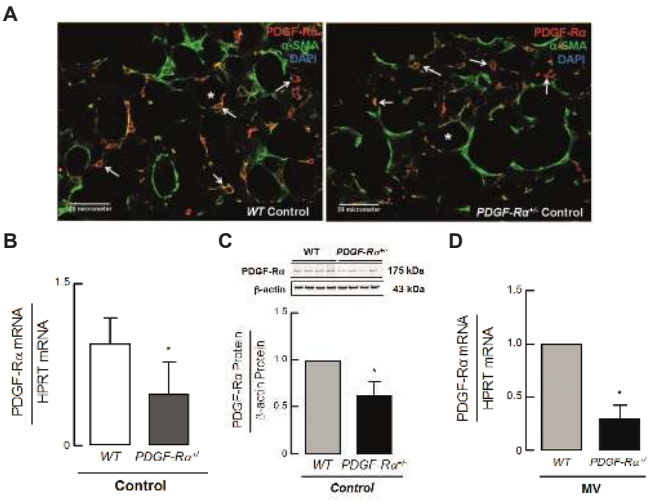

Figure A.1: Reduced PDGF-R-α abundance in PDGF-Rα happloinsufficient mice (**A**) Double staining for PDGF-Rα (red) and α-SMA (green) showed a co-localization of these two proteins as well as a reduced number of double positive cells (white arrows) in 6-7d old PDGF-R$\alpha^{+/-}$ mice (right panel) when compared to PDGF-R$\alpha^{+/+}$ (WT) littermates (left panel). * represents alveolar air space. (**B**) Quantitative RT-PCR and (**C**) Immunoblot analysis showing reduced PDGF-Rα protein and mRNA expression in lungs of PDGF-R$\alpha^{+/-}$ newborn mice when compared to WT littermates. $n = 4$/group. (**D**) Reduced PDGF-Rα transcript in newborn PDGF-R$\alpha^{+/-}$ mice upon MV-O_2 for 8h when compared to wildtype littermates. ($n = 3$ mice/group). In (B-C) the data is presented as Mean $\pm$ SD. *$p < 0.05$. Statistical test in (B-D) is Two-tailed unpaired Student's t test or Mann Whitney test.

littermates (Figure A.1A-C). For the study day 5-8 old neonatal mice both males and females were used. The experimental protocols were approved by the Bavarian government (TVA no. 55.2-1-54-2532-117-2010). The mice were kept under specified pathogen-free (SPF) conditions in a 12/12 hour light cycle in the fully-climate controlled rooms having set points to the new conventions 2007/526 EC in our central mouse facility. Mice had a two-week adaptation phase to their new environment and a handling by new nurses before putting them into the experiment. For each experiment, appropriate sample size ($n = 6 - 12$) was estimated considering the effect of MV-O_2 on viability of newborn mice.

Mechanical ventilation

We used 5-8 day-old (newborn/neonatal) C57B6 wild type (PDGF-R$\alpha^{+/+}$) and PDGF-Rα haploinsufficient (PDGF-R$\alpha^{+/-}$) mice, all born at term gestation weighing 4g (WT $3.98 \pm 0.55g$; PDGF-R$\alpha^{+/-}$ $3.93 \pm 0.66g$ bodyweight (bw)) to perform experiments in four groups of mice (14-16 mice per group). WT and PDGF-R$\alpha^{+/-}$ pups received mechanical ventilation with oxygen-rich gas (40% O_2) (MV-O_2) for 8h at 180 breaths/min (MicroVent 848; Harvard Apparatus) after tracheotomy under sedation with ketamine and xylazine (60 and $12\mu g/g$ bw), as previously described [9]. The ventilator setting mimicked the clinical setting to avoid severe lung injury (mean tidal volume $8\mu l/g$ bw; mean airway pressure (11-12 cmH_2O)). Tidal volumes were similar between the MV-O_2 groups (WT $8.3 \pm 0.5\mu l/g$ bw; PDGF-R$\alpha^{+/-}$ $7.9 \pm 0.3\mu l/g$ bw). The ventilation protocol was designed to avoid severe lung injury typically occuring in response to MV with very high inflation pressures and extreme hyperoxia. Hence, we used modest tidal volumes (mean $8.7\mu l/g$ bw) and airway pressures (peak 12-13 cmH_2O, mean 11-12 cmH_2O), and limited the FiO_2 to 40%, thereby simulating the MV strategy of choice for preterm

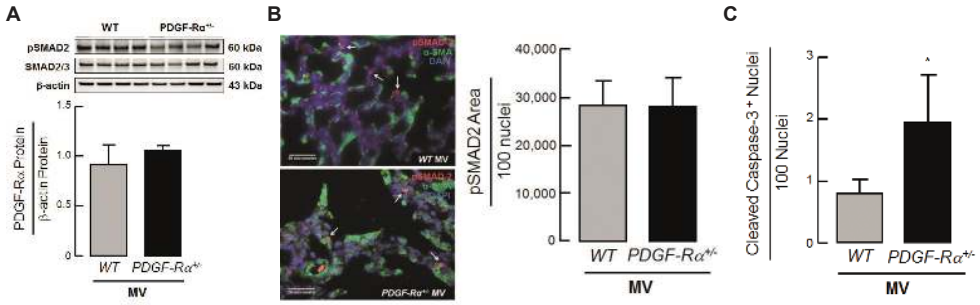

Figure A.2: (**A**) Immunoblot analysis showing similar pSMAD levels in whole lung homogenate of newborn WT as well as PDGF-R$\alpha^{+/-}$ mice. ($n = 3$ mice/group). (**B**) Representative immunofluorescence image showing similar pSMAD levels (red) in both newborn WT (upper panel) and PDGF-R$\alpha^{+/-}$ mice (lower panel). α-SMA is in green and nucleus is stained with DAPI (blue). Quantification of the image showing pSMAD-2 area to 100 nuclei. ($n = 3 - 4$ mice/group, 4 sections/mice, 10 images/section). (**C**) Increased apoptosis quantified by cleaved caspase-3 nuclei to 100 nuclei in newborn PDGF-R$\alpha^{+/-}$ compared to WT mice. ($n = 4$ mice/group). In (A-C) data is presented as Mean $\pm$ SD. *$p < 0.05$. Statistical test is Two-tailed unpaired Student's t test ($p = 0.0159$).

infants with respiratory failure. Respective controls spontaneously breathed 40% O_2 for 8h after receiving sham surgery (superficial neck incision) under mild sedation. During MV-O_2, mice were maintained at neutral thermal environment; sedation with ketamine and xylazine ($10\mu g/g$ bw, and $2\mu g/g$ bw, respectively) was repeated as needed to minimize spontaneous movement and assure comfort. At the end of each study, pups were euthanized with an intraperitoneal overdose of sodium pentobarbital, $\sim 150\mu g/g$ bw, and lungs were excised for various studies as described below including histological analysis, as well as protein measurement and RNA expression analysis from frozen lung tissue. For PDGF-A treatment, $10\mu l/g$ bw of sterile saline containing $25ng/ml$ PDGF-A was administered through the endotracheal tube immediately before the onset of MV-O_2 as described previously. In a subgroup of mice with or without PDGF-A treatment, tidal volume and maximum tracheal pressure (Ptramax) was measured by whole body plethysmography (Pulmodyn, Harvard Apparatus). Stepwise increase of the tidal volume allowed to assess quasi-static compliance [9].

All animals were viable with response to tactile stimulation and adequate perfusion at the end of each experiment. All surgical and animal care procedures were reviewed and approved by the Institutional Animal Care and Use Committee (Bavarian Government). Upon ventilation both the mouse strains showed similar activation of pSMAD-2 while neonatal PDGF-R$\alpha^{+/-}$ mice displayed increased apoptosis when compared to wildtype mice (Figure A.2A-C). Allocation of the newborn mice to the groups was performed on the basis of similarity in weight and age. When newborn mice from more than one cage were used for the experiments, all pups were randomized before distribution in the groups. Investigators were blinded for the sex of mice during allocation. Further the analysis of lungs were performed based on internal serial numbers allotted to mice blinding the investigator for genetic background and treatment (example controls or ventilated). All experimental procedures were carried out in a laboratory-controlled environment during day time.

Quantitative histology and immunostaining

Lungs ($n = 6 - 11$/group) were fixed intra-tracheally with 4% paraformaldehyde overnight at 20 cmH_2O, as previously described [7]. Fixed lungs were then excised and their volume was measured by fluid displacement [10]. Lungs were embedded in paraffin for isotropic uniform

random (IUR) sectioning, as described previously [10]. Tissue sections ($4\mu m$) were stained with hematoxylin and eosin (H&E) for quantitative assessment of alveolar area and number of incomplete and complete alveolar walls (septal density) in 2-3 independent random tissue sections per animal using the CAST image analysis system (CAST-Grid 2.1.5; Olympus, Ballerup, Denmark). Alveolar area, number of incomplete and complete alveolar walls (septal density) and radial alveolar counts providing an index of alveolar number and were assessed in a minimum number of 30 fields of view were quantitatively assessed in 2-3 independent random $4\mu m$ H&E tissue sections per animal (CAST-Grid 2.1.5; Olympus) [20]. Tissue sections were stained for PDGF-Rα, VEGF-A, cleaved caspase-3, CD31 and αSMA for further quantification (see Supplemental methods for detailed description).

Quantification of micro-vessels ($20-100\mu m$).

$20-100\mu m$ diameter blood vessels were assessed in H&E (normalized to 100 alveoli) and CD-31 stained slides obtained from 8h studies ($n = 6-8$/group) applying a previously described immunohistochemical and morphometric approach [9] in 30 fields of view in the distal lung/animal (400X magnification).

Protein extraction and immunoblot analysis

After 8h MV-O_2, protein extraction from snap-frozen total lungs was done using high urea buffer (KPO4, Urea, AppliChem) with Halt Protease Inhibitor (#1861280, Thermo Fisher Scientific). Primary lung fibroblasts were lysed with RIPA buffer with Halt Protease Inhibitor (mouse) or sodium vanedate (human) (#S6508, Sigma) and complete mini (#11836170001, Roche) followed by sonication. After measurement of protein concentrations (BCA, #23227, Pierce Scientific), immunoblots were performed using a Bis-Tris or a Tris-Acetate gel (#NP0321BOX, #EA0375BOX, Life Technologies) using the following antibodies: PDGF-Rα (C-20, Santa Cruz Biotechnology #338), VEGF-A (147, Santa Cruz Biotechnology #507), VEGF-R2 (Abcam, Cambridge, USA #Ab2349), VE-Cadherin (H-72, Santa Cruz Biotechnology #28644), cleaved caspase-3 (Cell Signalling Technology #9661), cleaved caspase-9 (Cell Signaling Technologies #7237), eNOS (Cell Signaling Technologies #5880), phospho-ERK (Cell Signalling Technologies #4370), total ERK (Cell Signalling Technologies #4695), RAS (Cell Signalling Technologies #8955), PI3K (Cell Signaling Technologies #13666), JAK-2 (Cell Signaling Technologies #3230), STAT-3 (Cell Signaling Technologies #9139). Images were detected by chemiluminescence (#RPN2232, GE Healthcare) and quantified by densitometry (Bio Rad). Details of immunoblot analysis could be found in Supplemental methods.

In vitro experiments

Mouse primary pulmonary myofibroblasts

Mouse myofibroblasts (MFBs) were extracted by excising lungs of 5-7 day old C57BL6 wild type mice after intraperitoneal overdose of sodium pentobarbital ($\sim 150\mu g/g$ bodyweight). Under sterile conditions lungs were flushed with PBS after cannulation of the right ventricle. Flushed lungs were then excised, diced into 1 mm pieces and distributed on a petridish (Corning #430167, Tewksbury MA, USA). Attachment to the dish was accomplished by incubation for 15 to 20 min at $37^{\circ}C$. Afterwards the tissue pieces were gently submerged in media (Gibco #41966-029, Darmstadt, Germany) containing Pen/Strep (Gibco, #15140-122) and Gentamycin (Lonza #BE02-012E, Basel, Switzerland) for 48 hours before changing to fresh media. Experiments were started at 70-80% confluency. Myofibroblasts were characterized with fluorescence activated cell sorter (FACS LSRII) using multicolor staining technique. Briefly

myofibroblasts were resuspended in FACS buffer (PBS+2% FCS+ 10mM HEPES+0.1% Na-Azide) and stained with CD90.2 APC FITC (BD Pharmingen, Heidelberg, Germany #561974), CD 105 PE (BD Pharmingen, Heidelberg, Germany #562759), CD45 FITC (BD Pharmingen, Heidelberg, Germany #553080), CD11b V450 (BD horizon, Heidelberg, Germany #560455), CD11c PerCpCy5.5 (Biolegend, Fell, Germany #117328). For detection of internal markers, Myofibroblasts were fixed with 4% PFA (Alpha Aesar GmbH, Germany #43368) followed by permeabilization with 0.2% TritonX-100 (Carl Roth GmbH + Co.KG, Karlsruhe, Germany #3051.2) and blocking with 1% BSA (Sigma) in PBS. Myofibroblasts were then stained in blocking solution with PDGF-Rα APC (eBiosciences #17-1401-81), α-Smooth Muscle Actin PE (R & D systems, Minneapolis, MN, USA #IC1420P) and Vimentin Alexa 488. Stained myofibroblasts were then acquired through BD^{TM}LSR II utilizing BD FACSDiva^{TM}software version 6.0 and analyzed using Flowjo version 9.6.1. As displayed in Supplemental Figure A.13B Myofibroblast culture constituted leukocytes (0.6±0.5% CD45$^+$), mesenchymal-like cells (8.5±4.5% CD105$^+$, 32±8.6% CD90$^+$), myofibroblasts (77.2±14% PDGF-Rα^+/Vimentin$^+$, 16.7±12% Vimentin$^+$ and 77.6±27% αSMA$^+$). Antibodies used were CD45 (BD Pharming #553080), CD105 (BD Pharming #562759), CD90 (BD Pharming Vimentin (Cell Signaling #561974), PDGF-Rα (eBiosciences #17-1401), #9854) and α-SMA (R&D systems #IC1420P).

Mechanical stretch

Myofibroblasts were seeded on flexible-bottomed laminin-coated culture plates (#BF-3001L, Flex Cell International Corporation) and stretched at 70-80% confluency (shape/sine; elongation min 0%, max 8%; frequency 2Hz; duty cycle 50%; cycles 43216) for 24h. A detailed description of mechanical stretch expriment is available in the Supplemental methods.

Protein analysis

Cells were lysed with RIPA buffer including Halt Protease Inhibitor Cocktail (mouse myofibroblasts) or sodium vanedate (catalog #S6508, Sigma) and complete mini (Roche, Penzberg, Germany #11836170001; human lung fibroblasts). After storage at $-80°C$, cell lysates were sonicated and processed for immunoblot analysis (as described in 'in vivo' methods).

siRNA transfection of pulmonary mouse myofibroblasts

Primary neonatal mouse myofibroblasts were transfected with either 100nM specific siRNA against PDGF-Rα (Santa Cruz Biotechnology, Inc., Germany #sc-29444) or 100nM control siRNA B (Santa Cruz Biotechnology #sc-44230) suspended in TurboFect (Thermo Fisher Scientific, Waltham, MA #R0531) or remained untreated controls in siRNA transfection media (Santa Cruz Biotechnology, Inc., Germany #sc-36868). Transfection with siRNA was repeated after 17 hours.

Caspase activity and immunoblot analysis in human umbilical vein endothelial cells

Mycoplasma tested Human umbilical vein endothelial cells (HUVECs) (Commercially obtained from Lonza #CC-2935) were cultured in EBM-2 Basal Media (#00190860, #cc-4176, Lonza, mycoplasma free) with EGM-2 Single Quots supplements (Lonza #cc-4176) on 0.2% gelatin (Sigma Aldrich #G1393) coated 96-well plates (5000 cells/well) or 6-well plates (150,000 cells/well). After obtaining stable culture conditions, HUVECs were incubated with culture supernatants collected from three groups of mouse myofibroblasts: I) untreated myofibroblasts (TurboFect), II) control siRNA treated myofibroblasts and III) myofibroblasts treated with siRNA against PDGF-Rα. For caspase activity assay, incubation with $40\mu g/ml$ anti-VEGF (C-1) antibody (#sc-7269, Santa Cruz) served as a positive control. Caspase activity was

assessed after 6 hours using the Caspase-Glo 3/7 assay kit (#G8091, Promega). After 6h of incubation, caspase activity was assessed using the Caspase-Glo 3/7 assay kit (Promega GmbH, Germany #G8091) according to the manufacturer's instructions. Cells plated in 6-well plate were lysed after 6h incubation and lysate was processed for immunoblot analysis with cleaved caspase 9 (Cell Signaling Technologies #9509) and eNOS (Cell Signaling Technologies #880) protein.

Luciferase assay

PDGF-Rα promoter inserted in a reporter plasmid was transfected in CCL206 stimulated with TGF-β1. Luciferase activity was assessed the next day using Dual Luciferase assay. For generation of reporter please refer to Supplemental methods.

Functional assays for myofibroblasts

Mouse and human myofibroblasts or lung fibroblasts were subjected to analysis of proliferation (Cell titer Glo assay and manual counting) and migration (Boyden chamber assay and scratch migration assay) followed by the application of stretch and TGF-β as shown in Supplemental Figure A.13C. Proliferation assays and scratch migration assay were performed after 48h of application while migration assay was done after 8h. For detailed description of proliferation, boyden chamber and scratch migration assays please refer to Supplemental methods.

Statistical analysis

All datasets are presented as mean $\pm$ SD. Statistical analysis was performed using Prism 5 and 6 software package (GraphPad, San Diego, CA). Two-way analysis of variance (ANOVA) and post-hoc test with Bonferroni correction was performed to compare controls and mechanically ventilated WT (PDGF-R$\alpha^{+/+}$) and haploinsufficient (PDGF-R$\alpha^{+/-}$) newborn mice. For in vitro experiments, One-way ANOVA and post-hoc test with Bonferroni correction was performed to compare more than two groups of Myofibroblasts (immunoblot, migration and proliferation analysis). For analysis of caspase activity to HUVECs non-parametric Kuskal Wallis test was performed. To compare datasets from two groups of either WT or PDGF-R$\alpha^{+/-}$ mice (immunoblot, migration and proliferation analysis, reporter assays), parametric unpaired student's t-test with Welchs correction or the non-parametric Mann-Whitney test (for datasets with a skewed distribution) was performed with two-tailed or one-tailed analysis. Test groups were always compared to control group. Differences were considered statistically significant when the p value was < 0.05. For microarray, data was analyzed in a target gene approach using the Pearsons correlation coefficient to correlate expression of PDGF-Rα and TGF-β in preterm infants with and without BPD. Correlation coefficients in preterm infants with and without BPD were tested using the R-packages psych. Statistical methods applied for the SNP analysis are outlined above.

Results

Enrichment of PDGF-Rα SNPs associated with reduced protein levels and migration of lung fibroblasts from ventilated preterm infants developing nCLD

We confirm reduced PDGF-Rα expression in lung fibroblasts isolated from ventilated preterm infants. This reduction in PDGF-Rα expression was correlated with increased duration of MV-O_2, as quantified by immunofluorescence and immunoblot analysis (Figure A.3A). Further,

a case-control analysis of PDGF-Rα in 1061 newborns ($n = 492$ with moderate or severe BPD) identified 14 SNPs out of 117 with nominal significance ($p <= 0.05$) (Figure A.3B). Three of these SNPs were highly statistically significant, with p-values below 0.001 (Supplemental Table A.1). The presence of at least one SNP at these 3 positions (rs12506783) was associated with reduced PDGF-Rα gene expression and PDGF-R as well as VEGF-A protein levels in blood from ventilated preterm inants (Figure A.3C-E, Supplemental Figure A.11). In human lung fibroblast this SNP is associated with reduced PDGF-Rα protein level in accordance with reduced migration (Figure A.3F-G). Analysis of SNPs cis-regulating gene expression for genes in the PDGF-pathway and its downstream pathways showed enrichment of low p-values for SNPs linked to the MAPKKK-cascade, JAK/STAT-cascade, apoptosis, cell cycle, DNA metabolism, lipid metabolism, protein metabolism, and actin and calcium ion homeostasis (Supplemental Table A.2). Together, these experiments indicate that MV-O_2 in humans results in a reduction of PDGF-Rα expression by alveolar fibroblasts, and suggests that genetic risk factors for reduced PDGF signaling in human infants is associated with an increased risk of developing nCLD.

PDGF-Rα haploinsufficiency drives the air sac pathology of nCLD in neonatal mice undergoing MV-O_2

In order to test whether attenuated PDGF signaling was indeed a risk factor for the development of nCLD as suggested by our human SNP data and not restricted to the air sac component, we obtained gene-targeted mice lacking one allele of PDGF-Rα and subjected them to MV-O_2 using a unique preclinical mouse model. We found that lungs of PDGF-Rα haploinsufficient newborn mice undergoing MV-O_2 for 8h showed a significant increase in distal airspace size and decrease in radial alveolar counts resembling nCLD pathology as assessed by quantitative morphometry when compared to unventilated controls (Figure A.4A-C), whereas their ventilated WT littermates were unaffected. As expected with this phenotype, there were fewer secondary septae in PDGF-R$\alpha^{+/-}$ neonatal mice after MV-O_2 for 8h as compared to WT mice (Figure A.4D), with no significant difference in lung volumes between the groups (WT control $55.3\pm7.0\mu l/g$ bw; WT MV-O_2 $56.2\pm14.2\mu l/g$ bw; PDGF-R$\alpha^{+/-}$ control $59.7\pm11.9\mu l/g$ bw; PDGF- R$\alpha^{+/-}$ MV-O_2 $57.6\pm23.7\mu l/g$ bw; mean and SD each). Atelectasis, as analyzed using ImageJ, involved 14-18% of the total lung in both groups undergoing MV-O_2 (WT MV-O_2 $17.2\pm9.6\%$; PDGF-R$\alpha^{+/-}$ MV-O_2 $22.8\pm10.4\%$; $p = 0.61$).

Immunoblot and mRNA analysis confirmed reduced pulmonary PDGF-Rα level (Figure A.4G, Figure A.1D), reflected by the reduced number of myofibroblasts localized on septal crests in ventilated PDGF-R$\alpha^{+/-}$ mice lungs compared to WT littermates (Figure A.4E-F). Diminished JAK-2 and STAT-3 in ventilated PDGF-R$\alpha^{+/-}$ mice reflects reduced PDGF-Rα downstream signaling (Figure A.4H-I).

PDGF-Rα haploinsufficiency drives reduced pulmonary micro-vessel density with increased endothelial cell apoptosis in neonatal mice undergoing MV-O_2

We next asked whether attenuated PDGF signaling would also reproduce the vascular defect of nCLD. Indeed, we demonstrated by histological analysis of PDGF-R$\alpha^{+/-}$ mice undergoing MV-O_2, a significant reduction in the number of alveolar micro-vessels ($20 - 100\mu m$), notably exceeding the effect observed in WT pups (Figure A.5A). This finding was corroborated by immunoblot analysis showing reduced lung protein levels of the endothelial cell markers, VEGF-R2 (Figure A.5B), and VE-Cadherin (Figure A.5C) in ventilated neonatal PDGF-R$\alpha^{+/-}$ mice, suggesting a net loss of endothelial cells. Co-staining for apoptosis and endothelial cell markers

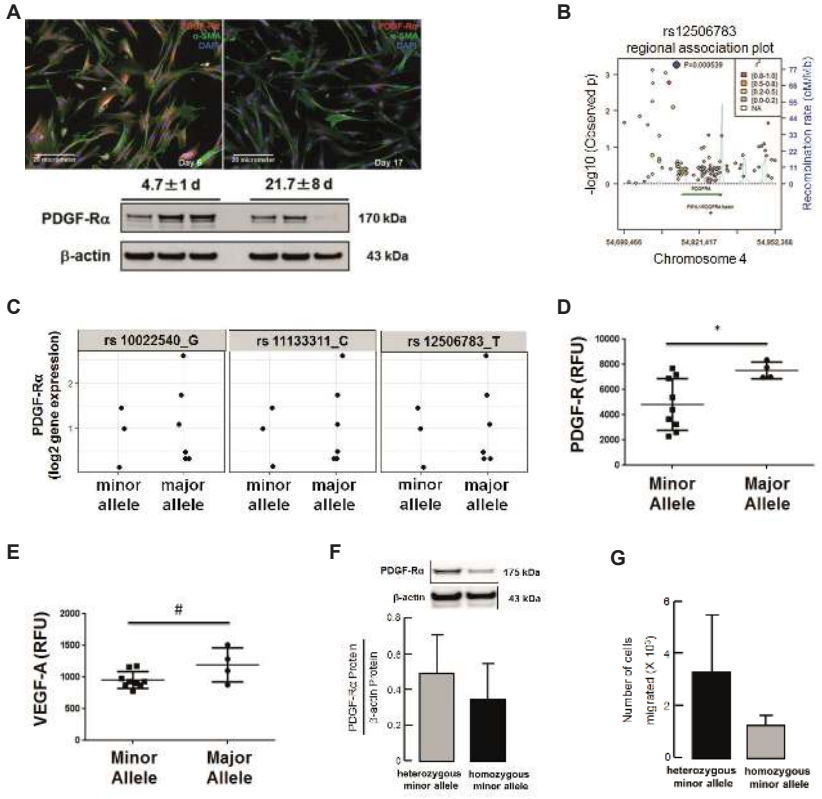

Figure A.3: Enrichment of PDGF-Rα SNPs associated with reduced protein levels and migration of lung fibroblasts from ventilated preterm infants developing nCLD (**A**) Decreased PDGF-Rα expression in human lung fibroblasts (hMFBs) from preterms undergoing MV-O_2 (21.7 ± 8 vs 4.7 ± 1 days of life; serial samples 2&5, 3&6) ($n = 3$ patients/group). (**B**) Regional association plot showing -log10 p-values (y-axis) of SNPs according to chromosomal positions (x-axis). Light blue: Estimated recombination rate (cM/Mb, HapMap CEU population); blue: most significant SNP (rs12506783); red: $r2 \geq 0.8$, white: $r2 \geq 0.2$. (**C**) Levels of PDGF-Rα gene expression in patients ($n = 9$) which are carrying at least one SNP (minor allele) compared to patients with no SNPs (major allele). Major alleles are given in the figure labels. Minor alleles of rs10022540 is A, in rs11133311 is T, and in rs12506783 is C. (**D**-**E**): PDGF-R (D) and VEGF-A (E) protein levels in separate patient cohort ($n = 13$) carrying at least one SNP (minor allele) at position rs12506783 compared to patients with no SNPs (major allele). Protein levels were quantified using SOMAlogic technique. Two-tailed unpaired Student's t test ($p = 0.0281 - 0.0863$). $\#p = 0.0863$. (**F**-**G**): Representative PDGF-Rα levels (F) and migratory potential assessed by boyden chamber assay (G) in fibroblasts isolated from tracheal aspirates of patients with nCLD. The fibroblast carrying SNP at both alleles (homozygote minor allele) displayed reduced PDGF-Rα levels and migration when compared to fibroblasts from patients carrying SNP at one allele (heterozygote minor allele). ($n = 3/4$ replicates). In (D-G) data is presented as Mean $\pm$ SD. *$p < 0.05$

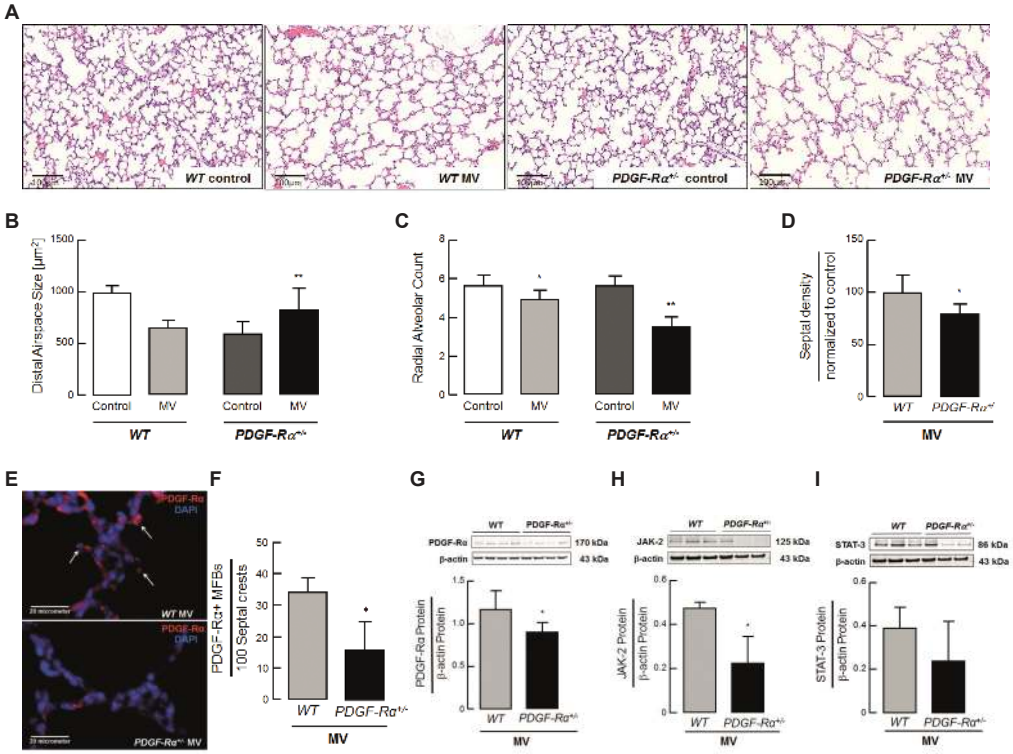

Figure A.4: PDGF-Rα haploinsufficiency drives the air sac pathology of nCLD in neonatal mice undergoing MV-O_2 (**A**) Representative lung tissue sections (200X) from 5-8d-old PDGF-R$\alpha^{+/+}$ (WT) and PDGF-R$\alpha^{+/-}$ mice after 8h MV-O_2 showing increased air space size compared to respective controls (O_2-control) spontaneously breathing 40% O_2 for 8h. (**B**) Quantitative analysis of lung tissue sections showed increased alveolar area after 8h MV-O_2 in PDGF-R$\alpha^{+/-}$ mice, whereas no significant change was observed in WT mice when compared to respective controls ($n = 6 - 11$ mice/group). (**C**) Radial alveolar counts (alveolar number) in lung tissue sections from WT and PDGF-R$\alpha^{+/-}$ mice were reduced after 8h MV-O_2 when compared to respective controls ($n = 6 - 11$ mice/group). (**D**) Septal density was significantly reduced in PDGF-R$\alpha^{+/-}$ mice when compared to WT littermates after 8h MVO_2 ($n = 6 - 8$ mice/group). (**E**) Immunofluorescence staining (400X, merged) for PDGF-Rα (red, white arrows; blue: DAPI) with decreased stain from the septal crests in lungs of ventilated PDGF-R$\alpha^{+/-}$ (lower panel) and WT (upper panel) mice undergoing MV-O_2. (**F**) Quantitative analysis of the immunofluorescence images (200X) showed reduced number of PDGF-Rα+ myofibroblasts located at the septal crests (presented myofibroblasts number per 100 septal crests; 10 fields of view in PDGF-Rα and α-smooth muscle actin co-stained sections/animal, 4 animals/group). (**G-I**) Immunoblot analysis of PDGF-Rα (G) and its downstream proteins JAK-2 (H) and STAT-3 (I) showing a significant reduction of protein level in PDGF-R$\alpha^{+/-}$ neonatal mice in contrast to WT mice after MV-O_2 for 8h($n = 3$ mice/group). PDGF-Rα levels are displayed as fold change of control. H and I are from same blot hence having same β-actin bands. In (B-D) and (F-I) data is presented as Mean $\pm$ SD. ***$p < 0.001$, **$p < 0.01$, *$p < 0.05$. Statistical analysis for (B-D) is Ordinary one way anova with Bonferroni's correction ($p = 0.0001 - 0.029$) and (F-I) is Two-tailed unpaired Student's t test or Mann Whitney test ($p = 0.024 - 0.028$).

demonstrated significantly increased vascular endothelial cell death in the lung periphery of ventilated neonatal PDGF-R$\alpha^{+/-}$ mice compared with WT littermates (Figure A.5E-F).

To further explore the link between reduced PDGF signaling and endothelial cell apoptosis, we focused on VEGF-A, a critical regulator of pulmonary microvascular development [21–25] With MV-O_2, pulmonary VEGF-A protein level was significantly reduced in PDGF-R$\alpha^{+/-}$ mice compared to WT littermates (Figure A.5D). Interestingly, vessel number did not differ compared to unventilated PDGF-R$\alpha^{+/-}$ mice (Supplemental Figure A.12).

In order to determine if this reduction was a direct consequence of reduced PDGF-Rα signaling in myofibroblasts, we isolated primary lung myofibroblasts from WT mice and measured their production of VEGF-A at baseline as well as following siRNA mediated knock-down of PDGF-Rα expression in vitro (Figure A.5H, I). We also administered conditioned supernatant from PDGF-Rα siRNA treated mouse myofibroblasts to human umbilical vein endothelial cells (HUVECs) in culture, and found reduced endothelial cell survival due to an increase in apoptosis (Figure A.5G, J) and a reduction in the permeability factor eNOS (Figure A.5K), comparable to the effect seen with an anti-VEGF-A antibody. These experiments together with Figure A.4G-I indicate that PDGF-Rα signaling in the myofibroblasts promotes VEGF-A expression, and corroborates that the microvascular phenotype is downstream of attenuated PDGF signaling.

Supplemental PDGF-A rescues both the air sac and microvascular nCLD phenotypes induced by MV-O_2 in neonatal PDGF-Rα haploinsufficient mice

As suggested by the human SNP data and our experiments above, if the attenuated PDGF signaling drives the pathogenesis of nCLD in all its manifestations, experimentally augmenting PDGF signaling in the lungs of ventilated haploinsufficient mice should ameliorate both the air sac and microvascular phenotypes. To directly test this prediction, we administered exogenous PDGF-A protein by endotracheal delivery at the onset of MV-O_2. The results showed both an increase in peripheral lung microvessel number ($20-100\mu m$) in treated versus untreated PDGF-R$\alpha^{+/-}$ neonatal mice undergoing MV-O_2, as well as a normalization of air sac defects, with increased alveolar and microvessel number compared with untreated controls (Figure A.6A-C). The reduction in JAK-2, STAT-3, VE-Cadherin and VEGF-A protein expression in the lungs of ventilated mice was also ameliorated with PDGF-A treatment, supporting reversal of the endothelial cell apoptosis (Figure A.6E-H). PDGF-A treatment further enhanced PDGF-Rα protein, associated with increased levels of AKT, suggesting a feed-forward mechanism where increased endosomal internalization leads to PDGF-Rα recycling in lung myofibroblasts with subsequent increase in receptor expression [26, 27] (Figure A.6D, I). The lung periphery of mechanically ventilated PDGF- R$\alpha^{+/-}$ neonatal mice also exhibited an increase in (secreted) VEGF-A protein immunolocalized near myofibroblasts, providing further support (Figure A.6J, M upper panel). Quantification of immunofluorescent staining confirmed a pronounced reduction in apoptotic (cleaved caspase-3 positive) surface area and individual cells, with dramatically increased CD31 surface area in PDGF-A treated mice (Figure A.6K-L,-M lower panel). A physiological rescue was also observed, with an improvement in quasi- static compliance by lung function testing in neonatal mice pre-treated with PDGF-A (Figure A.6N), with no significant difference in lung volume (PDGF-A $49.8\pm5.6\mu l/g$ bw vs no-PDGF-A $49.3\pm3.9\mu l/g$ bw; mean$\pm$SD, $p = 0.99$, Two-tailed Mann Whitney test).

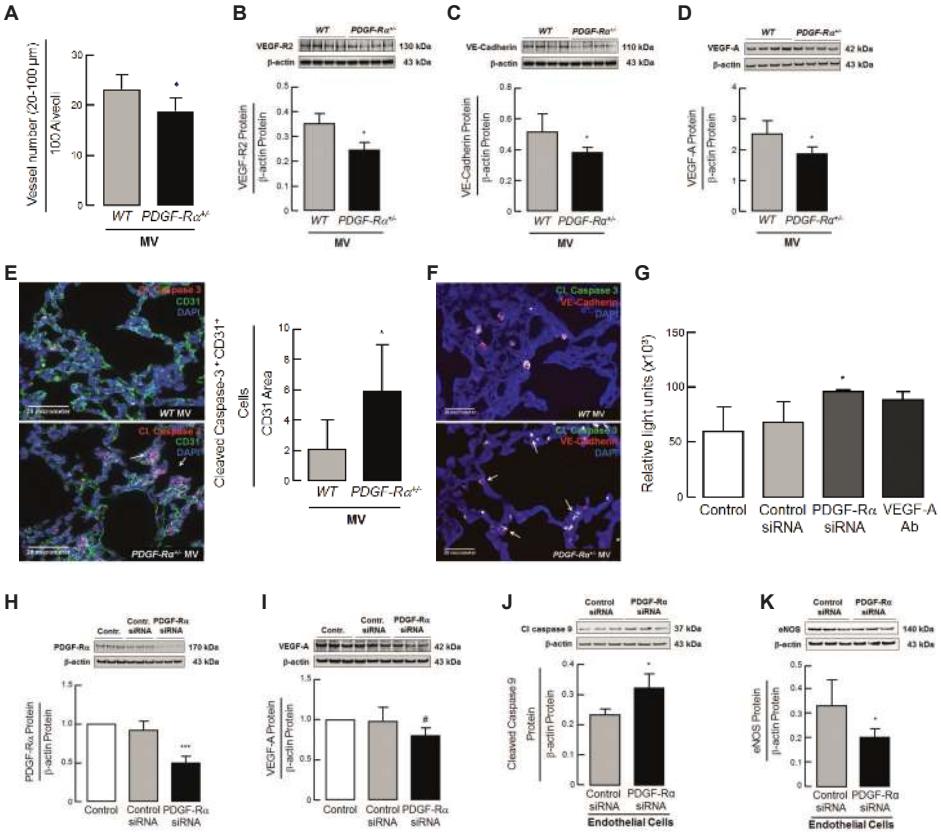

Figure A.5: PDGF-Rα haploinsufficiency drives reduced pulmonary micro-vessel density with increased endothelial cell apoptosis in neonatal mice undergoing MV-O_2 (**A-D**) Histologic and Immunoblot analysis displayed reduced small-vessel number ($20-100\mu m$ diameter) normalized to 100 alveoli as well as reduced pulmonary VEGF-R2, VE-Cadherin and VEGF-A protein levels respectively ($n = 6-8$ mice/group). (**E**) Immunofluorescent images of lung tissue (400X; merged) from neonatal PDGF-R$\alpha^{+/-}$ mice indicating increased cleaved Caspase-3 (red; white arrows; lower panel) after 8h MV-O_2 in contrast to WT mice (upper panel; green: CD31; blue: DAPI). Double stain revealed increased cleaved Caspase-3+/CD31+ cells normalized to CD31 area in PDGF-R$\alpha^{+/-}$ mice after 8h MV-O_2 ($n = 4$ mice/group, 4 sections/mice and 10 images/section). (**F**) Representative image confirming increased endothelial apoptosis in neonatal PDGF-R$\alpha^{+/-}$ mice after 8h MV-O_2 (lower panel; white arrows) with VE-Cadherin (red) and cleaved caspase-3 (green) and nucleus stained with DAPI (blue) when compared to WT mice (upper panel). ($n = 2$ mice/group). (**G** Increased caspase-3 activation in HUVECs upon incubation with supernatants for 6h obtained from lung mouse myofibroblasts after PDGF-Rα-siRNA treatment when compared to control-siRNA ($n = 3$ experiments). (**H-I**) In vitro application of PDGF-Rα-siRNA to primary lung mouse myofibroblasts from WT mice diminished PDGF-Rα (H) protein (normalized to control), associated with reduced VEGF-A protein (I). ($n = 3$ mice/group). (**J-K**) Increased cleaved caspase-9 and reduced eNOS protein levels in HUVECs upon incubation with supernatants for 6h obtained from lung mouse myofibroblasts after PDGF-Rα-siRNA treatment when compared to control-siRNA. ($n = 3$ mice/group). B and C are from same blot hence having same β-actin bands. Data is presented as Mean $\pm$ SD. ***$p < 0.001$, *$p < 0.05$ vs control, #$p < 0.05$ vs control-siRNA. Statistical test in (A-E) is Two-tailed unpaired Student's t test or Mann Whitney test, in (J-K) One-tailed Mann Whitney test ($p = 0.02 - 0.05$), in G is Kruskal Wallis H test ($p = 0.027$) and in I is Ordinary one way ANOVA with Bonferronis correction ($p = 0.0481$).

Elevated TGF-β levels causally relate with reduced PDGF-Rα expression in nCLD patients and mice undergoing MV-O_2 , reducing downstream signaling and migration in pulmonary myofibroblasts

Clinical and experimental studies have consistently demonstrated activation of pulmonary TGF-β signaling with MV-O_2 [28–35]. We therefore investigated how reduced PDGF-signaling and its demonstrated consequences are provoked in the neonatal lung. Hence, we characterized the two potential players mechanical stretch and TGF-β alone and in combination, with respect to their effect on primary mouse and human lung myofibroblasts.

Immunofluorescent images of tissue sections from nCLD patients ($n = 7$) showed reduced expression of PDGF-Rα associated with increased expression of pSMAD-2 compared with a control lung, supporting the relevance of the findings to patients suffering from nCLD (Figure A.7A). In parallel, we performed gene expression microarray analysis of blood samples obtained from 20 preterm infants in the first 72h after birth, which similarly demonstrated an inverse correlation between the levels of TGF-β1 and PDGF-Rα in patients who went on to develop nCLD that was not observed in patients who did not (Figure A.7B). We next analyzed TGF-β signaling activity in the lungs of ventilated WT mice, which demonstrated increased p-SMAD 2/3 protein with a concomitant reduction in PDGF-Rα+ alveolar myofibroblasts (Figure A.7C). To test the impact of TGF-β on PDGF-Rα promoter activity, we conducted a luciferase assay by transfecting CCL206 cells with a pGal vector carrying a PDGF-Rα promoter insert. Administration of TGF-β caused a 50% reduction in luciferase activity (Figure A.7D), indicating that TGF-β affects PDGF-Rα gene transcription, supporting the inverse relationship observed in nCLD is causal.

Figure A.6 (following page): Supplemental PDGF-A rescues both the air sac and microvascular nCLD phenotypes induced by MV-O_2 in neonatal PDGF-Rα haploinsufficient mice (**A**) Improved alveolar structure in 5-8d-old PDGF-R$\alpha^{+/-}$ mice undergoing 8h MV-O_2 after intra-tracheal treatment with PDGF-A ($10\mu l/g$ bw, 25ng/ml PDGF-A) when compared to mice receiving sterile saline (200x), confirmed by quantitative image analysis with increased alveolar counts (**B**) as well as vessel number normalized to 100 alveoli (**C**) ($20 - 100\mu M$) ($n = 2 - 4$ mice/group). (**D-I**) Immunoblot analysis of total lung homogenates showed increased PDGF-Rα (D) together with increased JAK-2 (E), STAT-3 (F), VEGF-A protein (G) VE-Cadherin (H) and AKT (I) protein levels in PDGF-A treated PDGF-R$\alpha^{+/-}$ mice after 8h MV-O_2 when compared to WT littermates ($n = 3 - 4$ mice/group). (**J-M**) Quantitative image analysis indicated increased VEGF-A to PDGF-Rα protein levels (K, M; upper panel) together with an increase in CD31 expression in relation to total tissue (K, M; lower panel) and a decrease in apoptotic (Cleaved caspase-3) CD31 expressing cells (L) in the lungs of PDGF-A treated PDGF-R$\alpha^{+/-}$ mice when compared to saline treated controls after 8h MV-O_2 ($n = 2 - 4$ mice/group). Upper panel in M is PDGF-R$\alpha^{+/-}$ mice treated with NaCl (left) or PDGF-A (right) sections stained with VEGF-A (green), PDGF-Rα (red) dual positive (orange, white arrows) and inserts show VEGF-A stain (green). Lower panel shows PDGF-R$\alpha^{+/-}$ mice treated with NaCl (left) or PDGF-A (right) sections stained with Cleaved-caspase 3 (green), CD31 (red) dual positive (orange, white arrows). Nucleus is stained with DAPI (blue). (**N**) Treatment with PDGF-A in ventilated neonatal PDGF-R$\alpha^{+/-}$ mice led to improved lung compliance displayed as a function of airway pressure (Ptramax) and tidal volume when compared to untreated mice ($n = 4$ mice/group). D-H and E-F are from same blot hence having same β-actin bands. In (B-L) the data is presented as Mean $\pm$ SD. ***$p < 0.001$, **$p < 0.01$, *$p < 0.05$, $^{\#}p < 0.065$. Statistical test used is One-tailed unpaired Student's t test ($p = 0.023 - 0.065$), in C and G is Two-tailed Mann Whitney and unpaired Student's t test ($p = 0.02 - 0.05$).

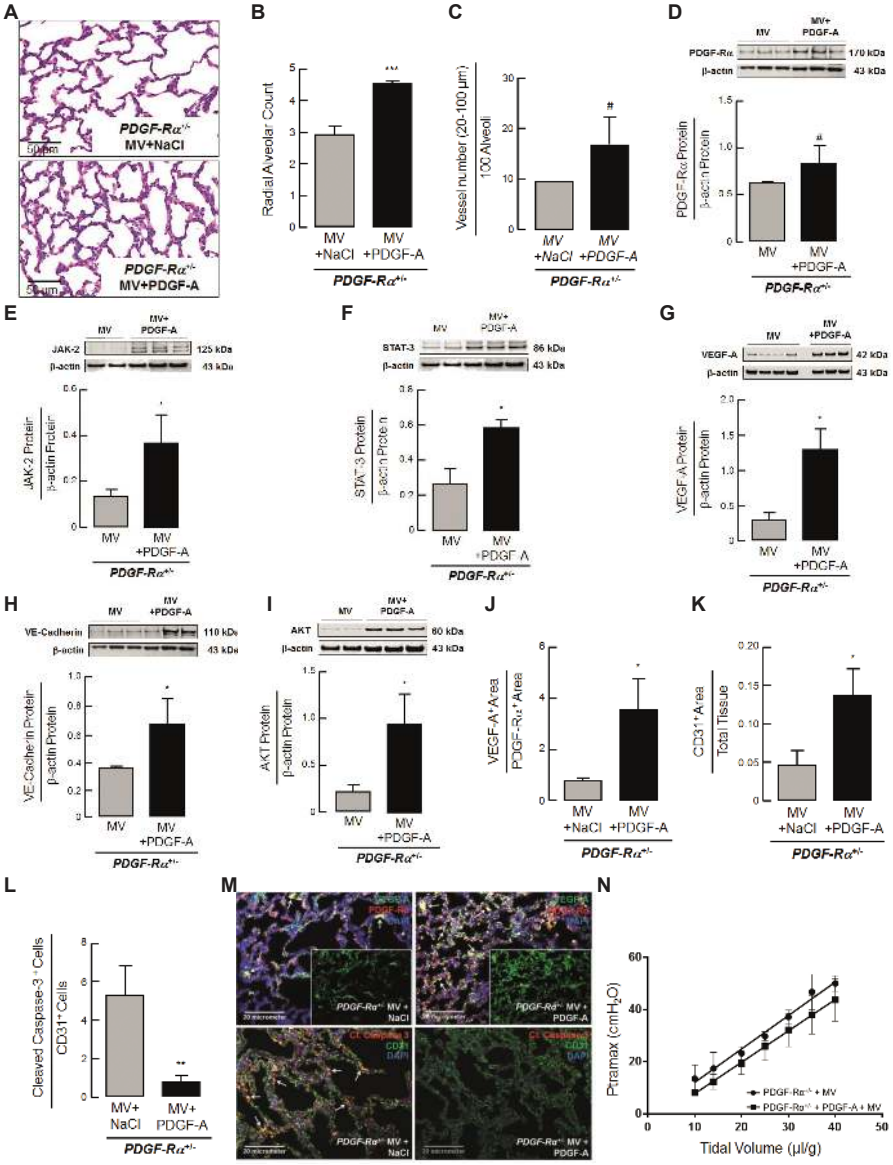
A
PDGF-Rα+/- MV+NaCl
PDGF-Rα+/- MV+PDGF-A
50 µm
B
Radial Alveolar Count
MV +NaCl
MV +PDGF-A
PDGF-Rα+/-
C
Vessel number (20-100 µm) / 100 Alveoli
MV +NaCl
MV +PDGF-A
PDGF-Rα+/-
D
MV
MV+ PDGF-A
PDGF-Rα
β-actin
170 kDa
43 kDa
PDGF-Rα Protein / β-actin Protein
MV
MV +PDGF-A
PDGF-Rα+/-
E
JAK-2
β-actin
125 kDa
43 kDa
JAK-2 Protein / β-actin Protein
MV
MV +PDGF-A
PDGF-Rα+/-
F
STAT-3
β-actin
86 kDa
43 kDa
STAT-3 Protein / β-actin Protein
MV
MV +PDGF-A
PDGF-Rα+/-
G
VEGF-A
β-actin
42 kDa
43 kDa
VEGF-A Protein / β-actin Protein
MV
MV +PDGF-A
PDGF-Rα+/-
H
VE-Cadherin
β-actin
110 kDa
43 kDa
VE-Cadherin Protein / β-actin Protein
MV
MV +PDGF-A
PDGF-Rα+/-
I
AKT
β-actin
60 kDa
43 kDa
AKT Protein / β-actin Protein
MV
MV +PDGF-A
PDGF-Rα+/-
J
VEGF-A+ Area / PDGF-Rα+ Area
MV +NaCl
MV +PDGF-A
PDGF-Rα+/-
K
CD31+ Area / Total Tissue
MV +NaCl
MV +PDGF-A
PDGF-Rα+/-
L
Cleaved Caspase-3+ Cells / CD31+ Cells
MV+ NaCl
MV+ PDGF-A
PDGF-Rα+/-
M
PDGF-Rα+/- MV + NaCl
PDGF-Rα+/- MV + PDGF-A
CC Caspase 3
CD31
DAPI
N
Pramax (cmH2O)
Tidal Volume (µl/g)
PDGF-Rα+/- + MV
PDGF-Rα+/- + PDGF-A + MV

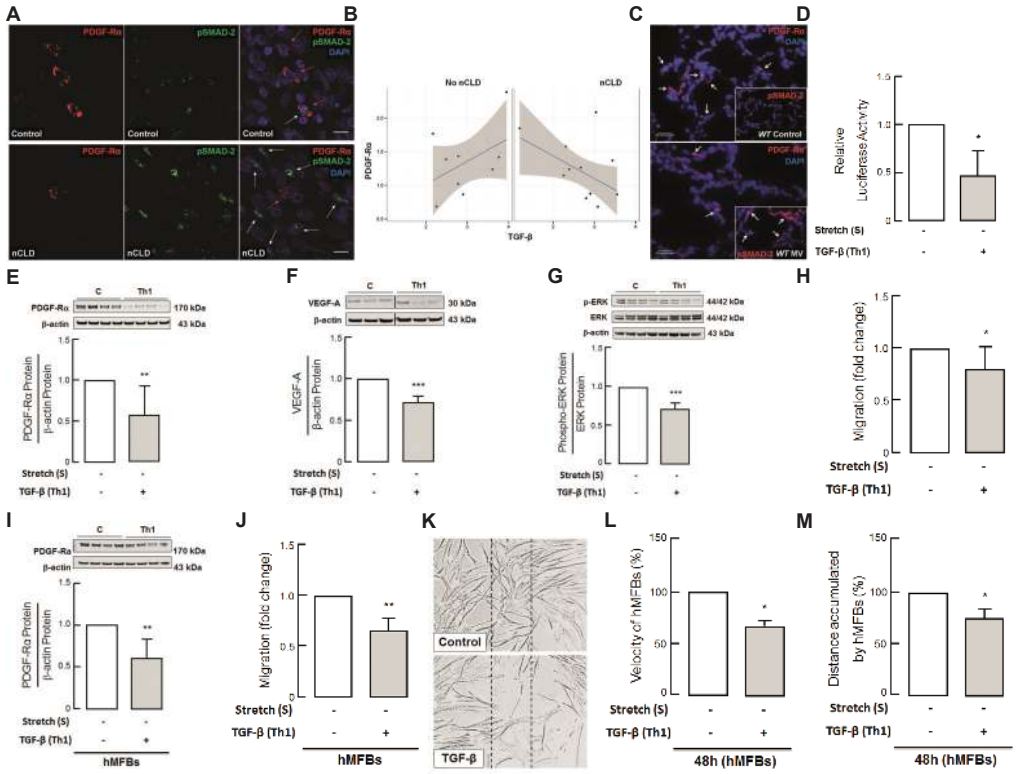

Figure A.7: Elevated TGF-β levels causally relate with reduced PDGF-Rα expression in nCLD patients and mice undergoing MV-O_2, reducing downstream signaling and migration in pulmonary myofibroblasts (**A**) Representative immunofluorescence images showing reduced expression of PDGF-Rα (red) in the lungs of patients ($n = 7$) developing nCLD (lower left panel, red stain; white arrows) together with increased pSMAD-2 expression (green; upper middle panel; green stain; white arrows) as compared to lung sections from a non-nCLD patient ($n = 1$) (upper panel) (200x). (**B**) Negative correlation between PDGF-Rα and TGF-β1 in transcriptome analysis 72h after birth in preterms with nCLD ($n = 11$) in contrast to non nCLD ($n = 9$; scatter plots log2-gene expression; linear regression (blue), CI (grey), ($p = 0.05$). (**C**) MV-O_2 reduced lung PDGF-Rα (main: red stain; white arrows) and increased pSMAD-2 levels (insert: red stain; white arrows) in neonatal PDGF-R$\alpha^{+/-}$ (lower panel) when compared to WT mice (upper panel); ($n = 4$ mice/group; 10 images/mouse; 200x). (**D**): Luciferase assay of CCL-206 cells transfected with pGL4.14 containing PDGF-Rα promoter revealing reduced promoter activity upon TGF-β application (normalized to control). ($n = 3$ experiments). (**E-G**) Immunoblot analysis showing reduced PDGF-Rα (E), pERK/EKR (F) and VEGF-A (G) protein levels upon TGF-β application alone in primary pulmonary myofibroblasts from 5-7d old WT mice ($n = 6-9$ mice/group). (**H**) Reduced migration of myofibroblasts (MFBs) from neonatal WT mice upon TGF-β application alone ($n = 5$ mice/group, 3 technical replicates). (**I-J**) Translation of the results in fibroblasts isolated from tracheal aspirates of ventilated preterm infants (hMFBs) displayed reduced PDGF-Rα levels (I) and migration assessed by boyden chamber assay (J) upon TGF-β application. ($n = 3 - 5$ patients/group). (**K-M**) Representative phase contrast images (100X) of scratch migration assays in human lung fibroblasts (hMFBs) after 48h of TGF-β incubation indicating decreased wound closure (K) quantified by reduced distance travelled (L) and velocity (M). ($n = 3$ patients/group). In (E-J) and (K-M) data is presented as Mean $\pm$ SD and normalized to control. Statistical test used is Two-tailed unpaired student's t test or Mann Whitney test ($p = 0.0002 - 0.039$). ***$p < 0.001$, **$p < 0.01$, *$p < 0.05$; C: un-stretched untreated control; Th1: un-stretched myofibroblasts subjected to 5ng/ml TGF-β (24h)

We further confirmed the effect of TGF-β on PDGF-Rα signaling in primary pulmonary myofibroblasts isolated from WT neonatal mice and fibroblasts isolated from tracheal aspirates of nCLD patients.This analysis showed a significant downregulation in PDGF-Rα level, its signalling measure by pERK/ERK and impaired function displayed as reduced migration (Figure A.7E-F, H). In accordance with the in vivo data, VEGF-A signaling associated with micro-vessel development was also diminished by 20% in pulmonary myofibroblasts from neonatal WT mice incubated with TGF-β (Figure A.7G). Translating this finding in human we demonstrate diminished PDGF-Rα levels and migration of fibroblasts (Figure A.7I). Reduced migration upon TGF-β was confirmed by boyden chamber and wound migration assays showing significantly abrogated velocity and distance travelled by fibroblasts in comparison to untreated controls (Figure A.7J-M).

Pronounced effect of TGF-β on pulmonary myofibroblasts from PDGF-R$\alpha^{+/-}$ mice and in concert with mechanical stretch on both mice and human myofibroblasts

The inhibitory effect of TGF-β on PDGF-Rα level and downstream proteins JAK-2, STAT-3 and pERK/ERK was dramatic in myofibroblasts isolated from PDGF-R$\alpha^{+/-}$ mice with more than 30-50% reduction in the respective proteins (Figure A.8A-C, E).This was accompanied by reduction in vascular marker VEGF-A and diminished migration (Figure A.8D, F).

Mechanical ventilation has been demonstrated to exert significant strain forces on the developing lung in infants requiring invasive and even non-invasive respiratory support [3]. We therefore dissected the contribution of mechanical stretch and the impact of growth factor

Figure A.8 (following page): Pronounced effect of TGF-β on pulmonary myofibroblasts from PDGF-R$\alpha^{+/-}$ mice and in concert with mechanical stretch on both mice and human myofibroblasts (**A-E**) TGF-β application (Th1) to myofibroblasts (MFBs) isolated from neonatal PDGF-R$\alpha^{+/-}$ mice reduced PDGF-Rα (A), JAK-2 (B), STAT-3 (C), VEGF-A (D) and pERK/ERK (E) protein levels when compared to control. ($n = 3-6$ mice/group). (**F**) Reduced migration assessed by boyden chamber in myofibroblasts (MFBs) isolated from PDGF-R$\alpha^{+/-}$ mice compared to WT mice. ($n = 5$ mice/group). (**G-J**): TGF-β application in combination with mechanical stretch (S+Th1) in myofibroblasts (MFBs) isolated from neonatal WT mice showed reduced PDGF-Rα (G) and VEGF-A (H) protein as well as migratory RAS (I) and pERK/ERK (J) protein levels when compared to control myofibroblsts as assessed by immunoblot assay. ($n = 6 - 9$ mice/group). (**K**) TGF-β application (Th1) as an additional dose (Th2) on stretched myofibroblasts (MFBs) from WT mice reduced migration as assessed by boyden chamber assay. ($n = 5$ mice/group). (**L-M**) TGF-β application in combination with stretch (S+Th1) reduced PDGF-Rα protein levels in fibroblasts (hMFBs) isolated from tracheal aspirates of nCLD patients when compared to control (C) or stretched (S) myofibroblasts (L) and as an additional dose (TH2) to stretched fibroblasts reduced migration (M). ($n = 3 - 6$ patients/group). A-E and B-C are from same blot hence having same β-actin bands. Values are normalized to the respective controls except for B-D. Data is presented as Mean $\pm$ SD. Statistical test used in (A, D-F) is Two-tailed and (B-C) is One-tailed student's t test or Mann Whitney test ($p = 0.004 - 0.05$) and in (G-M) is ordinary One way ANOVA with Bonferroni's correction ($p = 0.0001 - 0.04$). ***$p < 0.001$, **$p < 0.01$, *$p < 0.05$. C: Un-stretched untreated control; S: stretched myofibroblasts (24h); Th1: un-stretched myofibroblasts subjected to 5ng/ml TGF-β (24h); S+Th1: myofibroblasts stretched in parallel to TGF-β application (5ng/ml) (24h); Th2: re-incubation with 5ng/ml TGF-β (8h).

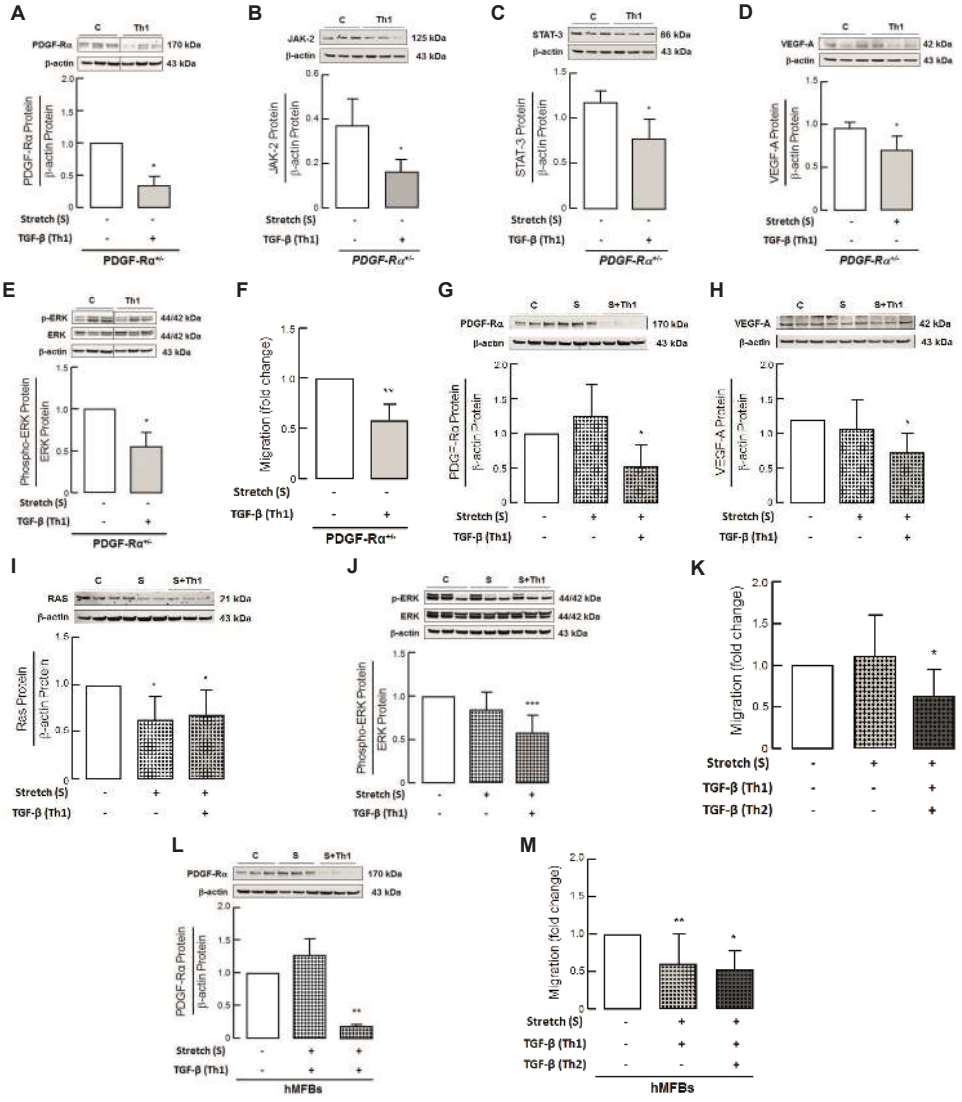
A
C
Th1
PDGF-Rα
170 kDa
β-actin
43 kDa
PDGF-Rα Protein / β-actin Protein
Stretch (S)
TGF-β (Th1)
PDGF-Rα+/-
B
JAK-2
125 kDa
JAK-2 Protein / β-actin Protein
C
STAT-3
86 kDa
STAT-3 Protein / β-actin Protein
D
VEGF-A
42 kDa
VEGF-A Protein / β-actin Protein
E
p-ERK
ERK
44/42 kDa
Phospho-ERK Protein / ERK Protein
F
Migration (fold change)
G
S
S+Th1
H
I
RAS
21 kDa
Ras Protein / β-actin Protein
J
K
TGF-β (Th2)
L
hMFBs
M

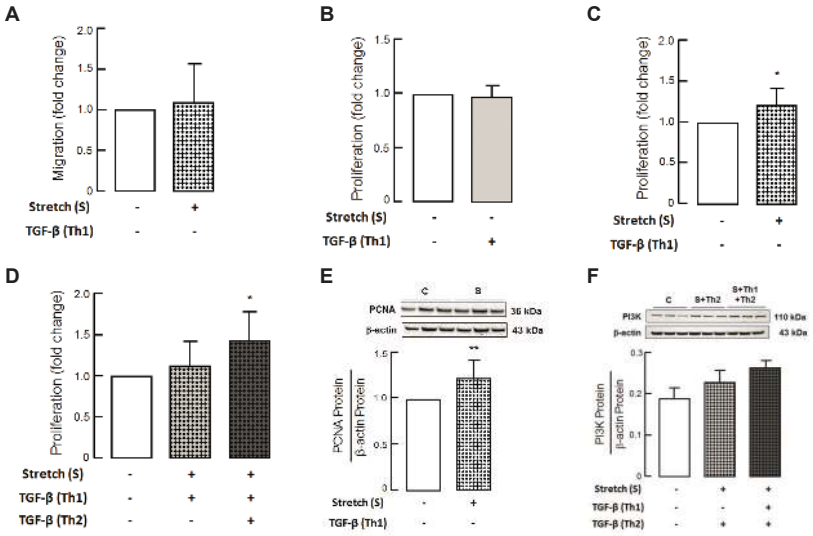

Figure A.9: Effect of TGF-β in combination with mechanical stretch on PDGF-Rα signaling and functional properties of fibroblasts (**A**) No change in migration of myofibroblasts (MFBs) from newborn WT mice with mechanical stretch ($n = 5$ mice/group). (**B-D**) Analysis of proliferation (Cell Titer Glo) exhibited no change upon TGF-β (B) or stretch (C) in mouse myofibroblasts (MFBs) from WT mice, while an increase in proliferation observed when mouse myofibroblasts were stretched in presence of TGF-β were subjected to an additional dose of TGF-β (D) ($n = 9$ mice/group). (**E-F**) Immunoblot analysis showing increased proliferation markers like PCNA (E) levels with mechanical stretch and PI3K (F) upon additional TGF-β incubation on stretched myofibroblasts (MFBs) from newborn WT mice ($n = 6$ mice/group). Values here are normalized to respective controls. Data is presented as Mean $\pm$ SD. Statistical analysis in (A-C, E) is Two-tailed unpaired Student's t test and in (D, F) is Ordinary one way ANOVA with Bonferroni's correction. $^{**}p < 0.01$, $^{*}p < 0.05$. (p value range $= 0.0080 - 0.0232$) C: Un-stretched untreated control; S: stretched myofibroblasts (24h); Th1: un-stretched myofibroblasts subjected to 5ng/ml TGF-β (24h); S+Th1: myofibroblasts stretched in parallel to TGF-β application (5ng/ml) (24h). S+Th2: myofibroblasts stretched for 24h followed by incubation with TGF-β (5ng/ml) for 24h.

exposure on PDGF signaling in vitro. Here we found that mechanical stretch in combination with TGF-β significantly reduced PDGF-Rα level in mouse myofibroblasts together with a matched reduction in VEGF-A expression confirming our in vivo findings (Figure A.8G-H). With respect to myofibroblast function, we found that mechanical stretch in the presence of single or repeat doses of TGF-β significantly reduced migration in primary pulmonary myofibroblasts from WT mice together with a significant reduction in RAS and downstream pERK/ERK protein level, a signaling downstream of PDGF-Rα with a crucial role in myofibroblasts migration (Figure A.8I-K) [36, 37]. In addition, mechanical stretch in the presence of TGF-β increased myofibroblast proliferation, together with proteins associated with proliferation PI3K and PCNA level (Figure A.9B-F). Whereas TGF-β in the absence of mechanical stretch was able to achieve comparable effects on myofibroblast migration, PDGF-Rα and VEGF-A protein level (Figure A.7E, G, H), mechanical stretch alone did not alter the migratory behaviour or protein expression in the lung myofibroblasts but did increase their proliferative behaviour (Figure A.8G, H, and Figure A.9A, C).

Translating these effects to primary human fibroblasts obtained from tracheal aspirates of preterm nCLD patients, we found a significant reduction in PDGF-Rα protein level and migration by TGF-β in combination with stretch (Figure A.8L-M). In line with this, repeated

application of TGF-β in combination with stretch markedly reduced the migration of human lung fibroblasts (Figure A.8M).

Taken together, these results indicate that elevated TGF-β signaling in the setting of MV-O_2 contributes to the development of nCLD, exacerbating the deficiency in PDGF signaling by inhibiting expression of PDGF-Rα on lung myofibroblasts.

The central role of the PDGF signaling cascade closely intertwined with upstream effectors and downstream effects with critical consequences for cellular functions in the injured neonatal lung as well as its recue with administration of PDGF-A is depicted in Figure A.10.

Discussion

Neonatal chronic lung disease (nCLD), formerly known as Bronchopulmonary Dysplasia, has long-term health consequences not only for lung but also neurologic function. Invasive and non-invasive mechanical ventilation with oxygen-rich gas (MV-O_2) is necessary for the survival of preterm babies suffering from respiratory failure due to lung immaturity and insufficient respiratory drive after birth. Nontheless, both treatments are known to contribute to adverse pulmonary outcome, i.e. the development of nCLD [3]. Hence it is critical to pursue medical treatments that can prevent or treat nCLD in neonatals requiring ventilatory support. Here, we provide causal evidence supporting a surprising cellular and molecular model for the development of nCLD. As shown in mouse and human, PDGF signaling not only affects secondary septation but significantly impacts on the micro-vascular structure in close relation with the omnipresent TGF-β in the injured neonatal lung (Figure A.10A). This close intertwinement of growth factor signalling in nCLD pathology with PDGF as a central driver holds promising potential for therapeutic approaches.

The integration of PDGF-Rα haploinsufficient mice with a unique pre-clinical model of nCLD, together with tailored biochemical and in vitro assays of human and mouse primary lung cells, allowed us to elucidate the molecular pathogenesis of this disease to an unprecedented level of understanding. Building upon previous observations suggesting a role for reduced PDGF-Rα signaling in lung pathology [13, 11, 38, 39, 12, 18], we dissected upstream and downstream molecular regulators of nCLD, including a crosstalk with VEGF-A and TGF-β with mechanical stretch (Figure A.10A).

Our finding that impairment of the PDGF signaling pathway - previously associated only with myofibroblast migration and secondary septation of air sacs - is capable to produce both the alveolar structural and microvascular pathology of nCLD is surprising. Is it possible that due to the dynamic intercellular crosstalks required to generate the highly stereotyped and architecturally complex arrangement of alveoli, disruption of a single program indirectly disrupts closely coordinated, but distinct, processes? There is some precedent for this model, since inhibition of VEGF in lung development has been shown to result in reduced epithelial proliferation and impaired sacculation [40]. However, as we show in the case of PDGF-Rα, the causal relationship may be more direct, since VEGF-A is apparently produced not only by lung epithelial cells, but also by myofibroblasts in response to PDGF and its down- stream signalling through JAK and STAT [41, 42]. Perhaps this additional level of patterned VEGF-A production is important for ensuring proper investment of newly-forming secondary septal walls by the microvascular network. In any case, our demonstration of the therapeutic activity of exogenously administered PDGF-A (Figure A.10B) for rescuing both the air sac septation and microvascular defects is highly promising, particularly since previous attempts to improve vascularization by administering exogenous VEGF-A not only failed to rescue nCLD, but actually induced capillary leakage [43].

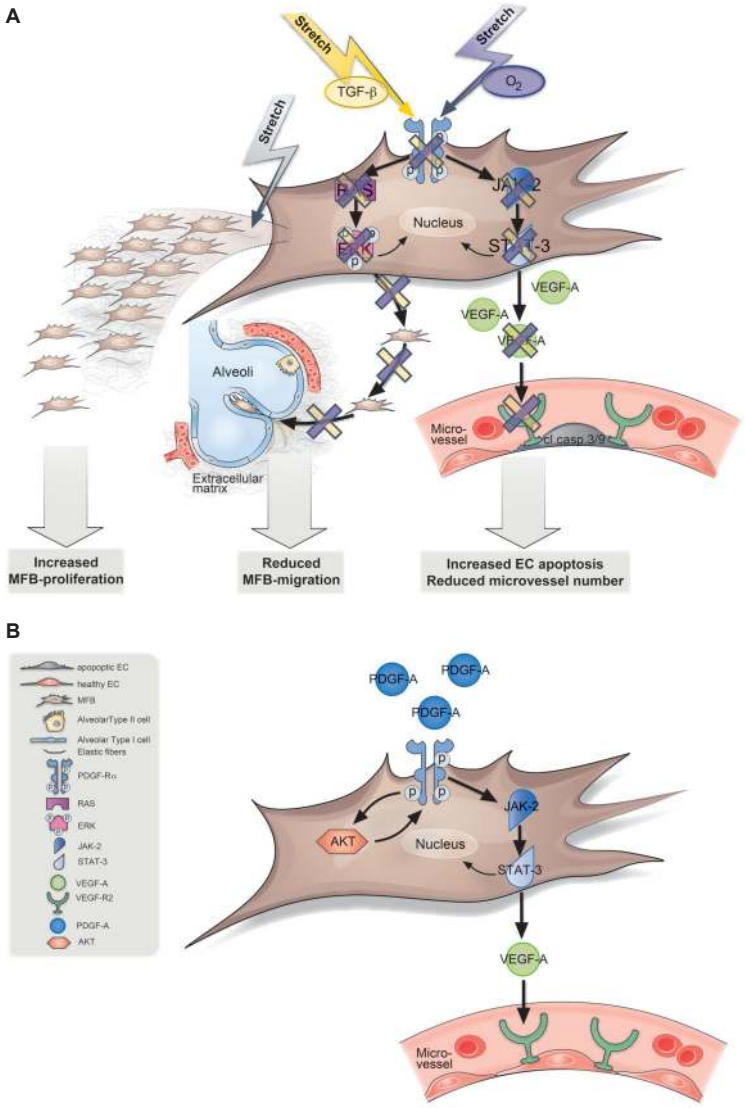

Figure A.10: Model for how attenuated PDGF signaling and positive pressure ventilation interact to produce the distinct phenotypic manifestations of nCLD (**A**) MV-O_2 in vivo, a combination of O_2 i.e. oxygen and stretch (purple arrow) and/or TGF-β alone or in combination with mechanical stretch in vitro (yellow arrow) reduce platelet derived growth factor receptor α (PDGF-Rα) levels and its downstream signaling through JAK-2 and STAT-3 in the pulmonary myofibroblast (MFB).This reduction in turn abrogates vascular endothelial growth factor expression (VEGF-A and VEGF-R2), leading to increased apoptosis in pulmonary endothelial cells (EC). Whereas myofibroblast migration is diminished through reduces RAS and pERK/ERK signaling, stretch alone increases their proliferation, hence depicting the differential effect of the most important denominators of nCLD development in the premature lung undergoing MV-O_2. (**B**) Application of PDGF-A to premature lung increases PDGF-Rα levels in an AKT dependent manner in turn activating the downstream cascade through JAK-2, STAT-3 signaling. This then activates VEGF-A secretion and VEGF-R2 activity reducing apoptosis in endothelial cells (ECs).

Supplemental methods

Study design

Preterm infants born below 32 weeks of gestational age and matched control infants with respect to gestational age, gender, percentage of individuals considered small for GA, and country of maternal origin were selected for the study. Exclusion criteria were oligo- or anhydramnios, severe congenital malformations, severe metabolic disorders and prepartum treatment of the mother with cytostatic or immunosuppressive medication other than for lung maturation.

Mice were randomly selected from each litter to undergo mechanical ventilation. 6-11 mice were utilized per group for histological analysis as well as 3-6 mice per group for protein analysis. Tissue sections from the respective mouse lungs were selected randomly for hematoxylin and eosin as well as immunostainings. In vitro experiments were performed on myofibroblasts obtained from 3-9 different mice. Functional assays on both mice myofibroblasts and human lung fibroblasts (proliferation and migration analysis) constituted 3 biological replicates consisting of 2-3 technical replicates each resulting in a total of 5-9 samples from different mice analyzed per condition (stretch and/or TGF-β treatment).

Human studies

SNP and protein analysis

All relevant perinatal diagnoses were provided for statistical analysis. Patients with moderate or severe BPD according to the definition by Jobe et al. from both cohorts were considered cases (Jobe, 2011). Exclusion criteria were oligo- or anhydramnios, severe congenital malformations, the diagnosis of severe metabolic disorders and prepartum treatment of the mother with cytostatic or immunosuppressive medication other than for lung maturation led to exclusion of the neonate. Cases (controls) had a median GA of 26.6 (27.0) weeks, 42.5 (45.7) % were female, and 28.0 (26.7) % were found to be small for GA. Duration of oxygen supplementation was 80 (15) days in median. Genotypes of PDGF-Rα SNPs (single nucleotide polymorphisms) were determined in neonates using Affymetrix Axiom microarrays based on the Axiom CEU array supplemented with some custom content. Among the 1061 individuals with genetic data passing QC, 492 developed BPD grade 2 or 3 and were considered cases. Cases and controls were balanced for sex, gestational age at birth, status 'small for gestational age', and country of origin of the mother. 117 SNPs within 100 kB upstream and downstream of PDGF-Rα, present on the array, and passing QC were selected for analysis; case-control analysis was adjusted for relatedness to account for multiple births. The PDGF signaling pathway and several pathways downstream of PDGF signaling were analyzed for evidence regarding genetic regulation of gene expression of their pathway elements. From our genome-wide dataset, genetic markers were identified either directly or via linkage disequilibrium as corresponding to SNPs found to contribute to genetic regulation of gene expression (i.e. eQTL SNPs) in several studies [22, 44–47]. The distribution of p-values for these SNPs was analyzed using the R-package snpMatrix [48] to identify pathways for which p-values in our BPD-association analysis showed nominally more evidence for association than would be expected by chance. A part of patients from this cohort ($n = 9$, Supplemental Table A.3A) were subjected to PDGF-Rα transcriptome analysis as described in microarray methods section.

A separate patient cohort consisting infants with or without later development of BPD and a GA < 32 weeks with excluding growth retardation was included at the Perinatal Center of the Ludwig-Maximilians-University, Campus Grosshadern ($n = 13$). Patient characteristics of this cohorts are given in Supplemental Table A.3B. Whole blood samples were collected at days 22-58 after birth in Ethylenediaminetetraacetic acid (EDTA) neonatal collection tubes. Generated plasma samples were stored at $-80°C$ and later subjected to proteomic

screening (SOMAscan^{TM}, SomaLogic, Boulder, USA). For the assay high quality samples were used and protein binding to 1129 individual high affinity molecules (SOMAmer®) was quantified by custom Agilent hybridization array [49]. Even low amount samples ($90 - 160\mu l$) showed high reproducibility. The SNP genotyping of this samples for the most significant SNP position rs12506783 was performed by Eurofins Genomics. Briefly, sequences forward CAAAATACCTGGAAGCTCTGGAG and reverse CCAGCATTCAATTCATACTTGCTG were generated using a re-sequencing approach. According to the reference sequence, the necessary primers were defined in order to create overlapping PCR fragments and for subsequent sequencing to have the region of interest covered in a satisfactory manner. PCR purification was performed with 10% PolyEthylenGlycol (PEG8000) in 30% Isopropyl alcohol/1M NaCl for precipitation and a washing step with 80% Ethanol. All sequences were generated using BigDye terminator chemistry (version 3.1), if necessary in combination with dGTP BigDye terminator chemistry (version 3.0) (Thermo Fisher Scientific, Waltham, MA USA) following standard protocols. For sequencing reactions peqStar 96 HPL (PEQLAB Biotechnologie GMBH, Erlangen, Germany) or GeneTouch (Biozym Scientific GmbH, Oldendorf, Germany) thermal cyclers were used. Sequencing reaction cleanup was done either manually or on a Hamilton Starlet robotic workstation (Hamilton Robotics GmbH, Martinsried, Germany) by gel-filtration through a hydrated Sephadex matrix filled into appropriate 96 well filter plates followed by a subsequent centrifugation step. Finally all reactions were run on ABI3730xl capillary sequencers equipped with 50 cm capillaries and POP7 polymer (Thermo Fisher Scientific, Waltham, MA USA). Sequencing data was generated using the original ABI Software including the KB-basecaller, which assigns quality values to all called bases similar to PHRED [50]. Additional basecalling was performed using the PeakTrace basecaller from Nucleics Pty Ltd (Woollahra, AUS) according to SOP_SEQ_PeakTrace to improve the single peak resolution and quality values and therefore increase the reading lengths. Primer sequences used were forward GTACTGGGATTACAGGTGTGAG and reverse ATAACATCCCAGGAGGCCTAC.

Human primary lung fibroblasts

Patients for tracheal aspirate analysis were recruited following the same in- and exclusion criteria as outlined above. Samples from 6 patients were used. Two patients provided serial samples; two patients were recruited with individual samples with respect to the early and later time point for PDGF-Rα expression analysis. Tracheal aspirates were obtained from preterm infants undergoing MV-O_2 who later developed nCLD, i.e. mild, moderate or severe BPD (gestational age 24 ± 1.4 weeks, birth weight $650 \pm 80.2g$, MV-O_2 43 ± 24 days (mean $\pm$ SD)). Patient characteristics are mentioned in Supplemental Table A.3C. First samples were obtained early after the initiation of MV-O_2 (4.7$\pm$1 day of life); second samples were taken during the third week of life (21.7$\pm$8 day of life). Primary human lung fibroblasts were cultured 80% confluent in DMEM medium with 20% FCS (PAN Biotech GmbH, Aidenbach, Germany), 2mM L-glutamine, and penicillin/streptomycin (Thermo Fisher Life Technologies, Carlsbad, CA). FACS analysis was performed to check the purity of the cultures as described in the manuscript.

Blood sampling, RNA isolation and microarray analysis

Briefly, blood was sampled from an indwelling umbilical artery catheter at birth. RNA isolation was performed according to the manufacturer's recommendations (PreAnalytiX). RNA was hybridized on CodeLink Human Whole Genome Bioarrays (GE Healthcare) using the CodeLink Expression Assay Kit (GE Healthcare) and samples processed using CodeLink Expression Software V4.1 (GE Healthcare). The dataset was initially prepared using the manufacturer recommended subtract background correction and median normalization. Data was then filtered for transcripts with high rates of missing values, low expressed values, or outlier values. Missing

values were imputed using the sequential nearest neighbor (SeqKNN) approach [51]. The dataset was then normalized using the quantile normalization method [52]. For data preparation the Bioconductor packages SeqKnn and limma for quantile normalization were used.

Human lung slides

Human slides were obtained from paraformaldehyde fixed and paraffin embedded autopsy lungs from preterm infants with different BPD grades ($n = 7$) and an infant that died from a non-pulmonary cause. Median gestational age of BPD patients was 26+0 weeks (25+4 - 31+0) and gestational age of the control infant was 26+5 weeks. All patients died between 28 and 66 days after birth and none were treated with extracorporeal membrane oxygenation. No chromosomal or other congenital anomalies were present in all patients. Tissue sections were stained for PDGF-Rα, and TGF-β for further quantification. The patient characteristics are mentioned in Supplemental Table A.3D.

In vivo studies

Assessment of protein expression in distal lung

PFA-fixed lung tissue sections were stained for PDGF-Rα (C-20) (Santa Cruz Biotechnology #sc-338), α-SMA (Sigma Aldrich #A5228), VEGF-A (C-1) (Santa Cruz Biotechnology #sc-7269), CD31 (Dianova, Hamburg Germany #DIA-310), cleaved caspase-3 (Cell Signaling Technology #9661S), VE-Cadherin (H-72, Santa Cruz Biotechnology #28644), pSMAD-2/3 (Santa Cruz Biotech #SC-8828) and DAPI (Sigma Aldrich #D8417) alone or in combination. Number of total nuclei as well cleaved caspase-3 and CD-31 positive cells were quantified in eight different fields of view/slide (400x magnification) using Imaris Software (Zurich, Switzerland). For cell surface or extracellular markers, areas with positive stain were quantified in separate color channels in 10 fields of view/animal (200x magnification) using the BIOQuant Software (BIOQUANT Image Analysis Corporation, Nashville, TN, USA).

Protein extraction and immunoblot analysis

Lungs from 8h studies ($n = 5-8$/group) were excised, weighed and snap-frozen in liquid N_2, and stored at $-80^{\circ}C$ for later protein extraction. Protein extraction was performed using high urea buffer (KPO_4 , Urea, AppliChem, Darmstadt, Germany) with added Halt Protease Inhibitor Cocktail (catalog #1861280, Thermo Fisher Scientific). Measurement of protein concentrations was done using the bicinchoninic acid (BCA) assay (catalog #23227, Pierce Scientific Rockford, IL, USA) and immunoblots were performed using a Bis-Tris (catalog #NP0321BOX, Life Technologies, Darmstadt, Germany) or a Tris-Acetate (catalog #EA0375BOX, Life Technologies) Gel according to the manufacturer's instructions. After protein transfer (Nitrocellulose/Filter Paper, catalog #LC2006, Life Technologies) and blocking using 5% skim milk (catalog #70166, Sigma Aldrich) in 0,1% TBS-T buffer, the membranes were incubated with the following antibodies at $4^{\circ}C$ overnight: PDGF-Rα (C-20, Santa Cruz Biotechnology #338), VEGF-A (147, Santa Cruz Biotechnology #507), VEGF-R2 (Abcam, Cambridge, USA #Ab2349), VE-Cadherin (H-72, Santa Cruz Biotechnology #28644), cleaved caspase-3 (Cell Signaling Technology #9661), phospho-ERK (Cell Signaling Technologies #4370), total ERK (Cell Signaling Technologies #4695), RAS (Cell Signaling Technologies #8955), PI3K (Cell Signaling Technologies #13666). After washing the membranes were incubated with secondary antibodies (1:5000 dilution) as follows: for PDGF-Rα, VEGF-A, VE-Cadherin, cleaved caspase-3, phosphor ERK, total ERK, RAS, PI3K: goat anti-rabbit IgG (Santa Cruz Biotechnology #2301) and for VEGF-R2: donkey anti-goat IgG-HRP (Santa Cruz Biotechnology #2020) conjugated to horseradish peroxidase for 1-2 hours at $4^{\circ}C$ followed by 3 washes. As an internal loading control, membranes were stripped

and re-probed with 1:5000 dilution of a mouse polyclonal anti-β-actin antibody (Santa Cruz Biotechnology #sc-81178) followed by 1:5000 dilution of goat anti-mouse IgG-HRP (Santa Cruz Biotechnology #2060). Images were detected by chemiluminescence ECL prime Detection Kit (GE Healthcare, Buckinghamshire, Great Britain #RPN2232) and quantified by densitometry using a Gel Documentation System (Bio Rad, Munich, Germany).

RNA extraction and quantitative real-time PCR

Lungs from 8h studies ($n = 4 - 5$/group) were excised, weighed, snap-frozen in liquid N_2, and stored at $-80°C$ for subsequent two-step mRNA extraction using Roti-Quick-Kit (Carl Roth GmbH #A979.1) and purification with peqlab-Gold Total RNA-Kit (Peqlab, Erlangen, Germany #12-6834- 01). Quantitative real-time PCR was applied to measure lung mRNA expression of PDGF-Rα (forward 5'-TGTGCCGTTTCTCACTTCTCCAG-3', reverse 5'- TACCTTTGTTTCTCACTTCTCCAG-3') using proprietary primer-probes (Eurofins mwg operon, Ebersberg, Germany).

In vitro experiments

Mechanical stretch experiment Human

lung fibroblasts and mouse myofibroblasts were seeded on flexible-bottomed laminin-coated culture plates (Flex Cell International Corporation catalog no.: BF-3001L) to undergo in vitro stretch at 70-80% confluence (cyclic strain by vacuum pressure: shape / sine; elongation min 0%, max 8%; frequency 2Hz; duty cycle 50%; cycles 43216; duration 24h) for 24h. As shown in Supplemental Figure A.13C, one set of myofibroblasts was kept as un-stretched untreated control (C). Myofibroblasts undergoing stretch for 24h were termed as S and those undergoing stretch with parallel application of 5ng/ml TGF-β for 24h were termed as S+Th1. A set of myofibroblasts was also subjected to 5ng/ml TGF-β alone i.e. without any additional application of stretch and was termed as Th1. This step was considered as first hit on the myofibroblasts. A part of pre-stretched myofibroblasts (S+Th1) was separated from group and re-incubated (second hit) with 5ng/ml TGF-β (S+Th1+Th2). The dose of TGF-β and stretching parameters caused the injury without inducing apoptosis in myofibroblasts (Supplemental Figure A.14A-B). Apoptosis was detected using Annexin V FITC stain (BD Pharmingen #51-65874X) and Propidium Iodide stain (Sigma Aldrich #P4864) as per manufacturer's instructions and the data was analyzed using fluorescence antibody cell sorting device (FACS LSRII). Viability was determined using luminescence based Cell titer glo assay (Promega GmbH, Germany #G757) as per manufacturer's instructions and reading were taken with Berthold multimode microplate reader LB 941 (Berthold Technologies GmbH, Germany)

Generation of reporter constructs and Luciferase assay

The mouse PDGF-Rα promoter construct spanning from -1074 to +280 from initiation of transcription manufactured by gene synthesis (Life Technologies) was cloned into pGL4.14 (Promega, Madison, WI). Construct sequence was confirmed by sequencing (Supplemental Figure A.15). CCL206 cells were stimulated with TGF-β1 1 ng/ml (Peprotech, Rocky Hill, NJ) followed by transfection (TurboFect, ThermoFisher) with reporter plasmids (1 μg) and PGK Renilla (50 ng, Promega). Luciferase activity was determined using the Dual Luciferase Assay (Promega) the next day and values of Firefly Luciferase were normalized to values of Renilla Luciferase. The baseline reporter activity of unstimulated cells was set to 1.0. α-smooth muscle actin expression was determined as positive control read-out to prove TGF-β1 activity using Western blot analysis 48 hours later.

Proliferation assay

After first hit of stretch with/without TGF-β as shown in supplemental figure A.12, mouse myofibroblasts and human lung fibroblasts were seeded in a 24 well plate (75000 cells) for manual counting or in 96 well plates (5000 cells/well) for luminescence based Cell titer glo assay while performing second hit of TGF-β keeping respective controls. For manual counting myofibroblasts were trypsinized after 48h of incubation with second hit of TGF-β and counted using Neubauer chamber. Cell titer glo assay was performed as per manufacturers instructions after 48h of incubation with second hit of TGF-β (Cell Titer-Glo assay kit; Promega GmbH, Germany, #G7571). Briefly, reagent equivalent to the amount of media in each well was added. Plates were shaken gently and kept at $37^{\circ}C$ for 10 min followed by reading the plate using plate reader (Berthold technologies Tristar LB 941, Bad Wildbad, Germany).

Boyden chamber or transwell migration assay

Cell culture inserts i.e. transwells ($8\mu m$ pore size), were placed in wells of 24 well plates containing media (10% FCS) either with 25ng/ml PDGF-A (control) or 25ng/ml PDGF-A and 5ng/ml TGF-β. PDGF-A acted as chemoattractant for migration of myofibroblasts. After first hit of stretch and/or TGF-β (Supplemental Figure A.13C), myofibroblasts were seeded in the wells as described above followed by incubation for 8h at $37^{\circ}C$. After washing off the media, myofibroblasts on the upper side of the membrane were scratched and removed. Migrated myofibroblasts on the lower side of the membranes were then fixed in Methanol for 20 min at $-20^{\circ}C$ and stained with $0.5\mu g/ml$ DAPI solution (Sigma Aldrich #D8417) for 10 min. After incubation with 4% PFA for 15 min, cut membranes were mounted with Fluorescent mounting media (Dako North America Inc. #S3023). Images were taken with fluorescence microscope and quantified using Imaris 8.1 software.

Scratch migration assay

Human lung fibroblasts were seeded in a 24 well plate and were grown until confluency of 90%. A scratch was prepared in the middle of the well followed by 5ng/ml TGF-β application keeping respective control. Images were taken every 10 min for 48h using a time lapse microscope. Quantitative analysis of velocity and distance accumulated by the cells was performed using ImageJ as well as chemotaxis and migration softwares.

Supplemental figures and tables

Table A.1: Genetic association results of PDGF-R related SNPs with BPD. Position information is referring to genome build hg18.
*$p \leq 0.05$, **$p \leq 0.001$

rs-number	Chr	Position	Allele A	Allele B	N homo minor	N hetero	N homo major	N missing	beta	SE	p-value
rs10010509	4	54851963	T	G	18	245	795	3	0.1034	0.1251	0.4089
rs10022540	4	54739808	A	G	174	518	369	0	-0.3038	0.0899	0.0008**
NA	4	54739883	A	G	266	509	275	11	-0.2333	0.0839	0.0055*
rs1004564	4	54937382	A	C	322	522	217	0	0.1206	0.0885	0.1734
rs11728027	4	54896943	A	G	144	489	425	3	0.0429	0.0902	0.6348
rs11735716	4	54896828	T	C	43	379	634	5	-0.1443	0.1045	0.1679
rs11737133	4	54717553	T	C	152	475	433	1	0.2192	0.0894	0.0144*
rs12233727	4	54768027	T	C	248	554	258	1	-0.2826	0.0898	0.0017*
rs12500279	4	54775074	T	C	94	444	523	0	0.256	0.0964	0.008*
rs12511976	4	54857028	T	C	893	160	7	1	-0.1854	0.1605	0.2484
rs13118725	4	54690466	T	C	630	364	67	0	-0.2356	0.1018	0.0208*
rs1492769	4	54952368	A	C	747	285	29	0	-0.1425	0.1195	0.2333

rs17084051	4	54782338	A	C	36	329	696	0	0.123	0.1135	0.2789
rs17084241	4	54946036	A	G	9	146	905	1	0.1937	0.1586	0.2222
rs17690091	4	54924101	T	C	48	380	632	1	0.1779	0.1065	0.095
rs17690232	4	54929582	C	G	697	324	40	0	-0.189	0.1119	0.0917
rs17739921	4	54859623	A	C	329	526	202	4	-0.1739	0.0883	0.0492*
rs17746992	4	54932752	C	G	40	325	696	0	0.1951	0.1119	0.0815
rs1907814	4	54940014	A	G	78	461	521	1	-0.0493	0.0994	0.6202
rs1994810	4	54924241	A	G	67	435	559	0	-0.095	0.1021	0.3523
rs2412564	4	54934704	A	G	248	527	286	0	0.1359	0.0881	0.1236
rs35597368	4	54834528	T	C	858	191	12	0	-0.0213	0.1457	0.8839
rs4572929	4	54940498	A	G	68	418	573	2	0.2292	0.1	0.0222*
rs4864510	4	54883219	T	C	370	501	188	2	-0.0968	0.0881	0.2725
rs6811920	4	54945988	C	G	168	505	386	2	-0.0349	0.0894	0.6964
rs6832891	4	54751401	T	C	587	412	62	0	-0.1216	0.1032	0.2386
rs6840522	4	54725132	A	G	795	247	19	0	-0.021	0.1297	0.8717
rs7656613	4	54836600	T	C	564	423	74	0	0.2	0.1002	0.0461*
rs7659654	4	54731166	T	C	536	429	95	1	-0.2163	0.0958	0.0241*
rs7660560	4	54829151	A	G	17	209	833	2	0.1542	0.1323	0.2442
rs7684220	4	54893055	T	C	351	517	186	7	-0.0898	0.088	0.308
rs894905	4	54916706	T	C	251	539	270	1	0.0684	0.0889	0.4419
rs9991165	4	54819348	A	G	791	247	23	0	-0.1153	0.1267	0.3629
rs2228230	4	54846797	T	C	19	250	792	0	0.0673	0.1294	0.6032
rs3690	4	54856570	A	C	798	244	19	0	-0.0888	0.1301	0.4951
rs56404781	4	54698999	T	G	793	251	17	0	0.0151	0.1308	0.9081
rs7378056	4	54739260	A	G	63	413	584	1	0.1423	0.1021	0.1638
rs34148754	4	54751806	A	G	52	415	591	3	0.1304	0.1034	0.2075
rs12506783	4	54781154	T	C	244	541	275	1	0.3076	0.0886	0.0005**
rs61320297	4	54782932	A	G	37	328	695	1	0.1306	0.112	0.2438
rs7673984	4	54783518	T	C	36	327	697	1	0.1073	0.1125	0.3404
NA	4	54784627	A	C	871	181	9	0	0.0443	0.1519	0.7708
rs2114039	4	54787383	T	C	583	403	74	1	-0.0667	0.1	0.5049
rs7678144	4	54797182	T	C	696	328	37	0	-0.0953	0.1132	0.3999
NA	4	54810805	C	G	0	139	915	7	-0.0824	0.1527	0.5896
rs7677751	4	54819217	T	C	17	219	824	1	0.0353	0.1331	0.791
rs73252946	4	54820749	A	G	22	243	796	0	0.117	0.1279	0.3605
rs58435984	4	54822747	T	C	834	209	17	1	-0.113	0.1364	0.4078
rs55947416	4	54824588	T	C	5	152	903	1	0.2635	0.1632	0.1067
rs67279506	4	54825439	A	G	835	209	16	1	-0.0655	0.1374	0.6337
rs58727676	4	54825551	T	G	837	207	17	0	-0.088	0.1372	0.5212
rs7688997	4	54826207	A	C	17	209	834	1	0.1276	0.1345	0.3431
rs56145315	4	54826446	T	C	17	209	835	0	0.1039	0.1369	0.4481
rs28600756	4	54826489	A	C	21	205	833	2	0.0951	0.1296	0.4635
rs67600360	4	54826919	A	G	834	209	17	1	-0.1168	0.1364	0.3921
rs28650939	4	54828716	T	C	17	207	837	0	0.1054	0.1372	0.4424
rs28528897	4	54829096	C	G	834	209	17	1	-0.0956	0.1364	0.4834
rs7691129	4	54829223	T	C	835	209	17	0	-0.1039	0.1369	0.4481
rs12641563	4	54830204	C	G	834	209	17	1	-0.0967	0.1364	0.4787
rs12506290	4	54830889	A	T	17	210	828	6	0.0818	0.1245	0.5112
rs10028020	4	54838334	A	G	11	186	862	2	0.0095	0.1423	0.947
rs4289498	4	54840189	A	G	775	256	22	8	-0.1087	0.1235	0.379
rs1547905	4	54841511	A	C	20	246	794	1	0.0349	0.1272	0.7838
rs2291591	4	54842526	T	C	7	158	894	2	-0.0988	0.1543	0.5219
rs7677708	4	54844015	A	G	784	254	22	1	-0.1039	0.1263	0.4108
rs55732997	4	54849648	T	C	792	249	20	0	-0.0755	0.1287	0.5578
rs10004857	4	54850737	A	G	18	244	796	3	0.0354	0.1253	0.7773
rs11133317	4	54850848	T	G	20	249	792	0	0.1086	0.1287	0.3989
rs2276948	4	54851157	A	G	19	245	792	5	0.1033	0.1212	0.394
rs13147194	4	54851891	T	G	792	248	21	0	-0.1163	0.1281	0.3639
rs55784333	4	54854148	C	G	798	245	18	0	-0.0805	0.1307	0.538
rs3733540	4	54856011	T	C	792	248	21	0	-0.1163	0.1281	0.3639
rs4864878	4	54868472	T	C	149	488	424	0	0.0743	0.0909	0.4138
rs6858442	4	54868690	A	G	192	497	370	2	0.0849	0.0875	0.3323
rs28889275	4	54870830	A	G	149	488	422	2	0.0661	0.0901	0.463
rs17084148	4	54891377	T	C	146	487	427	1	0.0782	0.0907	0.3886
rs73252935	4	54710879	T	C	874	180	7	0	0.004	0.155	0.9792
rs62297645	4	54732370	A	G	844	190	18	9	0.0601	0.1353	0.6571
rs6852007	4	54739176	A	G	11	193	856	1	0.0853	0.1436	0.5524
rs13135841	4	54740496	T	C	174	515	371	1	-0.281	0.0895	0.0017*
rs13145280	4	54751622	T	C	75	382	602	2	0.1935	0.0984	0.0494*
rs11133311	4	54762121	T	C	158	527	373	3	-0.3007	0.0904	0.0009**
rs28622224	4	54782850	T	C	74	404	582	1	0.1039	0.0995	0.2966
rs4864857	4	54784571	T	C	680	326	36	19	-0.0596	0.1083	0.5819
rs7698425	4	54785413	T	C	37	328	694	2	0.0793	0.1109	0.4749
rs1800810	4	54788788	C	G	692	327	37	5	-0.1224	0.1117	0.2733
rs1800813	4	54789224	A	G	34	330	696	1	0.0604	0.1132	0.594

rs7689569	4	54791155	A	G	35	326	698	2	0.0777	0.1118	0.4871
rs7679903	4	54792130	T	C	696	328	37	0	-0.0953	0.1132	0.3999
rs6554163	4	54797316	A	T	36	325	696	4	0.0678	0.1093	0.5347
rs67432867	4	54799211	A	T	694	329	37	1	-0.096	0.1128	0.3947
rs73252942	4	54799361	T	C	692	331	35	3	-0.0732	0.113	0.5172
rs4864864	4	54827082	T	C	17	209	834	1	0.0719	0.1346	0.5931
rs41279519	4	54828988	C	G	5	154	899	3	0.2559	0.1547	0.0985
rs869978	4	54834773	T	C	39	316	706	0	-0.0365	0.1128	0.7466
rs73252950	4	54836257	T	C	9	181	843	28	-0.0803	0.1026	0.4343
rs67388297	4	54837448	C	G	859	190	12	0	-0.0103	0.1459	0.9436
rs28698464	4	54837867	A	G	842	207	12	0	-0.1139	0.1423	0.4237
rs1316926	4	54838043	A	G	257	516	242	46	0.1026	0.0785	0.1915
rs28374326	4	54838078	T	C	5	192	859	5	-0.046	0.1397	0.7417
rs2412556	4	54840015	A	G	784	253	21	3	-0.1256	0.1263	0.3203
rs2162136	4	54756155	T	G	43	355	662	1	0.097	0.1088	0.3729
rs6832597	4	54770994	A	C	41	351	668	1	0.0933	0.1096	0.395
rs7681399	4	54785643	T	G	695	328	38	0	-0.1071	0.1127	0.3422
rs1800812	4	54789386	T	G	37	328	696	0	0.0953	0.1132	0.3999
rs4864862	4	54795246	A	G	37	328	696	0	0.0953	0.1132	0.3999
rs4864863	4	54795588	A	G	696	328	37	0	-0.0953	0.1132	0.3999
rs2229307	4	54824835	T	C	834	210	17	0	-0.1102	0.1367	0.4203
rs2307049	4	54824911	A	G	18	209	834	0	0.1195	0.1359	0.3796
rs7686588	4	54829385	A	G	832	210	18	1	-0.1202	0.1353	0.3746
rs12644709	4	54830337	A	G	834	208	17	2	-0.0955	0.1361	0.4832
rs1547904	4	54841146	T	C	20	249	792	0	0.0755	0.1287	0.5578
rs2412557	4	54844214	A	C	785	254	22	0	-0.0957	0.1267	0.45
rs4864872	4	54847041	T	G	20	256	782	3	0.1116	0.1227	0.3633
rs10020847	4	54847891	T	C	19	250	789	3	0.0256	0.124	0.8362
rs10021728	4	54848866	T	C	19	250	792	0	0.0673	0.1294	0.6032
rs11733839	4	54849284	C	G	22	253	786	0	0.1029	0.1268	0.4173

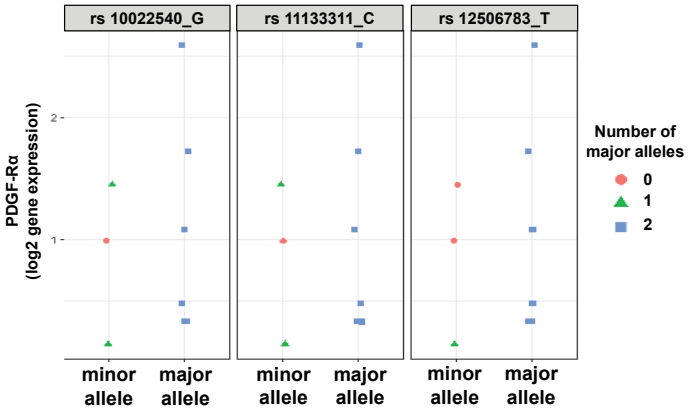

Figure A.11: Gene expression data based on SNP analysis in nCLD patients. PDGF-Rα gene expression in patients ($n = 8$) that carry at least one SNP (minor allele) compared to patients with no SNPs (homozygote major allele). Major alleles are given in the figure labels. Minor alleles of rs10022540 is A, in rs11133311 is T, and in rs12506783 is C. 0 represents homozygote minor allele, 1 represents heterozygote minor allele and 2 is homozygote major allele.

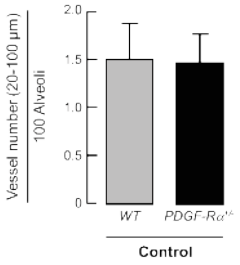

Figure A.12: Vessel count in wildtype and PDGF-R$\alpha^{+/-}$ mice. Histological analysis showed similar small-vessel number ($20 - 100\mu m$ diameter) normalized to 100 alveoli in both unventilated wildtype and PDGF-R$\alpha^{+/-}$ mice. ($n = 10 - 11$ mice/group).

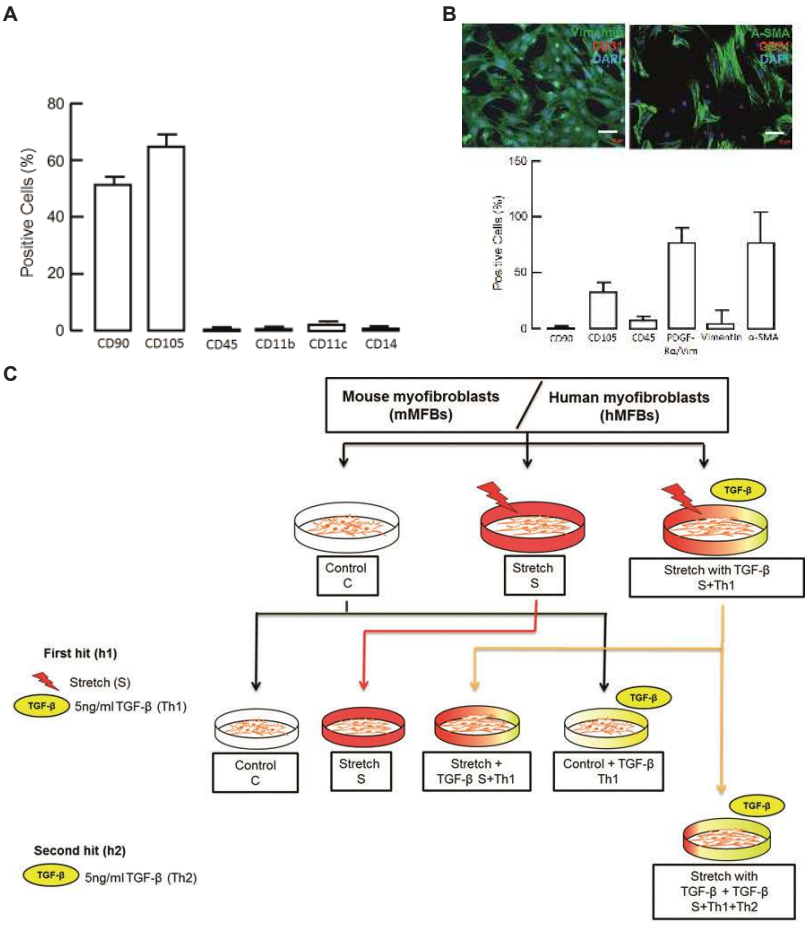

Figure A.13: Characterization of human lung fibroblasts and mouse myofibroblasts and experimental design for in vitro studies. (**A**-**B**) Quantitative analysis of characterization of (A) human lung fibroblasts and (B) mouse myofibroblasts performed using fluorescence antibody cell sorting (FACS) analysis indicated abundance of myofibroblast markers (CD90, CD105, PDGF-Rα, α-SMA and Vimentin). Data is displayed as percentage positive cells. For mouse myofibroblasts $n = 6$ mice/group and for human lung fibroblasts. ($n = 5$ samples/group). (**B**) Immunofluorescence images (200X) of mouse myofibroblasts co-stained for Vimentin or α-SMA (green), CD31 (red) and nucleus stained with DAPI (blue) are shown in figure. (**C**) Schematic representation of experimental strategy used for primary pulmonary mouse myofibroblasts and human lung fibroblasts. Briefly myofibroblasts underwent in vitro stretch with or without additional 5ng/ml TGF-β incubation for 24h (S+Th1 and S respectively). A set with only TGF-β application (Th1) and an un-stretched untreated control (C) was performed. This was considered to be the first hit model. A part from S+Th1 Myofibroblasts was re-incubated with 5ng/ml TGF-β for 24h (S+Th1+Th2). This was considered to be second hit model. In (A-B) the data is presented as mean $\pm$ SD. Statistical test is Two-tailed unpaired Student's t test or Mann Whitney test.

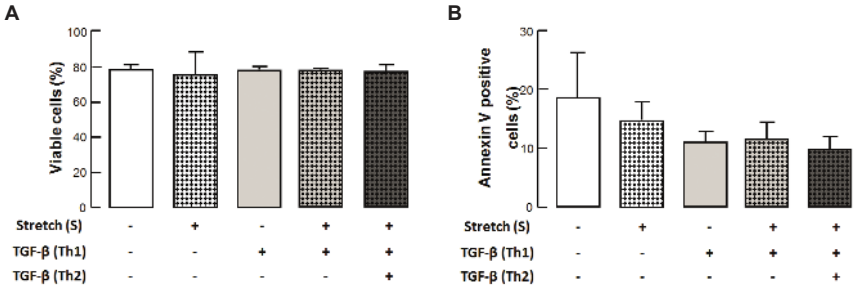

Figure A.14: Viability of mouse myofibroblasts upon application of stretch and TGF-β. Mouse myofibroblasts subjected to mechanical stretch with or without additional application of TGF-β as shown in supplemental Figure A.13. (**A**) For viability analysis Cell titer Glo assay was performed as per manufacturer's instructions. Luminometric readings displayed approximately 80% viable cells after all the applications for 24h-48h ($n = 3$ mice/group). (**B**) Annexin V FITC and propidium iodide staining of mouse myofibroblasts subjected to mechanical stretch with or without additional application of TGf-β as shown in Supplemental figure A.13, for analysis of apoptosis. FACS analysis revealed 10-15% apoptosis upon application of stretch with/without TGF-β application as first as well as second hit ($n = 3$ mice/group). In (A-B) the data is presented as Mean $\pm$ SD.

CATTCAAAAATAGAGCGCAAGTCGAAGGCCCTCCCTTCCCCCACCCGCTCCGGGAAGTCCCGCTTCGCCCAGGTT
TGGTTCCTGGAGTGTCAGCGCCCCCTTTCCCTCGCCAGCAGGATCGCCGTGTCCCAACTGTCTCTCGCTGGGTGT
CTTGGGTTCCCTGGTTTGTGGCTCAAACGTCCTGAAAGCTTTCCTAGGGTACGTCGCGTGCGACCCACTCGGAAG
GGTGGAATTTAGGAGGATAAAAATCCTTCTGCCATCAAGATGCAGAGGGCAGGCATTTGGTAGTCACGCCTAGCC
TGAGCGTTTTCATATGAAGATAGAAGAAGCGAGGACCAGATAACCCCCGAAAACAAAGGCAGGACCAGATAAGTG
GCTCCGAAGGGATAAAGGTCGTTCTTTCCTTCTTCCGGAGAACATCCCAAAGGTACGCCGAGCAACCGTTATTTG
CACACCGCCTCACAATCCAGCCTTTCAAAAACCCATCATCTTCCTATTAGACTCCACAGTTTCCTAATCCCATTA
AAGGATTAGCAACTACACGGCACTTTCCCTTAAGACCCCCAGTTCAAAACGACGCAGCCGCGTTAGAATTTCTCC
CCAGGGCCATATTTCTAGCGAGGCCCAGACTGTCTATAGAAAGGATAATTTGAATTCTAGATTTATATTCGTTTT
AGAAATGAGCAGCAATTTTACGTGTATTTTCTTTTCGAAGAGAATACAAAACAATAGCACCCCCACCCCCAAATT
GGGAAGTCAACTCATTTTGGAAATGATGGCTGTTTGTAGTTTCCTGAAACCTCTTTCCCGGCAGAACGTCAACAC
CTCCCCCTTCGGCCCCCCACCCCACCCCATCTGGTTTGCTCCCCCCTCCTCGTTGTTGTTGAAGTCTGGGGGTTG
GGACTGGCCCCCCTGATTGCATAAGAGCAAAAAGCAAAGAAGAGGTCTTGAGCCTGAGAGAGTCAGAGAGCAAGG
AGTCCTAGGGAAACTTTTATTTTGAAGAGACCAAGGGGGGGGGGGACTTCATTTCCTGACAGCTATTTACTTTAA
GCAAATGATTAGTTTTTGGAGGACGGACTATAACATTGAATCAATTACAAAATGCGGGTTTTGAGCCCATTACTG
TTGGAGCTTGAGGGAGAGAAACAAACGGAGGAGCTGCGGGGAAGGACTGGAAGCTTGGGGCTTACTTTTCACTCC
GGGTATCGGATTTTCTTTGCAAATTGACATAGAAGGAGAAGGTAAGGGAGAGGAAAAAGTGACTTTTGTTTCTCA
AGAAGGTCCCTGATCATAACTTGGGGCTGCAAGAAGCTAAGTAACTTCAAATTTTGGGCAACGAGGAAAACAAAA
ACAA

Figure A.15: SNPs in preterm infants with and without BPD

Table A.2: Analysis of SNPs in PDGF-related pathways PDGF-related pathways with overrepresentation of nominally BPD-associated cis-eQTL SNPs

Pathway	Nominally associated genes / all pathway genes	Nominally associated genes	Best p-values of nominally associated genes	Reference eQTL database
JAK / STAT Cascade	6 / 10	EPS8, GRB2, NUP62, PPP2CA, STAT1, STAT3	0.0013 - 0.044	dixon, fehrmann, kirsten_2014, seeQTL, zeller
MAPKKK Cascade	7 / 14	DUSP1, DUSP6, EGF, MAP2K1, MAPK9, PPP2CA, PRKCA	0.00015 - 0.044	dixon, fehrmann, kirsten_2014, seeQTL, zeller
Apoptosis	8 / 22	AKT1, LTA, NFKB1, NUP62, PPP2CA, PRKCA, RASA1, STAT1	0.00015 - 0.044	dixon, fehrmann, kirsten_2014, seeQTL, zeller
Cell Cycle	5 / 19	DUSP1, DUSP6, PPP2CA, PRKCA, STAT1	0.00015 - 0.044	dixon, fehrmann, kirsten_2014, seeQTL, zeller
DNA Metabolism	5 / 9	ATF2, CREB1, EGF, NUP62, PPP2CA	0.0013 - 0.044	dixon, kirsten_2014
Lipid Metabolism	3 / 9	PIK3R1, PPP2CA, PRKCA	0.00015 - 0.044	dixon, kirsten_2014, seeQTL, zeller
Protein Metabolism	14 / 39	ACTR2, AKT1, ATF2, CREB1, DUSP1, DUSP6, GSK3B, IKBKB, MAP2K1, MAP3K2, MAPK9, PPP2CA, PRKCA, RPS6KA5	0.00015 - 0.044	ding, dixon, fehrmann, kirsten_2014, seeQTL, zeller
Actin and Calcium Ion Homeostasis	6 / 15	ACTR2, EGF, PRKCA, RASA1, STAT1, STAT3	0.00015 - 0.042	ding, dixon, kirsten_2014, seeQTL, zeller

Table A.3: Characteristics of patients from which the samples for (A) protein data corresponding to SNP analysis and (B) gene expression data corresponding to SNP analysis were derived and those which were used for (C) isolation of fibroblasts and (D) immunostaining.

	A	B	C	D
Patients	$n = 9$	$n = 13$	$n = 6$	$n = 8$
BPD grades	0 ($n = 1$)	0/1 ($n = 9$)	0/1 ($n = 2$)	0 ($n = 1$)
	1/2/3 ($n = 7$)	2/3 ($n = 4$)	2/3 ($n = 4$)	1/2/3 ($n = 7$)
Gestational age (weeks)	26.5 ± 2.4	26.2 ± 1	25 ± 1	27.3 ± 2
Birth weight (grams)	858.9 ± 234	774.6 ± 136	563 ± 98	
Mechanical ventilation (days)		56.3 ± 14	74 ± 23	
Age of death (days)				37.75
Died of respository failure				$n = 6$
Males/females	$n = 6/n = 3$	$n = 5/n = 8$	$n = 4/n = 2$	$n = 5/n = 3$
Early onset infection		$n = 6$		
Days of culture			$3 - 14$	
Congenital infection			$n = 2$	

References

[1] Hargitai B, Szabo V, et al. Apoptosis in various organs of preterm infants: histopathologic study of lung, kidney, liver, and brain of ventilated infants. Pediatr Res. 2001;50(1):110–4.

[2] Jobe AH. The new bronchopulmonary dysplasia [Journal Article]. Curr Opin Pediatr. 2011;23(2):167–72.

[3] Konig K, Guy KJ. Bronchopulmonary dysplasia in preterm infants managed with non-invasive ventilation or surfactant and a brief period of mechanical ventilation: a 6-year cohort study [Journal Article]. J Matern Fetal Neonatal Med. 2014;27(6):608–11.

[4] Merritt TA, Deming DD, et al. The 'new' bronchopulmonary dysplasia: challenges and commentary [Journal Article]. Semin Fetal Neonatal Med. 2009;14(6):345–57.

[5] Doyle LW, Anderson PJ. Long-term outcomes of bronchopulmonary dysplasia [Journal Article]. Semin Fetal Neonatal Med. 2009;14(6):391–5.

[6] Ehrenkranz RA, Walsh MC, et al. Validation of the National Institutes of Health consensus definition of bronchopulmonary dysplasia [Journal Article]. Pediatrics. 2005;116(6):1353–60.

[7] Bland RD, Ertsey R, et al. Mechanical ventilation uncouples synthesis and assembly of elastin and increases apoptosis in lungs of newborn mice. Prelude to defective alveolar septation during lung development? [Journal Article]. Am J Physiol Lung Cell Mol Physiol. 2008;294(1):L3–14.

[8] Hamilton TG, Klinghoffer RA, et al. Evolutionary divergence of platelet-derived growth factor alpha receptor signaling mechanisms [Journal Article]. Mol Cell Biol. 2003;23(11):4013–25.

[9] Hilgendorff A. Increased risk for lung injury in PDGF-R deficient newborn mice [Journal Article]. European Respiratory Journal. 2011;42 (suppl 57).

[10] Scherle W. A simple method for volumetry of organs in quantitative stereology [Journal Article]. Mikroskopie. 1970;26(1):57–60.

[11] Bostrom H, Willetts K, et al. PDGF-A signaling is a critical event in lung alveolar myofibroblast development and alveogenesis [Journal Article]. Cell. 1996;85(6):863–73.

[12] Lindahl P, Karlsson L, et al. Alveogenesis failure in PDGF-A-deficient mice is coupled to lack of distal spreading of alveolar smooth muscle cell progenitors during lung development [Journal Article]. Development. 1997;124(20):3943–53.

[13] Bostrom H, Gritli-Linde A, et al. PDGF-A/PDGF alpha-receptor signaling is required for lung growth and the formation of alveoli but not for early lung branching morphogenesis [Journal Article]. Dev Dyn. 2002;223(1):155–62.

[14] Sun T, Jayatilake D, et al. A human YAC transgene rescues craniofacial and neural tube development in PDGFRalpha knockout mice and uncovers a role for PDGFRalpha in prenatal lung growth [Journal Article]. Development. 2000;127(21):4519–29.

[15] Bland RD, Albertine KH, et al. Impaired alveolar development and abnormal lung elastin in preterm lambs with chronic lung injury: potential benefits of retinol treatment [Journal Article]. Biol Neonate. 2003;84(1):101–2.

[16] Bland RD, Mokres LM, et al. Mechanical ventilation with 40of genes that regulate lung development and impairs alveolar septation in newborn mice [Journal Article]. Am J Physiol Lung Cell Mol Physiol. 2007;293(5):L1099–110.

[17] Powell PP, Wang CC, et al. Differential regulation of the genes encoding platelet-derived growth factor receptor and its ligand in rat lung during microvascular and alveolar wall remodeling in hyperoxia [Journal Article]. Am J Respir Cell Mol Biol. 1992;7(3):278–85.

[18] Popova AP, Bentley JK, et al. Reduced platelet-derived growth factor receptor expression is a primary feature of human bronchopulmonary dysplasia [Journal Article]. Am J Physiol Lung Cell Mol Physiol. 2014;307(3):L231–9.

[19] Jobe AH, Bancalari E. Bronchopulmonary dysplasia. Am J Respir Crit Care Med. 2001;163(7):1723–9.

[20] Emery JL, Mithal A. The number of alveoli in the terminal respiratory unit of man during late intrauterine life and childhood [Journal Article]. Arch Dis Child. 1960;35:544–7.

[21] Compernolle V, Brusselmans K, et al. Loss of HIF-2alpha and inhibition of VEGF impair fetal lung maturation, whereas treatment with VEGF prevents fatal respiratory distress in premature mice. Nat Med. 2002;8(7):702–10.

[22] Ding J, Gudjonsson JE, et al. Gene expression in skin and lymphoblastoid cells: Refined statistical method reveals extensive overlap in cis-eQTL signals [Journal Article]. Am J Hum Genet. 2010;87(6):779–89.

[23] Kamio K, Sato T, et al. Prostacyclin analogs stimulate VEGF production from human lung fibroblasts in culture [Journal Article]. Am J Physiol Lung Cell Mol Physiol. 2008;294(6):L1226–32.

[24] Nauck M, Roth M, et al. Induction of vascular endothelial growth factor by platelet-activating factor and platelet-derived growth factor is downregulated by corticosteroids [Journal Article]. Am J Respir Cell Mol Biol. 1997;16(4):398–406.

[25] Prochilo T, Savelli G, et al. Targeting VEGF-VEGFR Pathway by Sunitinib in Peripheral Primitive Neuroectodermal Tumor, Paraganglioma and Epithelioid Hemangioendothelioma: Three Case Reports [Journal Article]. Case Rep Oncol. 2013;6(1):90–7.

[26] Heldin CH. Targeting the PDGF signaling pathway in tumor treatment [Journal Article]. Cell Commun Signal. 2013;11:97.

[27] Wang Y, Pennock SD, et al. Platelet-derived growth factor receptor-mediated signal transduction from endosomes [Journal Article]. J Biol Chem. 2004;279(9):8038–46.

[28] Assoian RK, Fleurdelys BE, et al. Expression and secretion of type beta transforming growth factor by activated human macrophages [Journal Article]. Proc Natl Acad Sci U S A. 1987;84(17):6020–4.

[29] Groneck P, Gotze-Speer B, et al. Association of pulmonary inflammation and increased microvascular permeability during the development of bronchopulmonary dysplasia: a sequential analysis of inflammatory mediators in respiratory fluids of high-risk preterm neonates [Journal Article]. Pediatrics. 1994;93(5):712–8.

[30] Xu L, Rabinovitch M, et al. Altered expression of key growth factors (TGFalpha, TGF1, PDGF-A) and flawed formation of alveoli and elastin (Eln) in lungs of preterm (PT) lambs with chronic lung disease (CLD) [Journal Article]. The FASEB Journal. 2006;20 meeting abstract:A1442–A1443.

[31] Schultz C, Tautz J, et al. Prolonged mechanical ventilation induces pulmonary inflammation in preterm infants [Journal Article]. Biol Neonate. 2003;84(1):64–6.

[32] Vozzelli MA, Mason SN, et al. Antimacrophage chemokine treatment prevents neutrophil and macrophage influx in hyperoxia-exposed newborn rat lung [Journal Article]. Am J Physiol Lung Cell Mol Physiol. 2004;286(3):L488–93.

[33] Wu S, Capasso L, et al. High tidal volume ventilation activates Smad2 and upregulates expression of connective tissue growth factor in newborn rat lung [Journal Article]. Pediatr Res. 2008;63(3):245–50.

[34] Yamamoto H, Teramoto H, et al. Cyclic stretch upregulates interleukin-8 and transforming growth factor-beta1 production through a protein kinase C-dependent pathway in alveolar epithelial cells [Journal Article]. Respirology. 2002;7(2):103–9.

[35] Zhao Y, Gilmore BJ, et al. Expression of transforming growth factor-beta receptors during hyperoxia-induced lung injury and repair [Journal Article]. Am J Physiol. 1997;273(2 Pt 1):L355–62.

[36] Fuentes-Calvo I, Crespo P, et al. The small GTPase N-Ras regulates extracellular matrix synthesis, proliferation and migration in fibroblasts [Journal Article]. Biochim Biophys Acta. 2013;1833(12):2734–44.

[37] Liu J, Li M, et al. [Effects of blocking phospholipase C-gamma1 signaling pathway on proliferation and apoptosis of human colorectal cancer cell line LoVo] [Journal Article]. Ai Zheng. 2007;26(9):957–62.

[38] Chen L, Acciani T, et al. Dynamic regulation of platelet-derived growth factor receptor alpha expression in alveolar fibroblasts during realveolarization [Journal Article]. Am J Respir Cell Mol Biol. 2012;47(4):517–27.

[39] Lau M, Masood A, et al. Long-term failure of alveologenesis after an early short-term exposure to a PDGF-receptor antagonist [Journal Article]. Am J Physiol Lung Cell Mol Physiol. 2011;300(4):L534–47.

[40] Zhao L, Wang K, et al. Vascular endothelial growth factor co-ordinates proper development of lung epithelium and vasculature [Journal Article]. Mech Dev. 2005;122(7-8):877–86.

[41] Niu G, Wright KL, et al. Constitutive Stat3 activity up-regulates VEGF expression and tumor angiogenesis [Journal Article]. Oncogene. 2002;21(13):2000–8.

[42] Yu H, Jove R. The STATs of cancer–new molecular targets come of age [Journal Article]. Nat Rev Cancer. 2004;4(2):97–105.

[43] Akeson AL, Cameron JE, et al. Vascular endothelial growth factor-A induces prenatal neovascularization and alters bronchial development in mice [Journal Article]. Pediatr Res. 2005;57(1):82–8.

[44] Dixon AL, Liang L, et al. A genome-wide association study of global gene expression [Journal Article]. Nat Genet. 2007;39(10):1202–7.

[45] Fehrmann RS, Jansen RC, et al. Trans-eQTLs reveal that independent genetic variants associated with a complex phenotype converge on intermediate genes, with a major role for the HLA [Journal Article]. PLoS Genet. 2011;7(8):e1002197.

[46] Xia K, Shabalin AA, et al. seeQTL: a searchable database for human eQTLs [Journal Article]. Bioinformatics. 2012;28(3):451–2.

[47] Zeller T, Wild P, et al. Genetics and beyond–the transcriptome of human monocytes and disease susceptibility [Journal Article]. PLoS One. 2010;5(5):e10693.

[48] Devlin B, Roeder K. Genomic control for association studies [Journal Article]. Biometrics. 1999;55(4):997–1004.

[49] Rohloff JC, Gelinas AD, et al. Nucleic Acid Ligands With Protein-like Side Chains: Modified Aptamers and Their Use as Diagnostic and Therapeutic Agents [Journal Article]. Mol Ther Nucleic Acids. 2014;3:e201.

[50] Ewing B, Hillier L, et al. Base-calling of automated sequencer traces using phred. I. Accuracy assessment [Journal Article]. Genome Res. 1998;8(3):175–85.

[51] Kim KY, Kim BJ, et al. Reuse of imputed data in microarray analysis increases imputation efficiency [Journal Article]. BMC Bioinformatics. 2004;5:160.

[52] Bolstad BM, Irizarry RA, et al. A comparison of normalization methods for high density oligonucleotide array data based on variance and bias [Journal Article]. Bioinformatics. 2003;19(2):185–93.

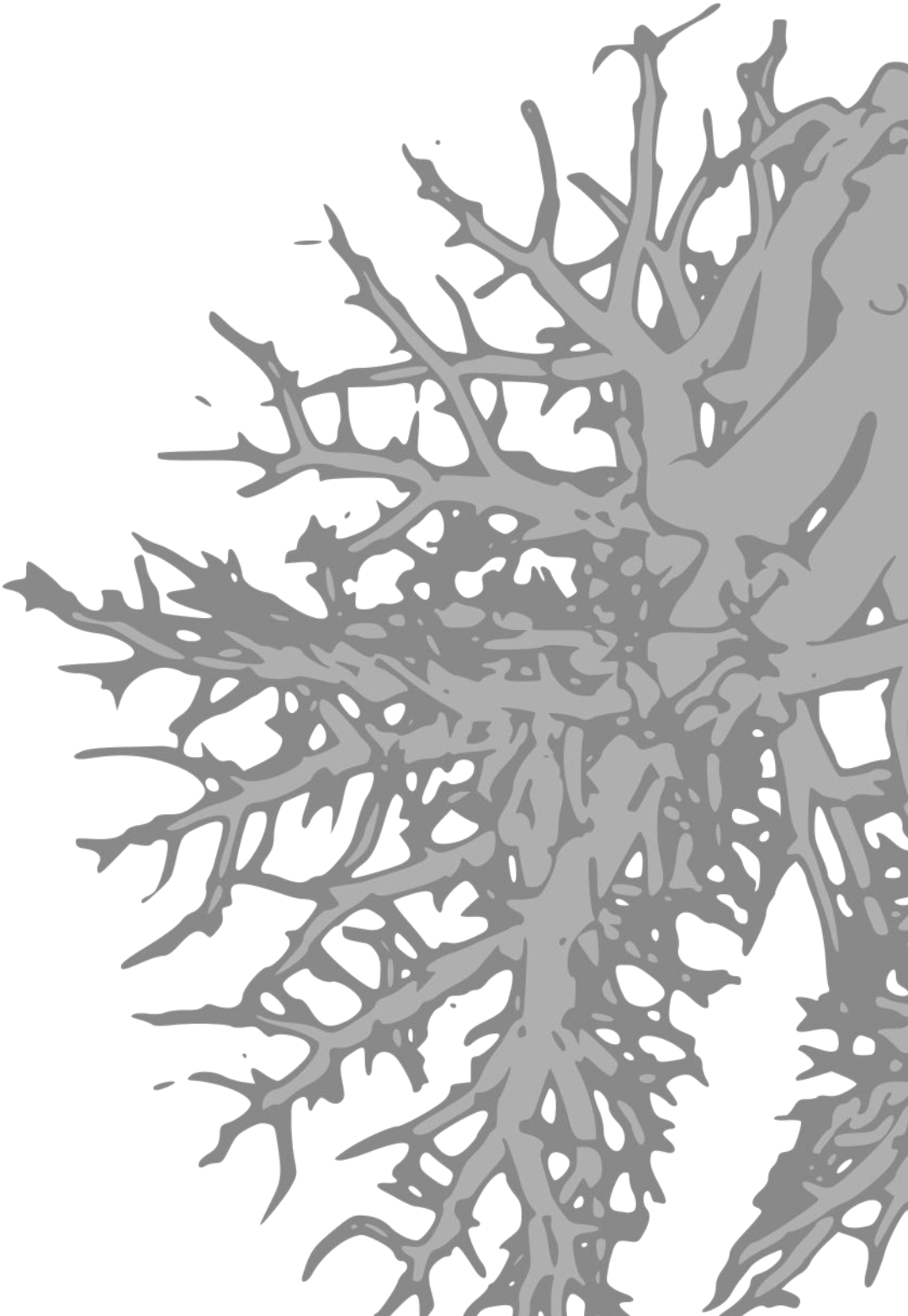

Summary

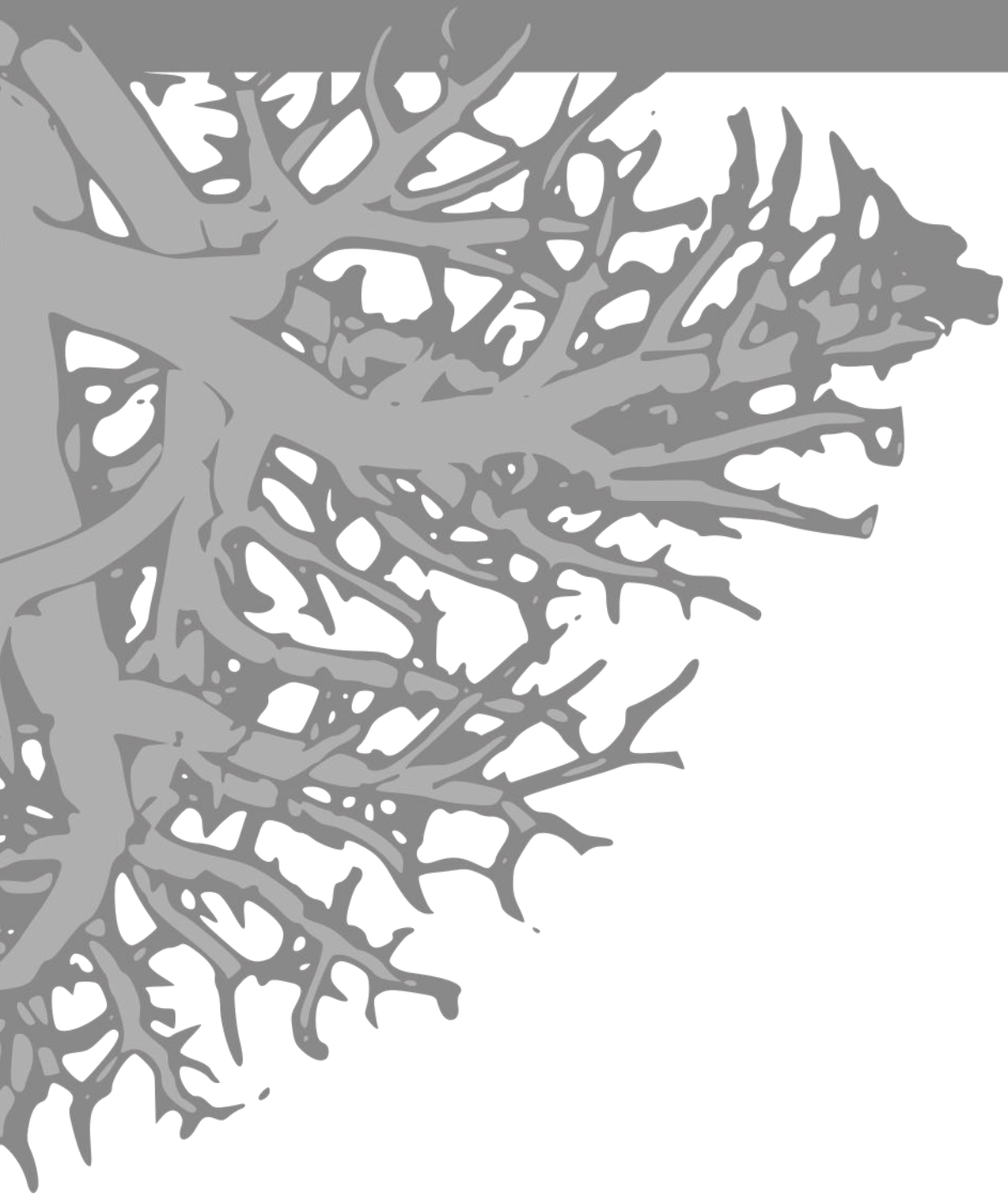

Summary

Congenital diaphragmatic hernia (CDH) is a severe anomaly characterized by a diaphragmatic defect, lung hypoplasia and pulmonary hypertension. Specific genetic abnormalities have been identified in some afflicted children, such as deletions in *FOG2*, *COUP-TFII* and *SOX7*, but in over 80% of cases the cause of CDH remains unknown. The associated pulmonary abnormalities are responsible for the high morbidity and mortality among patients with this disease. Vasodilator therapy often has no effect and little is known about the possibly aberrant expressions of the targeted factors of current drugs.

Chapter 1 describes the therapeutic approaches of CDH-related pulmonary hypertension over the years and the corresponding pathways. Both postnatally and antenatally, these approaches are still a matter of trial and error and have not been studied in randomized controlled trials or comparative effectiveness trials. Previous morphological studies have shown excessive muscularization of the pulmonary arteries and abnormal pulmonary vascular remodeling in patients with CDH, in which several pathways have found to be involved. Furthermore, a variety of chromosomal abnormalities have been reported. **Chapter 2** presents a review of the literature on pulmonary vascular development in health and in different diseases of the newborn associated with pulmonary vascular abnormalities, including CDH. In the study presented in **chapter 3** we focused on one of the pathways involved in CDH, transforming growth factor β (TGFβ). This pathway is regulated by retinoic acid signaling, which has been known to be disrupted in CDH. In the nitrofen rat model we found increased activation of TGFβ and reduced activation of bone morphogenetic protein.

Current treatment of pulmonary hypertension typically consists of targeting receptors and other important factors in the three major vasoactive pathways: the nitric oxide (NO), endothelin (ET) and prostacyclin (PGI_2) pathways. Although inhaled NO (iNO) is the most common used drug in the neonatal setting, studies failed to show consistency of its efficacy in CDH patients. Apart from iNO therapy, the phosphodiesterase-5 inhibitor sildenafil and prostacyclins are sporadically used as rescue therapy, with variable and unpredictable results. In the study presented in **chapter 4** we analyzed the expressions of the drug related factors in all three pathways. In human CDH lungs, we found upregulation of the endothelin A and B receptors and of the endothelin converting enzyme. The latter is a key molecule in the endothelin pathway, by converting endothelin-1 (ET-1) into its active form. Expression of the prostacyclin receptor in human control lungs gradually increased over time, but was decreased in CDH lungs in the fetal, preterm and term phases. The aberrant expressions of the above-mentioned factors could explain why treatment of pulmonary hypertension in patients with CDH fails.

As ultrasound studies at 20 weeks of gestation can already detect CDH, fetal treatment is a potential option. In the study presented in **chapter 5**, rats with nitrofen-induced CDH were antenally given sildenafil. We found that the decreased saccular airspaces had enlarged again, and that the pulmonary vessel wall was less muscularized. We expanded our study by analyzing the effect of antenatal treatment with the novel prostacyclin receptor agonist selexipag (NS-304) alone or in combination with sildenafil, as described in **chapter 6**. Treatment with NS-304 alone was followed by improvement in the aberrant cardiac and pulmonary vascularity. Combination therapy of sildenafil and NS-304 did not have added value to each of these compounds separately, indicating a limited effect of treatment with vasodilatory therapy at this stage of development or a different effect of activation of both pathways.

CDH is often associated with neonatal chronic lung disease (nCLD), as these patients are highly susceptible for oxygen and ventilation damage. The pathophysiology of both diseases seems to overlap. In both, multiple developmental signaling pathways are affected, with TGFβ, for example, as a shared factor. In the **appendix** we describe that in a mouse model of nCLD we found increased activation of TGFβ and reduced expression of platelet derived growth factor receptor α (PDGF-Rα), which corresponds to our findings in the nitrofen-CDH rat model.

The clinical implications of our research are discussed in **chapter 7**, which includes a recommendation to develop a precision medicine approach that might even already be applied antenatally.

Samenvatting

Congenitale hernia diafragmatica (CHD) is een ernstige aangeboren afwijking, met als kenmerken een gat in het middenrif, long hypoplasie en pulmonale hypertensie. Bij sommige patiënten zijn bepaalde genetische afwijkingen aangetoond, zoals deleties in FOG2, COUP-TFII en SOX7, maar in meer dan 80% van de gevallen blijft de oorzaak onbekend. De bijkomende longafwijkingen zijn verantwoordelijk voor de hoge morbiditeit en mortaliteit onder kinderen met CHD. Vaatverwijdende therapie helpt vaak niet en mogelijk vertonen de factoren waarop de huidige medicatie is gericht een afwijkende expressie.

Hoofdstuk 1 geeft een overzicht van de therapeutische aanpak van CHD-gerelateerde pulmonale hypertensie over de jaren en beschrijft de bijbehorende pathways. Zowel voor als na de zwangerschap vormt het vinden van de juiste therapie nog steeds een uitdaging. Dit is nog niet eerder onderzocht in gerandomiseerde gecontroleerde trials of vergelijkende effectiviteitsstudies. Morfologisch onderzoek heeft aangetoond dat bij kinderen met CHD de longvaten extreem verdikt zijn, en bij dit proces zijn verschillende pathways betrokken. **Hoofdstuk 2** geeft een overzicht van de literatuur over de normale ontwikkeling van het pulmonale vaatbed en de ontwikkeling bij verschillende aangeboren afwijkingen waarbij het pulmonale vaatbed abnormaal is, zoals CHD. **Hoofdstuk 3** richt zich op een van deze pathways, transforming growth factor β (TGFβ). Deze wordt gereguleerd door retinoïnezuur, waarvan de expressie verstoord is in CHD. In het nitrofen-CHD rat model vonden we een toegenomen activatie van TGFβ en een afgenomen activatie van bone morphogenetic protein, een andere belangrijke transcriptiefactor in dit pathway.

De huidige behandeling van pulmonale hypertensie is gericht op receptoren en andere belangrijke factoren in de drie belangrijke vasoactieve pathways: stikstofoxide (NO), endotheline en prostacycline. Inhaled NO (iNO) is het meest gebruikte middel onder pasgeborenen, maar het is nog niet duidelijk of het effect heeft bij kinderen met CHD. Naast iNO worden sildenafil en prostacylclines sporadisch gebruikt als een laatste redmiddel. Deze geven echter wisselende en onvoorspelbare resultaten. In **hoofdstuk 4** hebben we de expressie geanalyseerd van de factoren die aan deze middelen zijn gerelateerd; dit is gedaan voor alle drie bovengenoemde pathways. In longen van patiënten met CHD vonden we een toegenomen expressie van de type A en B endothelinereceptoren en het endotheline-converting enzym. Dit enzym is belangrijk omdat het de inactieve vorm van endotheline omzet naar de actieve vorm. De expressie van de prostacyclinereceptor nam toe gedurende de zwangerschap in gezonde longen, maar in CHD-longen was dit lager in alle zwangerschapsfasen. De afwijkende expressie van al deze factoren zou kunnen verklaren waarom de behandeling van pulmonale hypertensie bij kinderen met CHD niet goed aanslaat.

Omdat CHD al bij 20 weken zwangerschap ontdekt kan worden door middel van echografie, is behandeling tijdens de zwangerschap een mogelijke optie. In de studie beschreven in **hoofdstuk 5** hebben we ratten met door nitrofen geïnduceerde CHD tijdens de zwangerschap behandeld met sildenafil. Bij deze ratten waren de longblaasjes van normale grootte en was de vaatwand minder verdikt. In een vervolgstudie hebben we de werking geanalyseerd van een nieuw medicijn, selexipag (NS-304), afzonderlijk en in combinatie met sildenafil, zoals beschreven in **hoofdstuk 6**. Behandeling met alleen NS-304 gaf een verbetering van de afwijkingen in het hart en de longvaten. De combinatie van sildenafil en NS-304 had geen toegevoegde waarde boven elk van de afzonderlijke medicijnen. Het ziet ernaar uit dat vaatverwijdende therapie in deze fase van de ontwikkeling slechts een beperkt effect heeft. Ook kan het zijn dat deze twee medicijnen elk een ander effect hebben.

Patiënten met CHD hebben vaak ook neonatale chronische longziekte (nCLD), omdat zij gevoelig zijn voor schade door zuurstoftoediening en mechanische beademing. De onderliggende mechanismen van beide aandoeningen lijken te overlappen. In beide gevallen tonen meerdere pathways een abnormale ontwikkeling, waarvan TGFβ bijvoorbeeld een gezamenlijke factor is.

In de **appendix** beschrijven we een muismodel van nCLD waarin er een toegenomen activatie van TGFβ was en platelet derived growth factor receptor α (PDGF-Rα) een lagere expressie vertoonde. Dit komt overeen met onze bevindingen in het nitrofen-CHD ratmodel.

De implicaties van ons onderzoek voor de kliniek worden besproken in **hoofdstuk 7**. Dit hoofdstuk bevat tevens een aanbeveling voor een individueel gerichte behandeling die mogelijk al voor de geboorte kan worden toegepast.

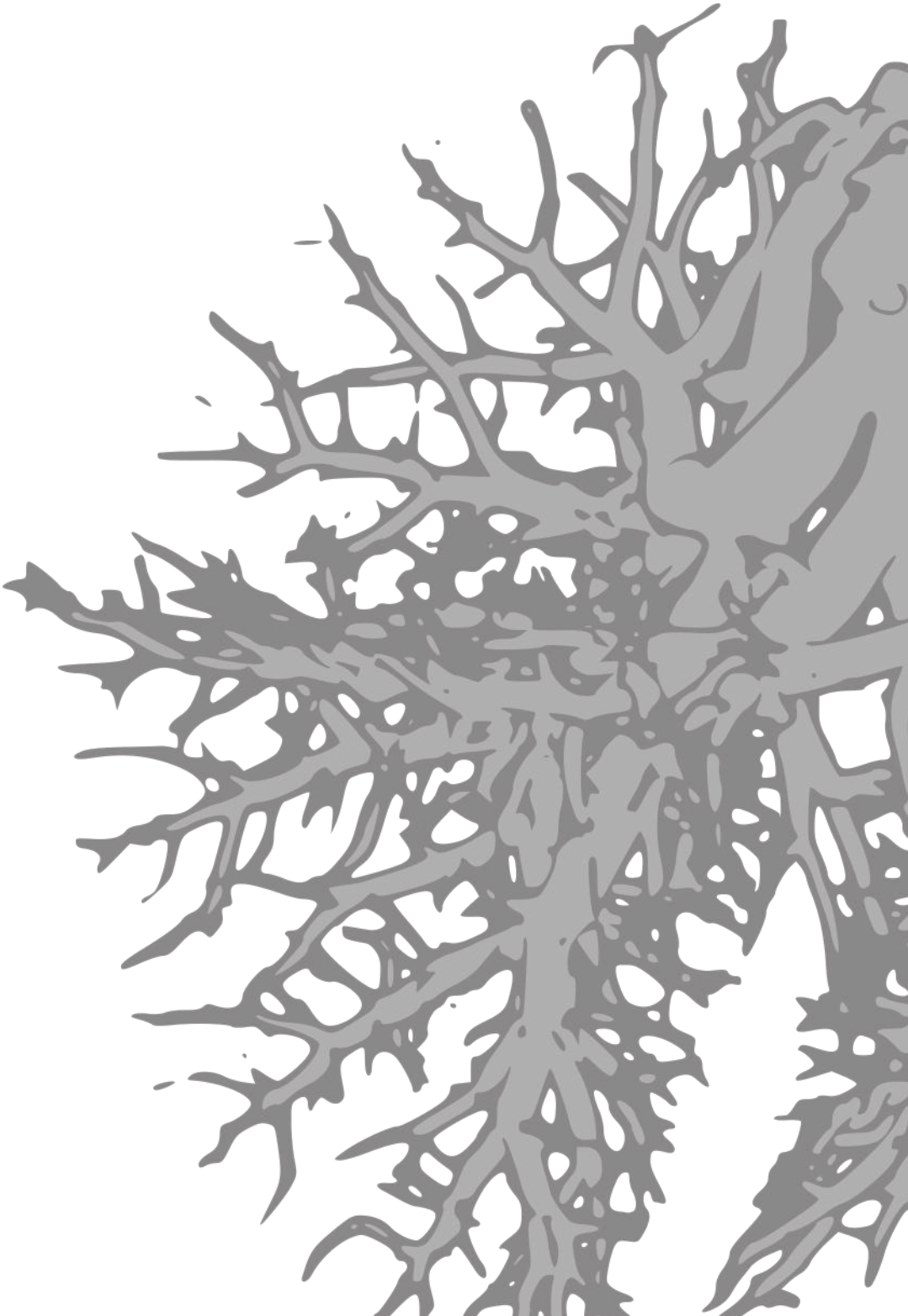

Addendum

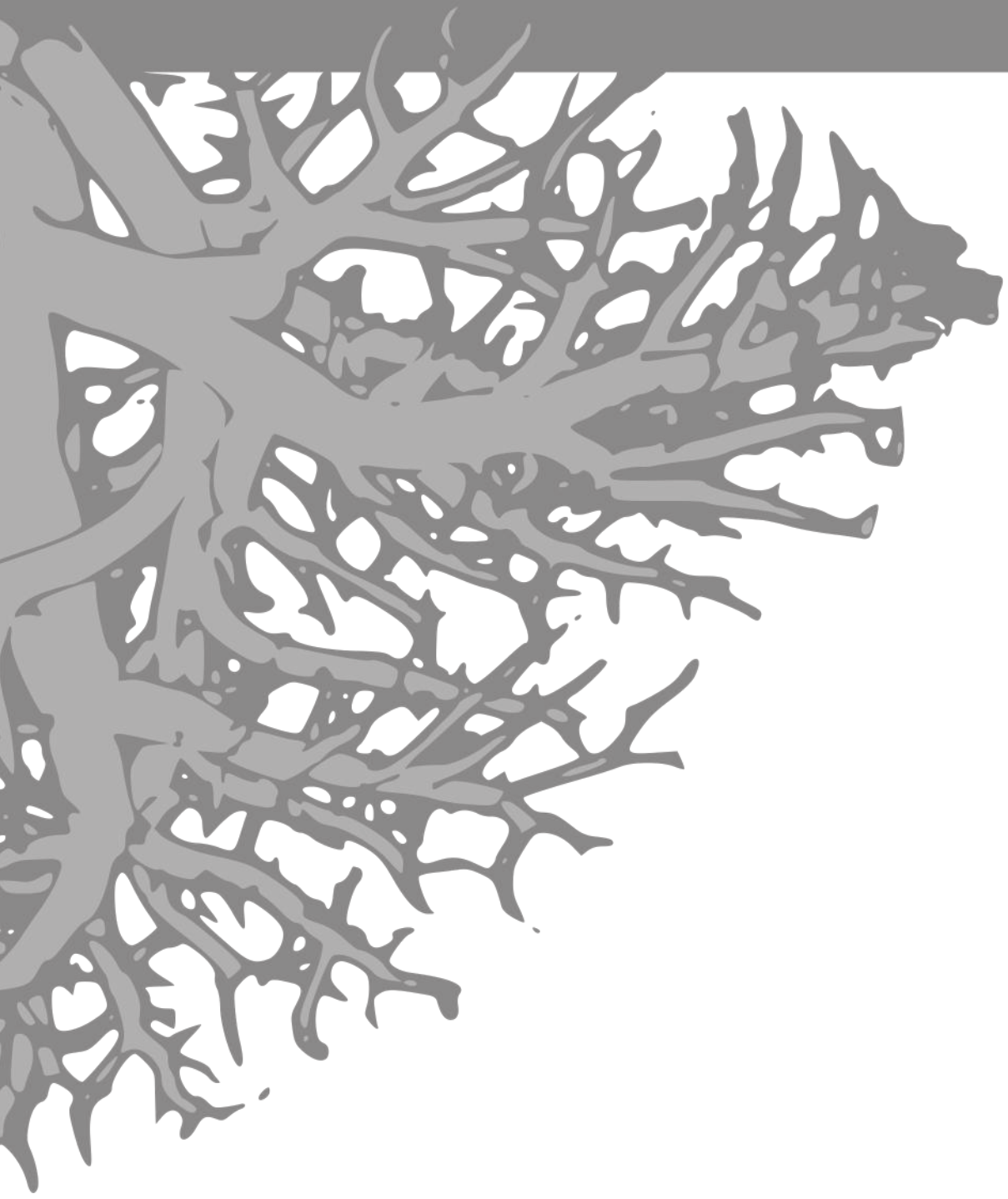

About the author

Daphne Stephanie Mous was born on February 7^{th} 1988 in Schiedam, the Netherlands. After completing Gymnasium at SG Spieringshoek in Schiedam, she started her medical training at the University of Leiden in 2005. During medical school she did her major internship at the department of pediatrics in the Juliana Children's Hospital in The Hague. After her graduation in 2011 she started working as a resident at the pediatric surgery department in the Erasmus Medical Centre – Sophia Children's Hospital in Rotterdam (2011–2017). In 2012 she started her research on the project that is described in this thesis next to her clinical work. As part of a collaboration, she performed some of her research at the Max Planck Institute for Lung and Heart Research in Bad Nauheim, Germany for a period of 5 months (2014–2015). In April 2017 she started working as a resident in Psychiatry at Rivierduinen in Leiden, awaiting a traineeship as a general practitioner, which she started in September 2017 at the Leiden University Medical Center.

Publications and manuscripts

Van Beelen NW, **Mous DS**, Brosens E, de Klein A, van de Ven CP, Vlot J, IJsselstijn H, Wijnen R. Increased incidence of hypertrophic pyloric stenosis in esophageal atresia patients. *Eur J Pediatr Surg.* 2014 Feb; 24(1): 20-4.

Mous DS, Kool H, Tibboel D, de Klein A, Rottier RJ. Pulmonary vascular development goes awry in congenital lung abnormalities. *Birth Defects Res C Embryo Today.* 2014 Dec; 102(4): 343-58.

Mous DS, Kool HM, Buscop-van Kempen MJ, Koning AH, Dzyubachyk O, Wijnen RMH, Tibboel D, Rottier RJ. Clinically relevant timing of antenatal sildenafil treatment reduces pulmonary vascular remodeling in congenital diaphragmatic hernia. *Am J Physiol Lung Cell Mol Physiol.* 2016 Oct 1; 311(4): L734-L742.

Leeuwen L, **Mous DS**, van Rosmalen J, Olieman JF, Andriessen L, Gischler SJ, Joosten KFM, Wijnen RMH, Tibboel D, IJsselstijn H, Spoel M. Congenital Diaphragmatic Hernia and Growth to 12 Years. *Pediatrics.* 2017 Aug; 140(2).

Oak P, Pritzke T, Thiel I, Koschlig M, **Mous DS**, Windhorst A, Jain N, Eickelberg O, Schulze A, Goepel, W, Reicherzer T, Ehrhardt H, Rottier RJ, Ahnert P, Gortner L, Desai TJ, Hilgendorff A. Attenuated PDGF signaling drives the alveolar pathology of neonatal chronic lung disease. *EMBO Mol Med.* 2017; epub ahead of print.

Förster K, Sass S, Dietrich O, Pomschar A, **Mous DS**, Rottier RJ, Nhrlich L, Oak P, Schulze A, Flemmer AW, Ehrhardt H, Hbener C, Eickelberg O, Theis FJ, Ertl-Wagner B, Hilgendorff A. Early identification of Bronchopulmonary Dysplasia using novel biomarkers by proteomic screening. *Accepted for publication – AJRCCM.* 2017, Sep.

Mous DS, Buscop-van Kempen MJ, Wijnen RMH, Tibboel D, Rottier RJ. Changes in vasoactive pathways in congenital diaphragmatic hernia associated pulmonary hypertension explain unresponsiveness to pharmacotherapy. *Provisionally accepted for publication – Respiratory Research.*

Mous DS, Kool HM, Burgisser PE, Buscop-van Kempen MJ, Nagata K, van Rosmalen J, Dzyubachyk O, Wijnen RMH, Tibboel D, Rottier RJ. Prenatal sildenafil and selexipag improve pulmonary vascularity in congenital diaphragmatic hernia. *Provisionally accepted for publication – Am J Physiol Lung Cell Mol Physiol.*

Mous DS, Kool HM, Wijnen RMH, Tibboel D, Rottier RJ. Pulmonary vascular development in congenital diaphragmatic hernia. *Submitted for publication.*

PhD portfolio

Name PhD student: Daphne Mous
Erasmus MC department: Pediatric Surgery, Sophia Children's hospital
PhD period: 2012-2017
Promotors: Prof.Dr. D. Tibboel, Prof.Dr. R.M.H. Wijnen
Supervisor: Dr. R.J. Rottier

	Year	Workload (ECTS)
General courses		
Introductory Course on Statistics and Survival analysis, Molmed, Erasmus MC	2012	0.5
Endnote, Erasmus MC	2012	0.2
Basic introduction course on SPSS, Molmed, Erasmus MC	2013	1.0
CPO mini course (patient orientated research and preparation for subsidy application, CPO, Erasmus MC	2013	0.3
BROK course, Erasmus MC	2013	1.0
Workshop on Photoshop, Illustrator and Indesign CS, Molmed, Erasmus MC	2013	0.3
Biomedical English writing course, Molmed, Erasmus MC	2013	2.0
Wetenschappelijke integriteit, Erasmus MC	2014	2.0
Specific courses		
Safely working in the laboratory, LUMC	2012	0.3
Cell and developmental biology, Cell biology, Erasmus MC	2013	3.0
Genetics course, Cell biology, Erasmus MC	2013	3.0
Symposia and workshops		
Symposium Applied Molecular Imaging, AMIE facility, Erasmus MC	2012	0.2
Advanced Pediatric Life Support, Erasmus MC	2013	0.3
Symposium orgaandonatie/tranplantatie bij kinderen, Groningen	2013	0.3
Symposium on Animal Models in Respiratory Research, NRS, Utrecht	2013/2016	0.6
MGC symposium, Rotterdam	2014	0.2
Longdagen, Utrecht	2015	0.3
Symposium Lung Repair and Regeneration, NRS, Amsterdam	2016	0.3
(Inter)national conferences		
International CDH workshop, Erasmus MC-Sophia Children's Hospital, Rotterdam, Netherlands: oral presentation (2x)	2013	3.0
Jubileumcongres Sophia 150 jaar, De Doelen, Rotterdam, Netherlands	2013	1.0
26th Symposium on International Paediatric Surgical Research, Cape Town, South-Africa: oral presentation	2013	2.0
12th Annual Retreat of the International Graduate Programme Molecular Biology and Medicine of the Lung, Giessen, Germany: oral presentation	2014	2.0
13th Annual Retreat of the International Graduate Programme Molecular Biology and Medicine of the Lung, Giessen, Germany: oral presentation	2015	2.0
International CDH workshop, Toronto, Canada: oral presentation	2015	2.0
Annual Meeting of the Canadian Association of Paediatric Surgeons, Niagara Falls, Ontario, Canada	2015	1.0
European Pediatric Surgery Annual Congress, Limassol, Cyprus: poster presentation (2x)	2017	3.0

Teaching activities		
Educational lectures for nurse practitioners and residents, pediatric surgery, Erasmus MC	2012-2017	0.2
Lectures on primary school, Calvijn College, Rotterdam	2013	1.0
Other		
Research meetings follow-up	2012-2014	0.3
Monday morning meetings Cell Biology, Erasmus MC: oral presentation (5x)	2012-2017	1.0
Research meetings Pediatric Surgery: oral presentation (2x)	2012-2017	0.5
EPAR PhD day, Erasmus MC	2013	0.2
Journal club Cell Biology	2013-2014	0.2
Sophia researchday, Erasmus MC-Sophia Children's Hospital, Rotterdam, Netherlands: poster presentation (1x), oral presentation (2x)	2013-2016	4.0
International exchange		
Temporary work for 5 months at the Max-Planck Institute for Heart and Lung Research, Bad Nauheim, Germany	2014-2015	
Grants		
Sophia Stichting Wetenschappelijk Onderzoek	2014	
COST project 'Short-Term Scientific Missions'	2015	
NRS Young Investigator Travel Grant	2015-2017	

Dankwoord

Na een hele leuke periode als ANIOS en PhD student bij de kinderchirurgie wil ik graag iedereen bedanken die mij de afgelopen jaren heeft geholpen en gesteund. Zonder jullie had ik dit niet kunnen doen!

Graag wil ik als eerste mijn beide promotoren, Dick Tibboel en René Wijnen, en co-promotor, Robbert Rottier, bedanken voor de begeleiding van mijn promotietraject. Dick, bedankt voor al je input in mijn onderzoek, jij stond altijd klaar met ideeën en was tot het laatste moment altijd bereikbaar voor overleg. René, zonder jou had ik nooit kunnen starten met dit onderzoek. Bedankt voor de mogelijkheid die je me hebt geboden om zowel klinisch werk als onderzoek te verrichten in de afgelopen jaren. Ook bedankt voor alle leuke activiteiten rondom de congressen; het bezoek aan Robben-Eiland bij Kaapstad, de Niagara Waterfalls bij Toronto en het drinken van cocktails op Cyprus! Robbert, bedankt voor al je steun, hulp en input in mijn onderzoek. Heel fijn dat je altijd beschikbaar was voor overleg en zelfs 's avonds laat of 's nachts nog reageerde op mijn mailtjes. Ik heb een hele leuke periode gehad bij jou op het lab met als hoogtepunt natuurlijk het avontuur met de groep op de Tafelberg in Kaapstad.

I would like to thank my reading committee, Irwin Reis, Karel Allegaert and Rory Morty. Irwin en Karel, bedankt voor het plaatsnemen in mijn kleine commissie en het lezen van mijn manuscript. Rory, thanks a lot for the great time I had in your lab in Bad Nauheim! It is an honor to have you in my committee! Rolf Berger en Harm Jan Bogaard, bedankt voor het plaatsnemen in mijn grote commissie en het aanwezig zijn bij mijn verdediging. Anne Hilgendorff, thank you for participating in my dissertation committee.

I also would like to thank all co-authors. Thanks for all the ideas, comments and help!

Natuurlijk wil ik ook mijn paranimfen bedanken. Lieve Evelien, super leuk dat je mijn paranimf wilde zijn! Ik heb het altijd heel gezellig gevonden om samen te werken, te lunchen, koffie te drinken en zelfs hard te lopen! Heel veel succes met het laatste stukje van jouw promotietraject, ik weet zeker dat dat helemaal goed gaat komen! Lieve Sabine, het stond al heel lang voor mij vast dat jij één van mijn paranimfen zou zijn! Want zoals je zelf al aangaf, jij ben niet alleen mijn zus, maar ook mijn beste vriendin! Heel leuk om jou nu naast mij te hebben staan, waar ik 2 jaar geleden naast jou stond!

Thanks to all colleages and former colleages of lab 1034: Heleen, Evelien, Marjon, Anne, Petra, Mieke, Jennifer, Koji, Hamed, Bob, Kim, Marta, Joshua and all students! Heleen, samen begonnen en samen geëindigd! Naast het hele fijne en leuke samenwerken hebben we ook genoten in Kaapstad en Toronto! Bedankt voor alle labskills die je me hebt geleerd en het behandelen van en helpen met de ratten! Jouw gezelschap maakte de woensdagen in het hok een stuk gezelliger! Heel veel succes met je eigen verdediging en je nieuwe baan en avontuur in Engeland! Marjon, zeker gedurende de laatste maanden was jij mijn rechterhand op het lab. Bedankt voor alle qPCR's, blotjes, gesneden blokjes en alle andere experimenten! Anne, Petra en Mieke, ook jullie bedankt voor alle hulp met kleuringen, microscopie en CT-scans! Thanks to all other colleages and former colleages of the department of Cell Biology!

Verder wil ik graag alle kinderchirurgen bedanken voor de leuke, gezellige en leerzame tijd die ik heb gehad op de afdeling Kinderchirurgie! Bedankt René, Conny, Pim, John, Hester, Claudia, Marco, Kees en Sheila! Ook alle assistenten en oud-assistenten, Lisette, Rosalie, Evelien, Kitty, Desiree, Rhiana en Willem en verpleegkundig specialisten, Susanna, Irene, Nicole, Thirza, Alwin, Klarieke en Kayleigh, bedankt voor de fijne samenwerking! Marja, bedankt voor alles wat je voor me hebt geregeld! En natuurlijk alle verpleegkundigen van afdeling 1 Zuid. Bedankt voor de samenwerking, het gezelschap tijdens de diensten en natuurlijk niet te vergeten het leuke weekend Winterberg!

Furthermore, I would like to thank all the members of the Morty lab in Bad Nauheim. I learned a lot from you all and had a really nice time over there! Jordi, Claudio, Ivana, Alessandro, Luciana, David, Diogo, Alberto, Ivonne, Agnieszka and Lina, it was fun playing football together! Thanks Ivana and Alessandro for the hospitality last year and it was really nice to have you here in the Netherlands. I hope we will keep visiting each other!

Naast mijn collega's wil ik ook graag al mijn vrienden en vriendinnen bedanken voor alle ontspanning en support. Lieve Aniek, bedankt voor alle biertjes die we samen hebben gedronken ter ontspanning en natuurlijk voor alle gezellige momenten samen met jou en Robbert! Fijn om te weten dat jullie altijd klaarstaan voor mij. Marije en Merijn, bedankt voor alle gezellige spelletjesavonden, wintersport en klusdagen! Sophie, Sven en Anne, onze klaverjasavondjes zijn helaas wat verminderd door alle drukte bij iedereen, maar van 'het varken' gaan we zeker nog wat leuks doen! Leuk dat we (bijna) allemaal collega huisartsen worden. Lieve voetbalteamgenoten, heerlijk om na een dag hard werken met jullie te kunnen sporten! Bedankt voor al jullie begrip en geduld als ik weer eens niet of niet op tijd kon komen voor trainingen en wedstrijden!

Verder wil ik mijn familie graag bedanken, met in het bijzonder mijn ouders. Lieve pap en mam, zonder jullie had ik dit alles niet kunnen bereiken! Jullie hebben mij en Sabine altijd in alles gesteund en staan altijd voor ons klaar. Bedankt voor jullie liefde en alle mogelijkheden die jullie ons hebben geboden! Lieve Sab, Frank en natuurlijk Eline, bedankt voor alle support en gezellige momenten! Lieve oma, ik vind het leuk dat u altijd zo geïnteresseerd bent in mijn werk. Lieve Paul B., Huib, Jeannine, Marise, Martijn, Willemien en Rob, wat heb ik toch een geweldige schoonfamilie getroffen! Met als 'extended family' natuurlijk ook Martin en Lisette! Bedankt voor alle leuke zeil- en wintersportvakanties, weekendjes, etentjes en andere sportieve en muzikale activiteiten!

Lieve Paul, jij bent het beste wat mij ooit is overkomen! Bedankt voor jouw eeuwige steun, geduld en liefde! Ondanks dat jij in een hele andere branch werkt, ben je altijd geïnteresseerd in wat ik doe en luister je naar al mijn verhalen. Verder is het heerlijk om naast het werk samen onze (vele) hobby's uit te voeren. Voetballen, hardlopen, duiken, muziek maken, dansen, tennissen, dagjes sauna, midden in de nacht taarten bakken of gewoon heerlijk series kijken. Jij bent altijd overal voor in, staat altijd voor me klaar en helpt bij alles! Ik ben ook super trots en blij dat jij de opmaak en kaft van dit boekje hebt gemaakt! Ik hou van jou!